NUREG-1754

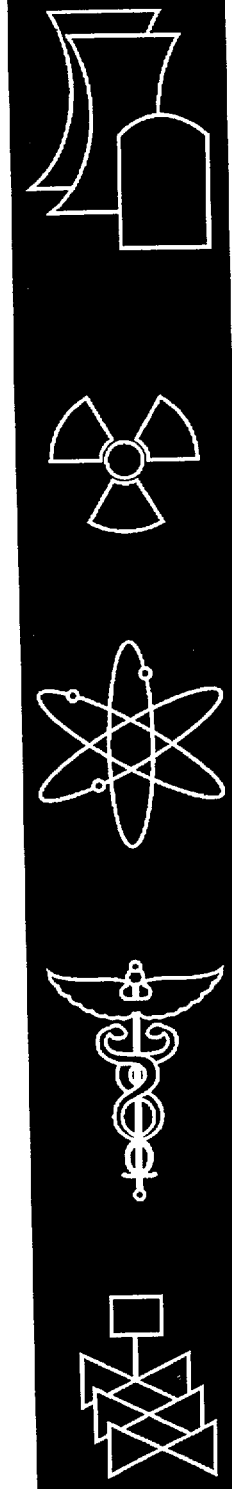

A New Comparative Analysis of LWR Fuel Designs

U.S. Nuclear Regulatory Commission
Office of Nuclear Regulatory Research
Washington, DC 20555-0001

AVAILABILITY OF REFERENCE MATERIALS IN NRC PUBLICATIONS

NRC Reference Material

As of November 1999, you may electronically access NUREG-series publications and other NRC records at NRC's Public Electronic Reading Room at www.nrc.gov/NRC/ADAMS/index.html.
Publicly released records include, to name a few, NUREG-series publications; *Federal Register* notices; applicant, licensee, and vendor documents and correspondence; NRC correspondence and internal memoranda; bulletins and information notices; inspection and investigative reports; licensee event reports; and Commission papers and their attachments.

NRC publications in the NUREG series, NRC regulations, and *Title 10, Energy*, in the Code of *Federal Regulations* may also be purchased from one of these two sources.

1. The Superintendent of Documents
   U.S. Government Printing Office
   Mail Stop SSOP
   Washington, DC 20402–0001
   Internet: bookstore.gpo.gov
   Telephone: 202-512-1800
   Fax: 202-512-2250
2. The National Technical Information Service
   Springfield, VA 22161–0002
   www.ntis.gov
   1–800–553–6847 or, locally, 703–605–6000

A single copy of each NRC draft report for comment is available free, to the extent of supply, upon written request as follows:

Address: Office of the Chief Information Officer,
Reproduction and Distribution
Services Section
U.S. Nuclear Regulatory Commission
Washington, DC 20555-0001
E-mail: DISTRIBUTION@nrc.gov
Facsimile: 301–415–2289

Some publications in the NUREG series that are posted at NRC's Web site address www.nrc.gov/NRC/NUREGS/indexnum.html are updated periodically and may differ from the last printed version. Although references to material found on a Web site bear the date the material was accessed, the material available on the date cited may subsequently be removed from the site.

Non-NRC Reference Material

Documents available from public and special technical libraries include all open literature items, such as books, journal articles, and transactions, *Federal Register* notices, Federal and State legislation, and congressional reports. Such documents as theses, dissertations, foreign reports and translations, and non-NRC conference proceedings may be purchased from their sponsoring organization.

Copies of industry codes and standards used in a substantive manner in the NRC regulatory process are maintained at—

The NRC Technical Library
Two White Flint North
11545 Rockville Pike
Rockville, MD 20852–2738

These standards are available in the library for reference use by the public. Codes and standards are usually copyrighted and may be purchased from the originating organization or, if they are American National Standards, from—

American National Standards Institute
11 West 42nd Street
New York, NY 10036–8002
www.ansi.org
212–642–4900

Legally binding regulatory requirements are stated only in laws; NRC regulations; licenses, including technical specifications; or orders, not in NUREG-series publications. The views expressed in contractor-prepared publications in this series are not necessarily those of the NRC.

The NUREG series comprises (1) technical and administrative reports and books prepared by the staff (NUREG–XXXX) or agency contractors (NUREG/CR–XXXX), (2) proceedings of conferences (NUREG/CP–XXXX), (3) reports resulting from international agreements (NUREG/IA–XXXX), (4) brochures (NUREG/BR–XXXX), and (5) compilations of legal decisions and orders of the Commission and Atomic and Safety Licensing Boards and of Directors' decisions under Section 2.206 of NRC's regulations (NUREG–0750).

NUREG-1754

A New Comparative Analysis of LWR Fuel Designs

Manuscript Completed: November 2001
Date Published: December 2001

Prepared by
G. M. O'Donnell, H. H. Scott, R. O. Meyer

Division of Systems Analysis and Regulatory Effectiveness
Office of Nuclear Regulatory Research
U.S. Nuclear Regulatory Commission
Washington, DC 20555-0001

A NEW COMPARATIVE ANALYSIS OF LWR FUEL DESIGNS

G. M. O'Donnell, H. H. Scott, and R. O. Meyer

ABSTRACT

In 1980, NRC published a comparative analysis of LWR fuel designs, and that report served as a handy reference for typical design and operating parameters for all types of fuel then in operation in U.S. power reactors. During the past twenty years, significant changes have been made in fuel designs, burnups, and analytical computer codes. The present report is an update of the earlier report. Typical fuel design parameters are tabulated for almost all fuel types in current operation, from BWR 8x8 bundles to PWR 17x17 assemblies. Cross-section diagrams are given for BWR fuel bundles and PWR fuel assemblies. Calculated values are plotted for thirteen operating parameters including fuel centerline temperature, cladding O.D. temperature, gap conductance, rod internal gas pressure, and cladding hoop stress. The calculated values are plotted as a function of fuel burnup to 65 GWd/t for a variety of power histories, covering a range from low to high linear heat ratings, which are constant early in life but decline later in a realistic manner.

Contents

Abstract iii

Foreword xvii

1. **Introduction** 1-1

2. **Input Parameters** 2-1
   - 2.1. Pitch 2-1
   - 2.2. Cladding Outer Diameter 2-9
   - 2-3. Cladding Thickness, Gap Thickness, and Pellet Diameter 2-9
   - 2-4. Dish Dimensions 2-12
   - 2-5. Plenum Length and Helium Fill Gas Pressure 2-12
   - 2-6. Plenum Spring Dimensions 2-13
   - 2.7. Coolant Flow Rates 2-13
   - 2.8 Other Parameters 2-13

3. **FRAPCON-3** 3-1
   - 3.1. MATPRO 3-1
   - 3.2. Fission Gas Release 3-1
   - 3.3. Oxide Thickness 3-1

4. **Axial Power Profile and Power Histories** 4-1
   - 4.1. Axial Power Profile 4-1
   - 4.2. Power Histories 4-1

5. **Calculations for BWR 8X8 Fuel** 5-1

6. **Calculations for BWR 9X9 Fuel** 6-1

7. **Calculations for BWR 10X10 Fuel** 7-1

8. **Calculations for PWR 14X14 Fuel** 8-1

9. **Calculations for PWR 15X15 Fuel** 9-1

10. **Calculations for PWR 16X16 Fuel** 10-1

11. **Calculations for PWR 17X17 Fuel** 11-1

12. **References** 12-1

Figures

2-1. Components of typical fuel rods 2-2
2-2. Cross sections of fuel bundles that are interchangeable in all BWRs 2-3
2-3. Cross sections of fuel assembles for Westinghouse and C-E 14x14 plants 2-4
2-4. Cross sections of fuel assemblies for Westinghouse and B&W 15x15 plants 2-5
2-5. Cross sections of fuel assemblies for C-E 16x16 and Westinghouse 17x17 plants 2-6
2.6. Relationship between outside dimension of fuel bundle, fuel rod pitch and cladding diameter 2-1
2-7. Cladding thickness as a function of cladding outer diameter determined from non-proprietary information 2-10
2-8. Gap thickness as a function of cladding outer diameter determined from non-proprietary information 2-11
4-1. Axial power profile used for code input 4-2
4-2. Power histories used for BWR 8x8 fuel design 4-3
4-3. Power histories used for BWR 9x9 fuel design 4-4
4-4. Power histories used for BWR 10x10 fuel design 4-5
4-5. Power histories used for PWR 14x14 fuel design 4-6
4-6. Power histories used for PWR 15x15 fuel design 4-7
4-7. Power histories used for PWR 16x16 fuel design 4-8
4-8. Power histories used for PWR 17x17 fuel design 4-9
5-1. Fuel temperatures and stored energy for a BWR 8x8 fuel rod with initial peak power of 7 kW/ft. 5-2
5-2. Cladding temperatures and fuel surface temperature for a BWR 8x8 fuel rod with initial peak power of 7 kW/ft 5-3
5-3. Gap thickness and gap conductance for a BWR 8x8 fuel rod with initial peak power of 7kW/ft. 5-4
5-4. Fission gas release and rod internal gas pressure for a BWR 8x8 fuel rod with initial peak power of 7kW/ft. 5-5
5-5. Oxide thickness at three axial locations for a BWR 8x8 fuel rod with initial peak power of 7 kW/ft. 5-6
5-6 Cladding hoop stress and hoop strain for a BWR 8x8 fuel rod with initial peak power of 7kW/ft. 5-7
5-7. Fuel temperatures and stored energy for a BWR 8x8 fuel rod with initial peak power of 9 kW/ft. 5-8
5-8. Cladding temperatures and fuel surface temperature for a BWR 8x8 fuel rod with initial peak power of 9 kW/ft. 5-9
5-9. Gap thickness and gap conductance for a BWR 8x8 fuel rod with initial peak power of 9 kW/ft. 5-10
5-10. Fission gas release and rod internal gas pressure for a BWR 8x8 fuel rod with initial peak power of 9 kW/ft. 5-11
5-11. Oxide thickness at three axial locations for a BWR 8x8 fuel rod with initial peak power of 9 kW/ft. 5-12
5-12. Cladding hoop stress and hoop strain for a BWR 8x8 fuel rod with initial peak power of 9 kW/ft. 5-13
5-13. Fuel temperatures and stored energy for a BWR 8x8 fuel rod with initial peak power of 11 kW/ft 5-14

Figures (cont.)

5-14. Cladding temperatures and fuel surface temperature for a BWR 8x8 fuel rod with initial peak power of 11 kW/ft 5-15
5-15 Gap thickness and gap conductance for a BWR 8x8 fuel rod with initial peak power of 11 kW/ft. 5-16
5-16. Fission gas release and rod internal gas pressure for a BWR 8x8 fuel rod with initial peak power of 11 kW/ft. 5-17
5-17. Oxide thickness at three axial locations for a BWR 8x8 fuel rod with initial peak power of 11 kW/ft. 5-18
5-18. Cladding hoop stress and hoop strain for a BWR 8x8 fuel rod with initial peak power of 11 kW/ft. 5-19
5-19. Fuel temperatures and stored energy for a BWR 8x8 fuel rod with initial peak power of 13 kW/ft. 5-20
5-20. Cladding temperatures and fuel surface temperature for a BWR 8x8 fuel rod with initial peak power of 13 kW/ft. 5-21
5-21. Gap thickness and gap conductance for a BWR 8x8 fuel rod with initial peak power of 13 kW/ft. 5-22
5-22. Fission gas release and rod internal gas pressure for a BWR 8x8 fuel rod with initial peak power of 13 kW/ft. 5-23
5-23. Oxide thickness at three axial locations for a BWR 8x8 fuel rod with initial peak power of 13 kW/ft. 5-24
5-24. Cladding hoop stress and hoop strain for a BWR 8x8 fuel rod with initial peak power of 13 kW/ft. 5-25
6-1. Fuel temperatures and stored energy for a BWR 9x9fuel rod with initial peak power of 7 kW/ft. 6-2
6-2. Cladding temperatures and fuel surface temperature for a BWR 9x9 fuel rod with initial peak power of 7 kW/ft. 6-3
6-3. Gap thickness and gap conductance for a BWR 9x9 fuel rod with initial peak power of 7 kW/ft. 6-4
6-4. Fission gas release and rod internal gas pressure for a BWR 9x9 fuel rod with initial peak power of 7 kW/ft. 6-5
6-5. Oxide thickness at three axial locations for a BWR 9x9 fuel rod with initial peak power of 7 kW/ft. 6-6
6-6. Cladding hoop stress and hoop strain for a BWR 9x9 fuel rod with initial peak power of 7 kW/ft. 6-7
6-7. Fuel temperatures and stored energy for a BWR 9x9fuel rod with initial peak power of 9 kW/ft. 6-8
6-8. Cladding temperatures and fuel surface temperature for a BWR 9x9 fuel rod with initial peak power of 9 kW/ft. 6-9
6-9. Gap thickness and gap conductance for a BWR 9x9 fuel rod with initial peak power of 9 kW/ft. 6-10
6-10. Fission gas release and rod internal gas pressure for a BWR 9x9 fuel rod with initial peak power of 9 kW/ft. 6-11
6-11. Oxide thickness at three axial locations for a BWR 9x9 fuel rod with initial peak power of 9 kW/ft. 6-12
6-12. Cladding hoop stress and hoop strain for a BWR 9x9 fuel rod with initial peak power of 9 kW/ft. 6-13

Figures (cont.)

6-13. Fuel temperatures and stored energy for a BWR 9x9fuel rod with initial peak power of 11 kW/ft. 6-14
6-14. Cladding temperatures and fuel surface temperature for a BWR 9x9 fuel rod with initial peak power of 11 kW/ft. 6-15
6-15. Gap thickness and gap conductance for a BWR 9x9 fuel rod with initial peak power of 11 kW/ft. 6-16
6-16. Fission gas release and rod internal gas pressure for a BWR 9x9 fuel rod with initial peak power of 11 kW/ft. 6-17
6-17. Oxide thickness at three axial locations for a BWR 9x9 fuel rod with initial peak power of 11 kW/ft. 6-18
6-18. Cladding hoop stress and hoop strain for a BWR 9x9 fuel rod with initial peak power of 11 kW/ft. 6-19
6-19. Fuel temperatures and stored energy for a BWR 9x9fuel rod with initial peak power of 12 kW/ft. 6-20
6-20. Cladding temperatures and fuel surface temperature for a BWR 9x9 fuel rod with initial peak power of 12 kW/ft. 6-21
6-21. Gap thickness and gap conductance for a BWR 9x9 fuel rod with initial peak power of 12 kW/ft. 6-22
6-22. Fission gas release and rod internal gas pressure for a BWR 9x9 fuel rod with initial peak power of 12 kW/ft. 6-23
6-23. Oxide thickness at three axial locations for a BWR 9x9 fuel rod with initial peak power of 12 kW/ft. 6-24
6-24. Cladding hoop stress and hoop strain for a BWR 9x9 fuel rod with initial peak power of 12 kW/ft. 6-25
7-1. Fuel temperatures and stored energy for a BWR 10x10 fuel rod with initial peak power of 5 kW/ft. 7-2
7-2. Cladding temperatures and fuel surface temperature for a BWR 10x10 fuel rod with initial peak power of 5 kW/ft. 7-3
7-3. Gap thickness and gap conductance for a BWR 10x10 fuel rod with initial peak power of 5 kW/ft. 7-4
7-4. Fission gas release and rod internal gas pressure for a BWR 10x10 fuel rod with initial peak power of 5 kW/ft. 7-5
7-5. Oxide thickness at three axial locations for a BWR 10x10 fuel rod with initial peak power of 5 kW/ft. 7-6
7-6. Cladding hoop stress and hoop strain for a BWR 10x10 fuel rod with initial peak power of 5 kW/ft. 7-7
7-7. Fuel temperatures and stored energy for a BWR 10x10 fuel rod with initial peak power of 7 kW/ft. 7-8
7-8. Cladding temperatures and fuel surface temperature for a BWR 10x10 fuel rod with initial peak power of 7 kW/ft. 7-9
7-9. Gap thickness and gap conductance for a BWR 10x10 fuel rod with initial peak power of 7 kW/ft. 7-10
7-10. Fission gas release and rod internal gas pressure for a BWR 10x10 fuel rod with initial peak power of 7 kW/ft. 7-11
7-11. Oxide thickness at three axial locations for a BWR 10x10 fuel rod with initial peak power of 7 kW/ft. 7-12

Figures (cont.)

7-12. Cladding hoop stress and hoop strain for a BWR 10x10 fuel rod with initial peak power of 7 kW/ft. 7-13
7-13. Fuel temperatures and stored energy for a BWR 10x10 fuel rod with initial peak power of 9 kW/ft. 7-14
7-14. Cladding temperatures and fuel surface temperature for a BWR 10x10 fuel rod with initial peak power of 9 kW/ft. 7-15
7-15. Gap thickness and gap conductance for a BWR 10x10 fuel rod with initial peak power of 9 kW/ft. 7-16
7-16. Fission gas release and rod internal gas pressure for a BWR 10x10 fuel rod with initial peak power of 9 kW/ft. 7-17
7-17. Oxide thickness at three axial locations for a BWR 10x10 fuel rod with initial peak power of 9 kW/ft. 7-18
7-18. Cladding hoop stress and hoop strain for a BWR 10x10 fuel rod with initial peak power of 9 kW/ft. 7-19
7-19. Fuel temperatures and stored energy for a BWR 10x10 fuel rod with initial peak power of 11 kW/ft. 7-20
7-20. Cladding temperatures and fuel surface temperature for a BWR 10x10 fuel rod with initial peak power of 11 kW/ft. 7-21
7-21. Gap thickness and gap conductance for a BWR 10x10 fuel rod with initial peak power of 11 kW/ft. 7-22
7-22. Fission gas release and rod internal gas pressure for a BWR 10x10 fuel rod with initial peak power of 11 kW/ft. 7-23
7-23. Oxide thickness at three axial locations for a BWR 10x10 fuel rod with initial peak power of 11 kW/ft. 7-24
7-24. Cladding hoop stress and hoop strain for a BWR 10x10 fuel rod with initial peak power of 11 kW/ft. 7-25
8-1. Fuel temperatures and stored energy for a PWR 14x14 fuel rod with initial peak power of 9 kW/ft. 8-2
8-2. Cladding temperatures and fuel surface temperature for a PWR 14x14 fuel rod with initial peak power of 9 kW/ft. 8-3
8-3. Gap thickness and gap conductance for a PWR 14x14 fuel rod with initial peak power of 9 kW/ft. 8-4
8-4. Fission gas release and rod internal gas pressure for a PWR 14x14 fuel rod with initial peak power of 9 kW/ft. 8-5
8-5. Oxide thickness at three axial locations for a PWR 14x14 fuel rod with initial peak power of 9 kW/ft. 8-6
8-6. Cladding hoop stress and hoop strain for a PWR 14x14 fuel rod with initial peak power of 9 kW/ft. 8-7
8-7. Fuel temperatures and stored energy for a PWR 14x14 fuel rod with initial peak power of 11 kW/ft. 8-8
8-8. Cladding temperatures and fuel surface temperature for a PWR 14x14 fuel rod with initial peak power of 11 kW/ft. 8-9
8-9. Gap thickness and gap conductance for a PWR 14x14 fuel rod with initial peak power of 11 kW/ft. 8-10
8-10. Fission gas release and rod internal gas pressure for a PWR 14x14 fuel rod with initial peak power of 11 kW/ft. 8-11

Figures (cont.)

8-11. Oxide thickness at three axial locations for a PWR 14x14 fuel rod with initial peak power of 11 kW/ft. 8-12
8-12. Cladding hoop stress and hoop strain for a PWR 14x14 fuel rod with initial peak power of 11 kW/ft. 8-13
8-13. Fuel temperatures and stored energy for a PWR 14x14 fuel rod with initial peak power of 13 kW/ft. 8-14
8-14. Cladding temperatures and fuel surface temperature for a PWR 14x14 fuel rod with initial peak power of 13 kW/ft. 8-15
8-15. Gap thickness and gap conductance for a PWR 14x14 fuel rod with initial peak power of 13 kW/ft. 8-16
8-16. Fission gas release and rod internal gas pressure for a PWR 14x14 fuel rod with initial peak power of 13 kW/ft. 8-17
8-17. Oxide thickness at three axial locations for a PWR 14x14 fuel rod with initial peak power of 13 kW/ft. 8-18
8-18. Cladding hoop stress and hoop strain for a PWR 14x14 fuel rod with initial peak power of 13 kW/ft. 8-19
8-19. Fuel temperatures and stored energy for a PWR 14x14 fuel rod with initial peak power of 15 kW/ft. 8-20
8-20. Cladding temperatures and fuel surface temperature for a PWR 14x14 fuel rod with initial peak power of 15 kW/ft. 8-21
8-21. Gap thickness and gap conductance for a PWR 14x14 fuel rod with initial peak power of 15 kW/ft. 8-22
8-22. Fission gas release and rod internal gas pressure for a PWR 14x14 fuel rod with initial peak power of 15 kW/ft. 8-23
8-23. Oxide thickness at three axial locations for a PWR 14x14 fuel rod with initial peak power of 15 kW/ft. 8-24
8-24. Cladding hoop stress and hoop strain for a PWR 14x14 fuel rod with initial peak power of 15 kW/ft. 8-25
8-25. Fuel temperatures and stored energy for a PWR 14x14 fuel rod with initial peak power of 16 kW/ft. 8-26
8-26. Cladding temperatures and fuel surface temperature for a PWR 14x14 fuel rod with initial peak power of 16 kW/ft. 8-27
8-27. Gap thickness and gap conductance for a PWR 14x14 fuel rod with initial peak power of 16 kW/ft. 8-28
8-28. Fission gas release and rod internal gas pressure for a PWR 14x14 fuel rod with initial peak power of 16 kW/ft. 8-29
8-29. Oxide thickness at three axial locations for a PWR 14x14 fuel rod with initial peak power of 16 kW/ft. 8-30
8-30. Cladding hoop stress and hoop strain for a PWR 14x14 fuel rod with initial peak power of 16 kW/ft. 8-31
9-1. Fuel temperatures and stored energy for a PWR 15x15 fuel rod with initial peak power of 9 kW/ft. 9-2
9-2. Cladding temperatures and fuel surface temperature for a PWR 15x15 fuel rod with initial peak power of 9 kW/ft. 9-3
9-3. Gap thickness and gap conductance for a PWR 15x15 fuel rod with initial peak power of 9 kW/ft. 9-4

Figures (cont.)

9-4. Fission gas release and rod internal gas pressure for a PWR 15x15 fuel rod with initial peak power of 9 kW/ft. 9-5
9-5. Oxide thickness at three axial locations for a PWR 15x15 fuel rod with initial peak power of 9 kW/ft. 9-6
9-6. Cladding hoop stress and hoop strain for a PWR 15x15 fuel rod with initial peak power of 9 kW/ft. 9-7
9-7. Fuel temperatures and stored energy for a PWR 15x15 fuel rod with initial peak power of 11 kW/ft. 9-8
9-8. Cladding temperatures and fuel surface temperature for a PWR 15x15 fuel rod with initial peak power of 11 kW/ft. 9-9
9-9. Gap thickness and gap conductance for a PWR 15x15 fuel rod with initial peak power of 11 kW/ft. 9-10
9-10. Fission gas release and rod internal gas pressure for a PWR 15x15 fuel rod with initial peak power of 11 kW/ft. 9-11
9-11. Oxide thickness at three axial locations for a PWR 15x15 fuel rod with initial peak power of 11 kW/ft. 9-12
9-12. Cladding hoop stress and hoop strain for a PWR 15x15 fuel rod with initial peak power of 11 kW/ft. 9-13
9-13. Fuel temperatures and stored energy for a PWR 15x15 fuel rod with initial peak power of 13 kW/ft. 9-14
9-14. Cladding temperatures and fuel surface temperature for a PWR 15x15 fuel rod with initial peak power of 13 kW/ft. 9-15
9-15. Gap thickness and gap conductance for a PWR 15x15 fuel rod with initial peak power of 13 kW/ft. 9-16
9-16. Fission gas release and rod internal gas pressure for a PWR 15x15 fuel rod with initial peak power of 13 kW/ft. 9-17
9-17. Oxide thickness at three axial locations for a PWR 15x15 fuel rod with initial peak power of 13 kW/ft. 9-18
9-18. Cladding hoop stress and hoop strain for a PWR 15x15 fuel rod with initial peak power of 13 kW/ft. 9-19
9-19. Fuel temperatures and stored energy for a PWR 15x15 fuel rod with initial peak power of 15 kW/ft. 9-20
9-20. Cladding temperatures and fuel surface temperature for a PWR 15x15 fuel rod with initial peak power of 15 kW/ft. 9-21
9-21. Gap thickness and gap conductance for a PWR 15x15 fuel rod with initial peak power of 15 kW/ft. 9-22
9-22. Fission gas release and rod internal gas pressure for a PWR 15x15 fuel rod with initial peak power of 15 kW/ft. 9-23
9-23. Oxide thickness at three axial locations for a PWR 15x15 fuel rod with initial peak power of 15 kW/ft. 9-24
9-24. Cladding hoop stress and hoop strain for a PWR 15x15 fuel rod with initial peak power of 15 kW/ft. 9-25
10-1. Fuel temperatures and stored energy for a PWR 16x16 fuel rod with initial peak power of 9 kW/ft. 10-2
10-2. Cladding temperatures and fuel surface temperature for a PWR 16x16 fuel rod with initial peak power of 9 kW/ft. 10-3

Figures (cont.)

10-3. Gap thickness and gap conductance for a PWR 16x16 fuel rod with initial peak power of 9 kW/ft. 10-4
10-4. Fission gas release and rod internal gas pressure for a PWR 16x16 fuel rod with initial peak power of 9 kW/ft. 10-5
10-5. Oxide thickness at three axial locations for a PWR 16x16 fuel rod with initial peak power of 9 kW/ft. 10-6
10-6. Cladding hoop stress and hoop strain for a PWR 16x16 fuel rod with initial peak power of 9 kW/ft. 10-7
10-7. Fuel temperatures and stored energy for a PWR 16x16 fuel rod with initial peak power of 11 kW/ft. 10-8
10-8. Cladding temperatures and fuel surface temperature for a PWR 16x16 fuel rod with initial peak power of 11 kW/ft. 10-9
10-9. Gap thickness and gap conductance for a PWR 16x16 fuel rod with initial peak power of 11 kW/ft. 10-10
10-10. Fission gas release and rod internal gas pressure for a PWR 16x16 fuel rod with initial peak power of 11 kW/ft. 10-11
10-11. Oxide thickness at three axial locations for a PWR 16x16 fuel rod with initial peak power of 11 kW/ft. 10-12
10-12. Cladding hoop stress and hoop strain for a PWR 16x16 fuel rod with initial peak power of 11 kW/ft. 10-13
10-13. Fuel temperatures and stored energy for a PWR 16x16 fuel rod with initial peak power of 13 kW/ft. 10-14
10-14. Cladding temperatures and fuel surface temperature for a PWR 16x16 fuel rod with initial peak power of 13 kW/ft. 10-15
10-15. Gap thickness and gap conductance for a PWR 16x16 fuel rod with initial peak power of 13 kW/ft. 10-16
10-16. Fission gas release and rod internal gas pressure for a PWR 16x16 fuel rod with initial peak power of 13 kW/ft. 10-17
10-17. Oxide thickness at three axial locations for a PWR 16x16 fuel rod with initial peak power of 13 kW/ft. 10-18
10-18. Cladding hoop stress and hoop strain for a PWR 16x16 fuel rod with initial peak power of 13 kW/ft. 10-19
10-19. Fuel temperatures and stored energy for a PWR 16x16 fuel rod with initial peak power of 14 kW/ft. 10-20
10-20. Cladding temperatures and fuel surface temperature for a PWR 16x16 fuel rod with initial peak power of 14 kW/ft. 10-21
10-21. Gap thickness and gap conductance for a PWR 16x16 fuel rod with initial peak power of 14 kW/ft. 10-22
10-22. Fission gas release and rod internal gas pressure for a PWR 16x16 fuel rod with initial peak power of 14 kW/ft. 10-23
10-23. Oxide thickness at three axial locations for a PWR 16x16 fuel rod with initial peak power of 14 kW/ft. 10-24
10-24. Cladding hoop stress and hoop strain for a PWR 16x16 fuel rod with initial peak power of 14 kW/ft. 10-25

Figures (cont.)

11-1. Fuel temperatures and stored energy for a PWR 17x17 fuel rod with initial peak power of 7 kW/ft. 11-2
11-2. Cladding temperatures and fuel surface temperature for a PWR 17x17 fuel rod with initial peak power of 7 kW/ft. 11-3
11-3. Gap thickness and gap conductance for a PWR 17x17 fuel rod with initial peak power of 7 kW/ft. 11-4
11-4. Fission gas release and rod internal gas pressure for a PWR 17x17 fuel rod with initial peak power of 7 kW/ft. 11-5
11-5. Oxide thickness at three axial locations for a PWR 17x17 fuel rod with initial peak power of 7 kW/ft. 11-6
11-6. Cladding hoop stress and hoop strain for a PWR 17x17 fuel rod with initial peak power of 7 kW/ft. 11-7
11-7. Fuel temperatures and stored energy for a PWR 17x17 fuel rod with initial peak power of 9 kW/ft. 11-8
11-8. Cladding temperatures and fuel surface temperature for a PWR 17x17 fuel rod with initial peak power of 9 kW/ft. 11-9
11-9. Gap thickness and gap conductance for a PWR 17x17 fuel rod with initial peak power of 9 kW/ft. 11-10
11-10. Fission gas release and rod internal gas pressure for a PWR 17x17 fuel rod with initial peak power of 9 kW/ft. 11-11
11-11. Oxide thickness at three axial locations for a PWR 17x17 fuel rod with initial peak power of 9 kW/ft. 11-12
11-12. Cladding hoop stress and hoop strain for a PWR 17x17 fuel rod with initial peak power of 9 kW/ft. 11-13
11-13. Fuel temperatures and stored energy for a PWR 17x17 fuel rod with initial peak power of 11 kW/ft. 11-14
11-14. Cladding temperatures and fuel surface temperature for a PWR 17x17 fuel rod with initial peak power of 11 kW/ft. 11-15
11-15. Gap thickness and gap conductance for a PWR 17x17 fuel rod with initial peak power of 11 kW/ft. 11-16
11-16. Fission gas release and rod internal gas pressure for a PWR 17x17 fuel rod with initial peak power of 11 kW/ft. 11-17
11-17. Oxide thickness at three axial locations for a PWR 17x17 fuel rod with initial peak power of 11 kW/ft. 11-18
11-18. Cladding hoop stress and hoop strain for a PWR 17x17 fuel rod with initial peak power of 11 kW/ft. 11-19
11-19. Fuel temperatures and stored energy for a PWR 17x17 fuel rod with initial peak power of 13 kW/ft. 11-20
11-20. Cladding temperatures and fuel surface temperature for a PWR 17x17 fuel rod with initial peak power of 13 kW/ft. 11-21
11-21. Gap thickness and gap conductance for a PWR 17x17 fuel rod with initial peak power of 13 kW/ft. 11-22
11-22. Fission gas release and rod internal gas pressure for a PWR 17x17 fuel rod with initial peak power of 13 kW/ft. 11-23
11-23. Oxide thickness at three axial locations for a PWR 17x17 fuel rod with initial peak power of 13 kW/ft. 11-24

11-24. Cladding hoop stress and hoop strain for a PWR 17x17 fuel rod with initial peak power of 13 kW/ft. 11-25

Tables

2-1. Typical Fuel Design Parameters used for Code Input 2-7
2-2. Consequence of variations in fill pressure for PWR 17x17 at 11 kW/ft with 10-in. plenum 2-12
2-3. Consequence of variations in plenum length for PWR 17x17 at 11 kW/ft with 350 psi fill pressure 2-12
2-4. Consequence of variations in fill pressure for BWR 9x9 at 11 kW/ft with 10-in. plenum 2-12
2-5 Consequence of variations in plenum length for BWR 9x9 at 11 kW/ft with 100 psi fill pressure 2-13

Tables (Cont.)

A1 Non-proprietary BWR Fuel Design Parameters A-1
A2 Non-Proprietary PWR Fuel Design Parameters A-2

FOREWORD

The USNRC is conducting an integrated fuel program consisting of experiments and analyses. The goal of the program is to ensure safety as new fuel designs, materials, and higher burnup levels are proposed. Realistic experiments and analyses are intended to help maintain safety, improve agency efficiency and effectiveness, and reduce unnecessary regulatory burdens. This comparative analysis of LWR fuel designs is part of that overall effort.

Jack E. Rosenthal, Chief
Safety Margins & Systems Analysis Branch
Office of Nuclear Regulatory Research

A NEW COMPARATIVE ANALYSIS OF LWR FUEL DESIGNS

G. M. O'Donnell, H. H. Scott, and R. O. Meyer

1. Introduction

In 1980, D. L. Acey and J. C. Voglewede published a comparative analysis of LWR fuel designs, and that report served as a handy reference for typical design and operating parameters for all types of fuel then in operation in U.S. power reactors.[1] During the past twenty years, significant changes have been made in fuel designs, burnups have increased more than fifty percent, and computer codes to analyze fuel behavior have been improved. The present report, therefore, is an update of the earlier report and provides current fuel design information and newly calculated fuel performance parameters out to 65 GWd/t, just beyond the present NRC fuel burnup limit of 62 GWd/t.

Changes in fuel rod design that affect performance calculations include smaller cladding diameters in BWRs corresponding to the introduction of 9x9 and 10x10 fuel bundles. Increases in plenum length and fill gas pressure in both BWRs and PWRs also affect the calculations. Several new cladding types and alloys have been introduced, but they have a minimal effect on calculated performance parameters except for corrosion (discussed later). These changes have been made to accommodate somewhat higher power levels and large burnup increases from around 40 GWd/t in 1980 up to 62 GWd/t (average for the peak rod) in 2000.

The earlier study was done with a March 1980 version (Revision 1) of the GAPCON-THERMAL-2 computer code, which was representative of a number of similar codes used at that time by the nuclear industry for fuel thermal performance analysis.[2,3] The present study has been done with FRAPCON-3, which is an updated version of a code that combined the best features of GAPCON-THERMAL-2 and another code called FRAP-S. FRAPCON-3 has been validated out to 65 GWd/t burnup, and this peer-reviewed code is the code currently being used by NRC for auditing licensee's analyses and for research applications.[4-6]

2. INPUT PARAMETERS

Figure 2-1 identifies the components of typical fuel rods, and typical fuel assembly cross sections are shown in Figs. 2-2 and 2-5. The shrouded fuel arrays in BWRs are usually called bundles whereas the open-lattice PWR fuel arrays are called assemblies.

Typical fuel design parameters that were used as code input are shown in Table 2-1 for all major fuel types currently in use in the U.S. These parameters are all based on non-proprietary values that are available in the literature.[7-9] Available non-proprietary fuel design parameters for a number of different fuel types are shown in Tables A1 and A2 in the Appendix, and two things are readily apparent from these tables. First, no information is available on the BWR 10x10 fuel design except the number of fuel rods in a bundle. Second, even within a given fuel type (e.g., BWR 8x8), there are variations in some of the parameters between different vintages and manufacturers. The second observation shows that single fixed design parameters do not exist for each fuel type, but rather there are ranges of values.

For our calculations, therefore, we sought typical values that were within these ranges although not necessarily corresponding to any specific design variant. Because design parameters were not available for the BWR 10x10 fuel type, we deduced suitable values of all the parameters needed for code input. The methods of selecting typical values for Table 2-1 are described below.

2.1. Pitch

The pitch was known for all of the fuel types except the 10x10. The value used was determined from calculations involving fuels of other array sizes. Since the 8x8 and 9x9 fuel bundles can be replaced with the 10x10 fuel bundles it is necessary for the outer dimensions of the bundle to be the same. The outer dimensions of the 8x8 and 9x9 fuel bundles were determined by multiplying their respective pitches by their respective array sizes minus one. One rod diameter was added to that value to determine the outside dimensions of the bundle. Figure 2-6

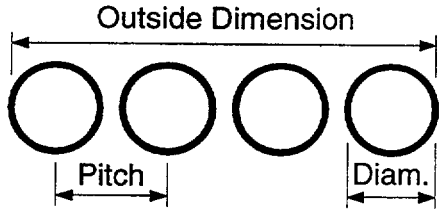

Fig. 2-6. Relationship between outside dimension of fuel bundle, fuel rod pitch and cladding diameter

illustrates the relationship of the outside dimension of the bundle to the pitch and cladding diameter. The values found for the 8x8 and 9x9 were averaged together for the value used. Using the rod diameter for the 10x10 (how that was determined is explained later), it is possible to determine the pitch. The equations are shown below.

8x8: $(8-1) \times 0.640 + 0.483 = 4.963$

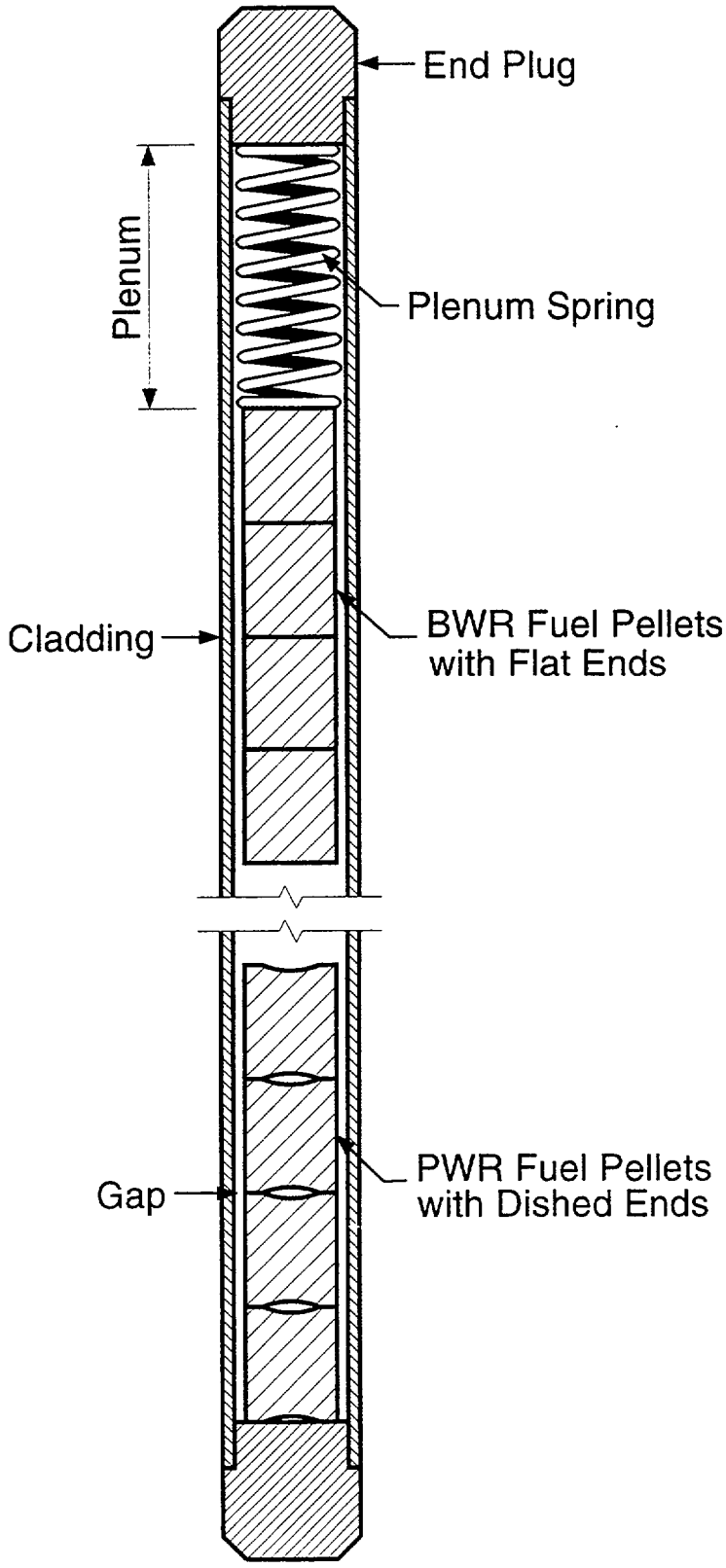

Fig. 2-1. Components of typical fuel rods

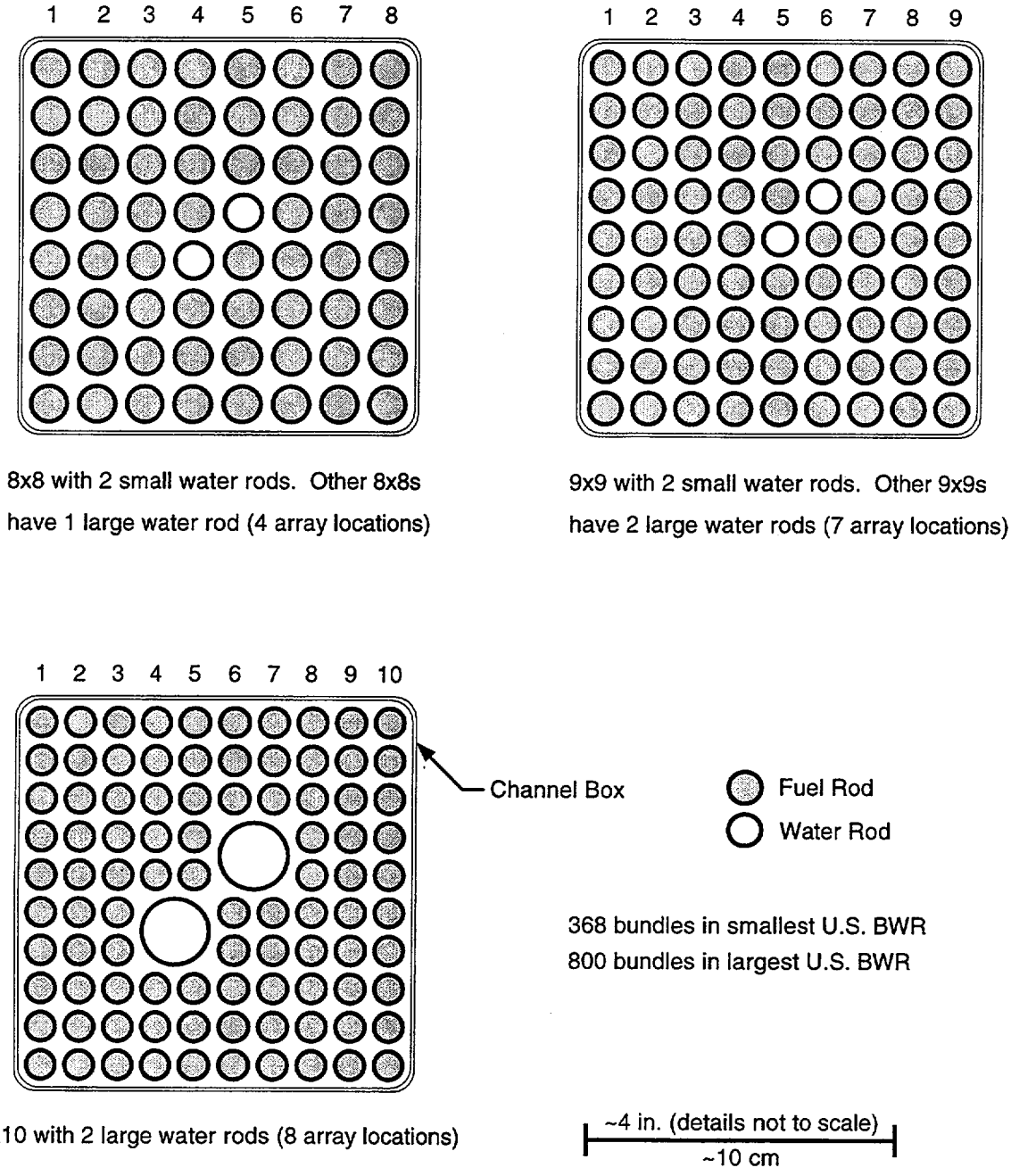

Fig. 2-2. Cross sections of fuel bundles that are interchangeable in all BWRs

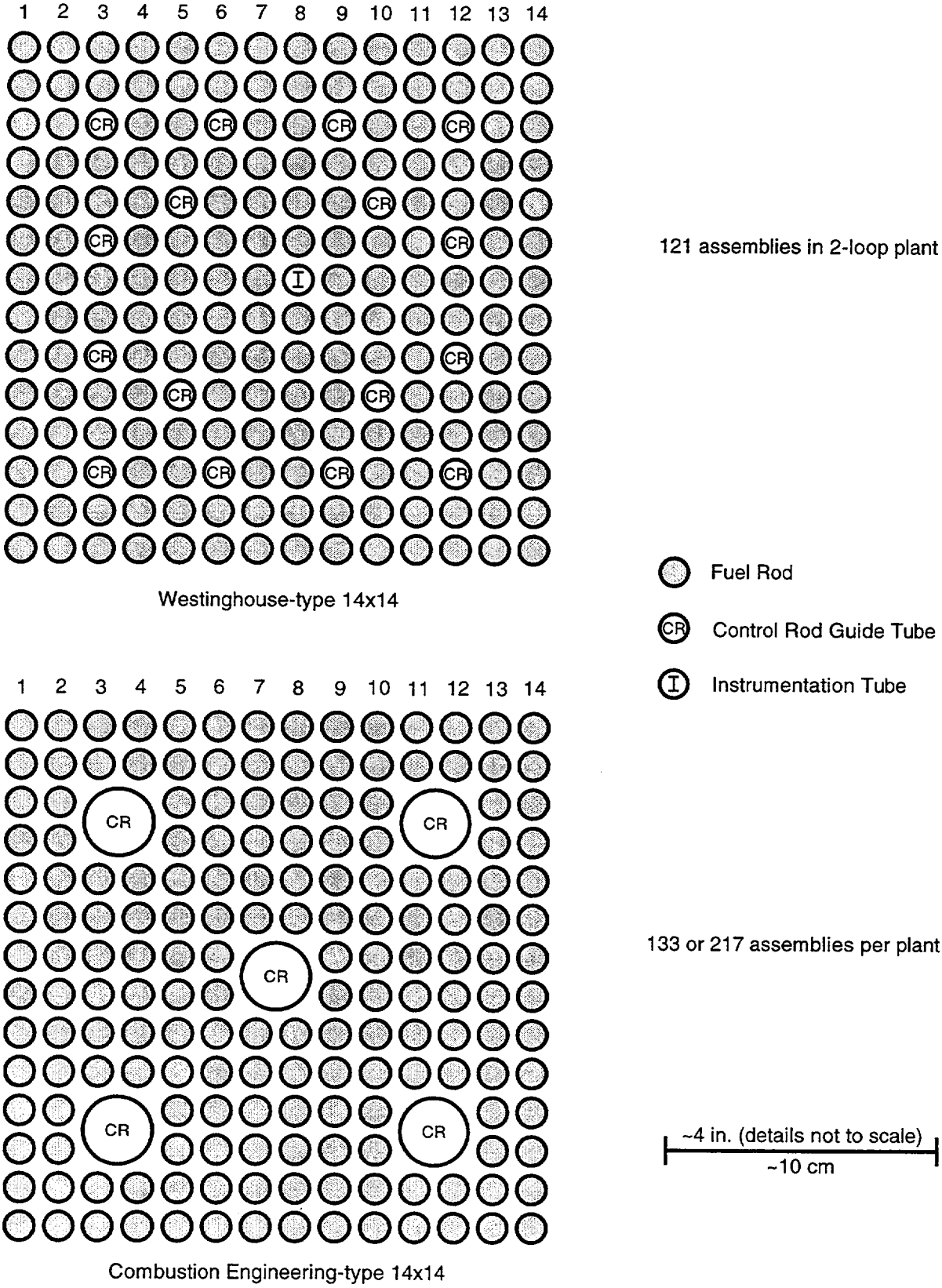

Fig. 2-3. Cross sections of fuel assemblies for Westinghouse and C-E 14x14 plants

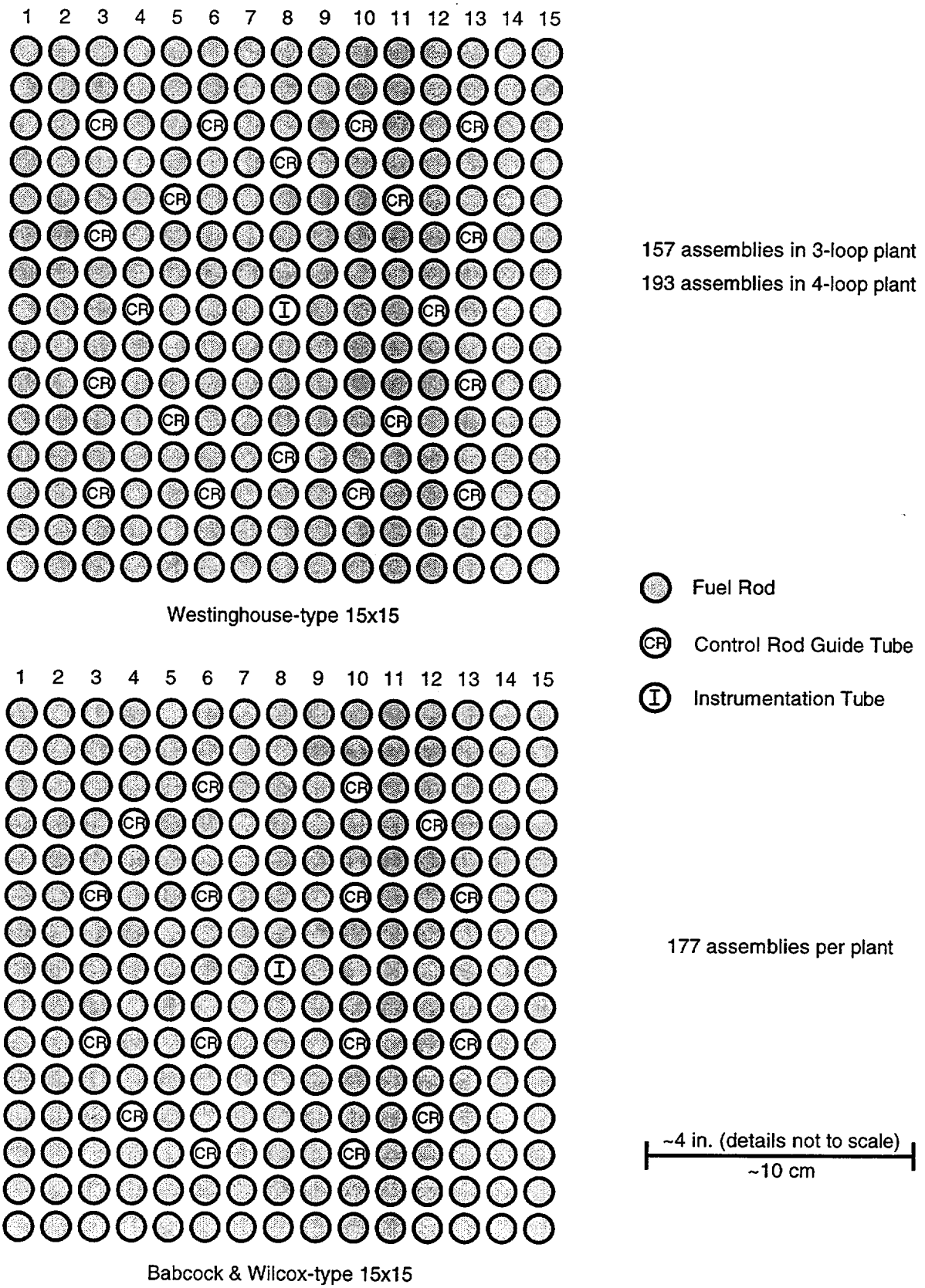

Fig. 2-4. Cross sections of fuel assemblies for Westinghouse and B&W 15x15 plants

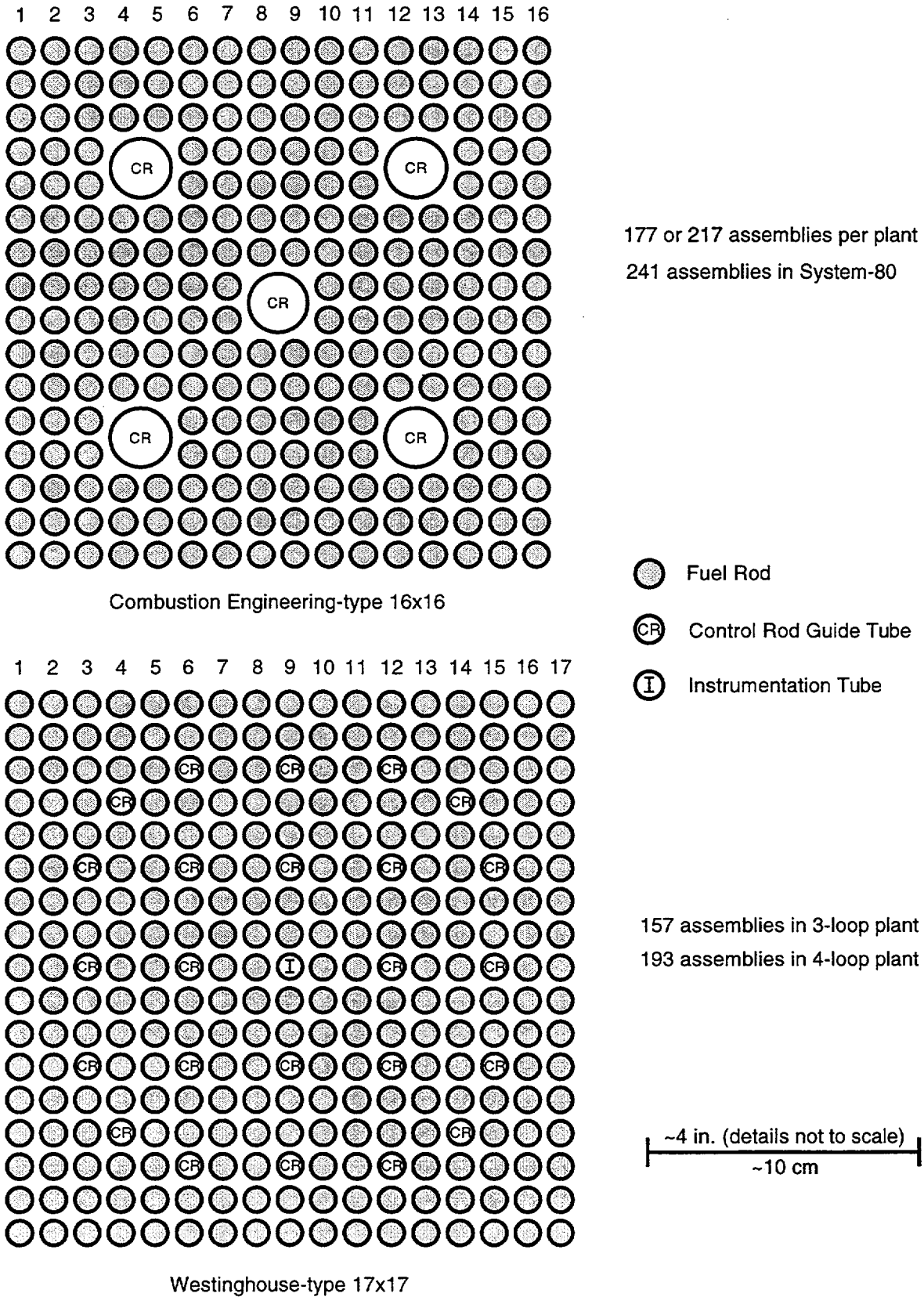

Fig. 2-5. Cross sections of fuel assemblies for C-E 16x16 and Westinghouse 17x17 plants

Table 2-1. Typical Fuel Design Parameters used for Code Input

Fuel Type	BWR 8x8	BWR 9x9	BWR 10x10	PWR 14x14	PWR 15x15	PWR 16x16	PWR 17x17
Pitch (mm, *in.*)	16.3 *0.640*	14.5 *0.572*	13.0 *0.510*	14.7 *0.580*	14.3 *0.563*	12.9 *0.506*	12.6 *0.498*
Cladding OD (mm, *in.*)	12.3 *0.483*	10.8 *0.424*	10.0 *0.395*	11.2 *0.440*	10.7 *0.423*	9.7 *0.382*	9.4 *0.370*
Cladding Thickness (mm, *in.*)	0.813 *0.032*	0.711 *0.028*	0.660 *0.026*	0.737 *0.029*	0.711 *0.028*	0.635 *0.025*	0.610 *0.024*
Gap Thickness (mm, *in.*)	0.112 *0.0044*	0.097 *0.0038*	0.089 *0.0035*	0.102 *0.0040*	0.097 *0.0038*	0.086 *0.0034*	0.084 *0.0033*
Fuel Pellet and Plenum Spring Diameter (mm, *in.*)	10.4 *0.410*	9.1 *0.360*	8.5 *0.336*	9.5 *0.374*	9.1 *0.359*	8.3 *0.325*	8.0 *0.315*
Pellet Length (mm, *in.*)	11.4 *0.45*						
Dish Diameter (mm, *in.*)	0 *0*			4.75 *0.187*	4.52 *0.178*	4.14 *0.163*	4.01 *0.158*
Dish Depth (mm, *in.*)	0 *0*			0.287 *0.0113*			
Plenum Length (mm, *in.*)	254 *10*						
Turns in the Plenum Spring	37	33	31	34	33	30	28
Plenum Spring Wire Diameter (mm, *in.*)	1.27 *0.05*						
Helium Fill Gas Pressure (MPa, *psi*)	0.69 *100*			2.41 *350*			
Active Fuel Length (m, *in.*)	3.66 *144*						

(cont'd)

Table 2-1. (cont'd) Typical Fuel Design Parameters used for Code Input

Fuel Type	BWR 8x8	BWR 9x9	BWR 10x10	PWR 14x14	PWR 15x15	PWR 16x16	PWR 17x17
System Pressure (MPa, *psi*)	7.14 *1035*			15.5 *2250*			
Coolant Inlet Temperature (°C, *°F*)	277 *530*						
Coolant Flow Rate (x10^6 kg/m^2-hr, *x10^6 lb/ft^2-hr*)	5.57 *1.14*	5.38 *1.10*	5.13 *1.05*	13.00 *2.65*	12.76 *2.61*	12.57 *2.57*	12.47 *2.55*
Enrichment (atom %)	4.0			4.5			
Pellet density (% TD)	95						
Temperature at which pellets were sintered (°C,*°F*)	1599 *2911*						
Limit on pellet density increase (% TD)	0.9						
Limit on pellet swelling (%)	5						
Fuel surface roughness (mm, *in.*)	7.6×10^{-4} *3×10^{-5}*						
Cladding surface roughness (mm, *in.*)	5.1×10^{-4} *2×10^{-5}*						
Initial crud thickness (mm, *in.*)	0 *0*						

9x9: (9-1) x 0.572 + 0.424 = 5.000

(4.963 + 5.000)/2 = 4.982

(4.982 - 0.395)/(10-1) = 0.510

The value determined for the pitch of the 10x10 fuel bundle is thus 0.510 inches. The pitch size for other fuel types was taken directly from Tables A1 and A2.

2.2. Cladding Outer Diameter

The cladding dimensions were known for all fuel types except the 10x10. Using known dimensions from bundles with other array sizes, an approximation was made for the 10x10 cladding dimensions. It was assumed that the fuel volume of the bundles would be same since each bundle should supply the same amount of power. Knowing the outer diameter of the 8x8 and 9x9 fuel rods and how many rods are in a typical bundle for each array size, it was possible to determine an approximate diameter for the 10x10 rods. Although the number of fuel rods in 8x8, 9x9, and 10x10 fuel bundles vary, the numbers we had available at the time this estimate was made were 62, 79, and 92 fuel rods, respectively, in each of the bundle types. Equations for the 10x10 cladding outer diameter are shown below. All π's cancel out and are not shown. The length of all the rods are the same and also cancel out.

8x8: $62 \times (0.483)^2 = 14.46$

9x9: $79 \times (0.424)^2 = 14.20$

$(14.46 + 14.20)/2 = 14.33$

$(14.33/92)^{1/2} = 0.395$

The outer diameter for the 10x10 fuel was assumed to be 0.395 inches. The cladding outer diameters for other fuel types were taken from known values listed in Tables A1 and A2.

2.3. Cladding Thickness, Gap Thickness, and Pellet Diameter

We noticed that the Siemens (SNP) cladding and fuel pellet dimensions were identical for their BWR 9x9 fuel and their PWR 15x15 fuel. This suggested that there was just a single population of dimensional design parameters for BWRs and PWRs rather than two different populations and that we could look for trends with the combined set of dimensional values. Therefore, we decided to look at cladding thickness and gap thickness as a function of cladding OD and we found very good correlations. These plots are shown in Figs. 2-7 and 2-8. From these plots, we selected typical cladding thickness and gap thickness values for all of the fuel types including the BWR 10x10 for which there was no available information. Fuel pellet diameter could be determined once the gap thickness was known as well as the cladding outer diameter and thickness. The gap thickness and cladding thickness were subtracted from half of the cladding outer diameter to give the fuel pellet radius. This value was doubled for the fuel pellet diameter.

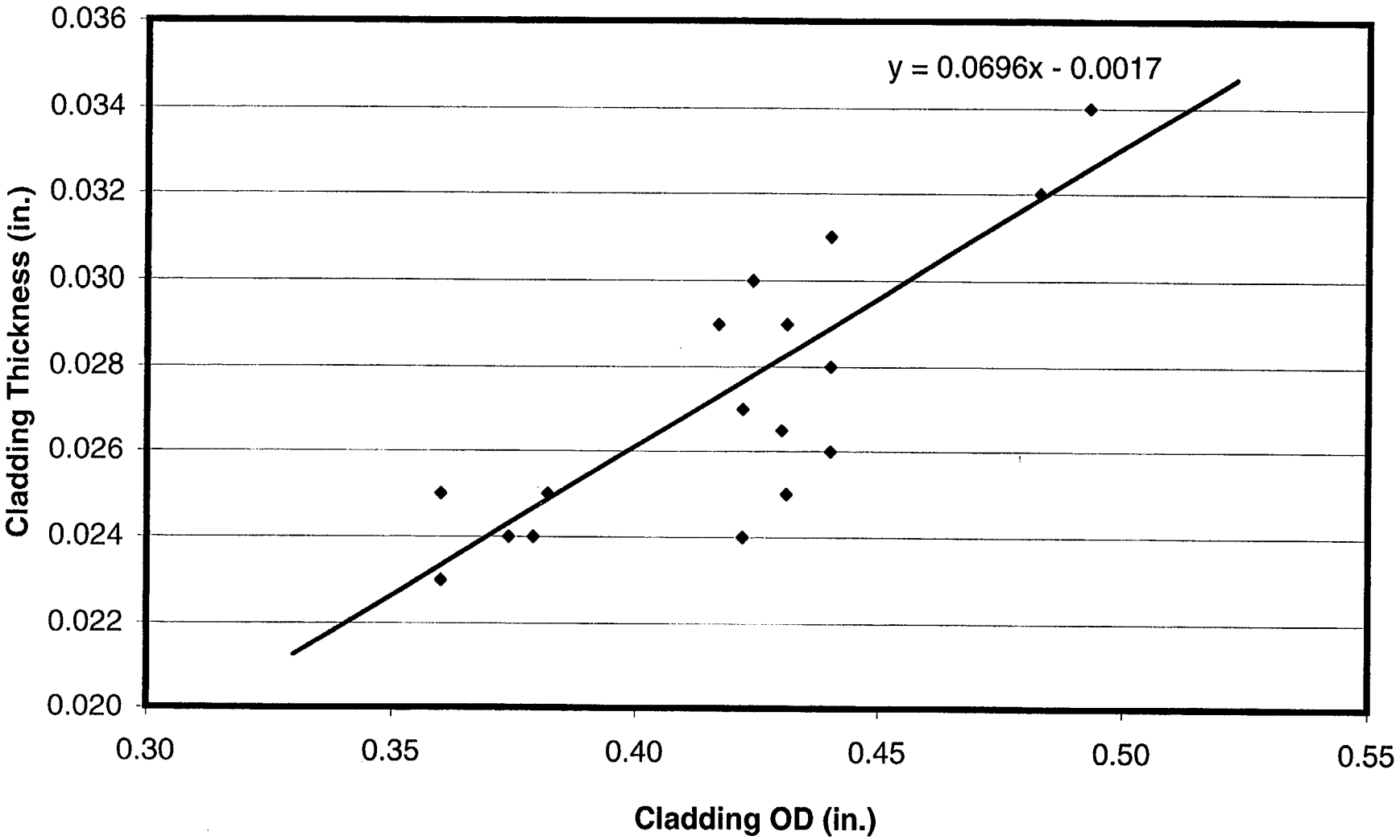

Fig. 2-7. Cladding thickness as a function of cladding outer diameter determined from non-proprietary information

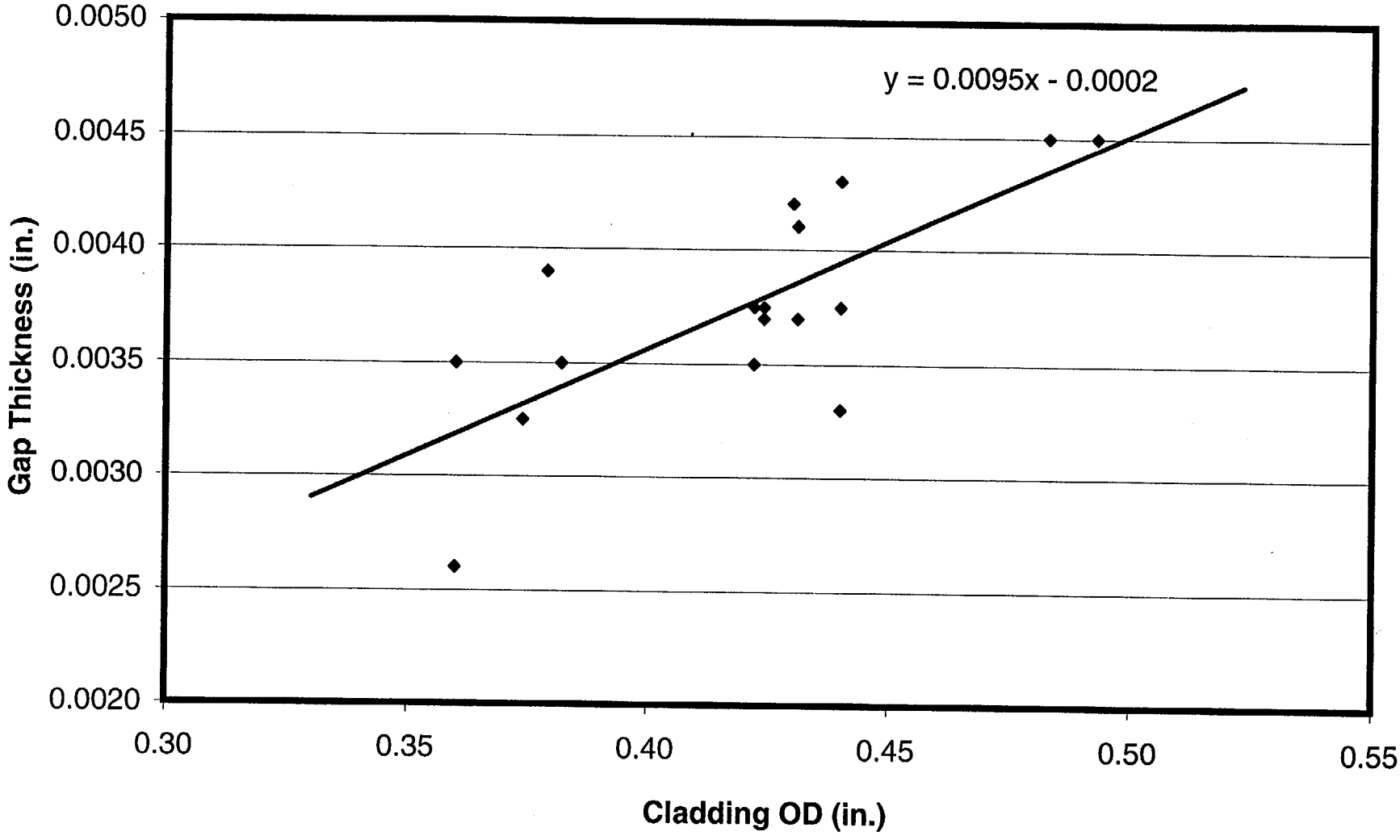

Fig. 2-8. Gap thickness as a function of cladding outer diameter determine from non-proprietary information

2.4. Dish Dimensions

Dish dimensions were only added if the fuel was known to be dished. None of the BWR cases were run with dished pellets. The dimensions of the dish were based on the size of the fuel pellet. The diameter of the dish was assumed to be 50% of the diameter of the fuel pellet. The dish depth was assumed to be 2.5% of the height of the fuel pellet. This was based on dimensions used in the assessment section of the FRAPCON-3 manual.

2.5. Plenum Length and Helium Fill Gas Pressure

Plenum length and helium fill gas pressure are used as variables by fuel designers to tailor a particular fuel load to target burnups and power levels. Mid-range values were used as code input although large variations are made in manufacturing, and these variations produce significant changes in end-of-life (EOL) fission gas release (FGR), EOL rod pressure, and plastic strain due to creep deformation (creep down). Tables 2-2 and 2-3 show typical code output changes for a PWR, and Tables 2-4 and 2-5 show typical changes in code output for a BWR. No EOL gap opening due to creep out was observed in any of the calculations.

Table 2-2. Consequence of variations in fill pressure for PWR 17x17 at 11 kW/ft with 10-in. plenum

Fill Pressure	EOL FGR	EOL Pressure	Max. Plastic Strain
250 psi	8.3%	1553 psi	-0.87%
350 psi	7.3%	1848 psi	-0.79%
450 psi	6.9%	2231 psi	-0.69%

Table 2-3. Consequence of variations in plenum length for PWR 17x17 at 11 kW/ft with 350 psi fill pressure

Plenum	EOL FGR	EOL Pressure	Max. Plastic Strain
6 in.	6.0%	2556 psi	-0.70%
10 in.	7.3%	1848 psi	-0.79%
14 in.	8.0%	1541 psi	-0.81%

Table 2-4. Consequence of variations in fill pressure for BWR 9x9 at 11 kW/ft with 10-in. plenum

Fill Pressure	EOL FGR	EOL Pressure	Max. Plastic Strain
50 psi	8.4%	879 psi	-0.44%
100 psi	7.2%	945 psi	-0.39%
150 psi	6.3%	1041 psi	-0.33%

Table 2-5. Consequence of variations in plenum length for BWR 9x9 at 11 kW/ft with 100 psi fill pressure

Plenum	EOL FGR	EOL Pressure	Max. Plastic Strain
6 in.	5.4%	1279 psi	-0.35%
10 in.	7.2%	945 psi	-0.39%
14 in.	8.7%	801 psi	-0.40%

Trends of EOL pressure and maximum plastic strain are as expected. The higher the fill pressure or the shorter the plenum, the higher will be the EOL rod pressure. Notice that the nominal fill pressure in combination with the shortest plenum resulted in EOL fuel rod pressures that are larger than the reactor system pressure. Plastic strain shows the same kind of trend. The cases that result in higher pressures experience less plastic strain (smaller pressure differential), which is negative in all cases (creep down).

The trends in fission gas release are not so easy to explain, however. In the Massih gas release model, the saturation concentration, which must be attained at a grain boundary prior to release, depends on the rod internal gas pressure (this is called P_{ext} in equation A.7, page A.5, of Ref. 4). The higher the gas pressure, the higher the saturation concentration, and vice versa. Thus, the larger plenum volume provides the lower gas pressure, which provides the lower saturation concentration, which permits earlier and larger FGR. What is observed is thus a natural consequence of the Massih model and is believed to be real.

2.6. Plenum Spring Dimensions

The plenum spring dimensions used for input are based on dimensions used in the assessment section of the FRAPCON-3 manual. Three cases were listed in the manual for fuel rods that are about 12 feet long. The spring volumes in these cases were compared to the volumes of the plenum. The percentages of plenum volume taken by these springs were 9.95%, 4.72%, and 3.40%. The volume percentage used in this report is 6% (the average of the three). The diameter of the spring is equal to the fuel pellet diameter for this report. A constant wire diameter was used for all fuel types. The number of turns in the spring was used to adjust the volume of the spring.

2.7. Coolant Flow Rates

The coolant flow rates used as input were based on flow rates used in the assessment section of the FRAPCON-3 manual. The coolant flow rate was adjusted to give a reasonable temperature rise through the core at all power levels examined. The temperature rise for each case changes since the flow rate is constant for all power levels.

2.8. Other Parameters

Nominal values were used for other parameters in Table 2-1 and were kept constant for each reactor type (BWR and PWR) to avoid additional variability in the output.

3. FRAPCON-3

FRAPCON-3 analyzes the thermal and mechanical performance of fuel rods during steady-state operation. Changes in power are possible but must occur slowly enough to be considered steady-state. FRAPCON-3 can calculate many properties such as temperatures, strain, swelling, densification, and fission gas release.

FRAPCON-3 has some limitations. Some of the major limitations that apply to this study are

1. The code has not been assessed to predict cladding strains resulting from pellet-cladding interaction.
2. Very limited assessment has been performed for fuel rods containing gadolinia.
3. It is not possible to model axially changing gadolinia concentrations which are common in modern fuel.
4. FRAPCON-3 only models standard Zircaloy cladding and not low-tin cladding.

3.1. MATPRO

FRAPCON-3 uses the MATPRO materials package to enable it to calculate materials properties to high burnup (65 GWd/t). MATPRO calculates properties such as the thermal conductivity and thermal expansion of the various materials in the fuel rod at high burnup.

3.2. Fission Gas Release

The fission gas release models available in FRAPCON-3 are the ANS-5.4 model and the Massih model. The model to be used is determined from the input. For all cases in this study, the Massih model was used. The Massih model is new to the FRAPCON series and was chosen because it is the best model for grain-boundary gas release. The Massih model is used unless the low temperature fission gas release model predicts more of a release.

3.3. Oxide Thickness

The cladding oxidation model used in FRAPCON-3 is not the model used in MATPRO. MATPRO predictions for oxide thickness were found to be different from measured oxide thicknesses by a factor of four or five. The model used in FRAPCON-3 to predict oxide thickness is based on the EPRI-developed ESCORE model. This ESCORE model has been assessed against in-reactor data with reasonably accurate results.

The oxide thickness is strongly dependent on the temperature of the metal-oxide interface. This temperature in turn is strongly affected by changing the mass flux of the coolant which is defined in the input. Therefore for an accurate oxide thickness calculation it is important to define a reasonable coolant mass flux. Oxide thickness is also greatly affected by the initial crud thickness.

4. AXIAL POWER PROFILE AND POWER HISTORIES

4.1. Axial Power Profile

The axial power shape changes during the lifetime of the fuel. In PWRs the power shape typically peaks at a lower axial position at beginning of life (BOL) and gradually changes to peak at higher axial positions at end of life (EOL). The result of this change is an average axial profile that is flat in the middle. In BWRs the peak is located in a lower axial position due to increased voiding at the top. Pellets enriched with gadolinia are used to flatten the axial profile for BWRs. Modeling the changing axial power profile on FRAPCON-3 is possible; however, for this report, a constant axial power profile was assumed. The constant profile was necessary to obtain understandable plots of the peak power node parameters. For example, plotting the centerline temperature of the peak power node with a constant axial power profile may show that the temperature rose during a burnup interval. If a changing axial profile were used, the peak power node may change from one step to the next. The temperature of the new peak node may not be as high as the temperature from the previous peak node and the plot of the centerline temperature would show that the temperature decreased. Plotting the peak power node would not show the true trend of the parameters if a changing axial power profile were used. The axial power profile used was derived from a burnup profile taken at EOL and is shown in Fig. 4-1. The same axial power profile was used for both PWRs and BWRs.

4.2. Power Histories

Each fuel design, except the 14x14, was given four power histories for analysis. The 14x14 was given five power histories so that one power (9 kW/ft) would be common in the calculations for all the fuel designs. The power histories used are simple and within reason. All power histories begin at their peak power, which is held constant for awhile, and end at 65 GWd/t with a power of 5 kW/ft. Figures 4-2 through 4-8 show the power histories used for each fuel type. From the highest power to lowest power, the ramp down to 5 kW/ft begins at 20, 30, 40, and 50 GWd/t, respectively. The power histories used were designed to provide a full range of realistic cases. The figures also show the time it took each case to burn up to 65 GWd/t.

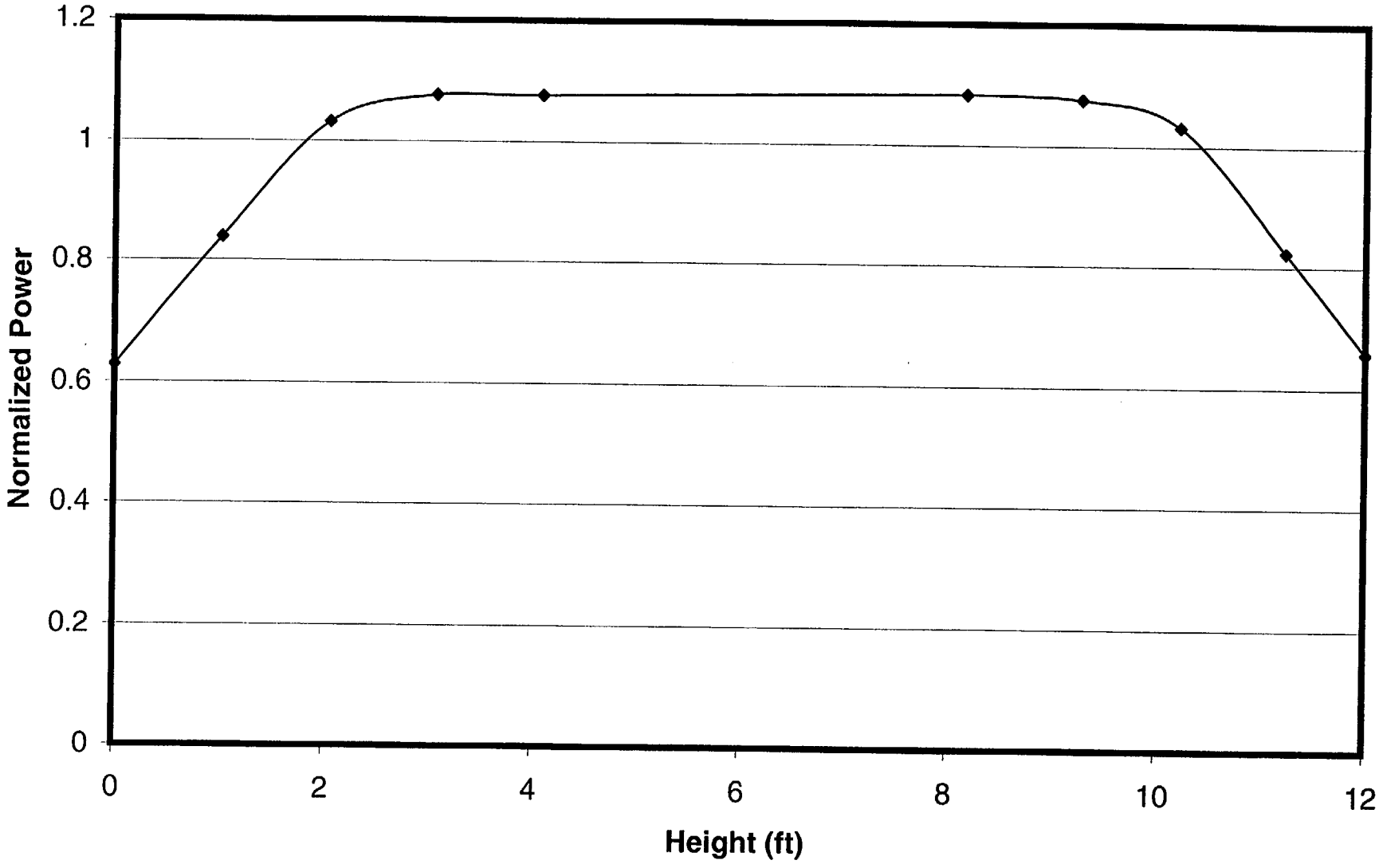

Fig. 4-1. Axial power profile used for code input

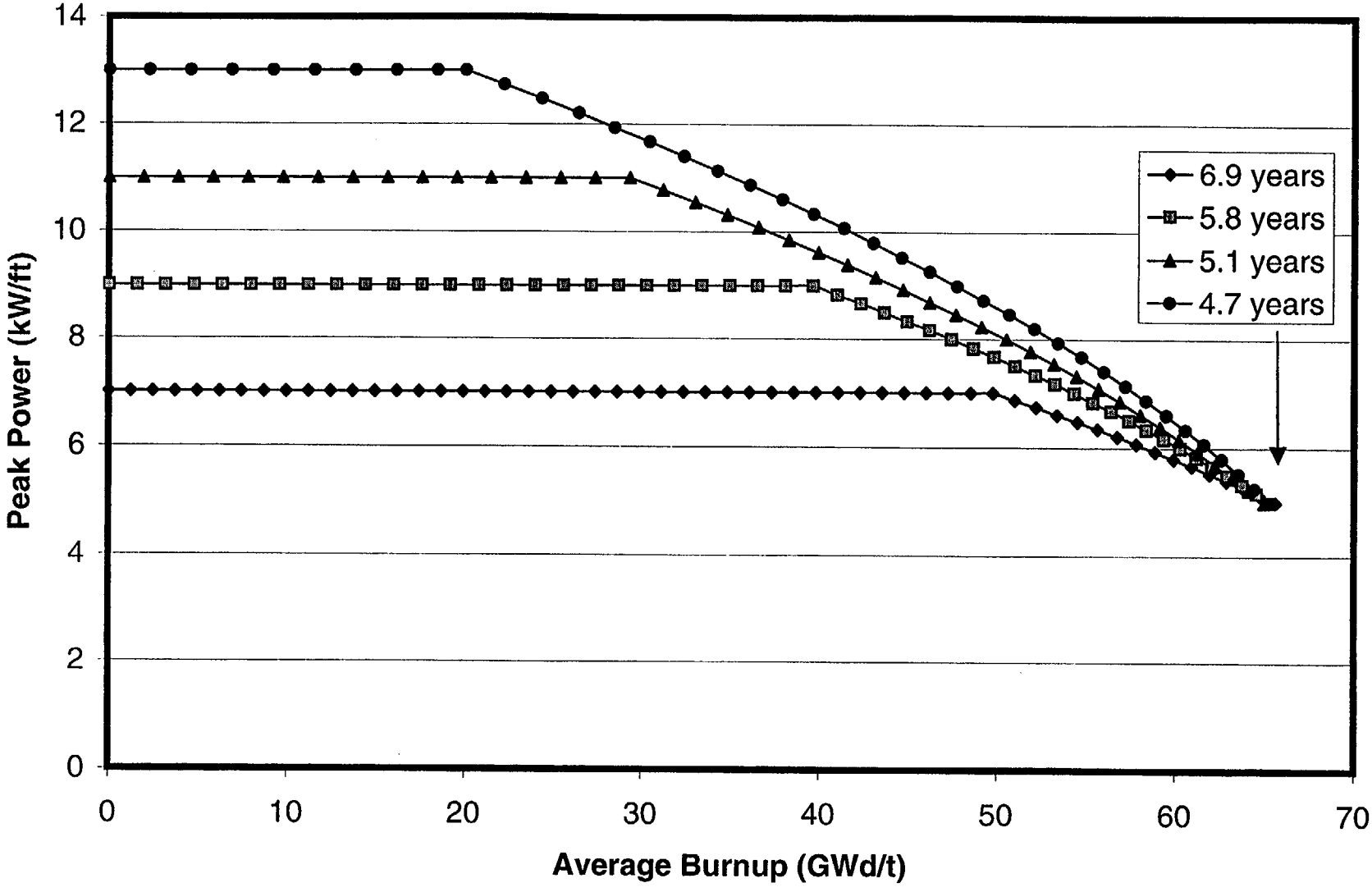

Fig. 4-2. Power histories used for BWR 8x8 fuel design

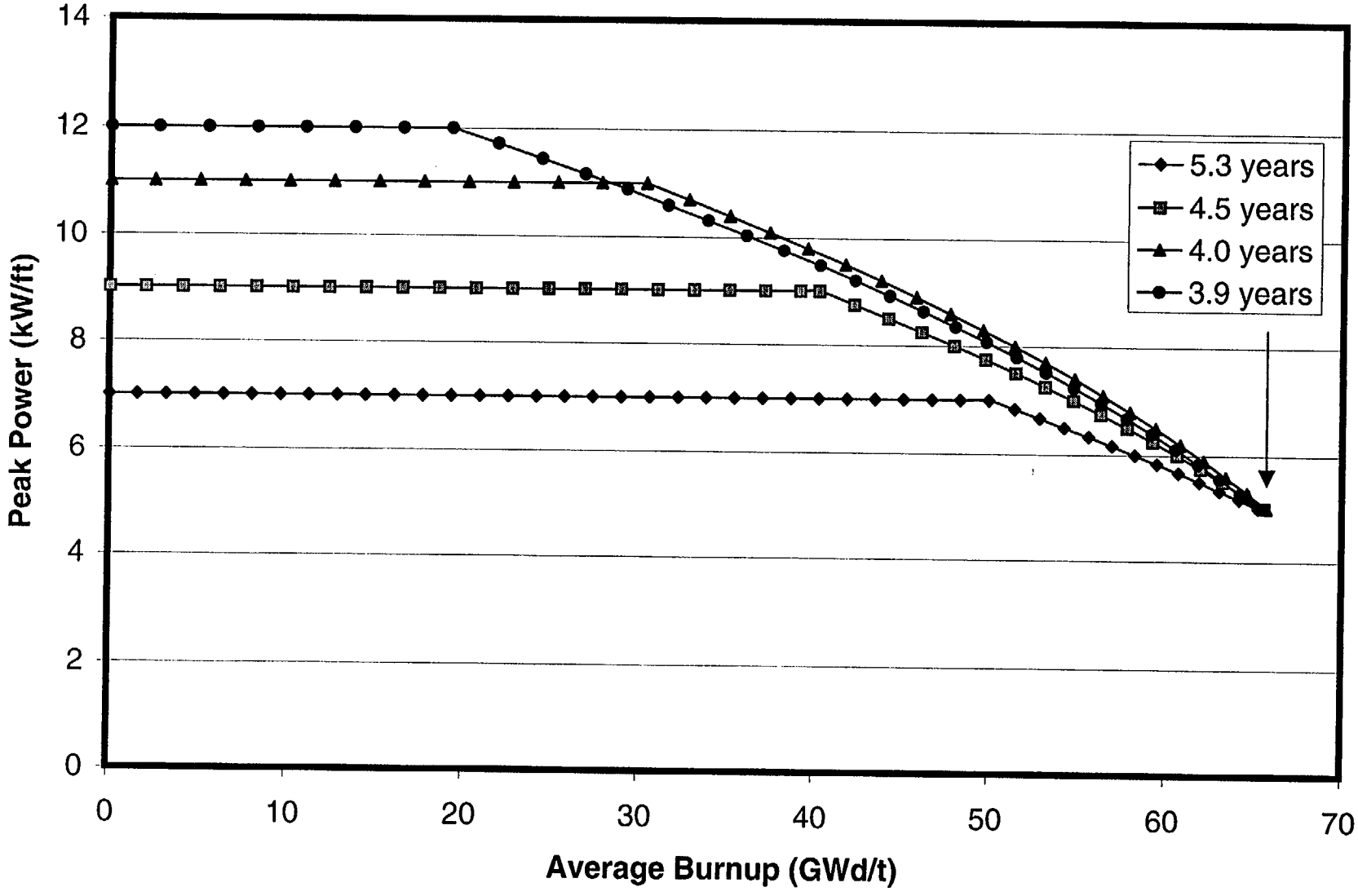

Fig. 4-3. Power histories used for BWR 9x9 fuel design

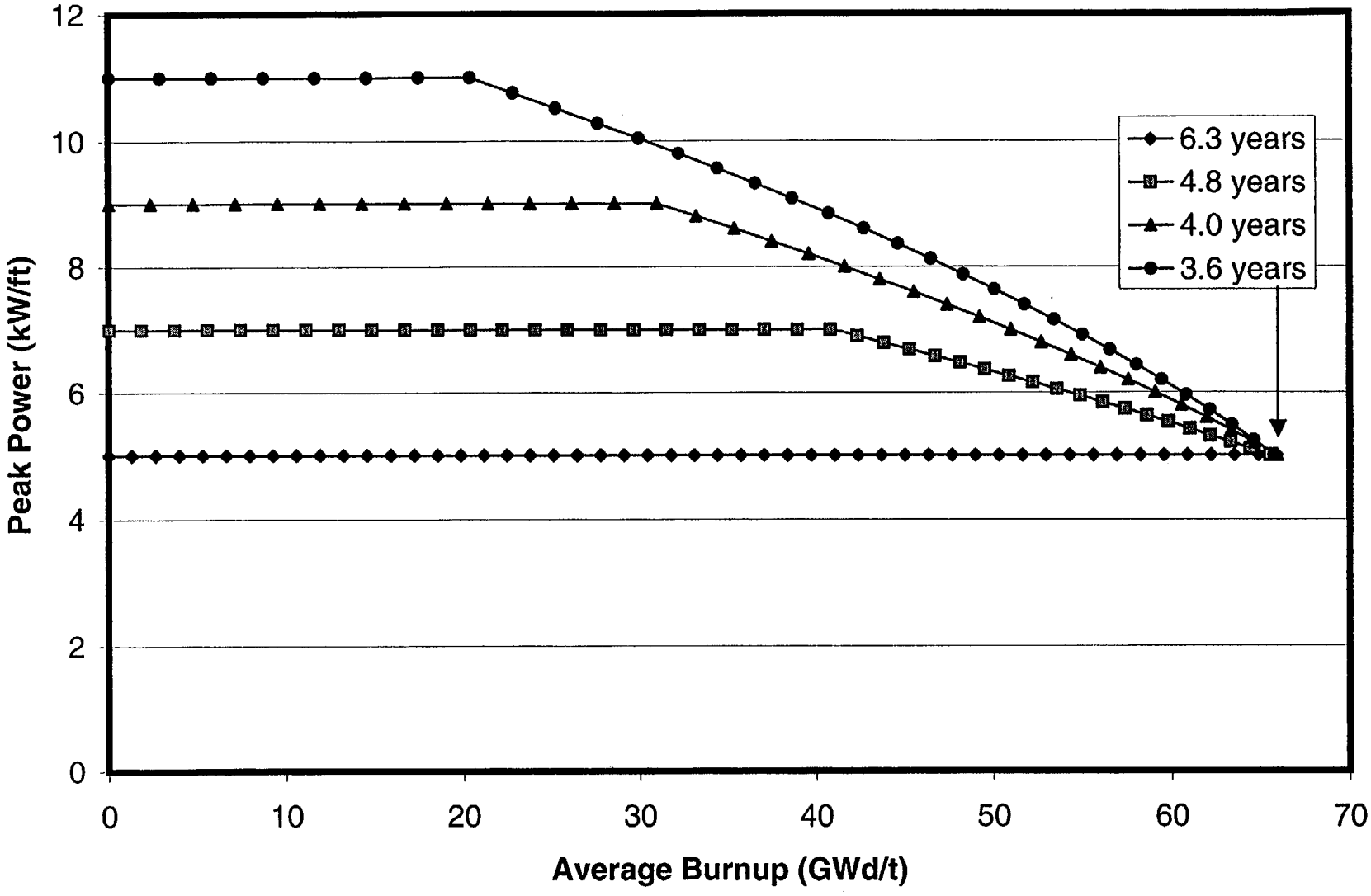

Fig. 4-4. Power histories used for BWR 10x10 fuel design

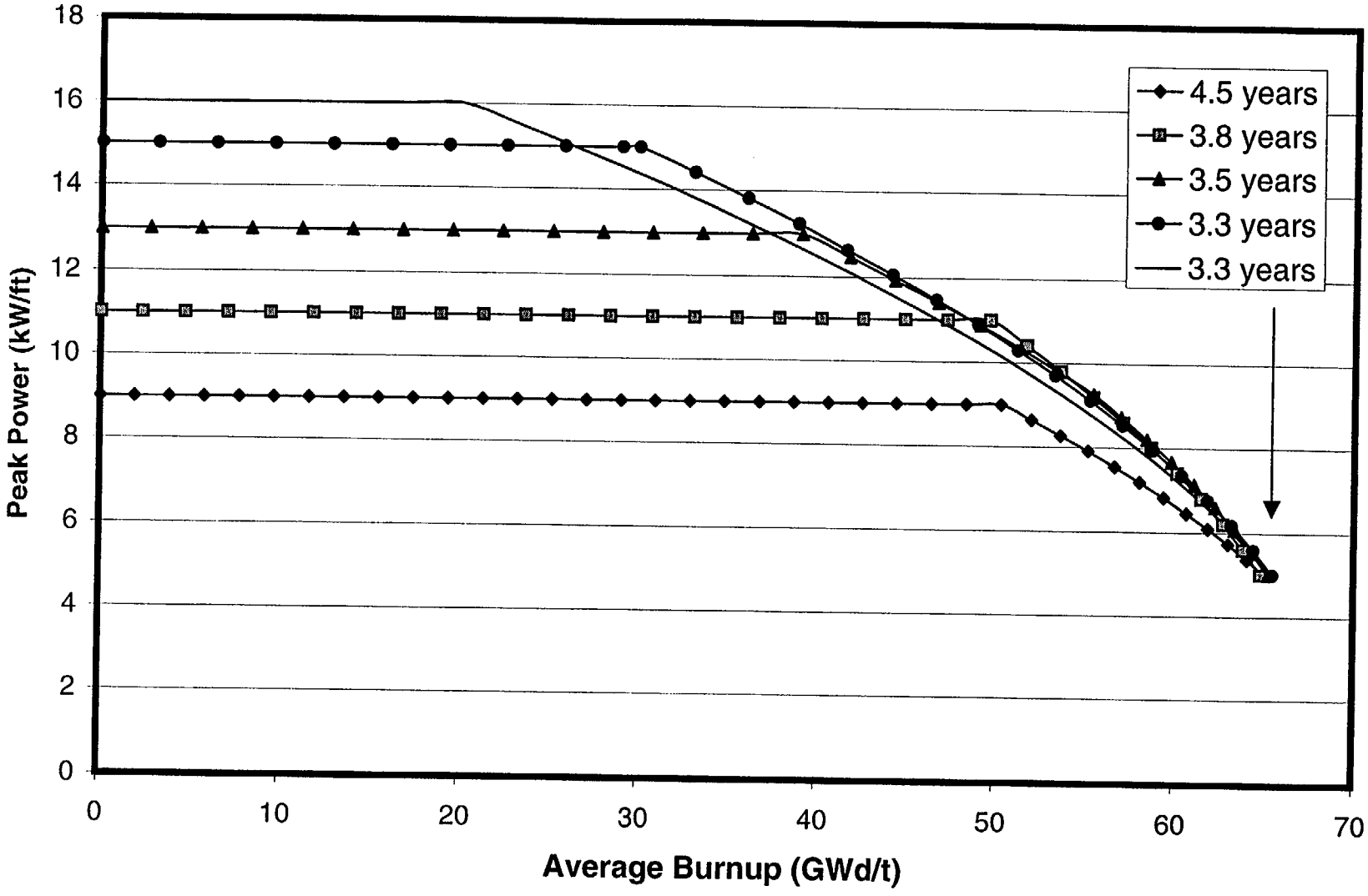

Fig. 4-5. Power histories used for PWR 14x14 fuel design

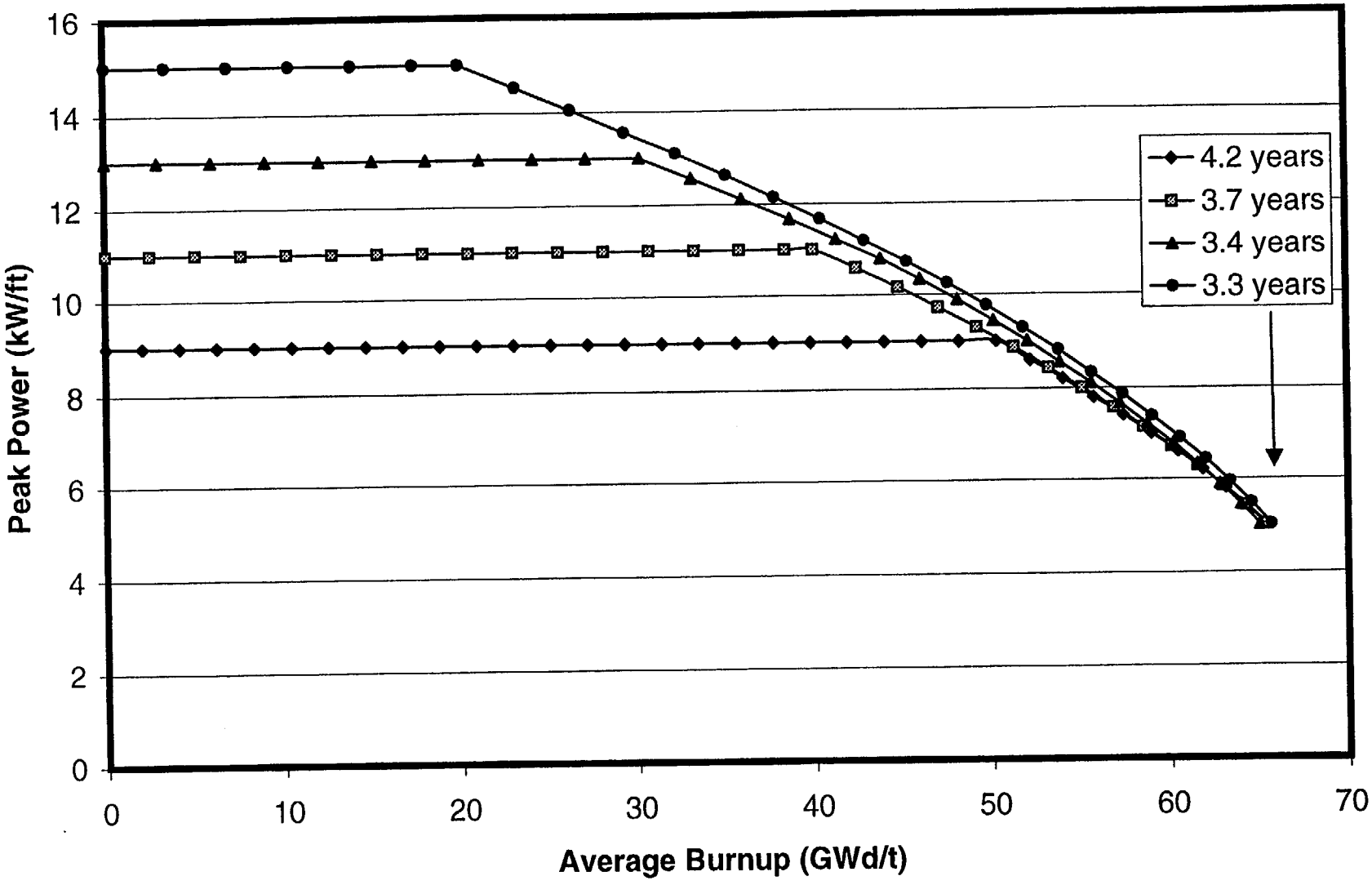

Fig. 4-6. Power histories used for PWR 15x15 fuel design

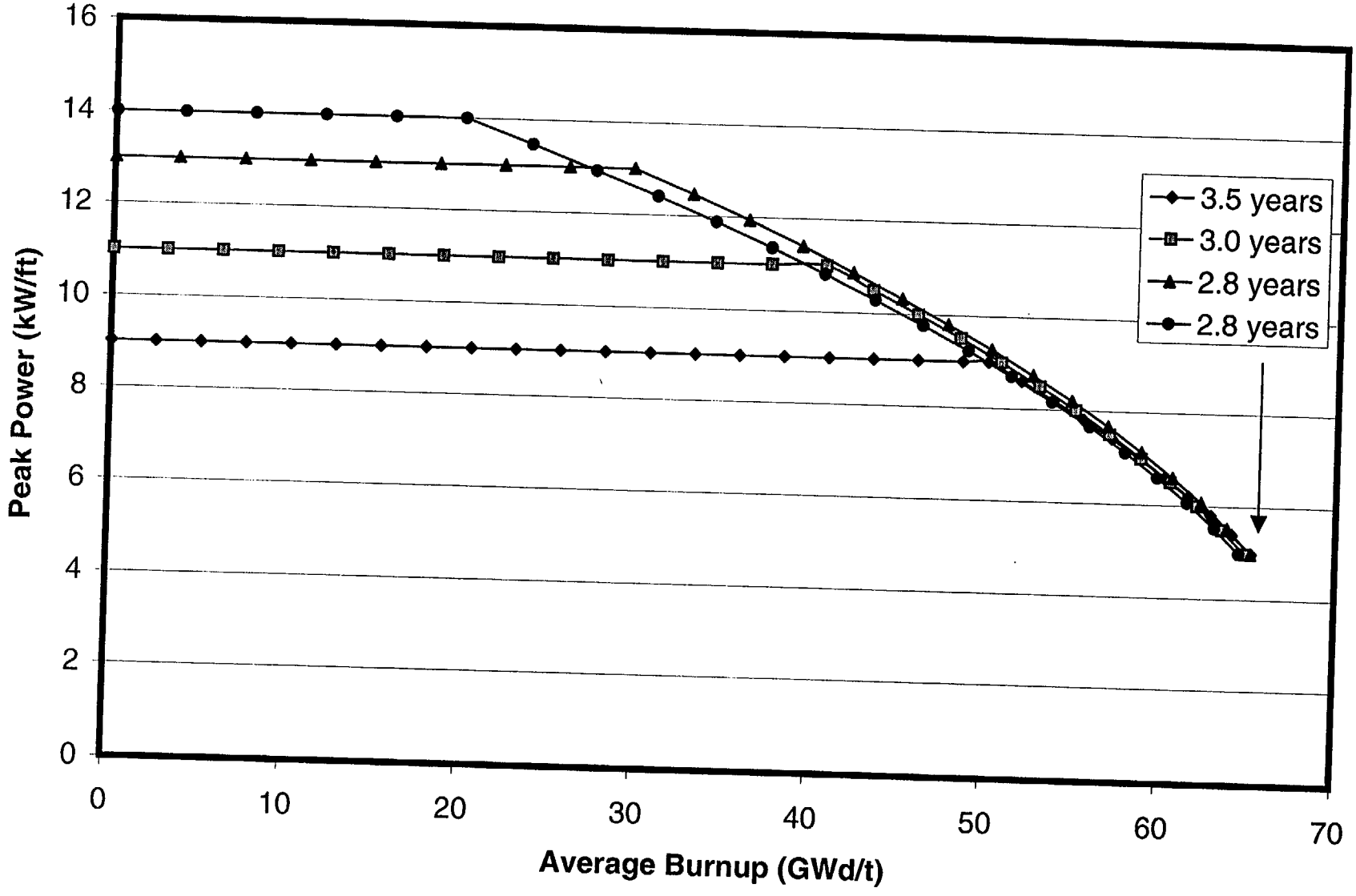

Fig. 4-7. Power histories used for PWR 16x16 fuel design

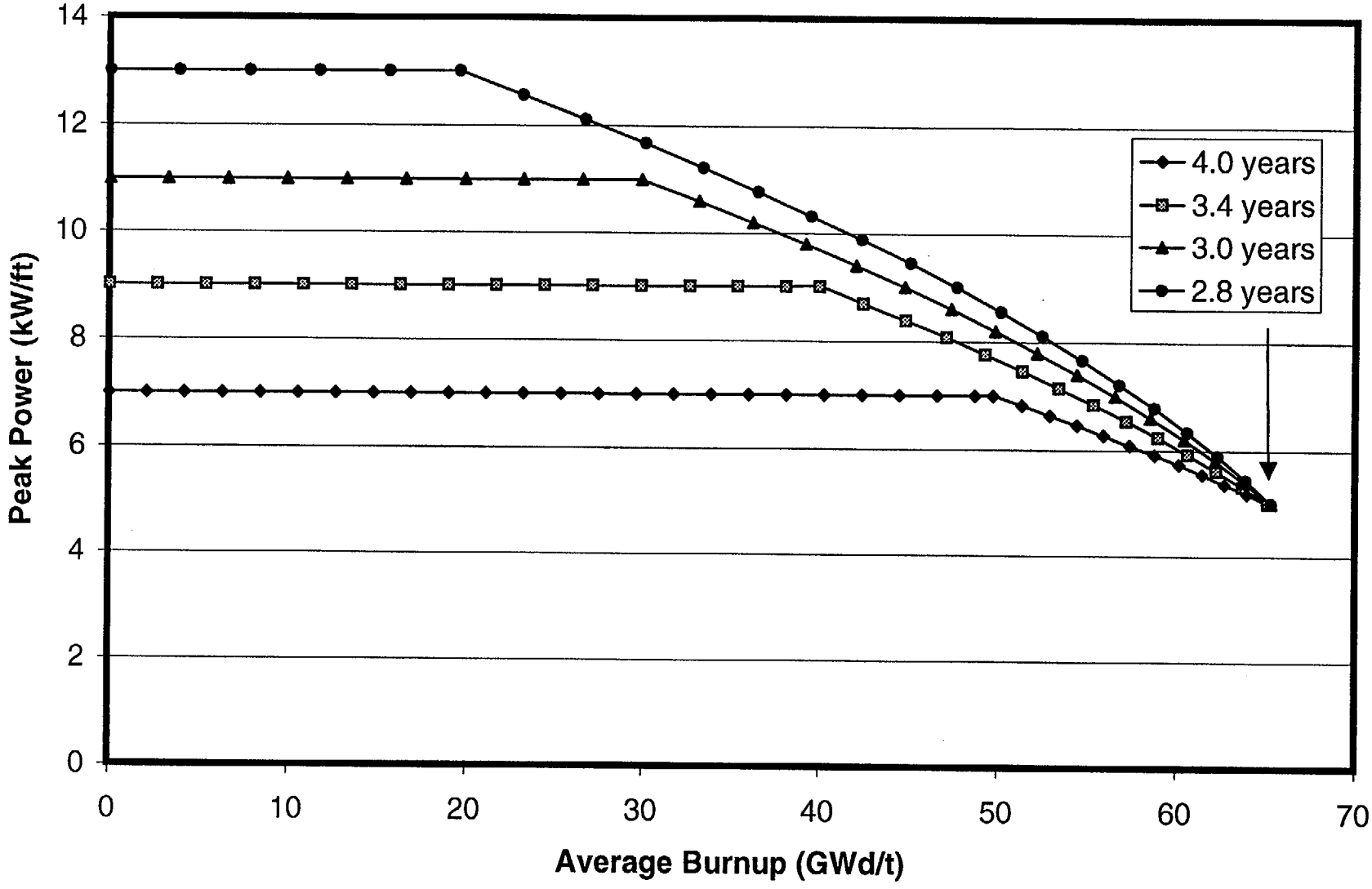

Fig. 4-8. Power histories used for PWR 17x17 fuel design

5. Calculations for BWR 8x8 Fuel

In the following figures, calculated values for BWR 8x8 fuel are plotted as a function of burnup for the parameters listed below:

Fuel centerline temperature
Average fuel temperature
Stored energy
Fuel O.D. temperature
Cladding I.D. temperature
Cladding O.D. temperature
Gap thickness
Gap conductance
Fission gas release
Rod internal gas pressure
Oxide thickness
Cladding hoop stress
Cladding hoop strain

Several general observations can be made about the calculated results:

- Within the first few GWd/t of burnup, a temperature peak is observed that is the result of fuel densification.

- Gap closure results in (a) the coming together of temperatures for fuel O.D. and cladding I.D. and (b) a sharp increase in gap conductance. The gap conductance increases again after a few time steps when the interaction between the pellet and cladding affects the contact conductance calculated for a closed gap. At this point there is also a large increase in stress, and the permanent strain changes directions.

- Some of the fission gas is released in spurts according to the Massih model in FRAPCON-3. This effect is apparent in many of the figures. Shorter time steps would produce slightly different looking curves, but the trend of gas release and the end-of-life gas release would be about the same.

- The burnup enhancement of fission gas release is readily seen in the lower power cases, but it is obscured in the highest power cases by the magnitude of prior gas release.

- Rod internal gas pressure increases with the accumulation of released fission gas. In the higher power PWR cases, as the power drops off near the end of life, the reduction in the plenum temperature offsets the increasing moles of fission gas.

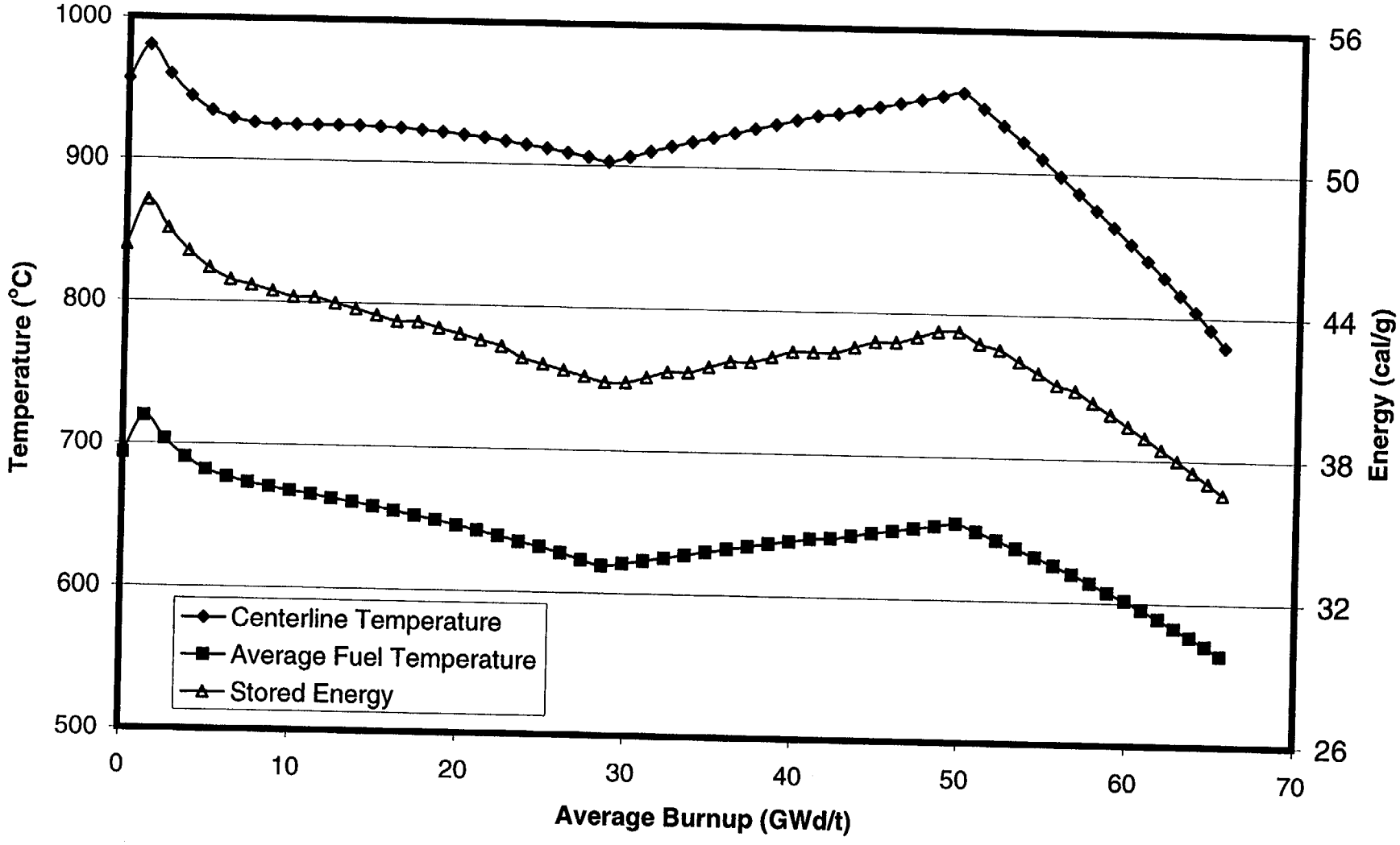

Fig. 5-1. Fuel temperatures and stored energy for a BWR 8x8 fuel rod with initial peak power of 7 kW/ft.

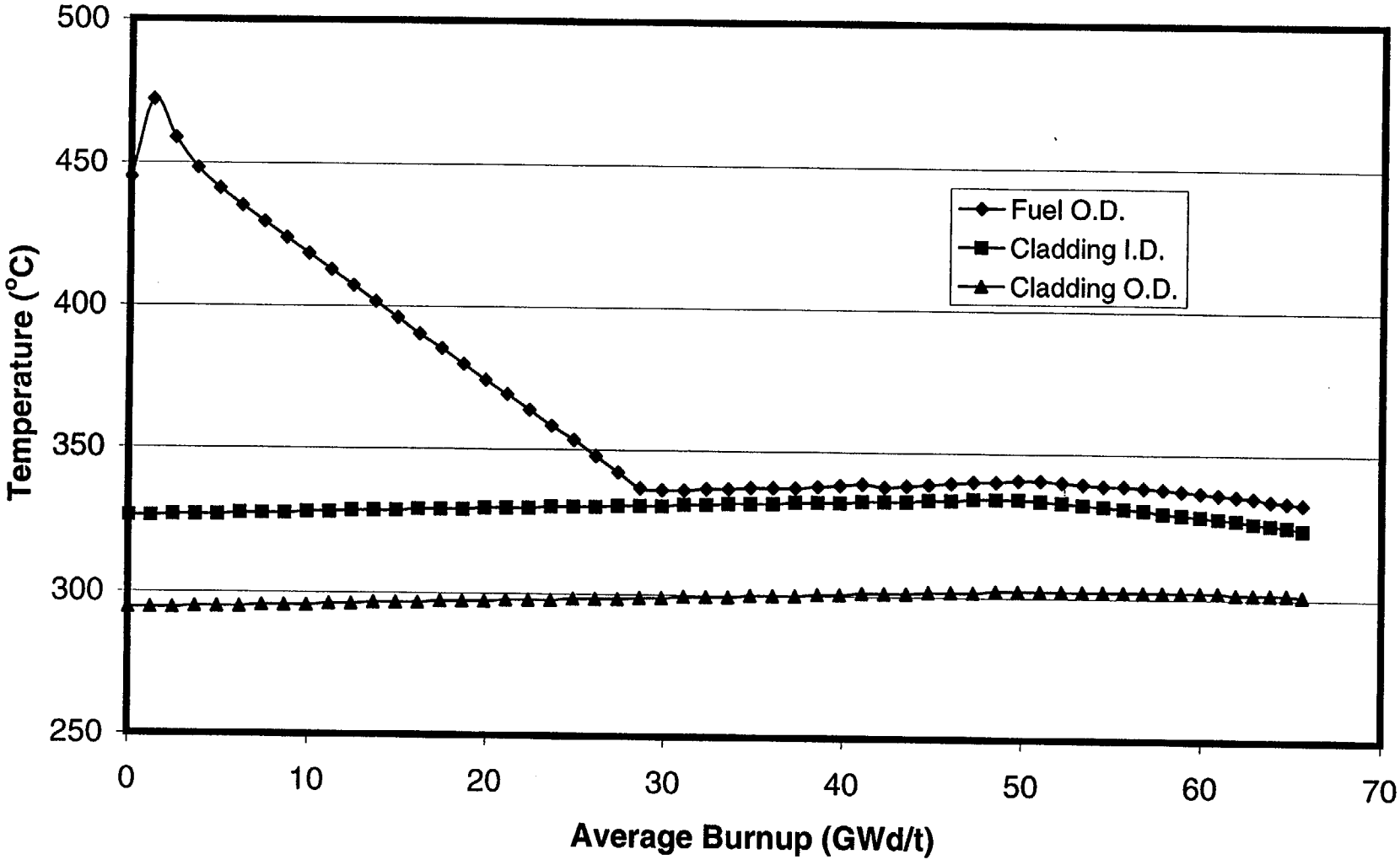

Fig. 5-2. Cladding temperatures and fuel surface temperature for a BWR 8x8 fuel rod with initial peak power of 7 kW/ft.

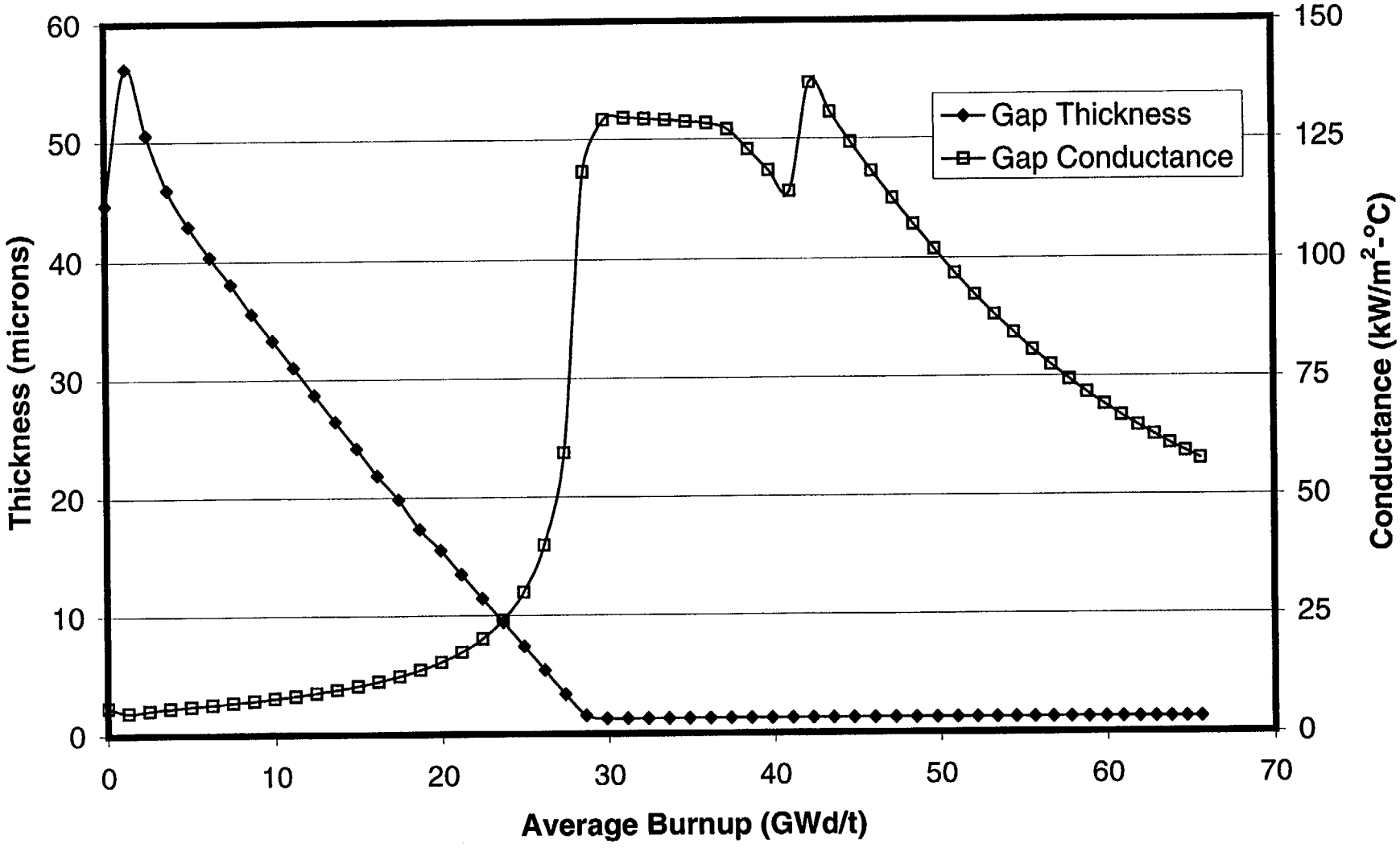

Fig. 5-3. Gap thickness and gap conductance for a BWR 8x8 fuel rod with initial peak power of 7 kW/ft.

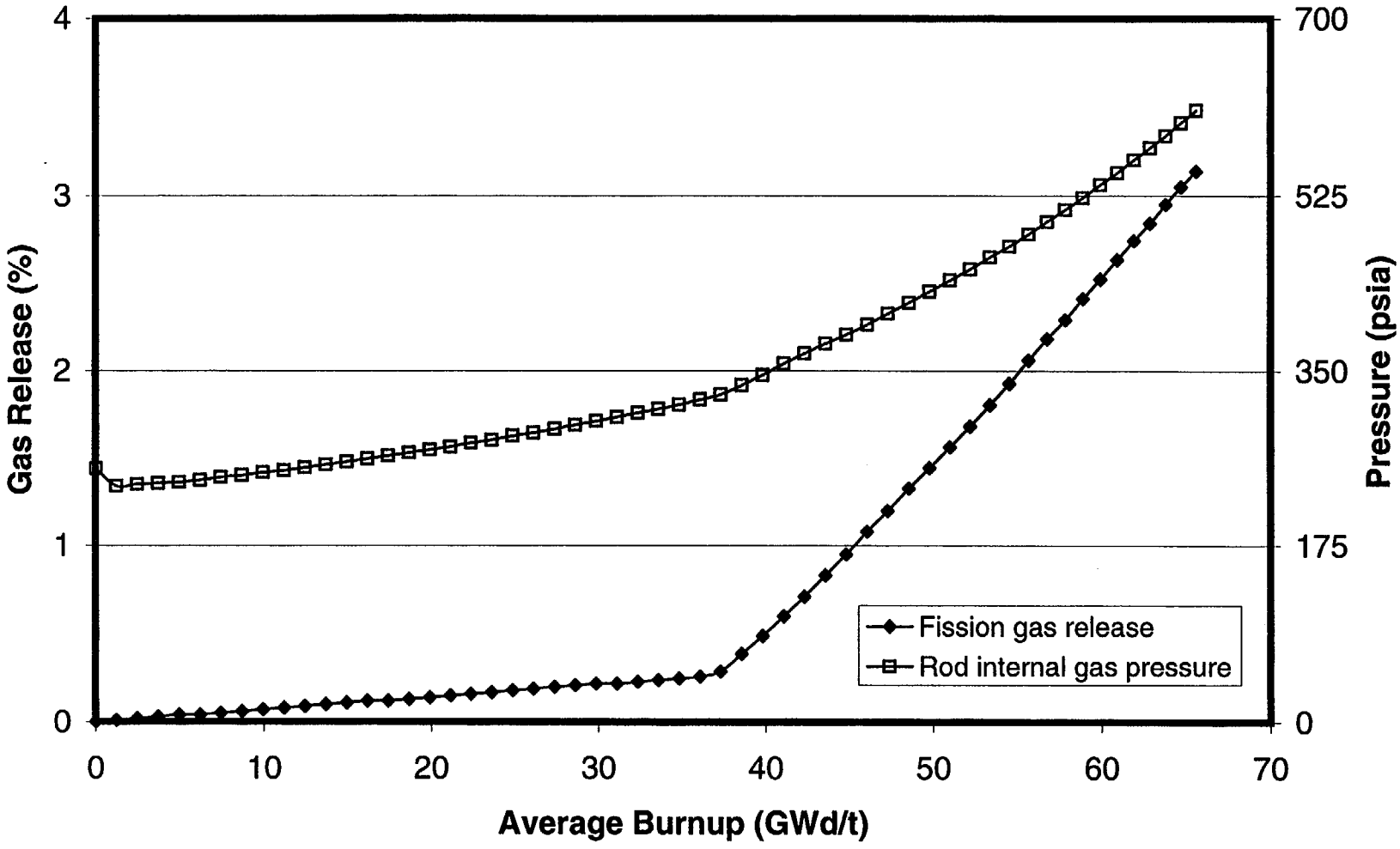

Fig. 5-4. Fission gas release and rod internal gas pressure for a BWR 8x8 fuel rod with initial peak power of 7 kW/ft.

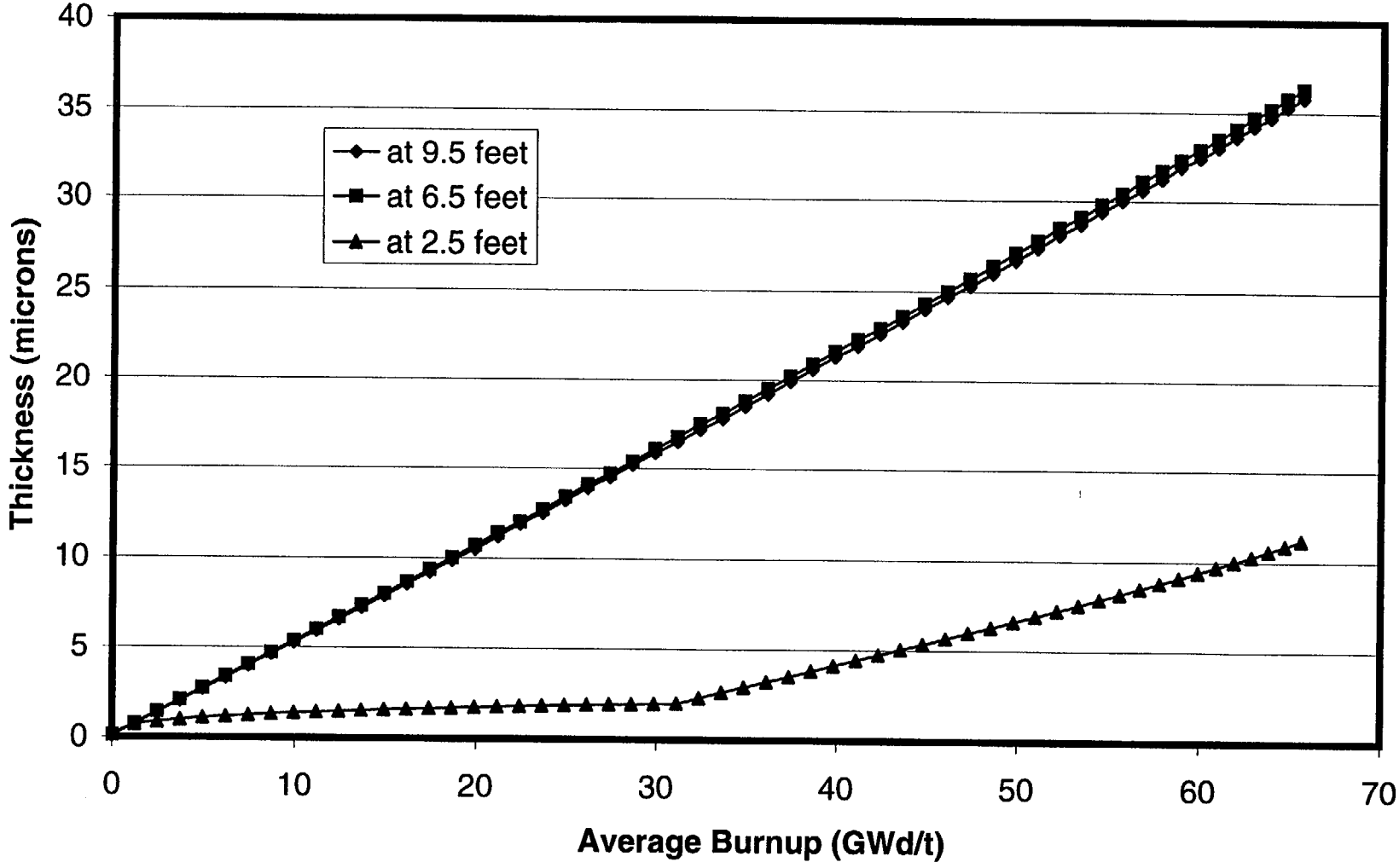

Fig. 5-5. Oxide thickness at three axial locations for a BWR 8x8 fuel rod with initial peak power of 7 kW/ft.

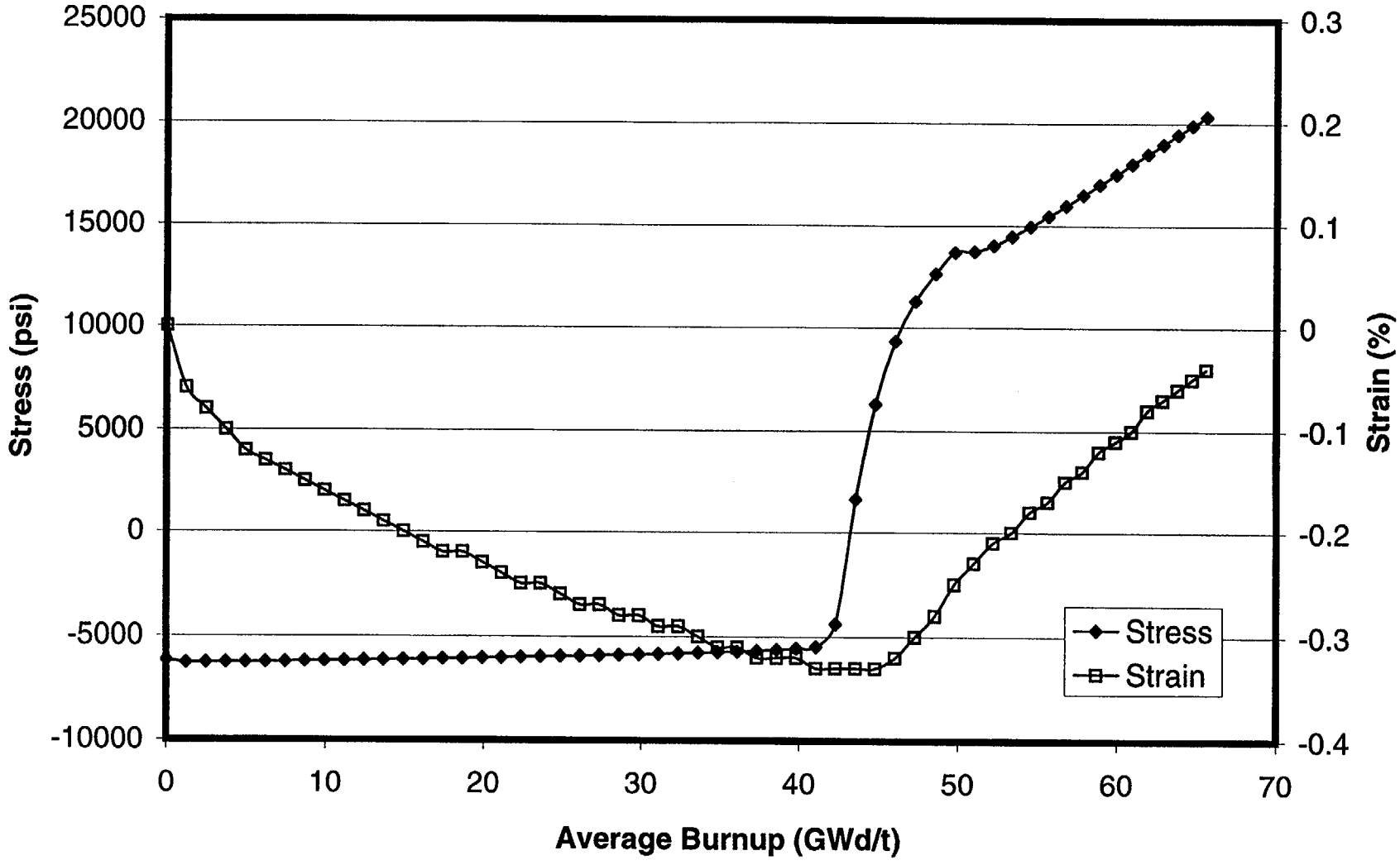

Fig. 5-6. Cladding hoop stress and hoop strain for a BWR 8x8 fuel rod with initial peak power of 7 kW/ft.

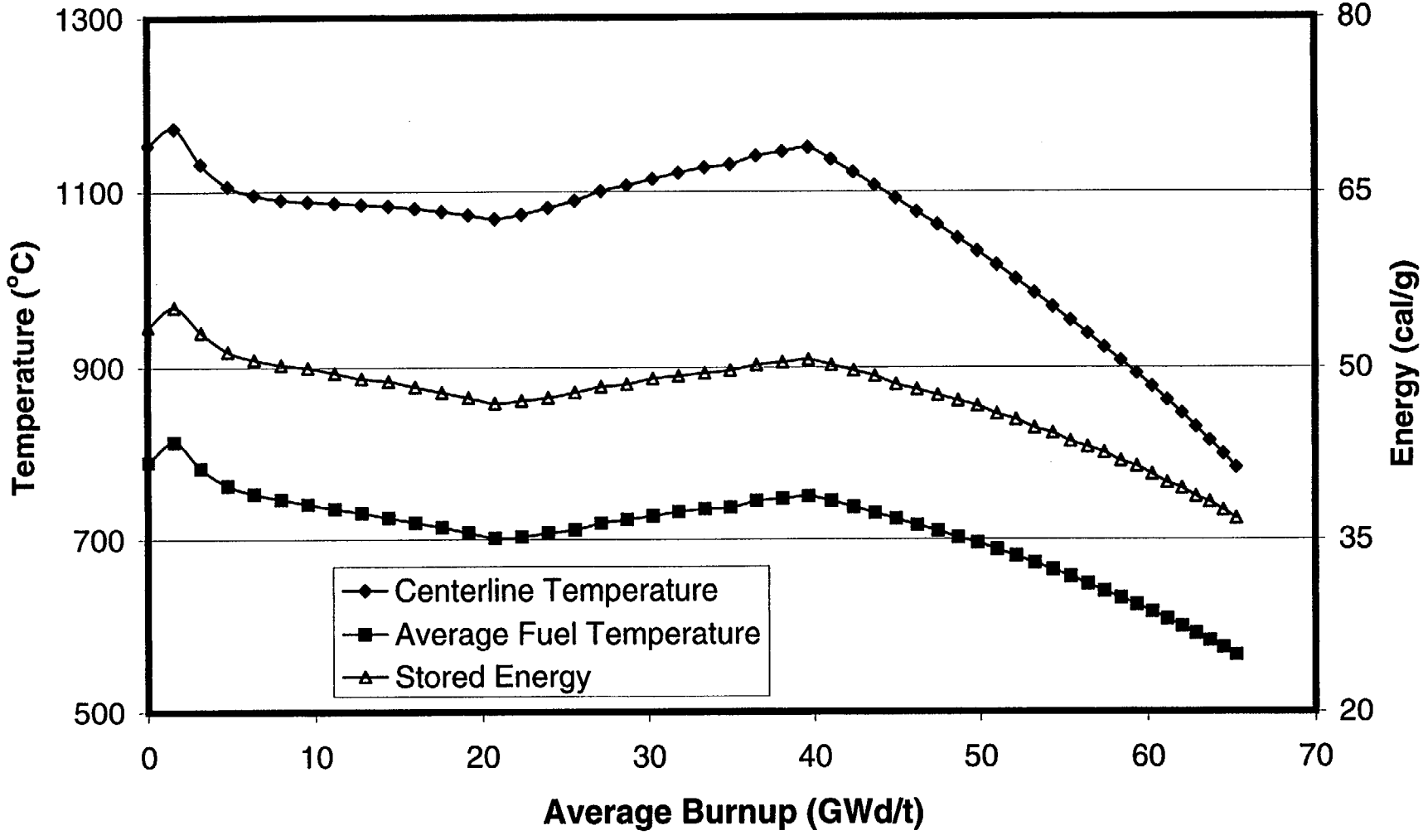

Fig. 5-7. Fuel temperatures and stored energy for a BWR 8x8 fuel rod with initial peak power of 9 kW/ft.

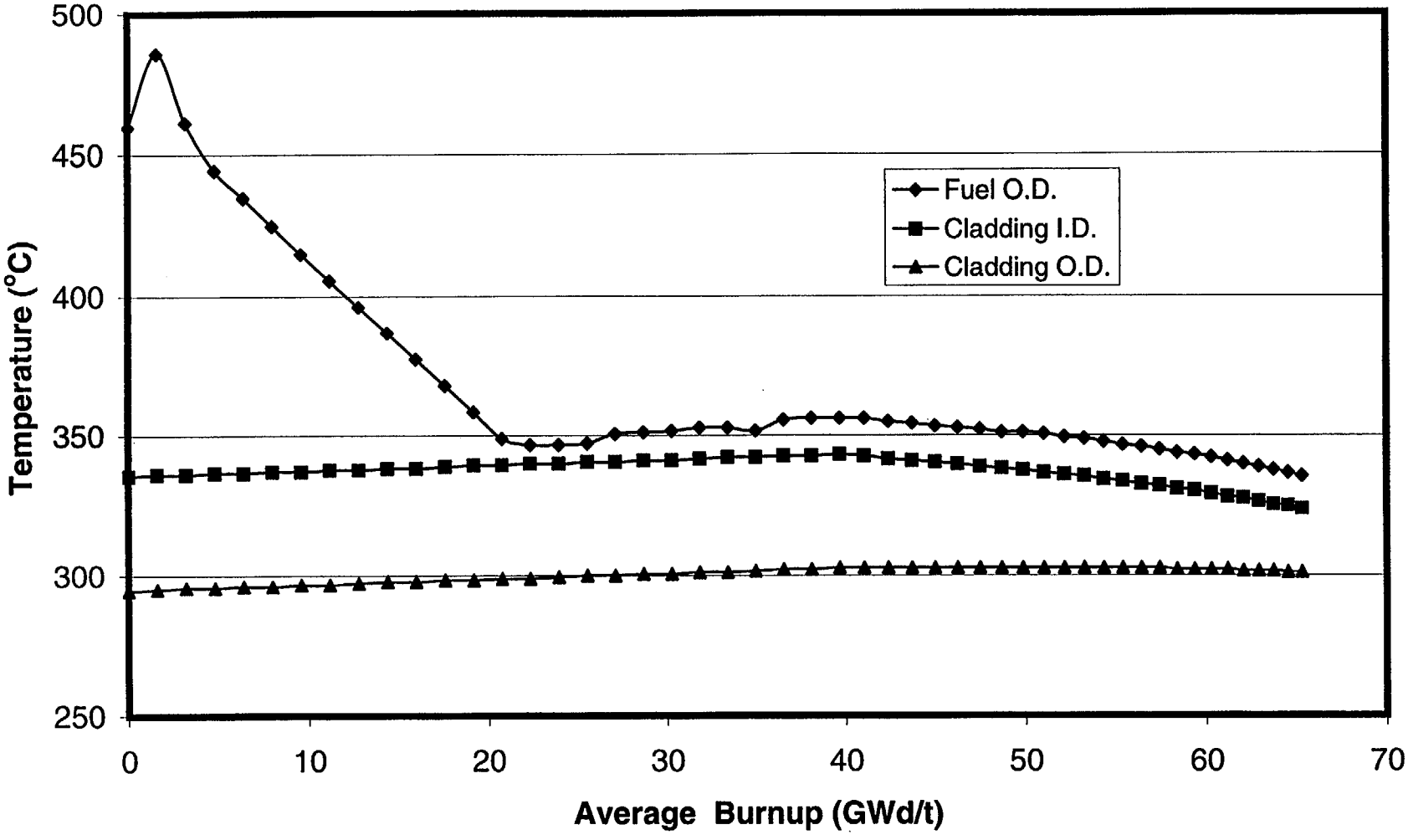

Fig. 5-8. Cladding temperatures and fuel surface temperature for a BWR 8x8 fuel rod with initial peak power of 9 kW/ft.

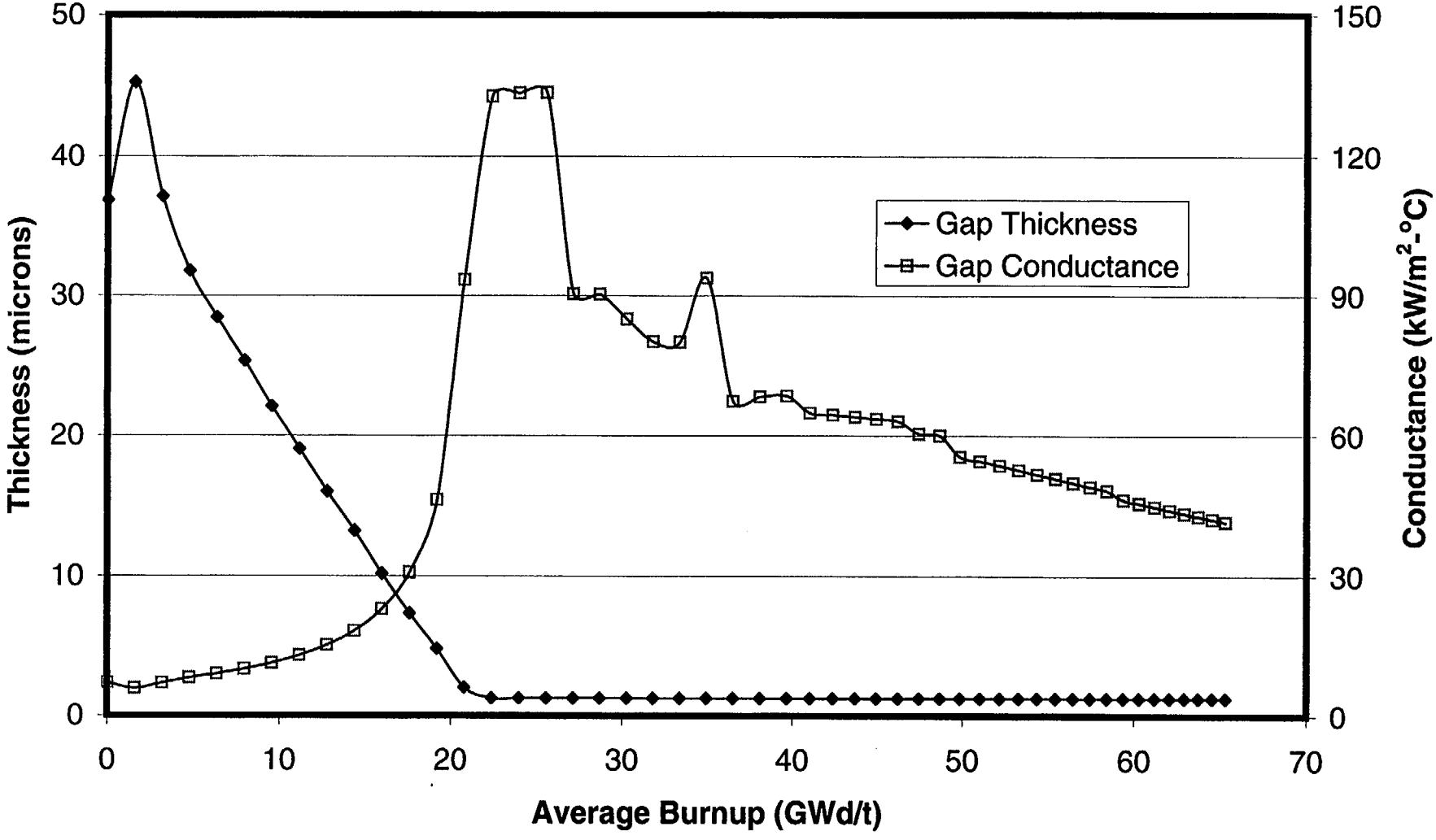

Fig. 5-9. Gap thickness and gap conductance for a BWR 8x8 fuel rod with initial peak power of 9 kW/ft.

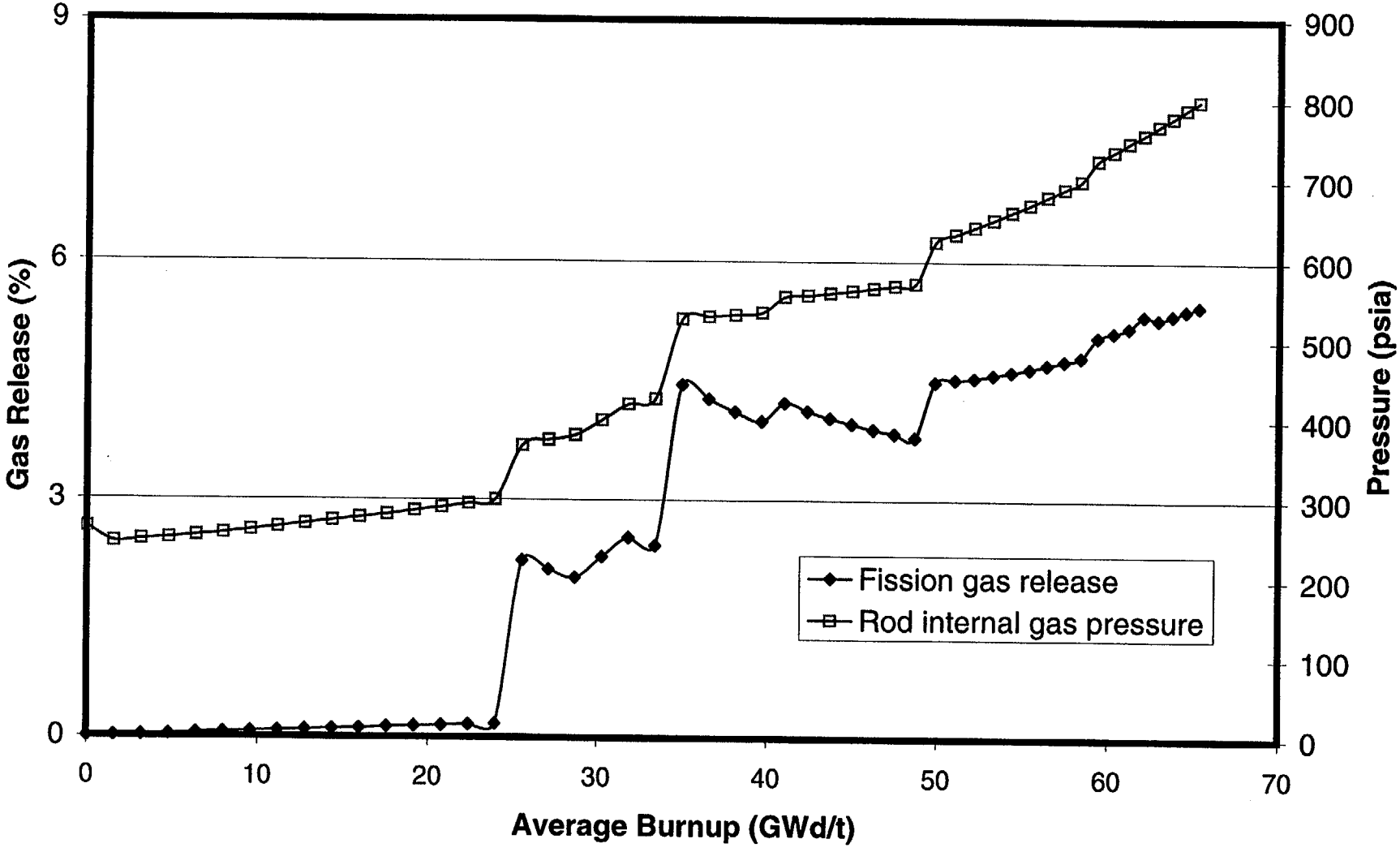

Fig. 5-10. Fission gas release and rod internal gas pressure for a BWR 8x8 fuel rod with initial peak power of 9 kW/ft.

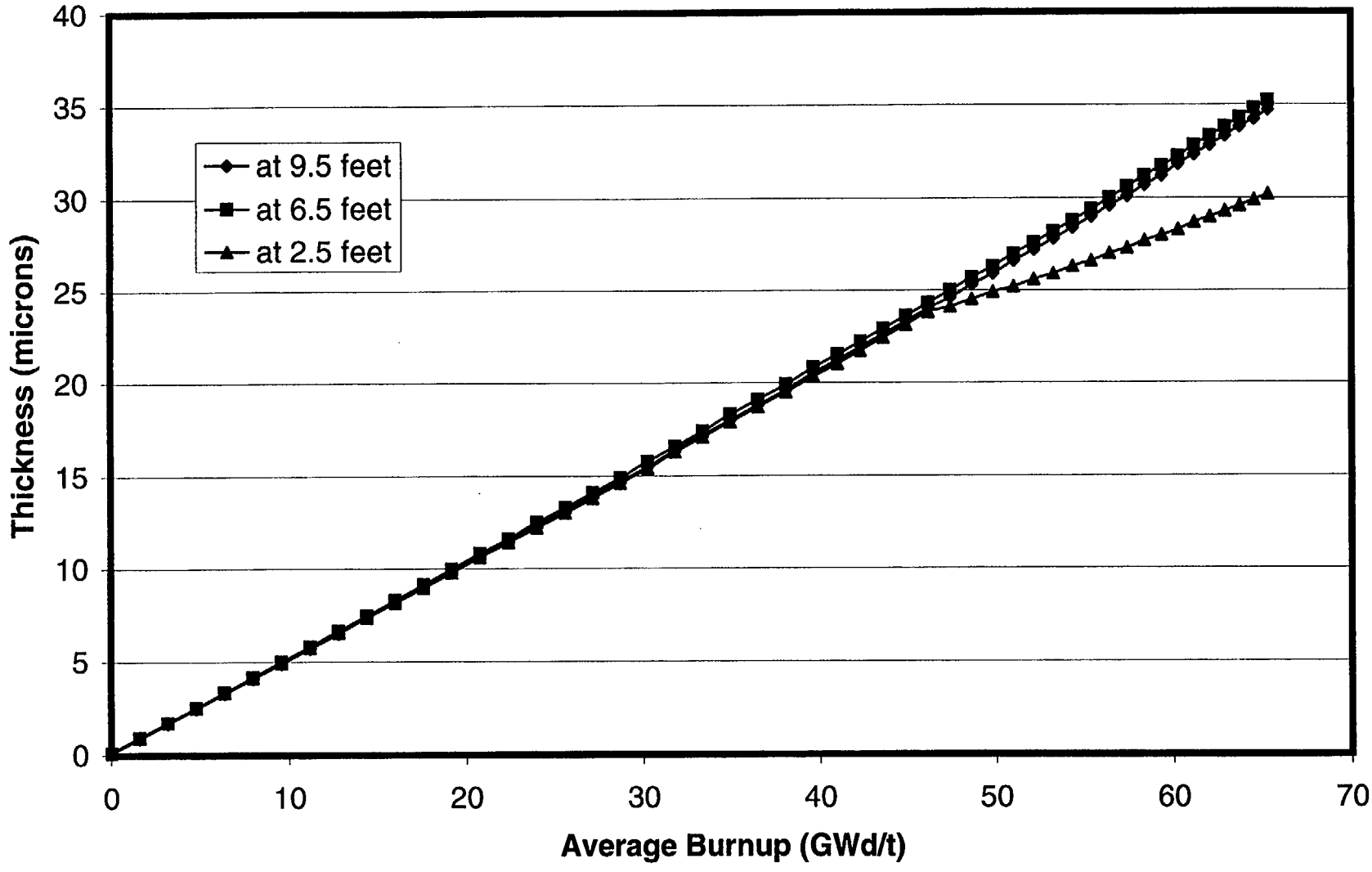

Fig. 5-11. Oxide thickness at three axial locations for a BWR 8x8 fuel rod with initial peak power of 9 kW/ft.

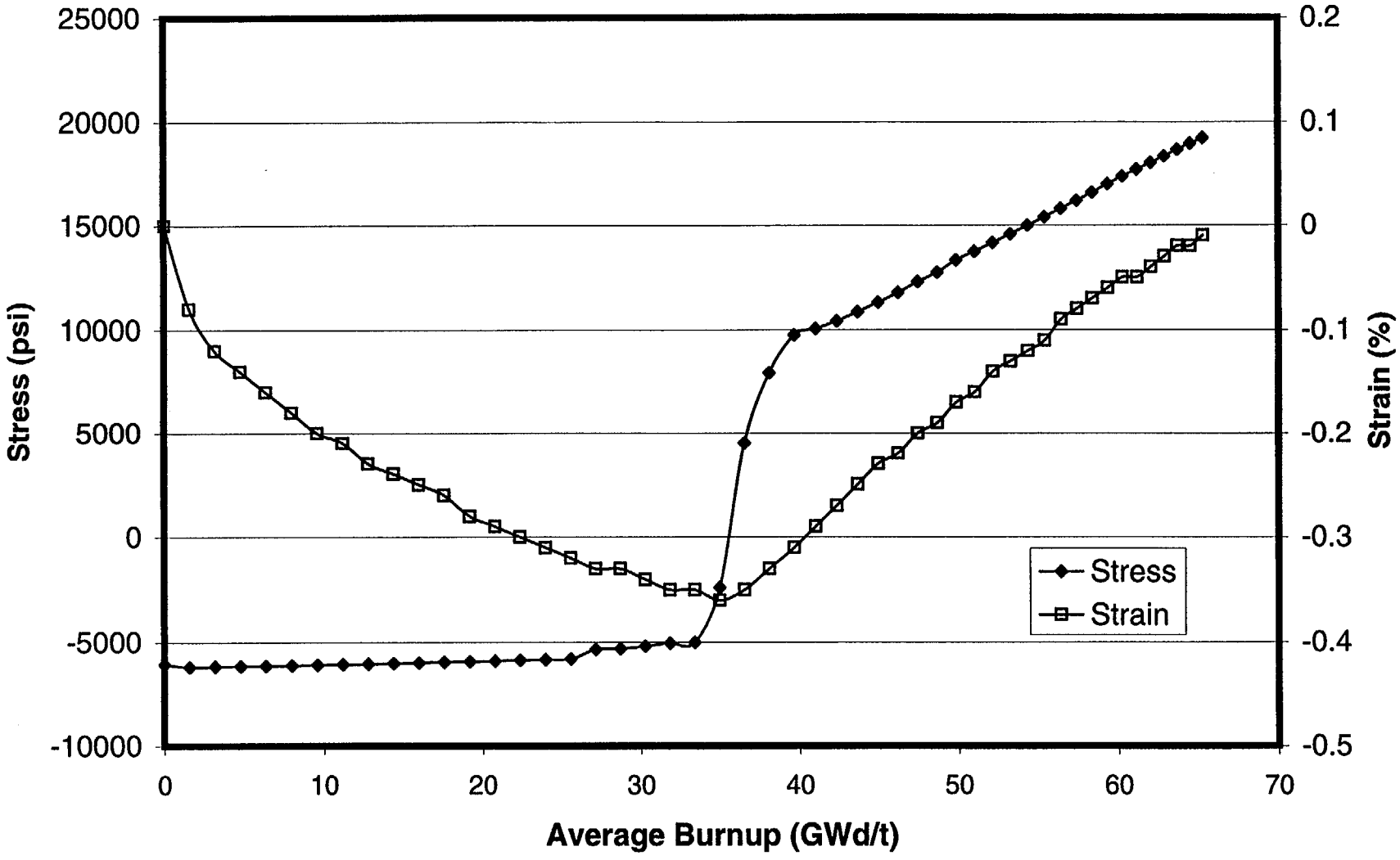

Fig. 5-12. Cladding hoop stress and hoop strain for a BWR 8x8 fuel rod with initial peak power of 9 kW/ft.

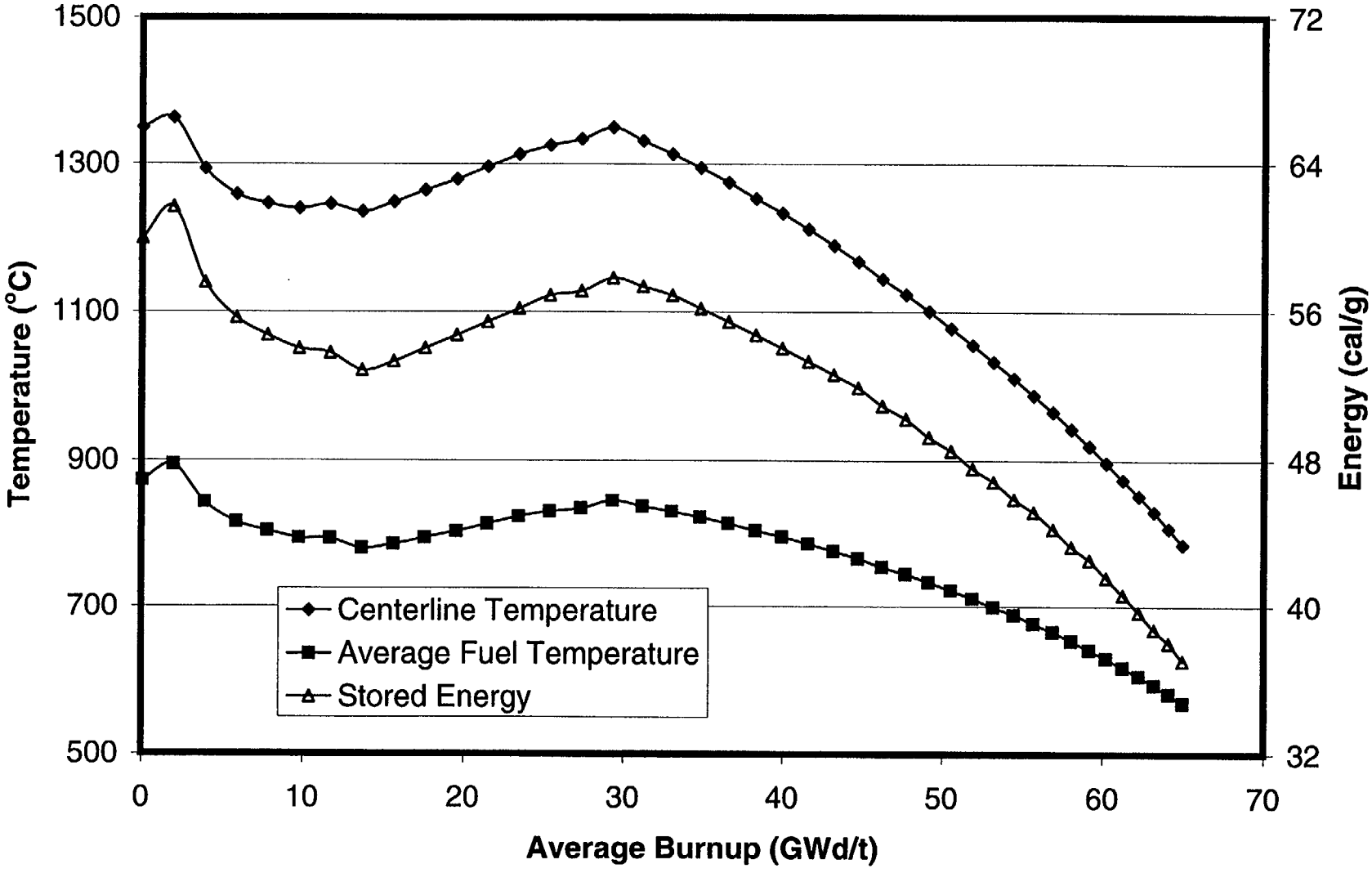

Fig. 5-13. Fuel temperatures and stored energy for a BWR 8x8 fuel rod with initial peak power of 11 kW/ft.

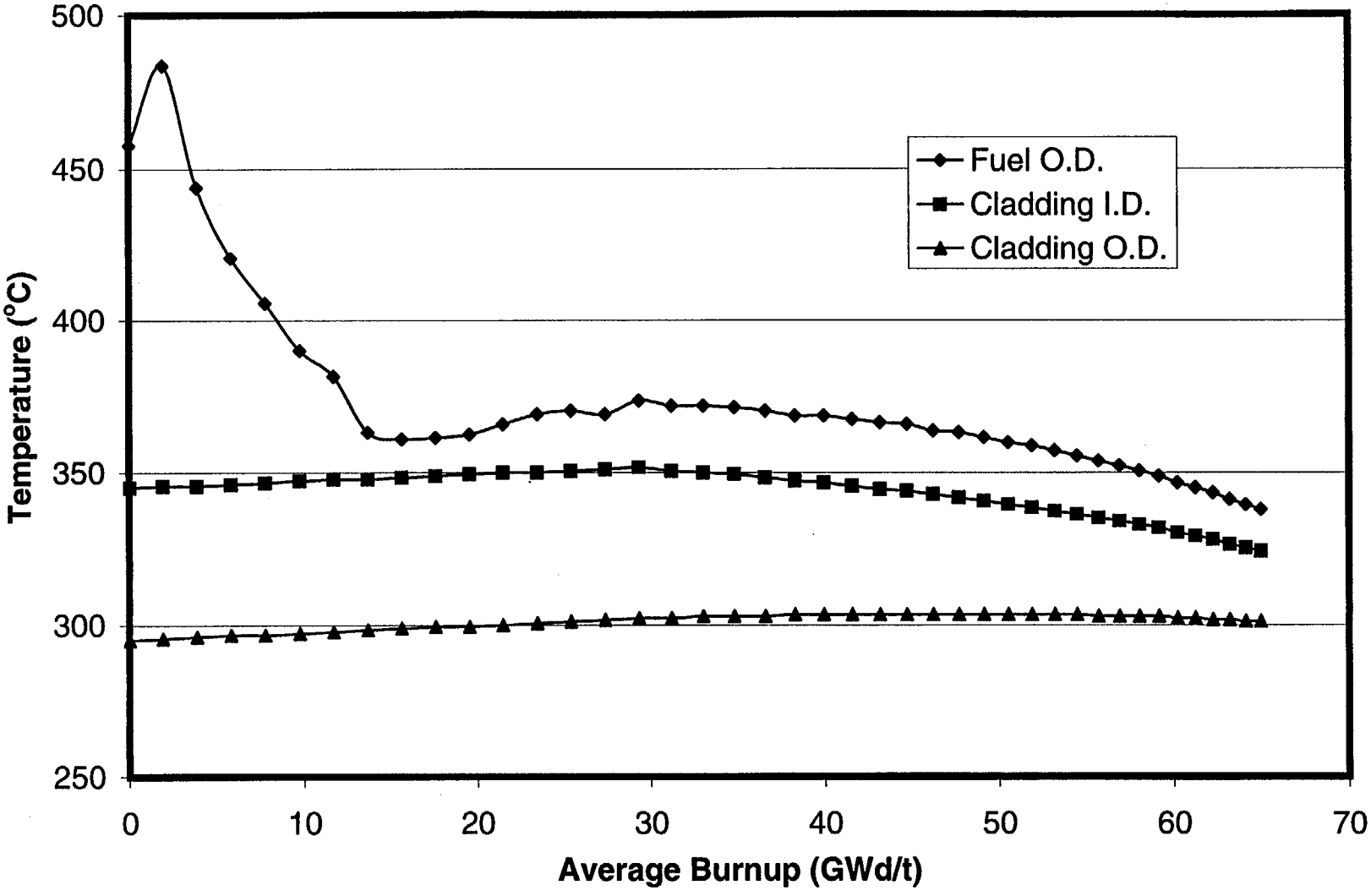

Fig. 5-14. Cladding temperatures and fuel surface temperature for a BWR 8x8 fuel rod with initial peak power of 11 kW/ft.

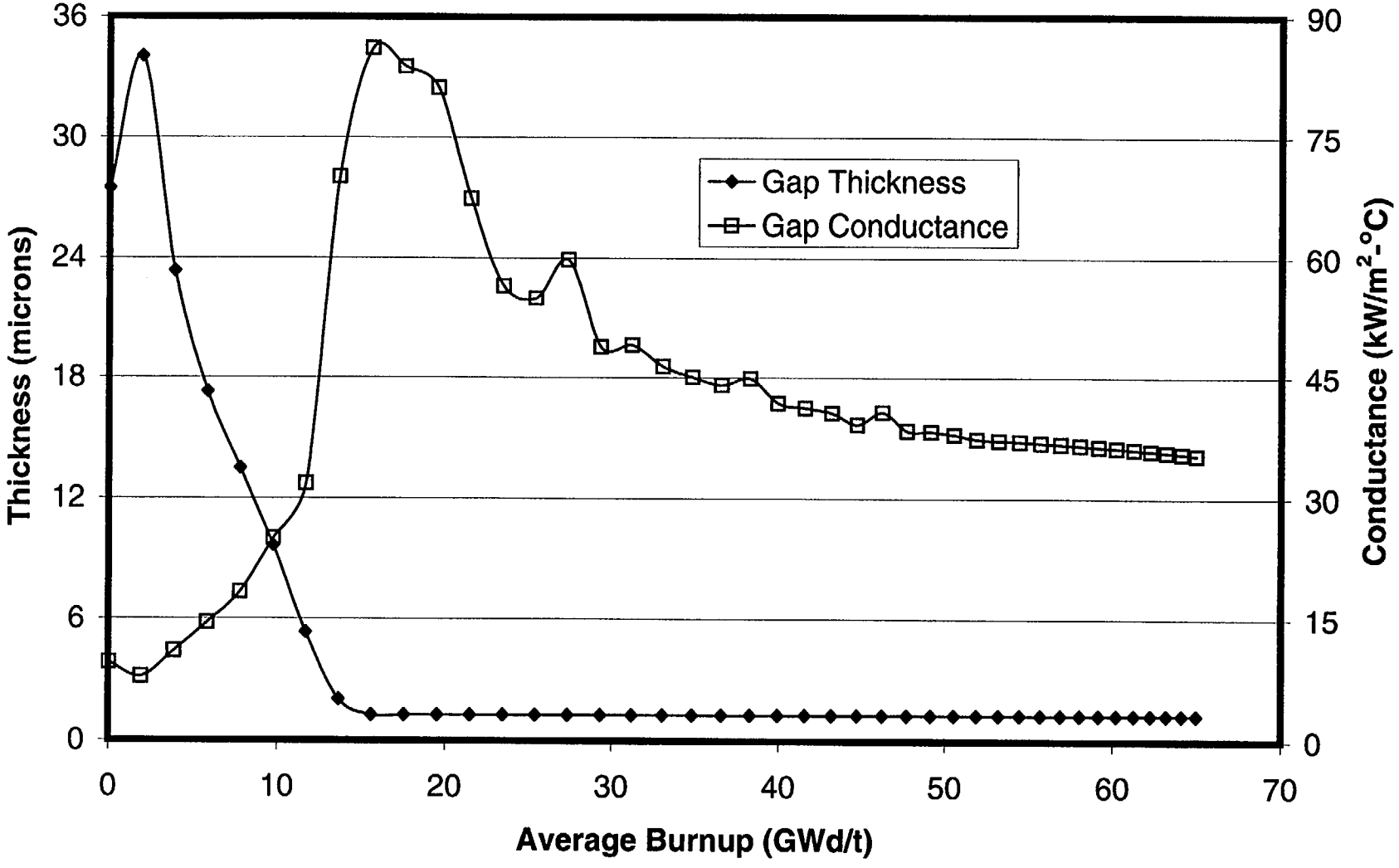

Fig. 5-15. Gap thickness and gap conductance for a BWR 8x8 fuel rod with initial peak power of 11 kW/ft.

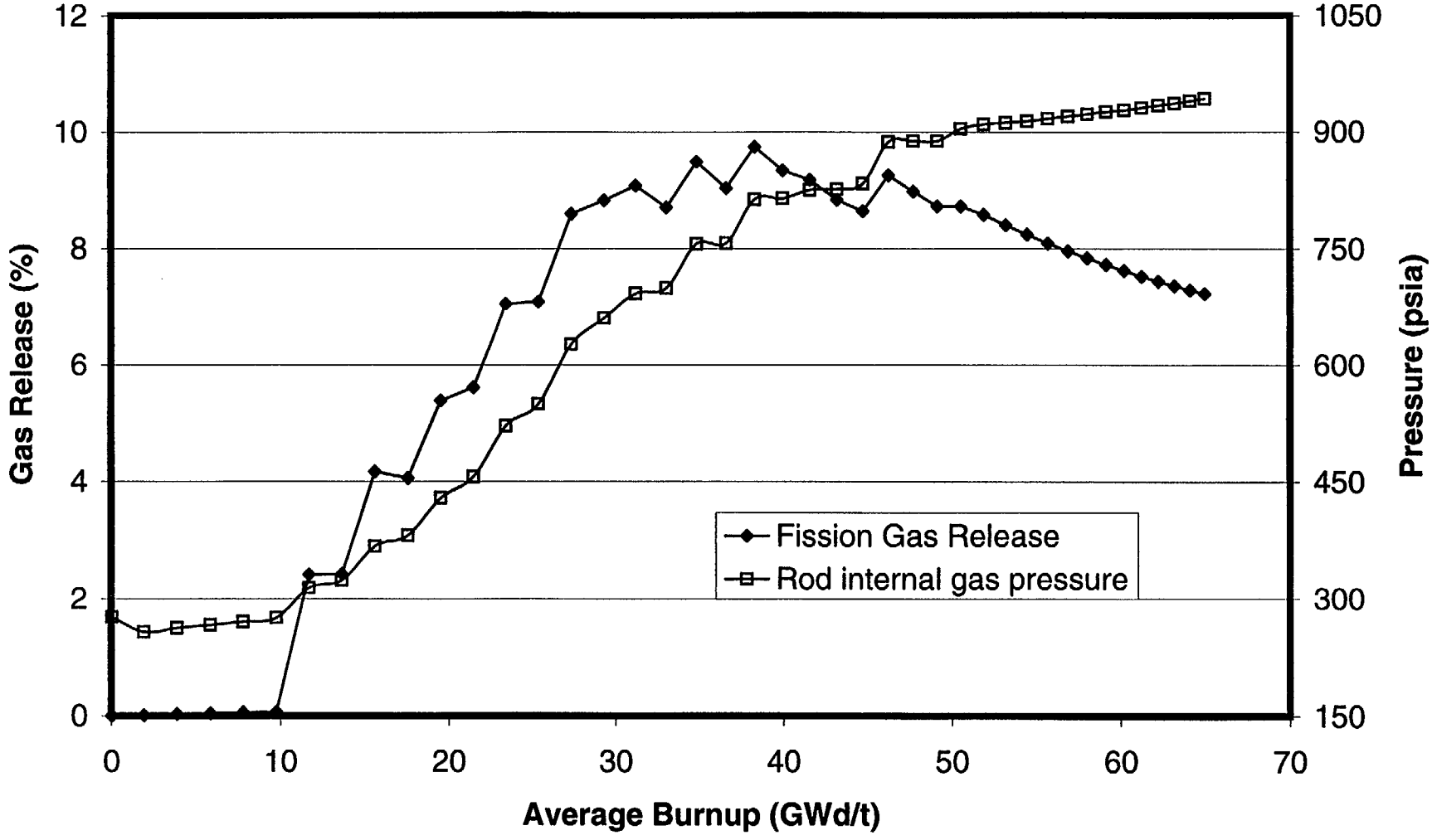

Fig. 5-16. Fission gas release and rod internal gas pressure for a BWR 8x8 fuel rod with initial peak power of 11 kW/ft.

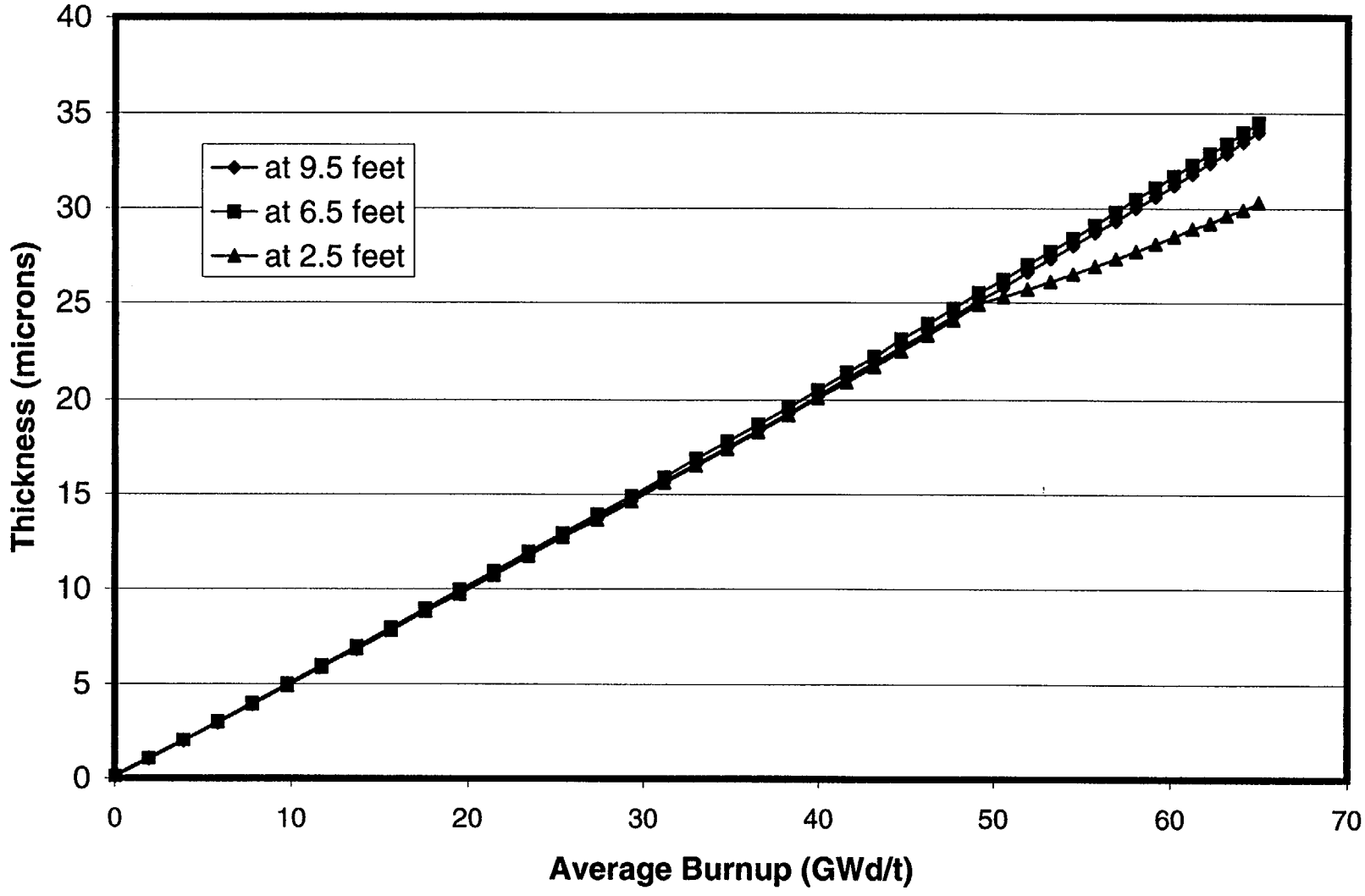

Fig. 5-17. Oxide thickness at three axial locations for a BWR 8x8 fuel rod with initial peak power of 11 kW/ft.

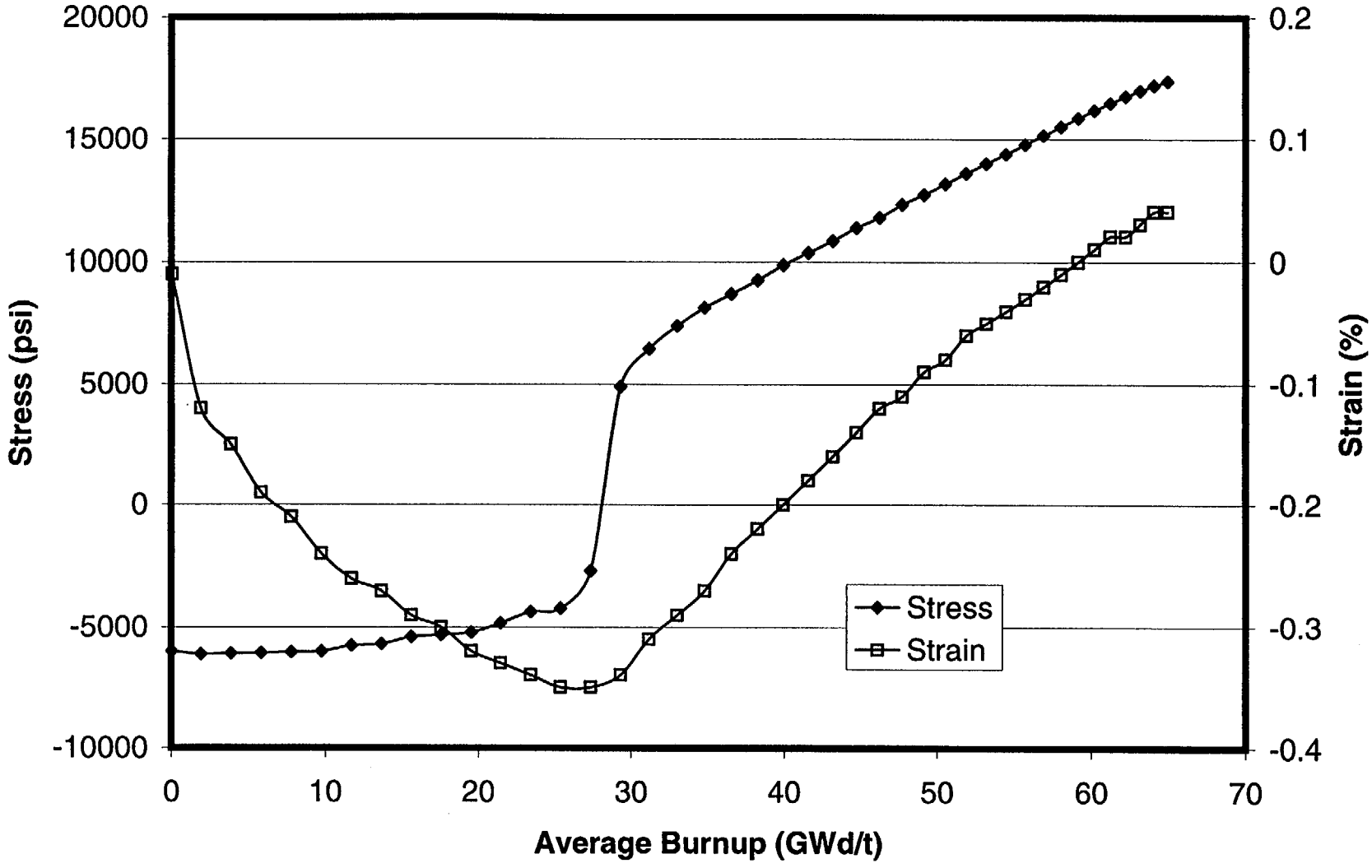

Fig. 5-18. Cladding hoop stress and hoop strain for a BWR 8x8 fuel rod with initial peak power of 11 kW/ft.

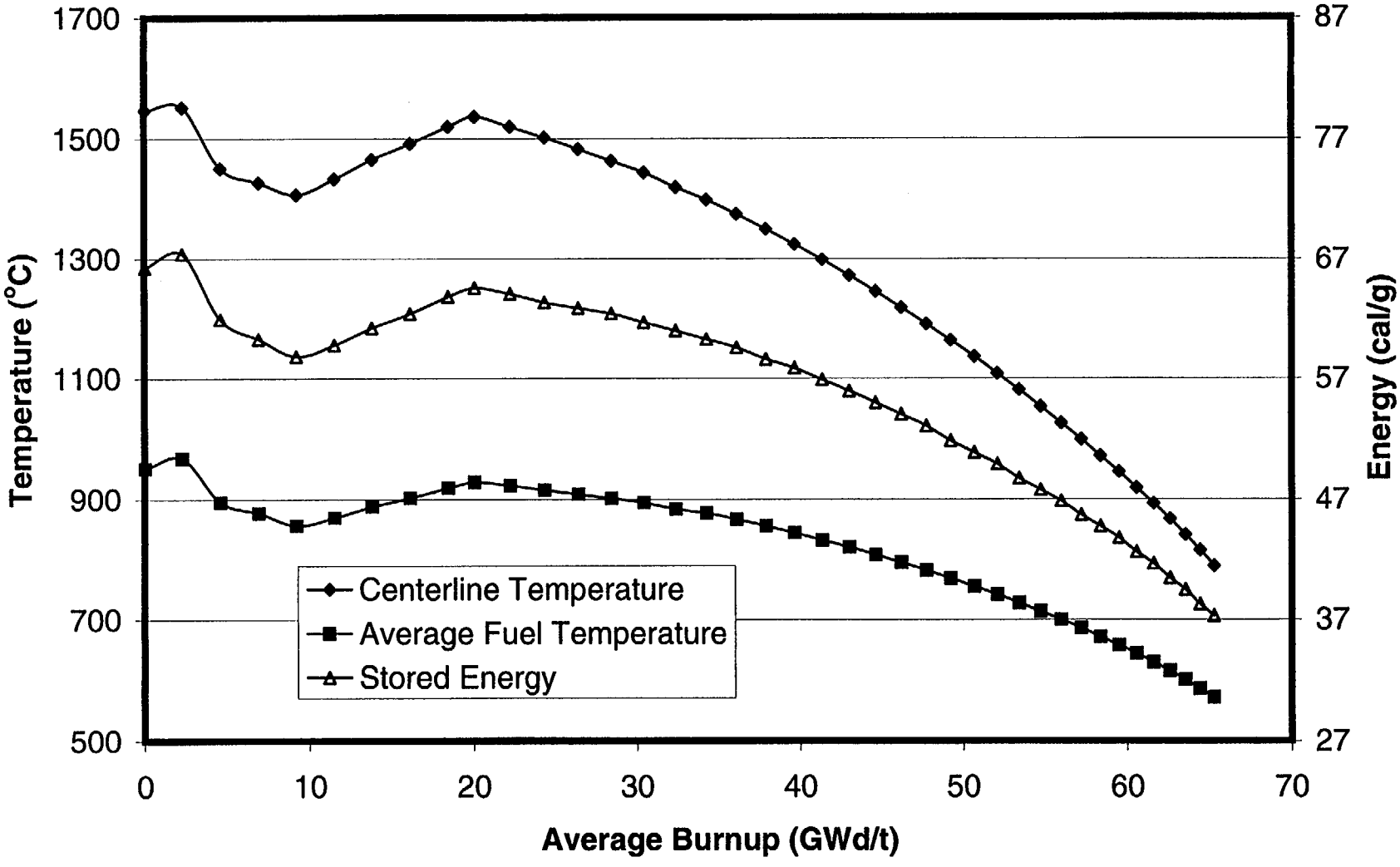

Fig. 5-19. Fuel Temperatures and stored energy for a BWR 8x8 fuel rod with initial peak power of 13 kW/ft.

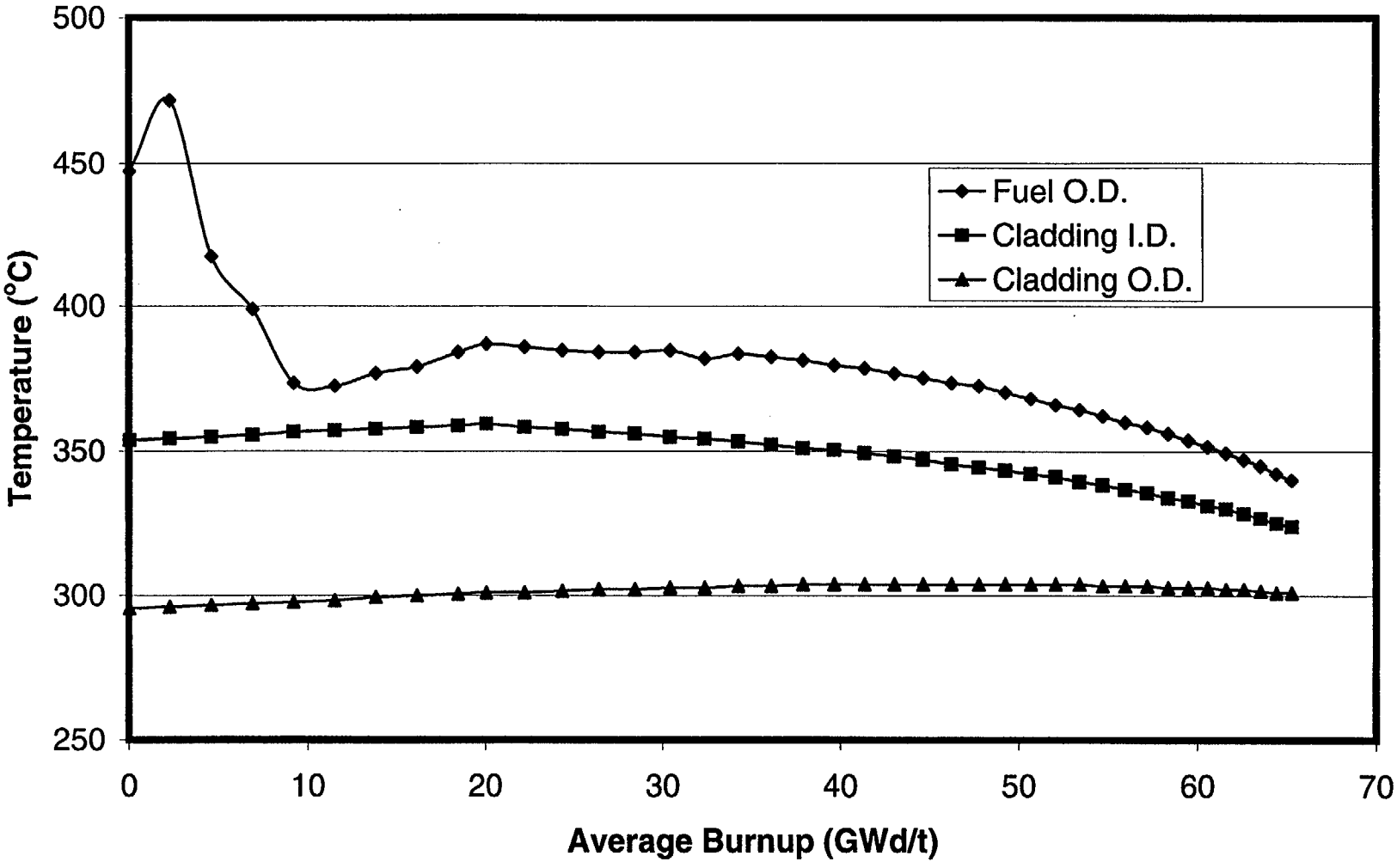

Fig. 5-20. Cladding temperatures and fuel surface temperature for a BWR 8x8 fuel rod with initial peak power of 13 kW/ft.

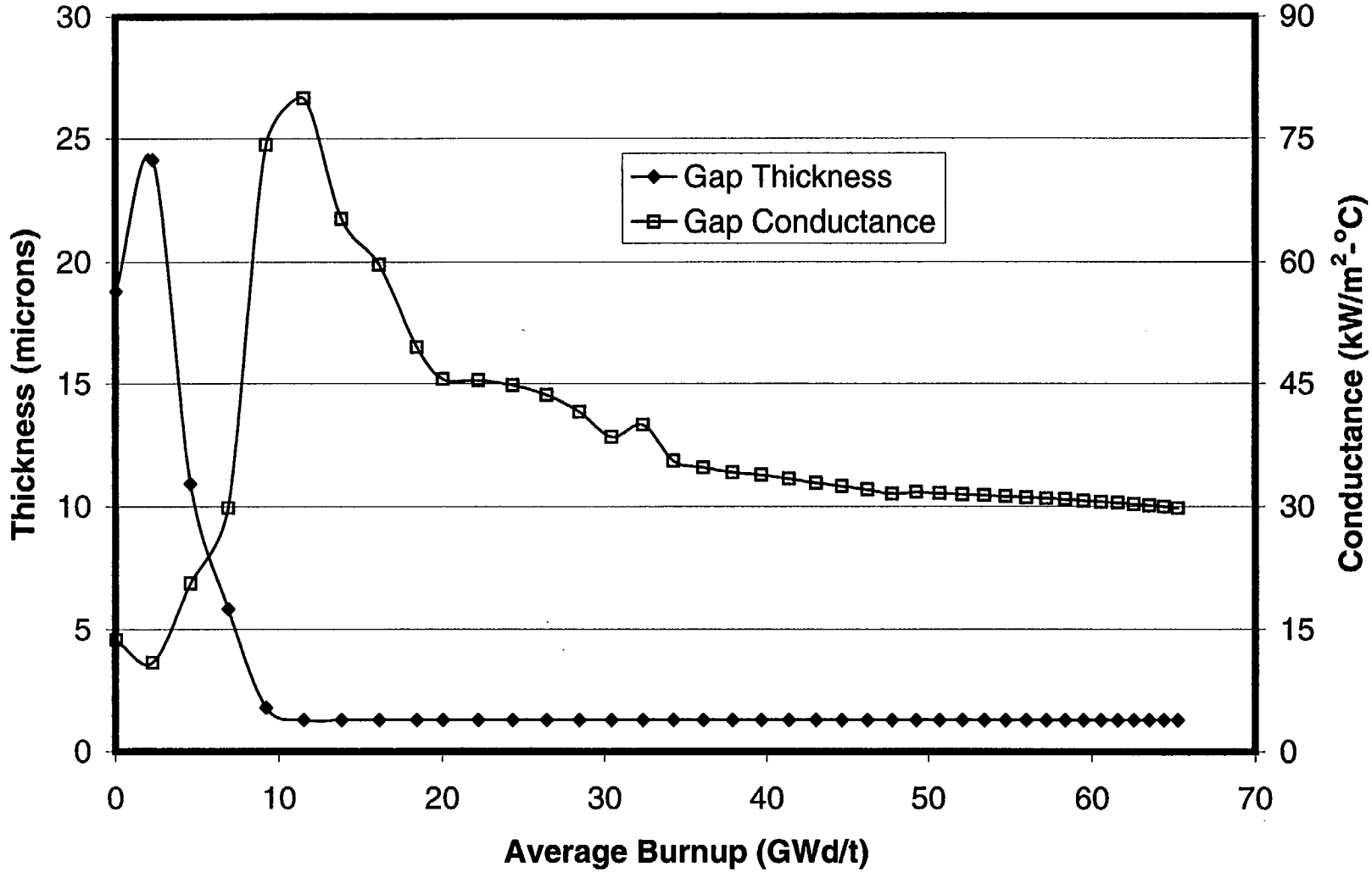

Fig. 5-21. Gap thickness and gap conductance for a BWR 8x8 fuel rod with initial peak power of 13 kW/ft.

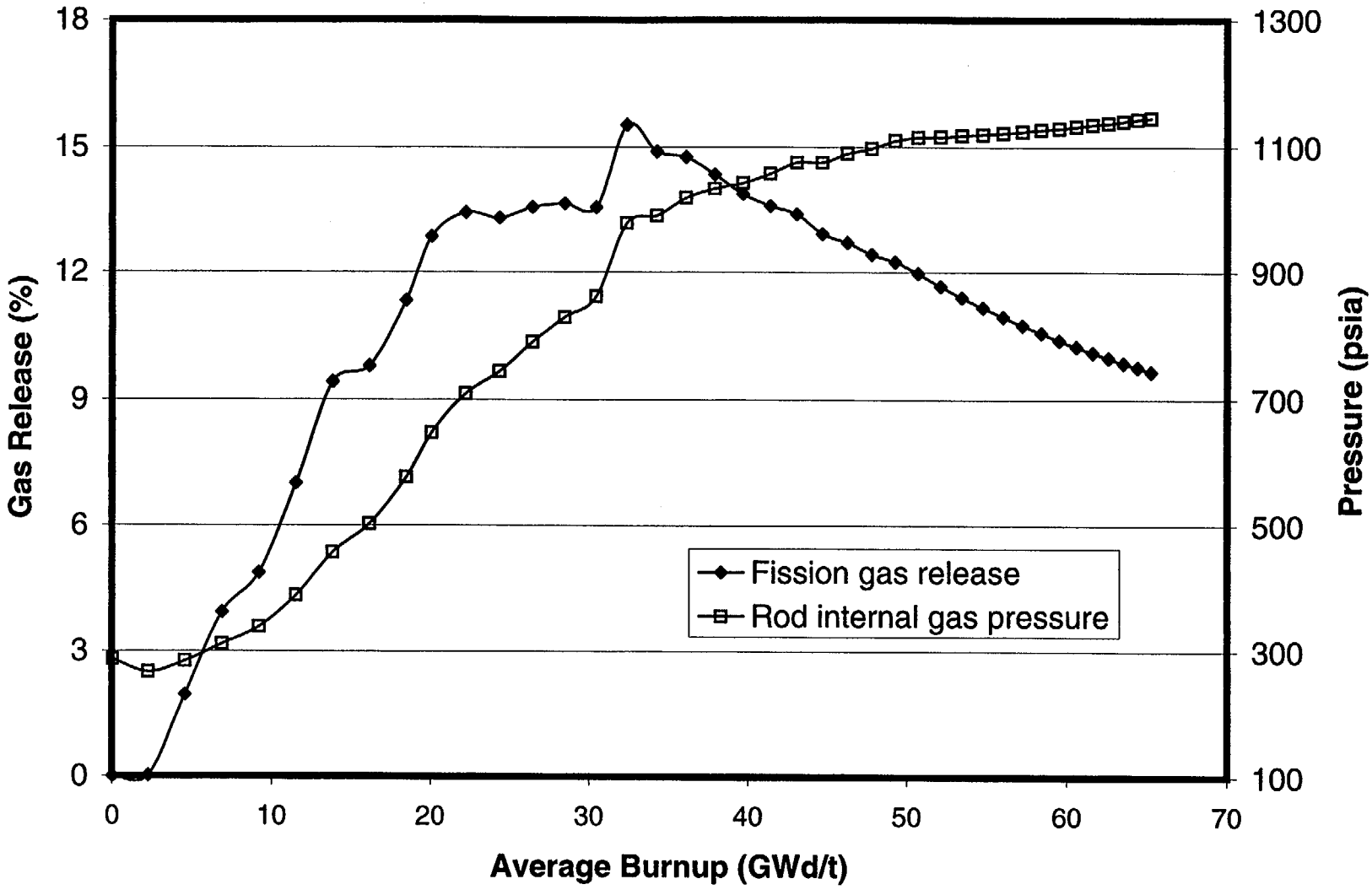

Fig. 5-22. Fission gas release and rod internal gas pressure for a BWR 8x8 fuel rod with initial peak power of 13 kW/ft.

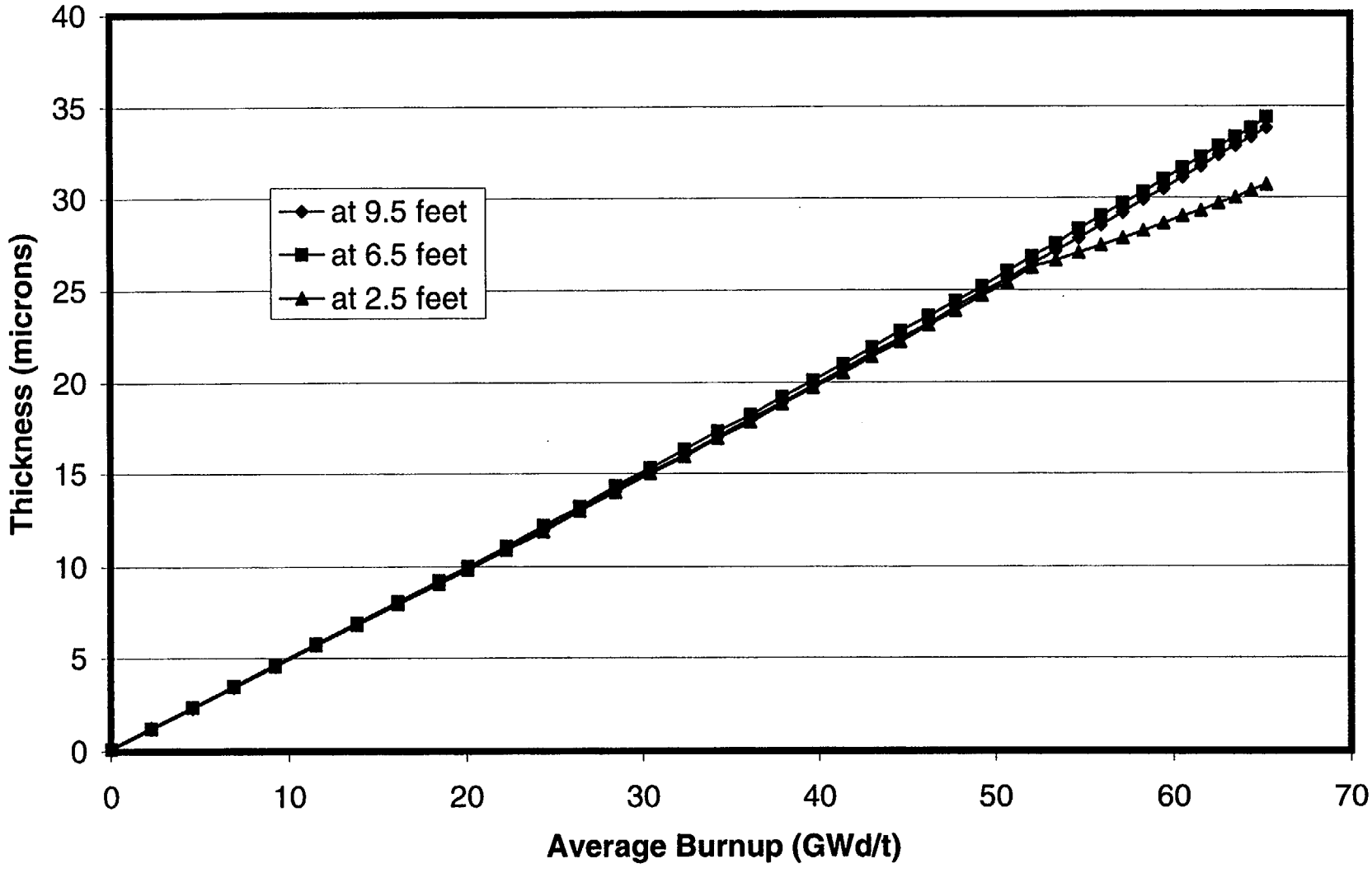

Fig. 5-23. Oxide thickness at three axial locations for a BWR 8x8 fuel rod with initial peak power of 13 kW/ft.

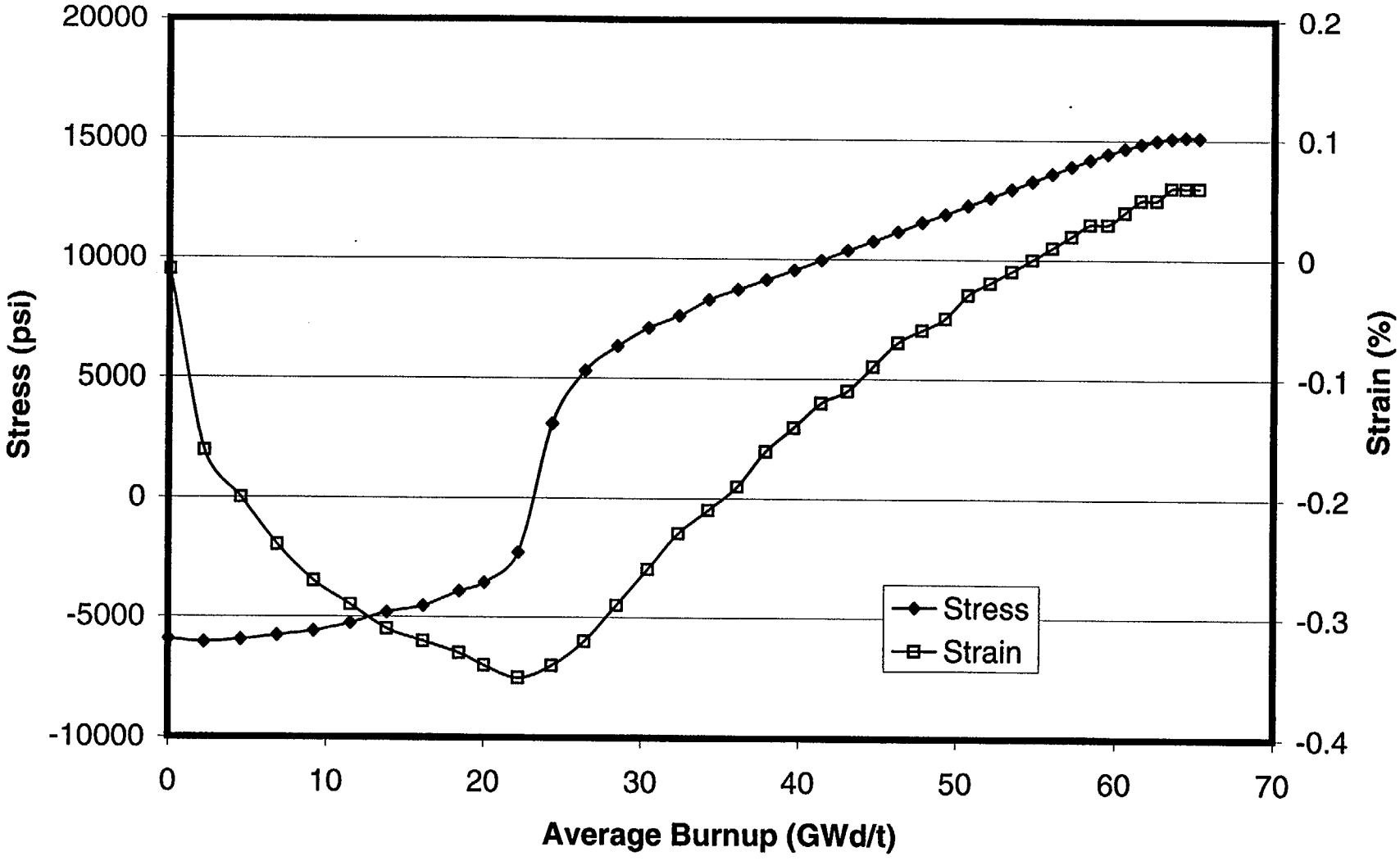

Fig. 5-24. Cladding hoop stress and hoop strain for a BWR 8x8 fuel rod with initial peak power of 13 kW/ft.

6. Calculations for BWR 9x9 Fuel

In the following figures, calculated values for BWR 9x9 fuel are plotted as a function of burnup for the parameters listed below:

Fuel centerline temperature
Average fuel temperature
Stored energy
Fuel O.D. temperature
Cladding I.D. temperature
Cladding O.D. temperature
Gap thickness
Gap conductance
Fission gas release
Rod internal gas pressure
Oxide thickness
Cladding hoop stress
Cladding hoop strain

Several general observations can be made about the calculated results:

- Within the first few GWd/t of burnup, a temperature peak is observed that is the result of fuel densification.

- Gap closure results in (a) the coming together of temperatures for fuel O.D. and cladding I.D. and (b) a sharp increase in gap conductance. The gap conductance increases again after a few time steps when the interaction between the pellet and cladding affects the contact conductance calculated for a closed gap. At this point there is also a large increase in stress, and the permanent strain changes directions.

- Some of the fission gas is released in spurts according to the Massih model in FRAPCON-3. This effect is apparent in many of the figures. Shorter time steps would produce slightly different looking curves, but the trend of gas release and the end-of-life gas release would be about the same.

- The burnup enhancement of fission gas release is readily seen in the lower power cases, but it is obscured in the highest power cases by the magnitude of prior gas release.

- Rod internal gas pressure increases with the accumulation of released fission gas. In the higher power PWR cases, as the power drops off near the end of life, the reduction in the plenum temperature offsets the increasing moles of fission gas.

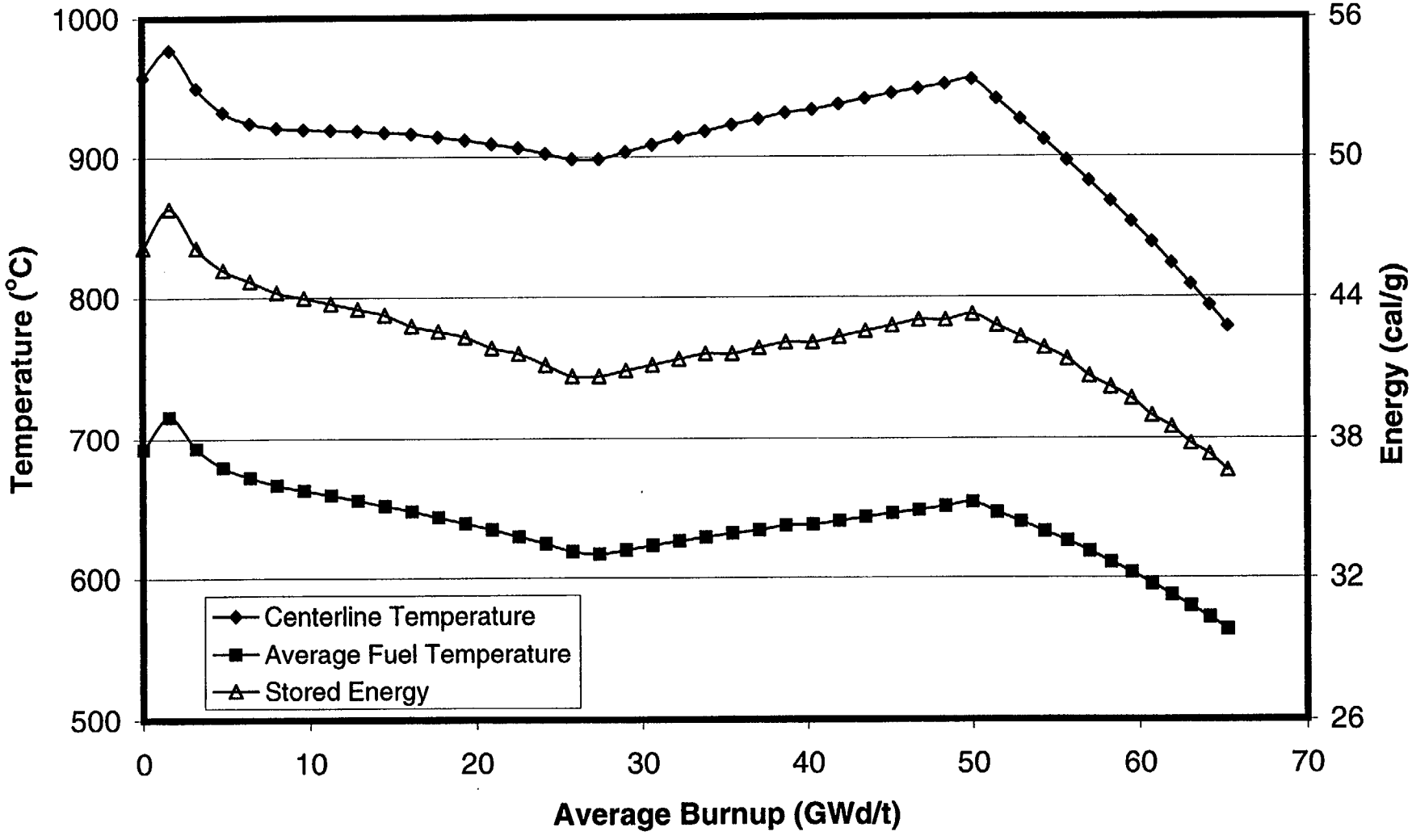

Fig. 6-1. Fuel temperatures and stored energy for a BWR 9x9 fuel rod with initial peak power of 7 kW/ft.

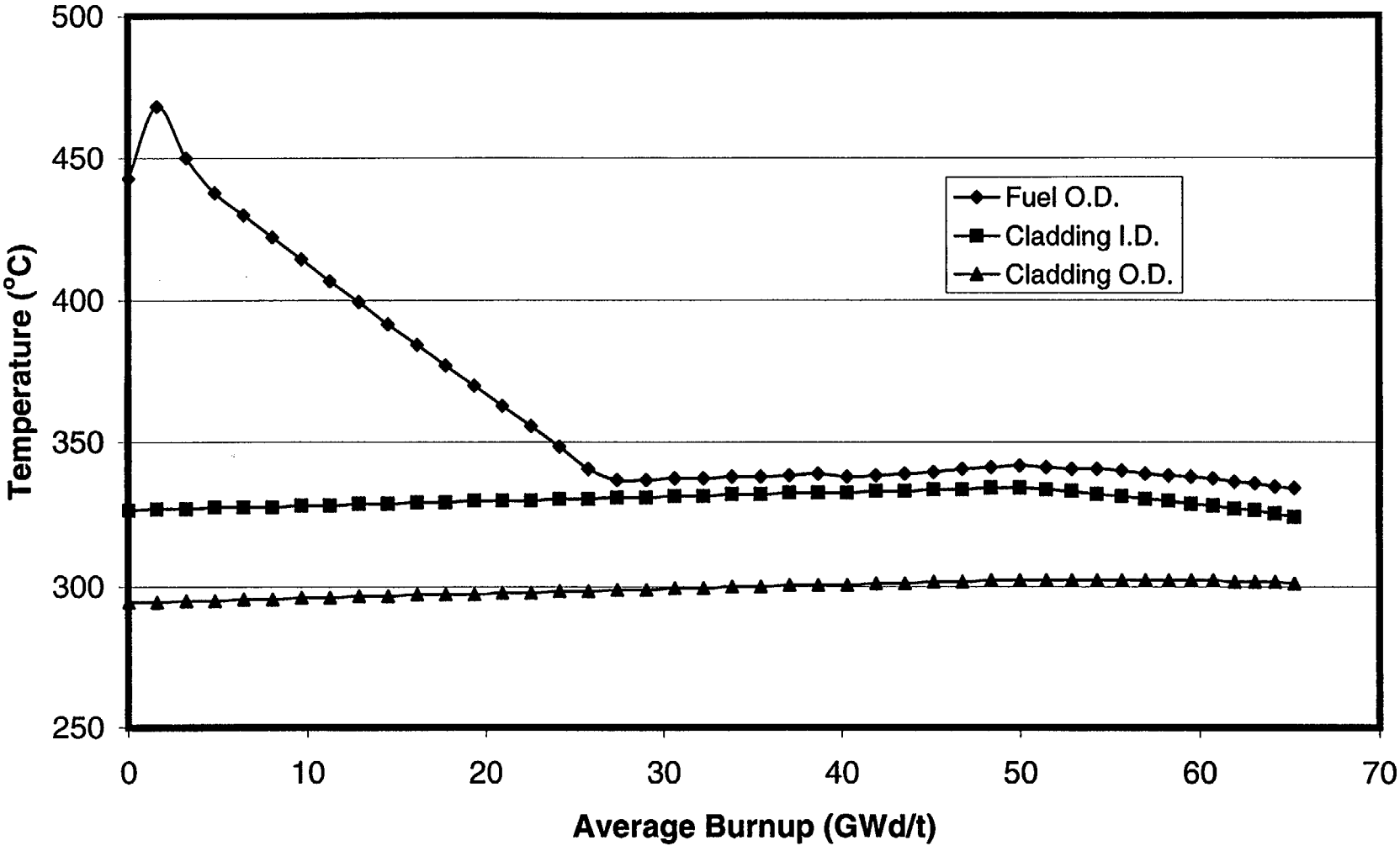

Fig. 6-2. Cladding temperatures and fuel surface temperature for a BWR 9x9 fuel rod with initial peak power of 7 kW/ft.

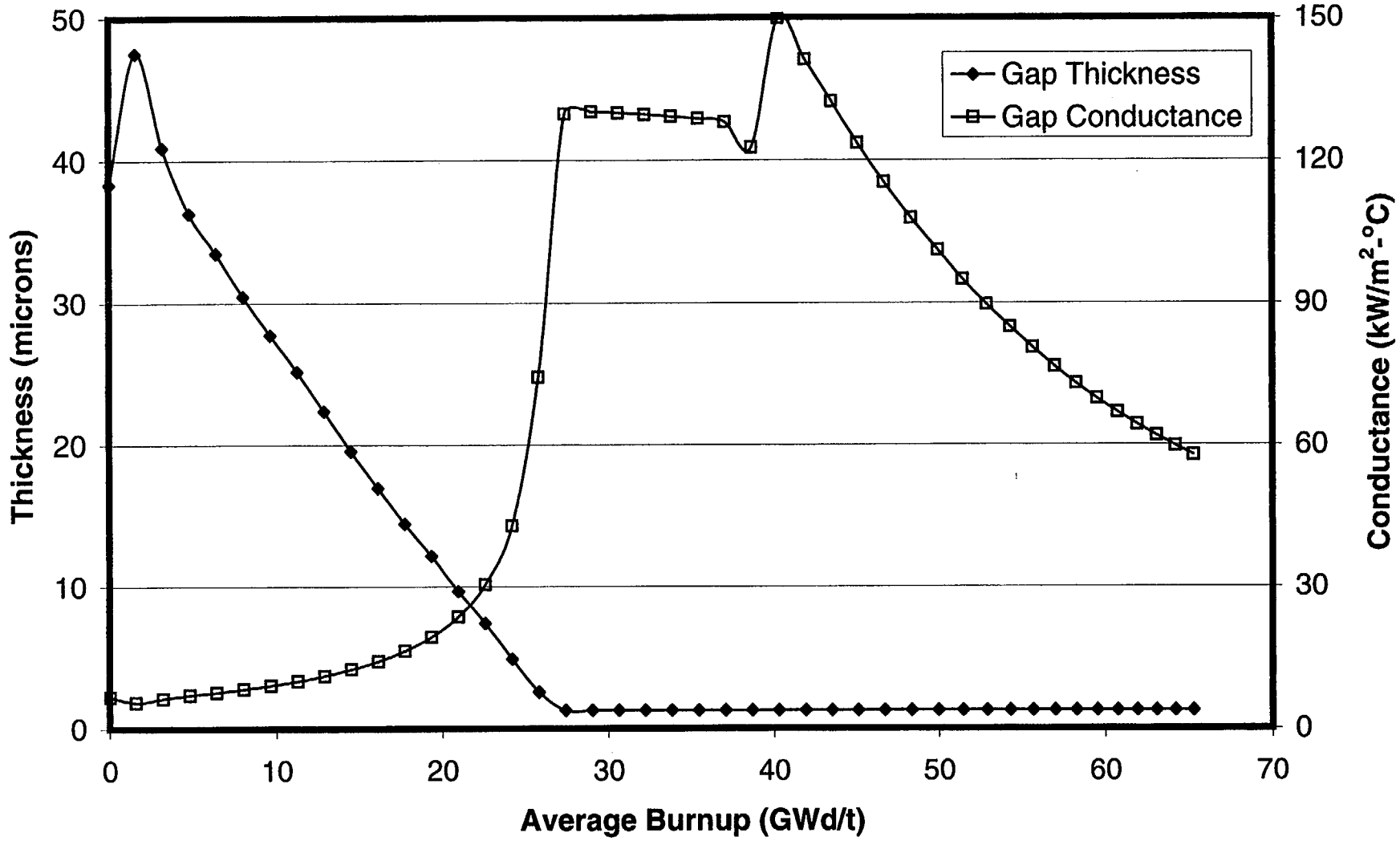

Fig. 6-3. Gap thickness and gap conductance for a BWR 9x9 fuel rod with initial peak power of 7 kW/ft.

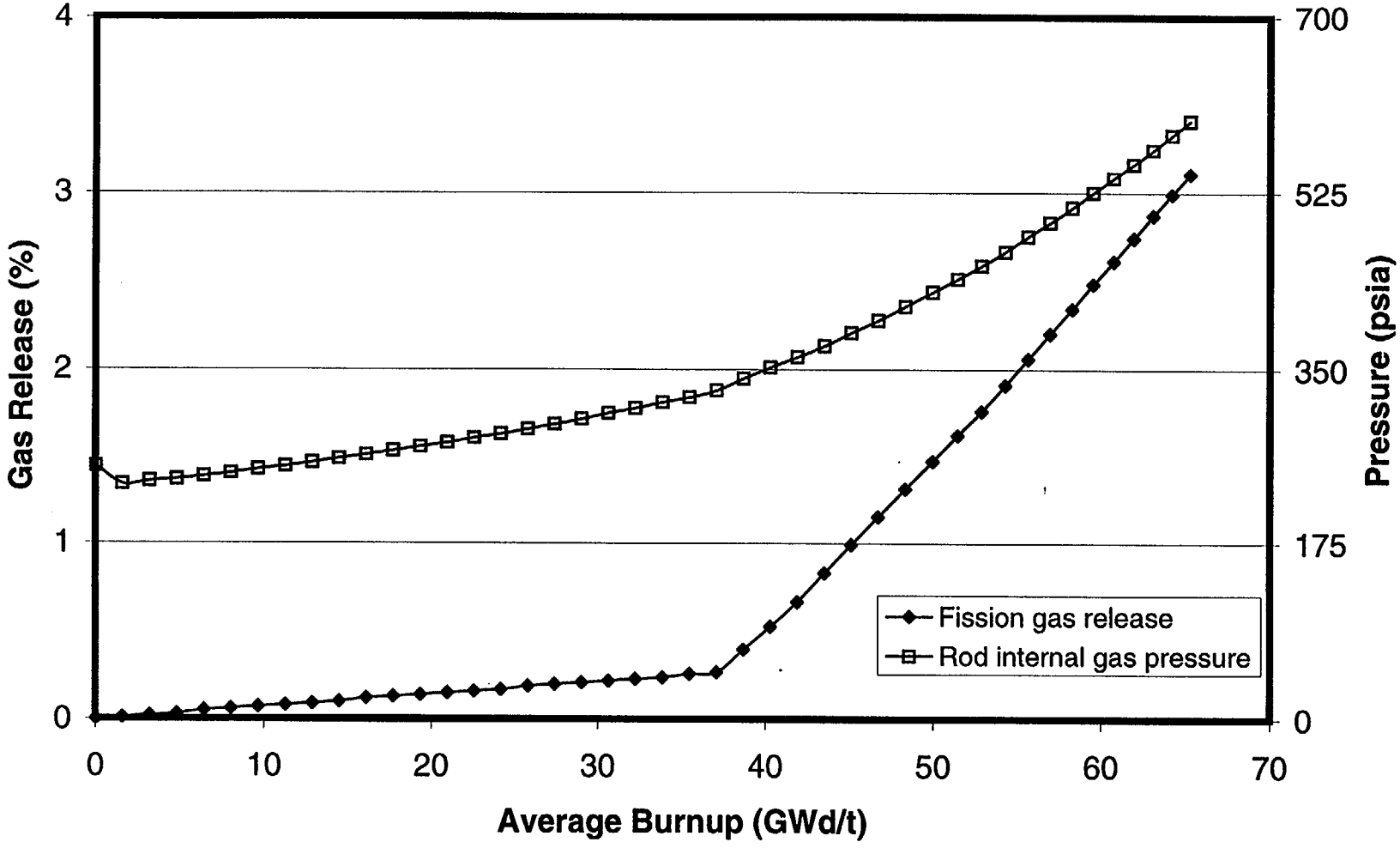

Fig. 6-4. Fission gas release and rod internal gas pressure for a BWR 9x9 fuel rod with initial peak power of 7 kW/ft.

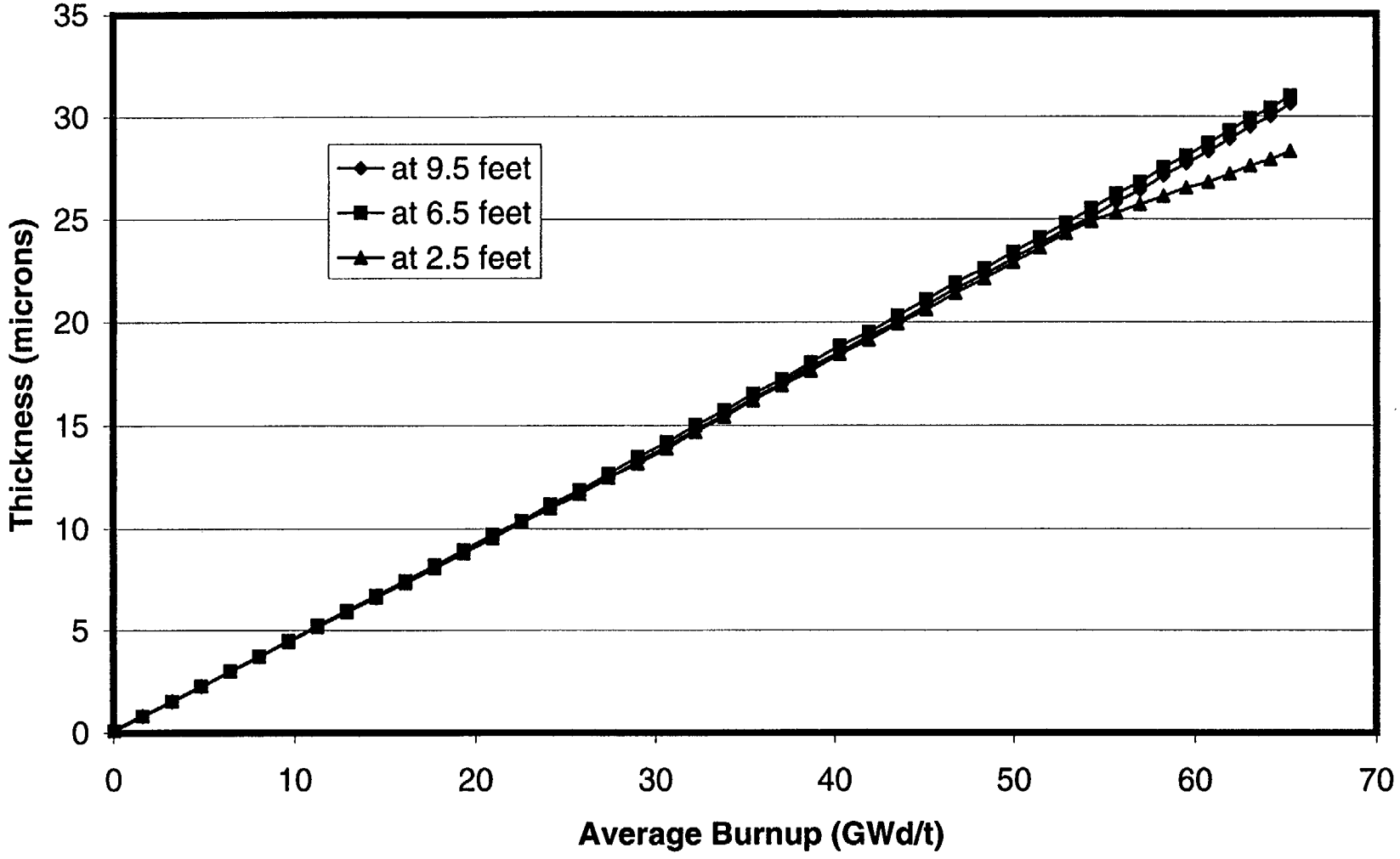

Fig. 6-5. Oxide thickness at three axial locations for a BWR 9x9 fuel rod with initial peak power of 7 kW/ft.

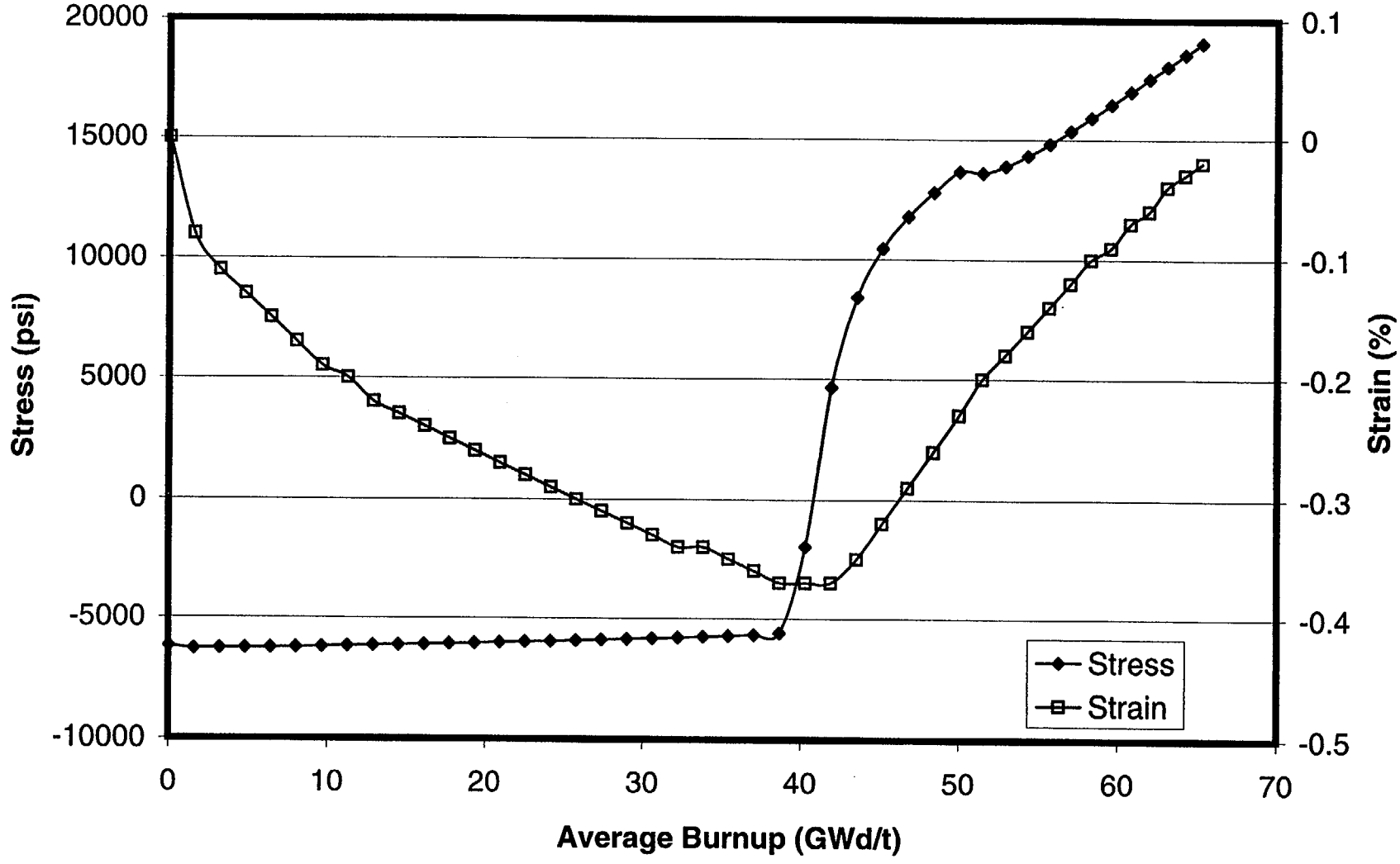

Fig. 6-6. Cladding hoop stress and hoop strain for a BWR 9x9 fuel rod with initial peak power of 7 kW/ft.

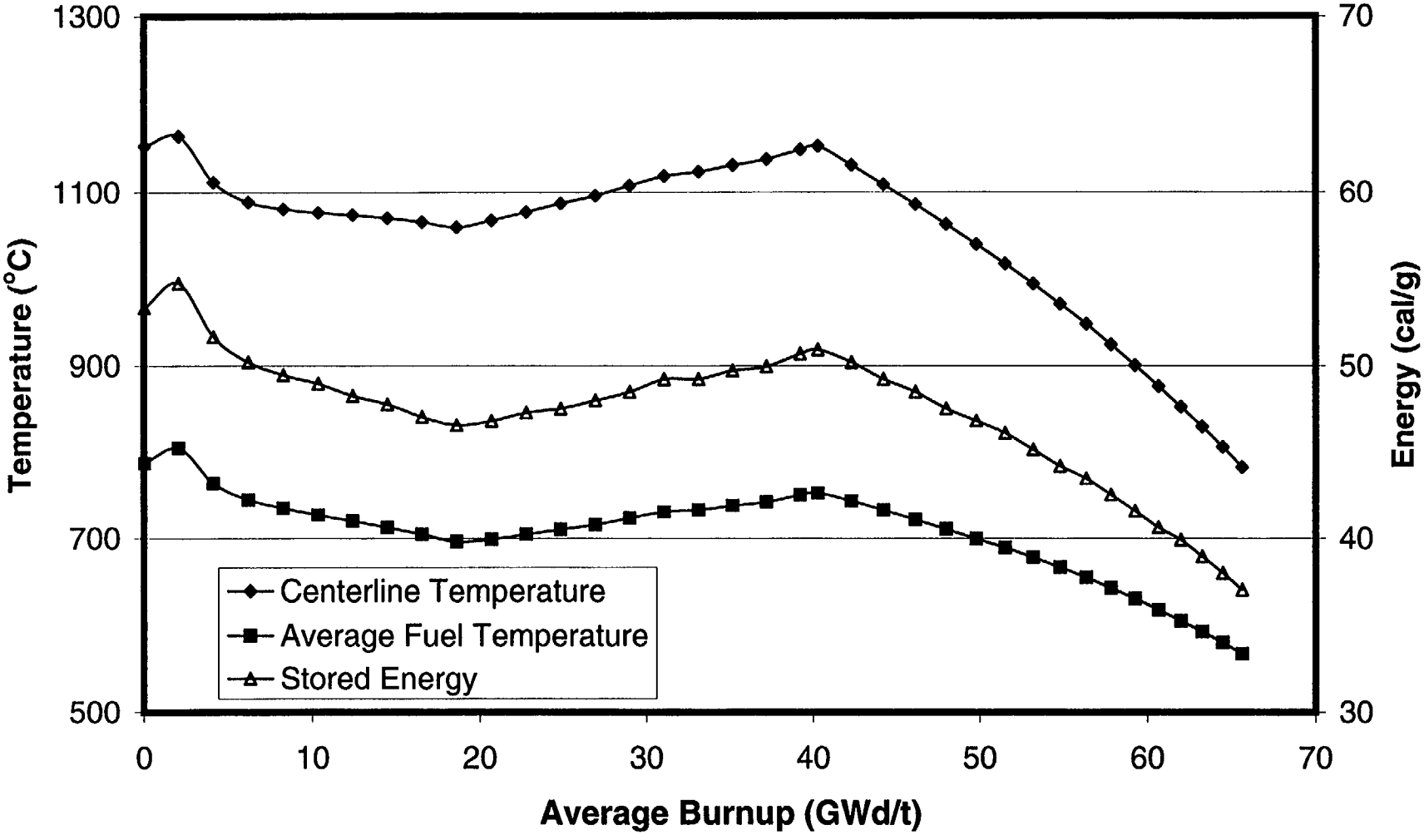

Fig. 6-7. Fuel temperatures and stored energy for a BWR 9x9 fuel rod with initial peak power of 9 kW/ft.

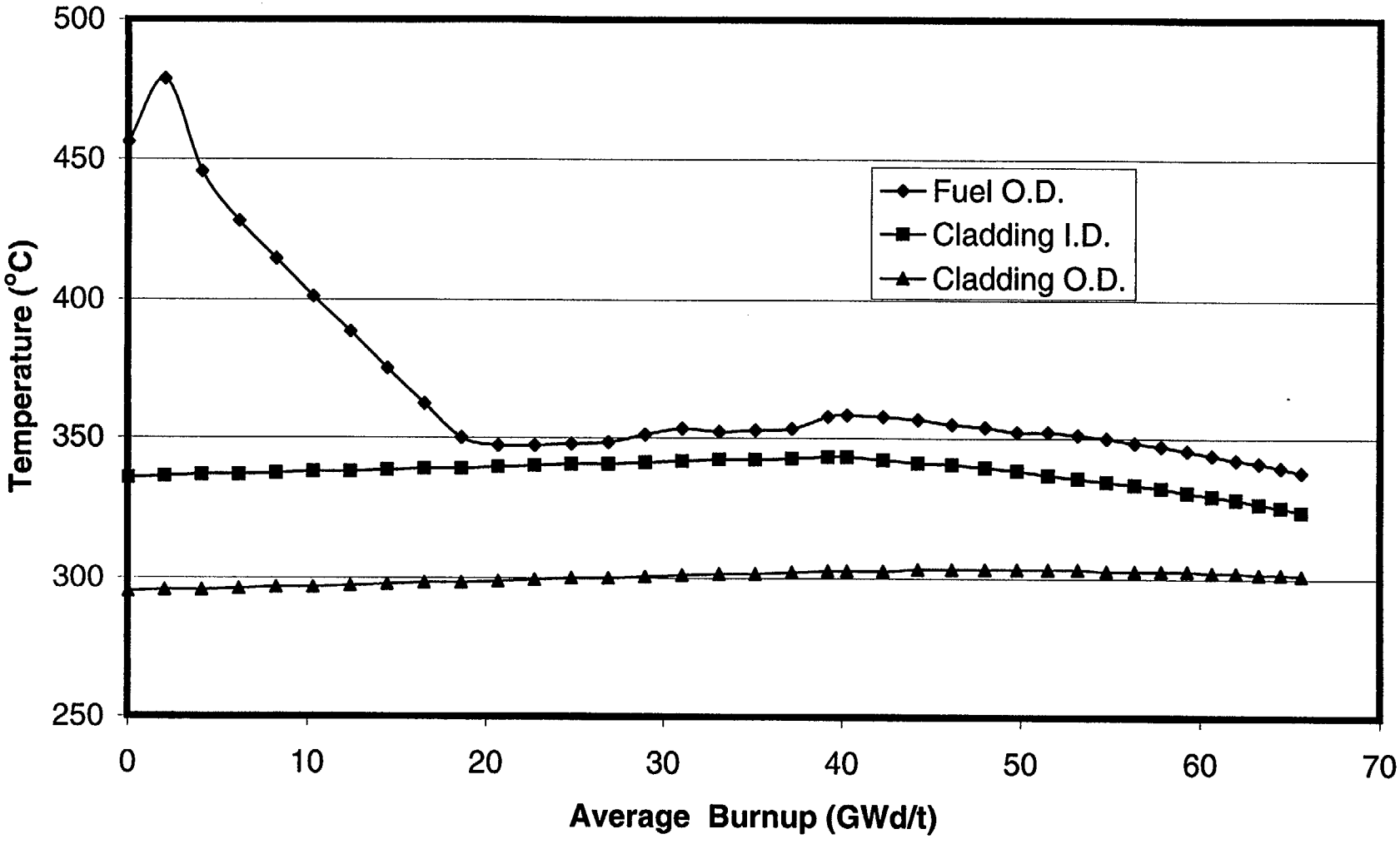

Fig. 6-8. Cladding temperatures and fuel surface temperature for a BWR 9x9 fuel rod with initial peak power of 9 kW/ft.

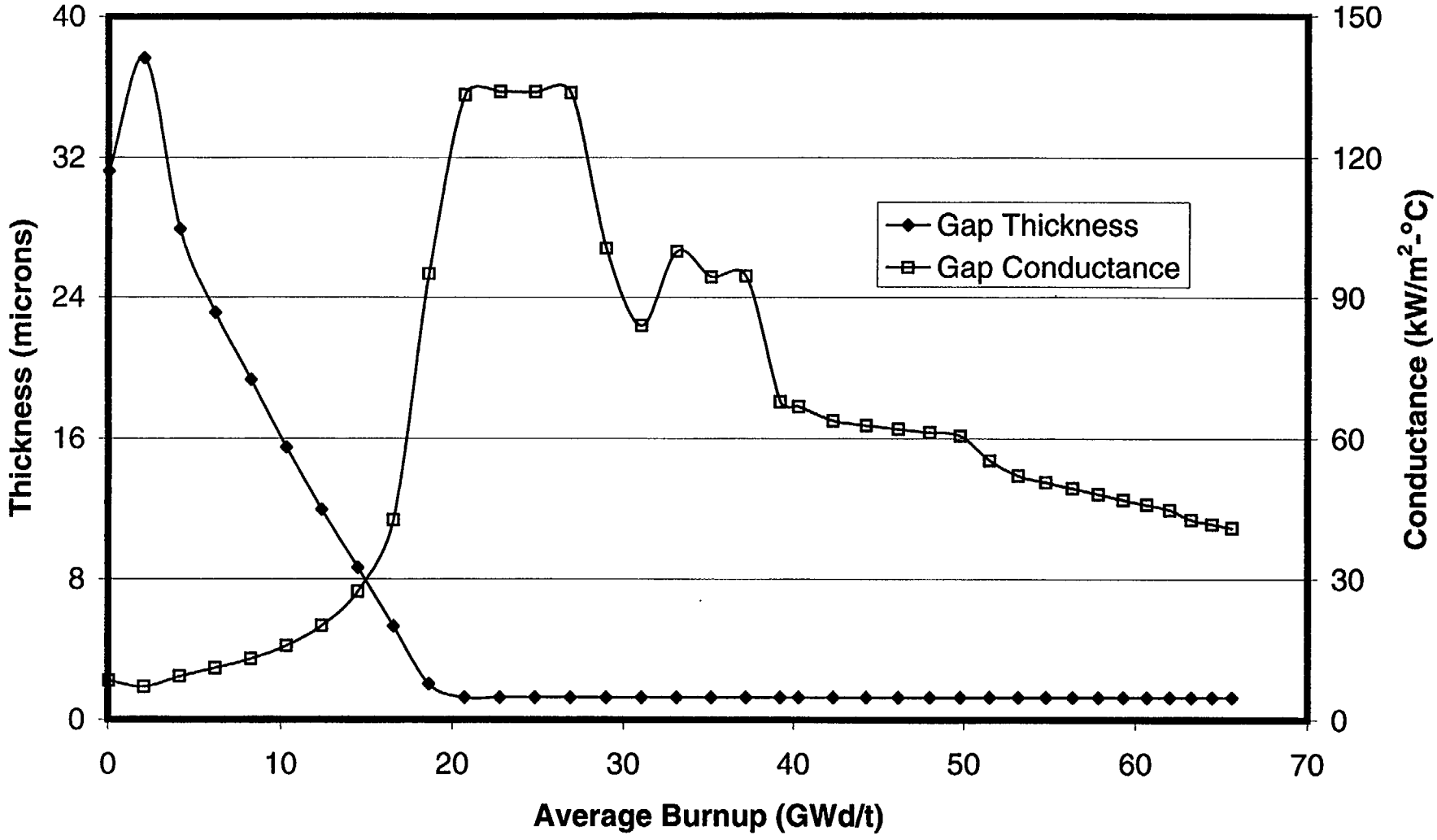

Fig. 6-9. Gap thickness and gap conductance for a BWR 9x9 fuel rod with initial peak power of 9 kW/ft.

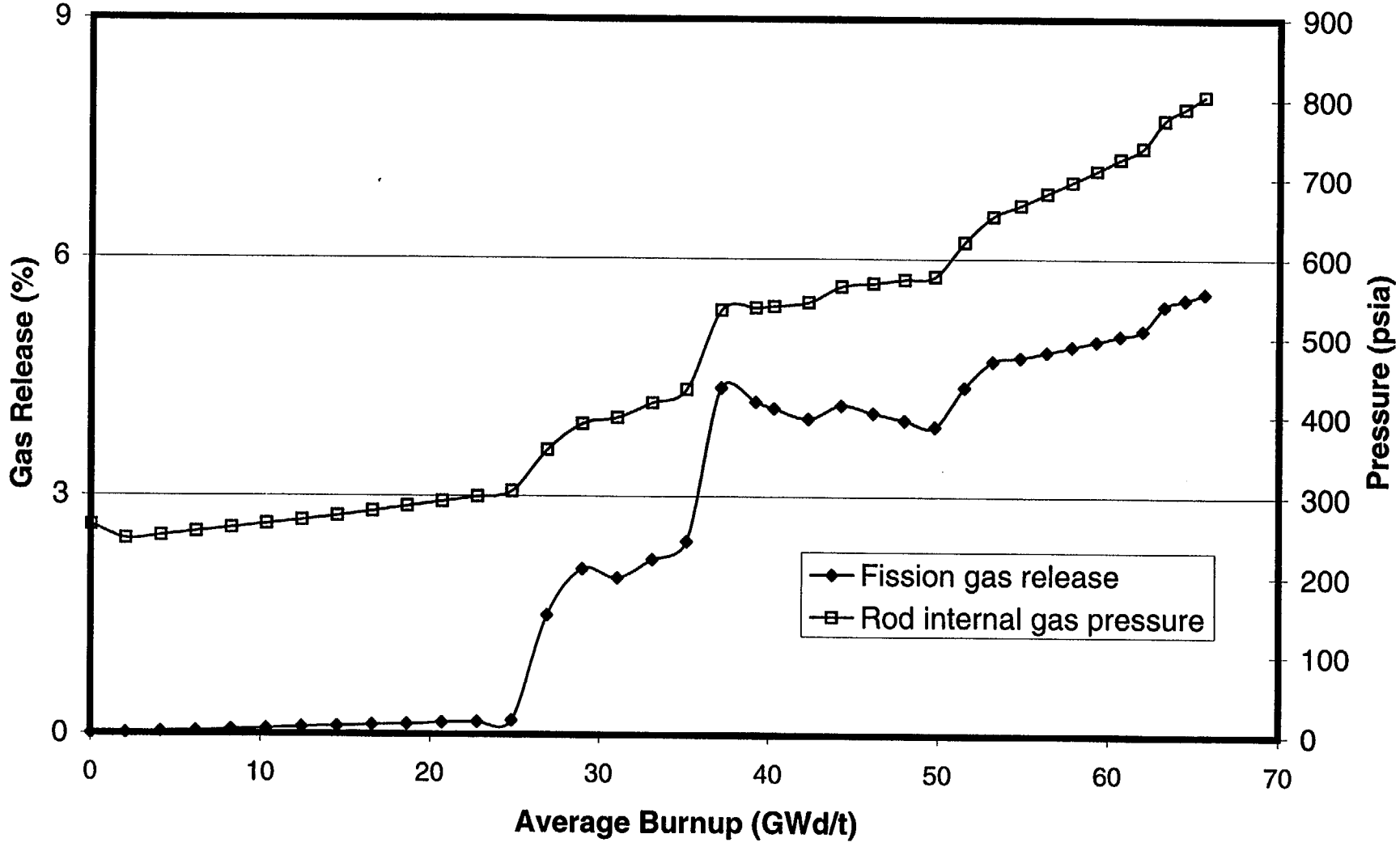

Fig. 6-10. Fission gas release and rod internal gas pressure for a BWR 9x9 fuel rod with initial peak power of 9 kW/ft.

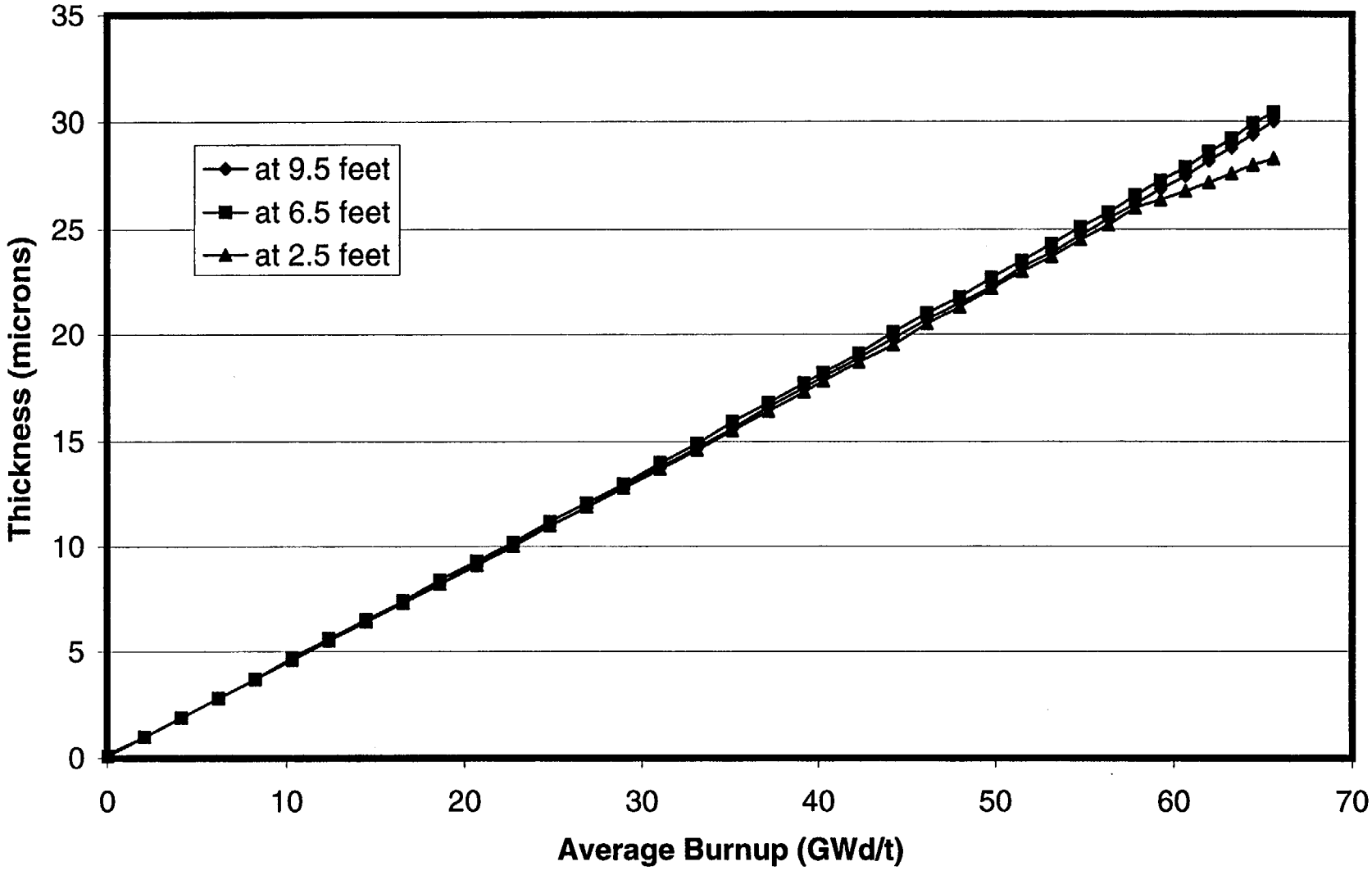

Fig. 6-11. Oxide thickness at three axial locations for a BWR 9x9 fuel rod with initial peak power of 9 kW/ft.

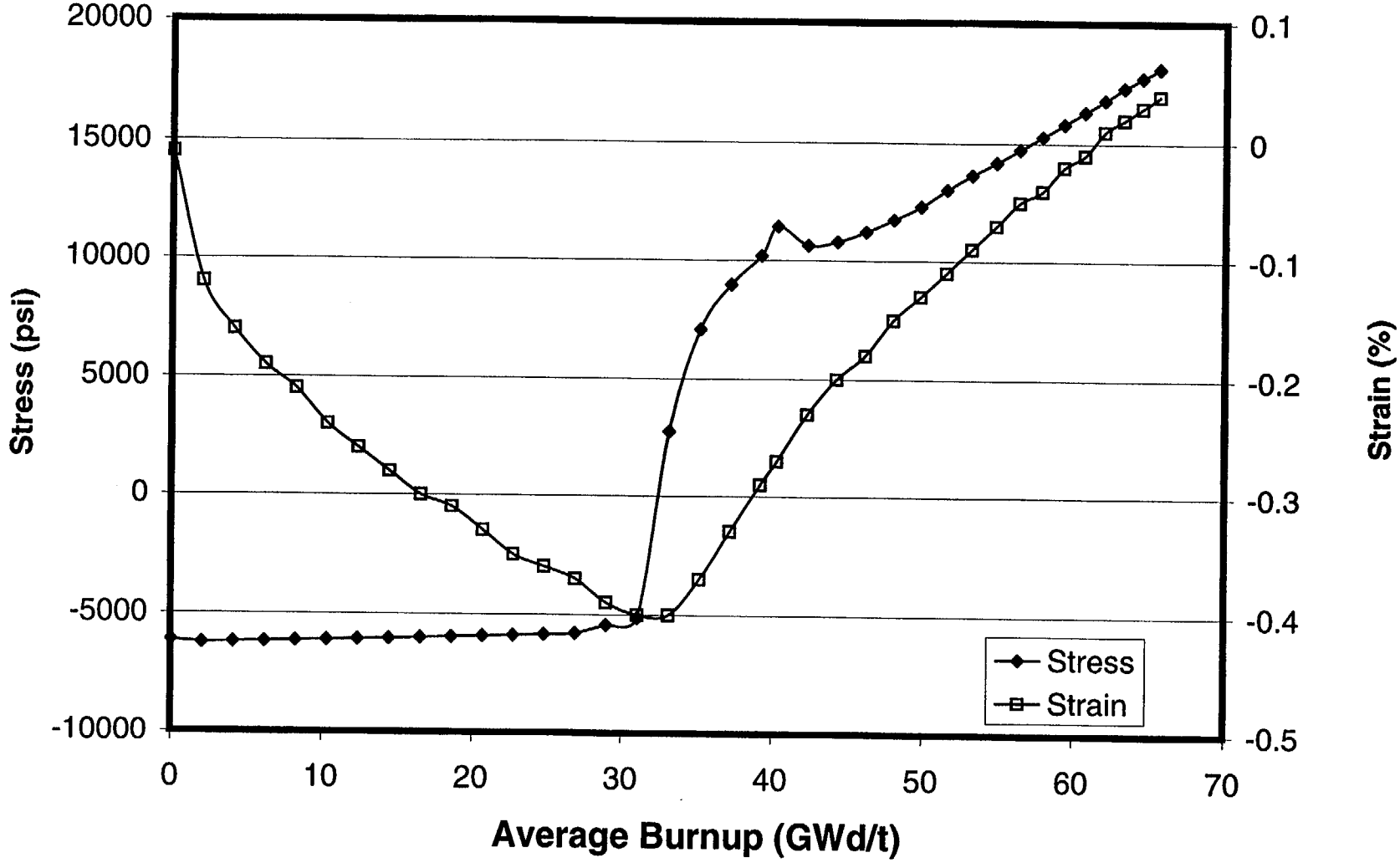

Fig. 6-12. Cladding hoop stress and hoop strain for a BWR 9x9 fuel rod with initial peak power of 9 kW/ft.

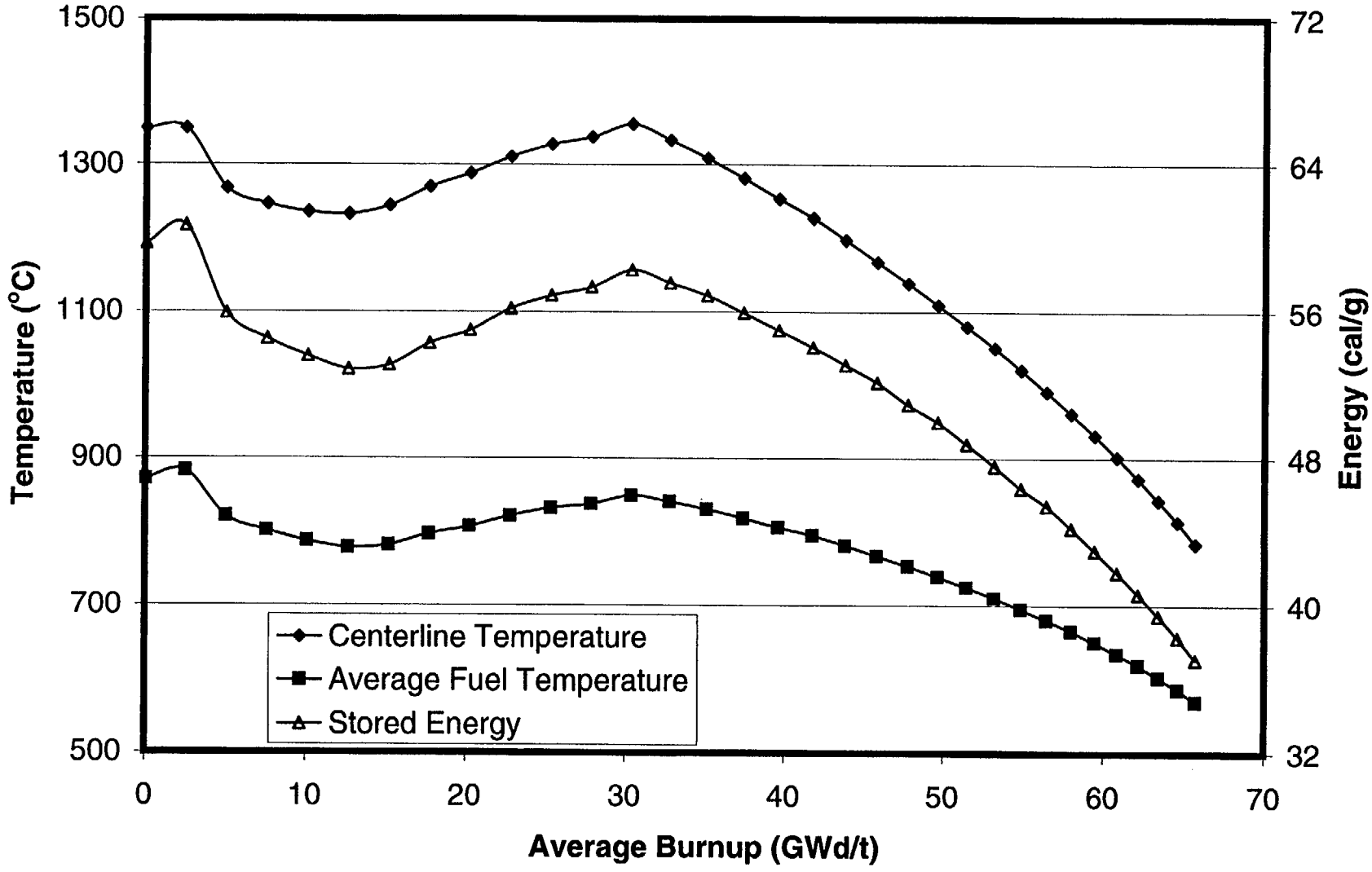

Fig. 6-13. Fuel temperatures and stored energy for a BWR 9x9 fuel rod with initial peak power of 11 kW/ft.

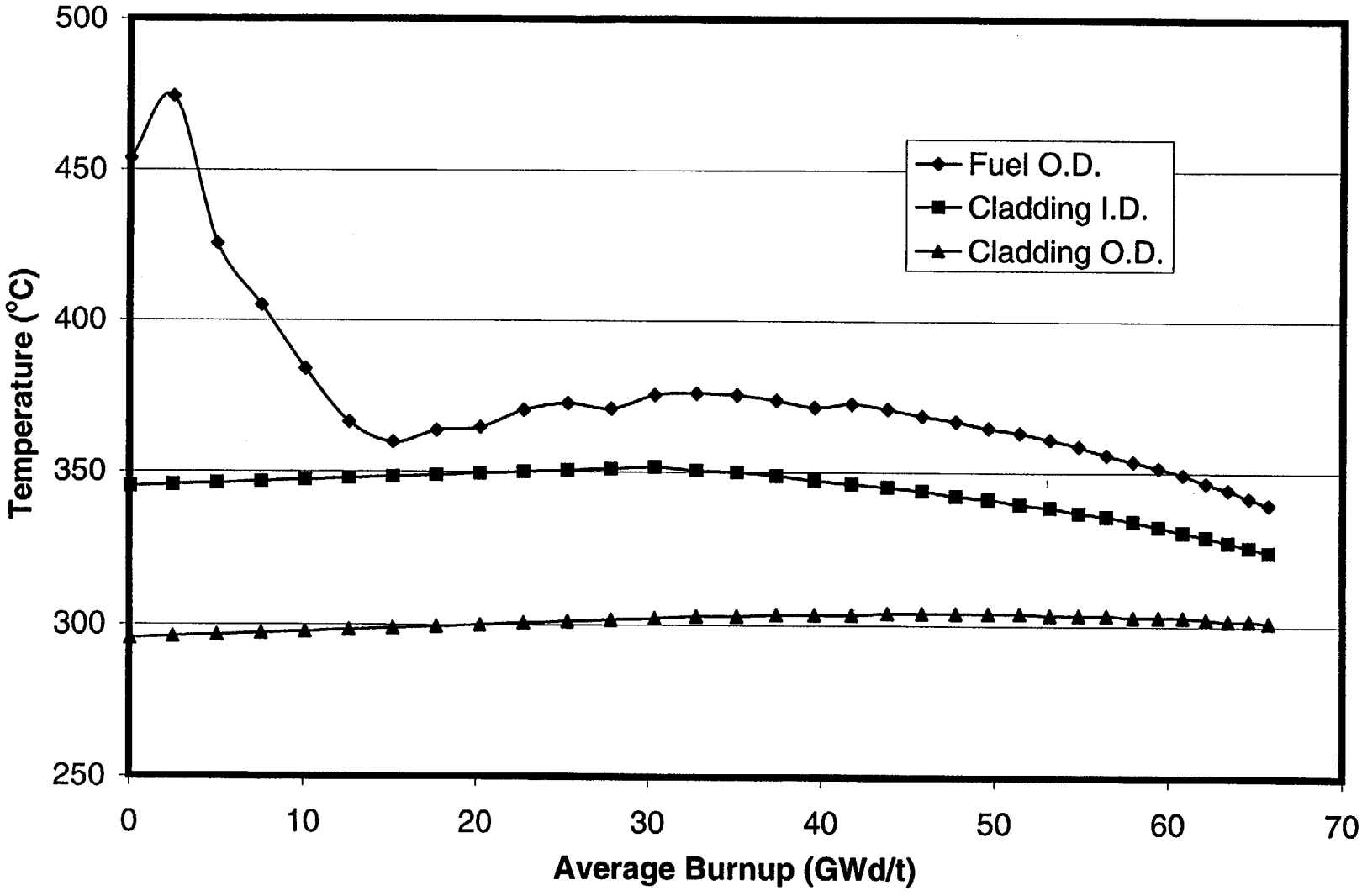

Fig. 6-14. Cladding temperatures and fuel surface temperature for a BWR 9x9 fuel rod with initial peak power of 11 kW/ft.

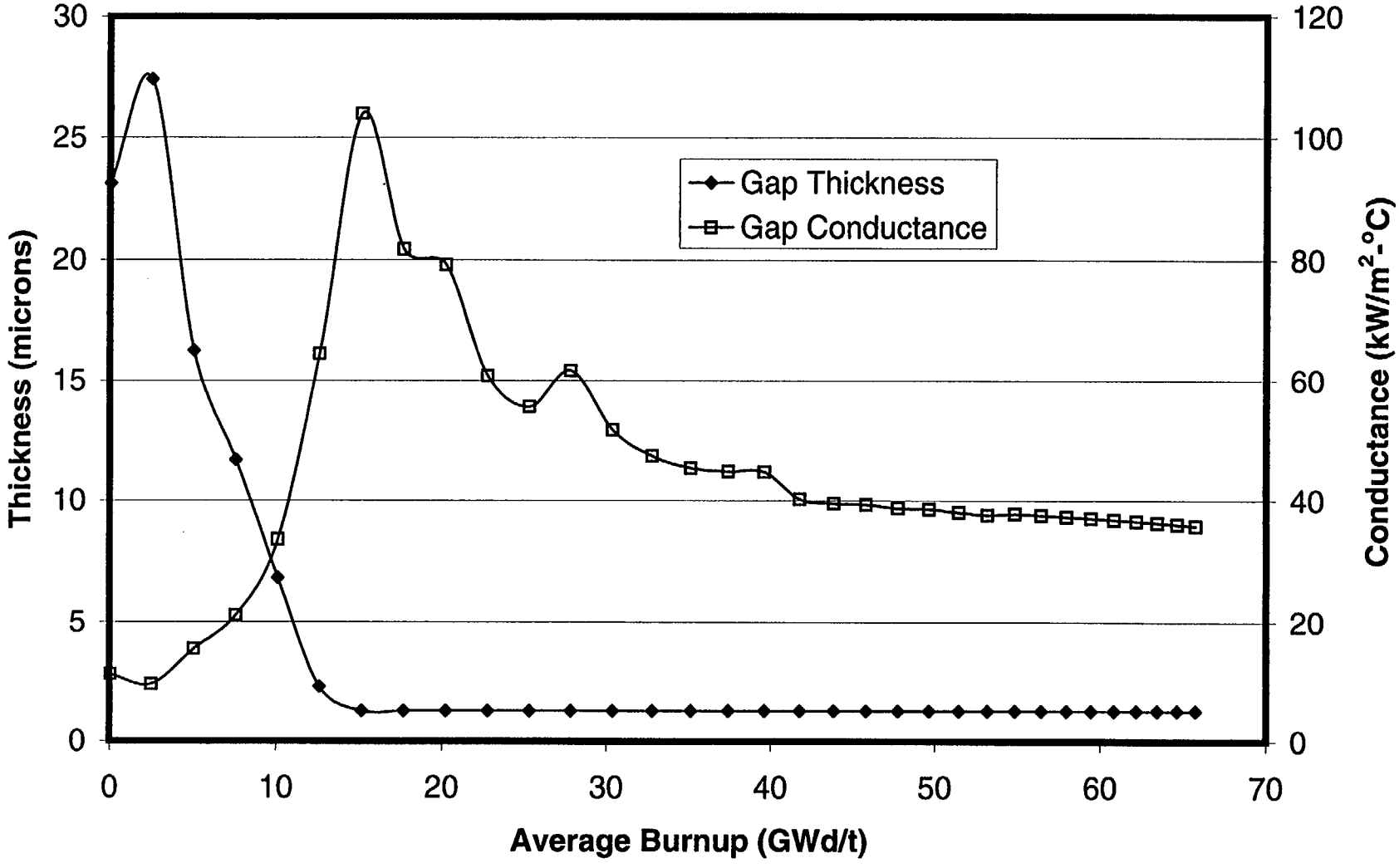

Fig. 6-15. Gap thickness and gap conductance for a BWR 9x9 fuel rod with initial peak power of 11 kW/ft.

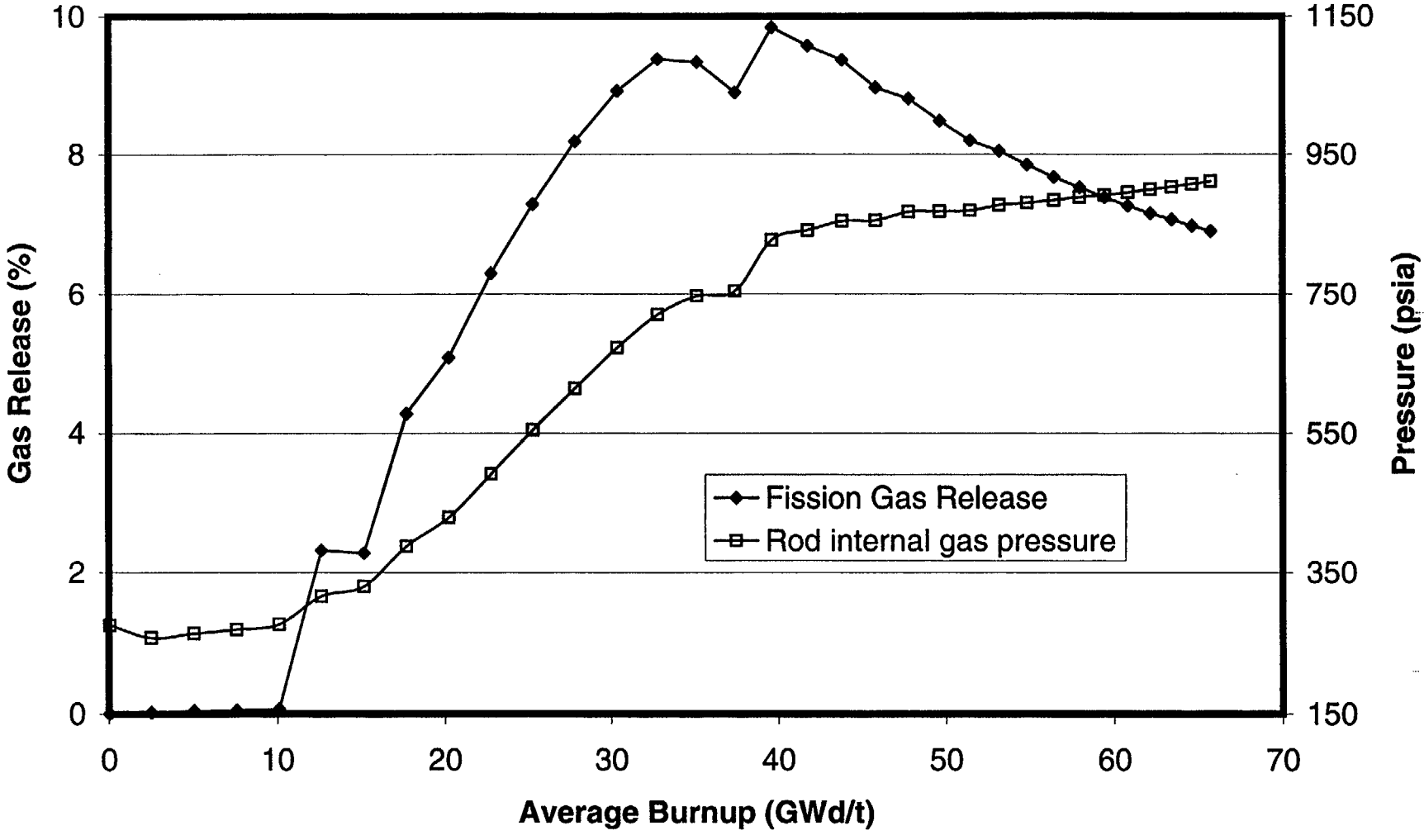

Fig. 6-16. Fission gas release and rod internal gas pressure for a BWR 9x9 fuel rod with initial peak power of 11 kW/ft.

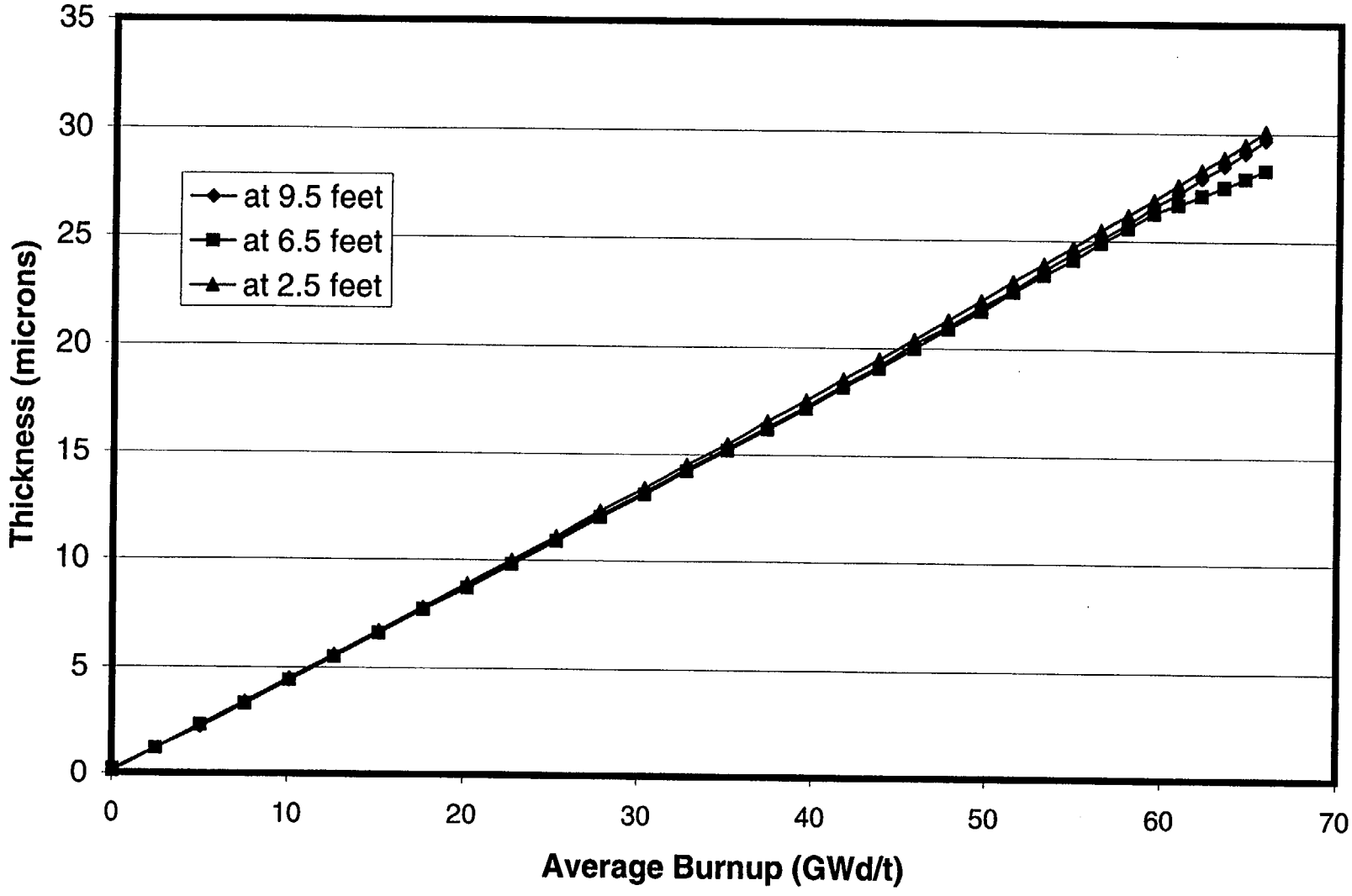

Fig. 6-17. Oxide thickness at three axial locations for a BWR 9x9 fuel rod with initial peak power of 11 kW/ft.

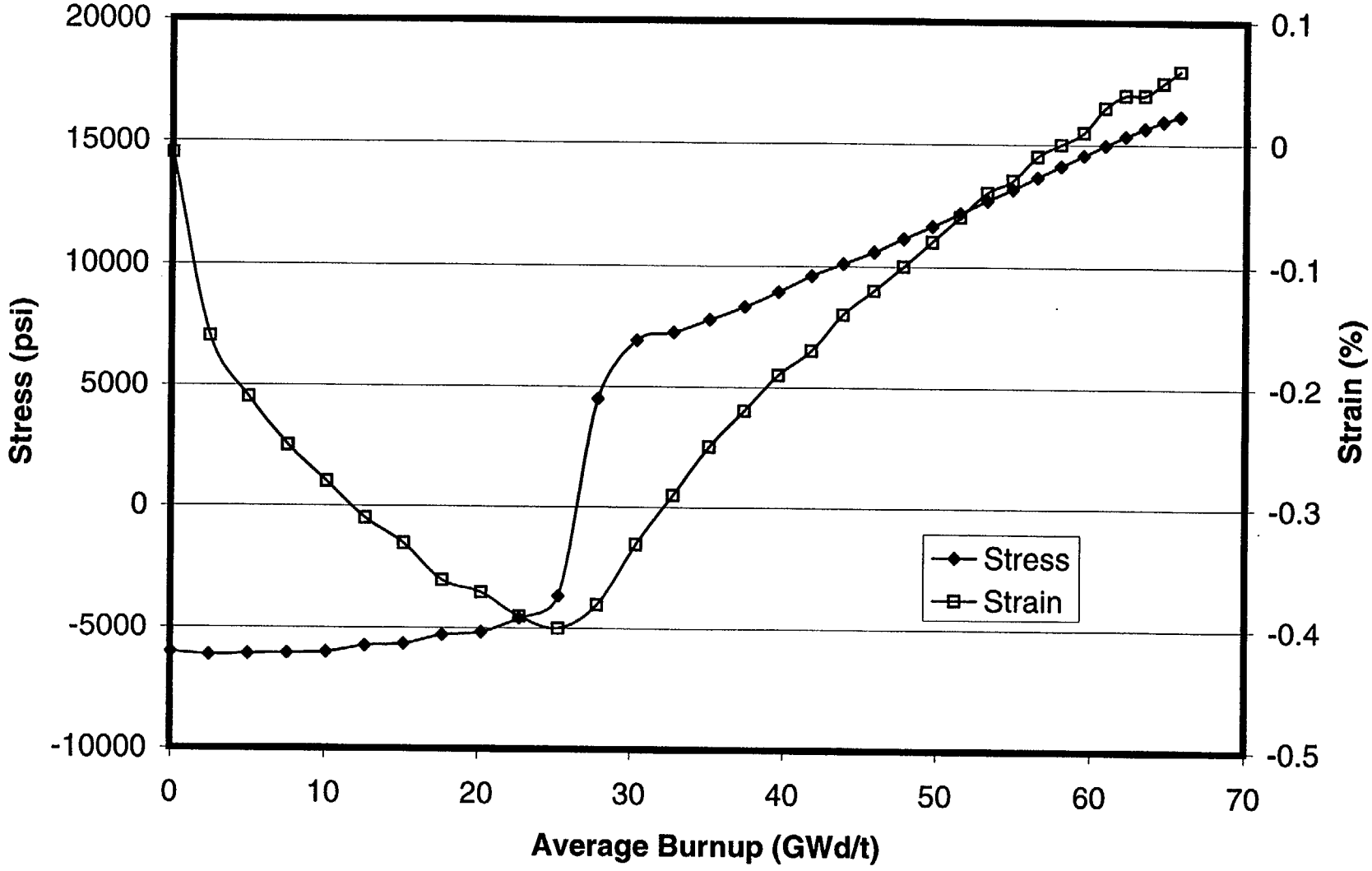

Fig. 6-18. Cladding hoop stress and hoop strain for a BWR 9x9 fuel rod with initial peak power of 11 kW/ft.

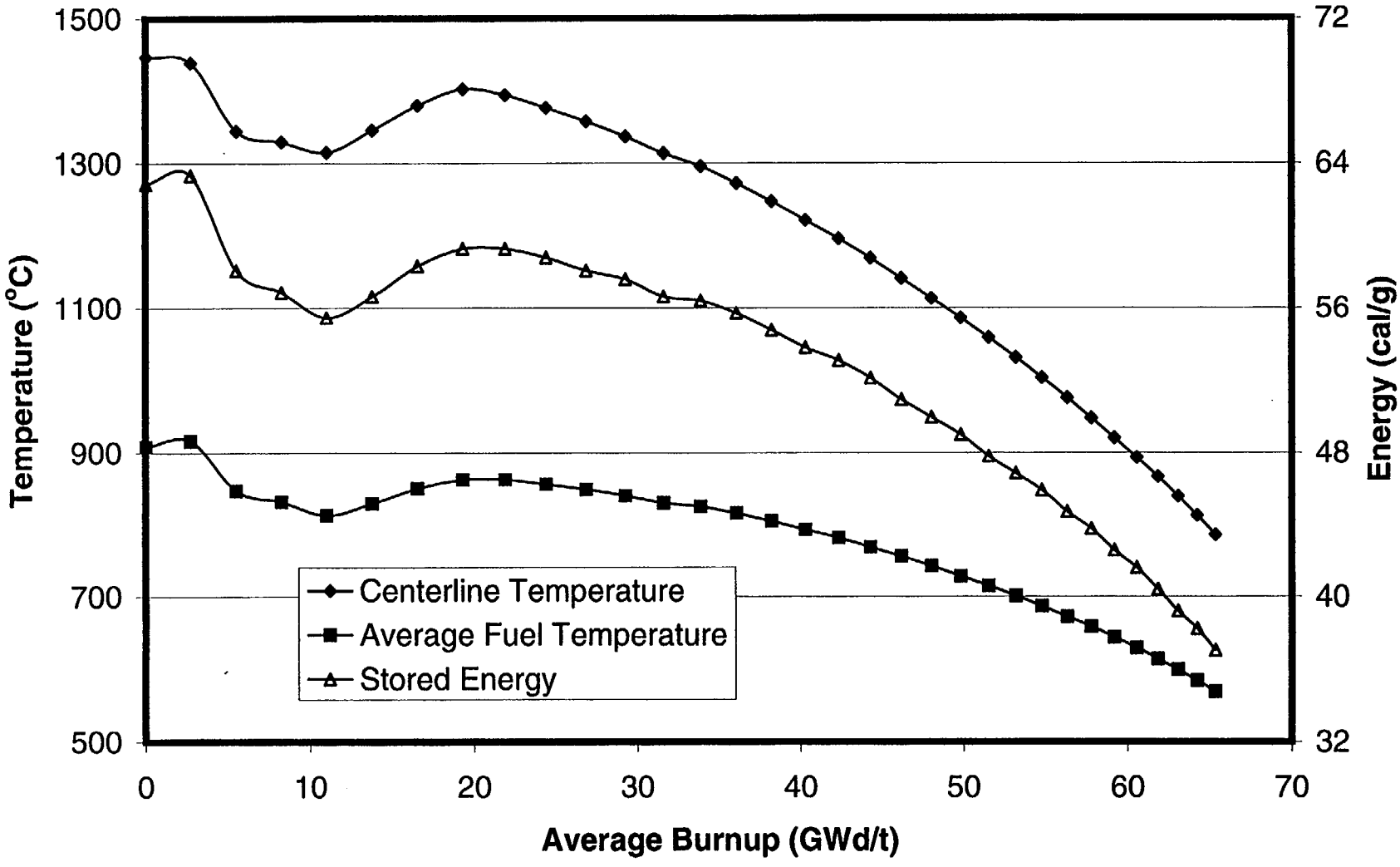

Fig. 6-19. Fuel Temperatures and stored energy for a BWR 9x9 fuel rod with initial peak power of 12 kW/ft.

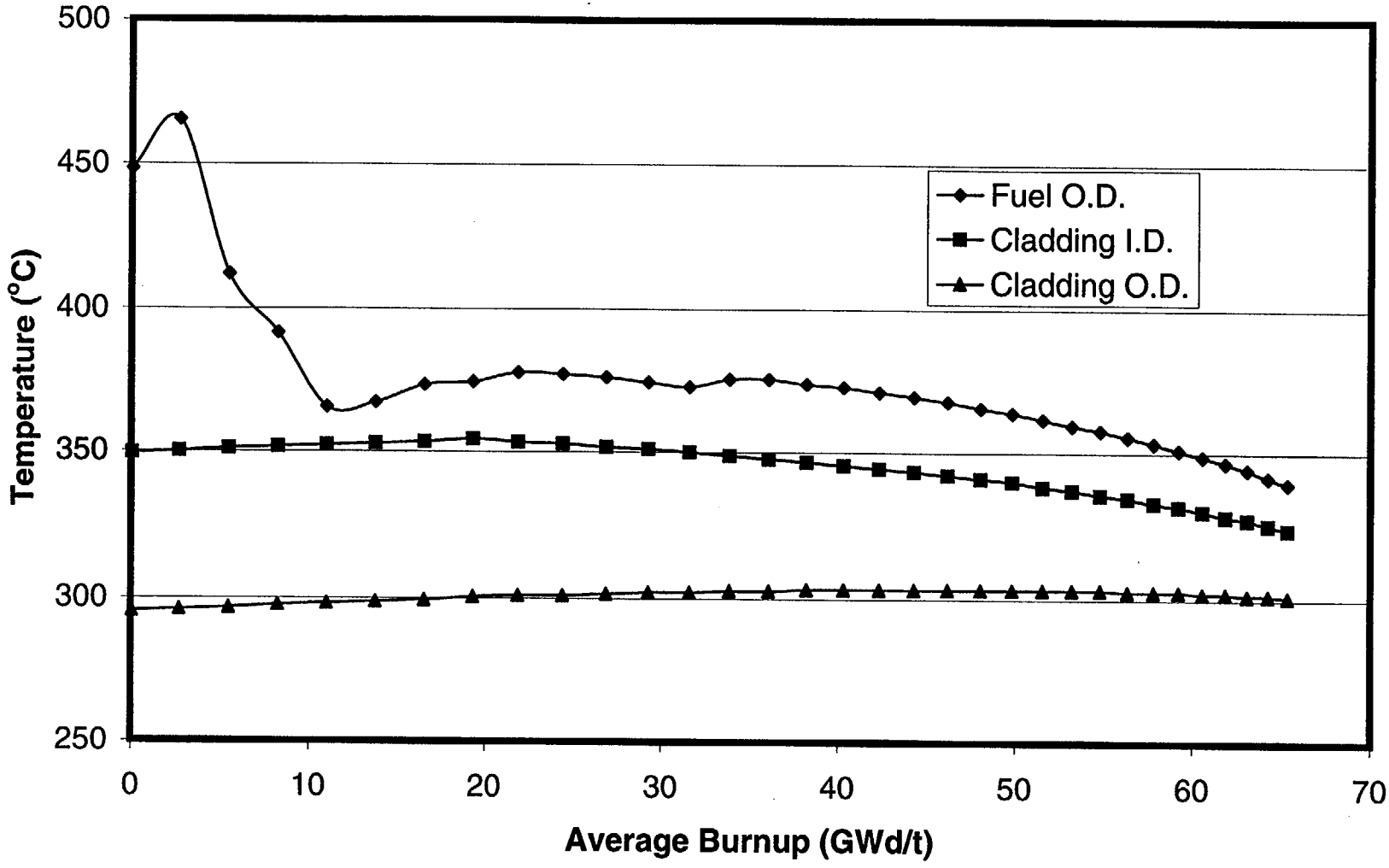

Fig. 6-20. Cladding temperatures and fuel surface temperature for a BWR 9x9 fuel rod with initial peak power of 12 kW/ft.

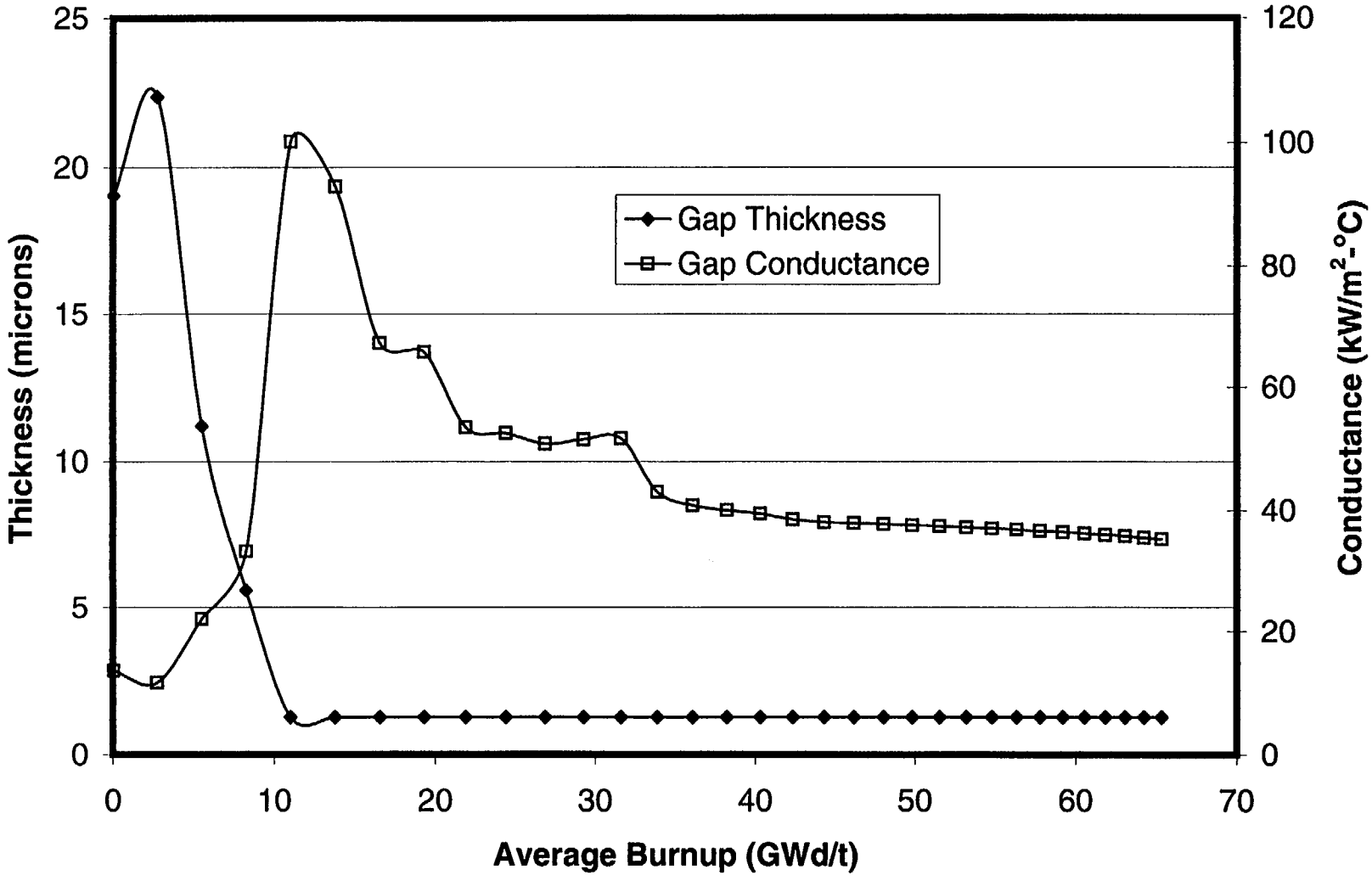

Fig. 6-21. Gap thickness and gap conductance for a BWR 9x9 fuel rod with initial peak power of 12 kW/ft.

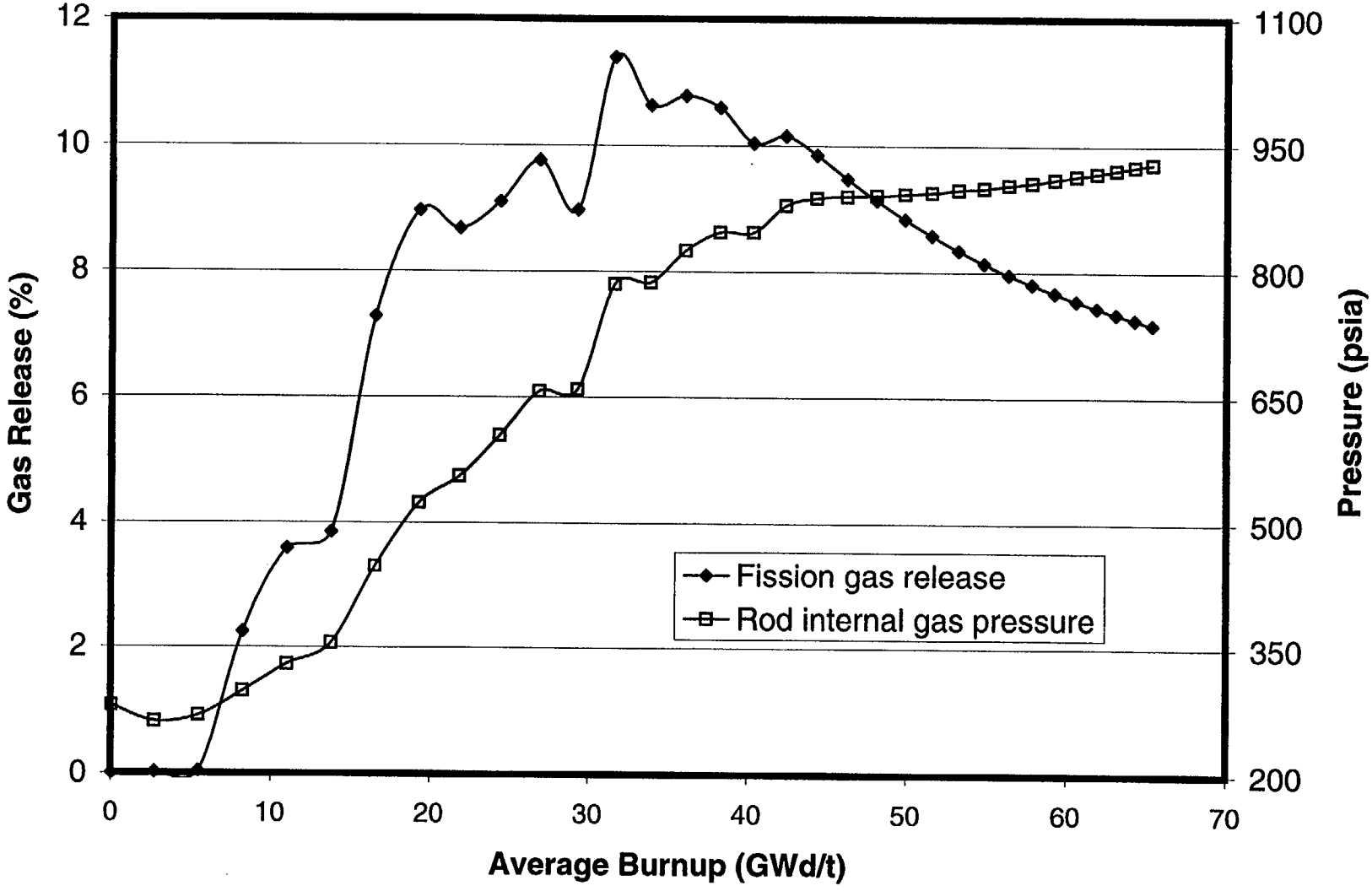

Fig. 6-22. Fission gas release and rod internal gas pressure for a BWR 9x9 fuel rod with initial peak power of 12 kW/ft.

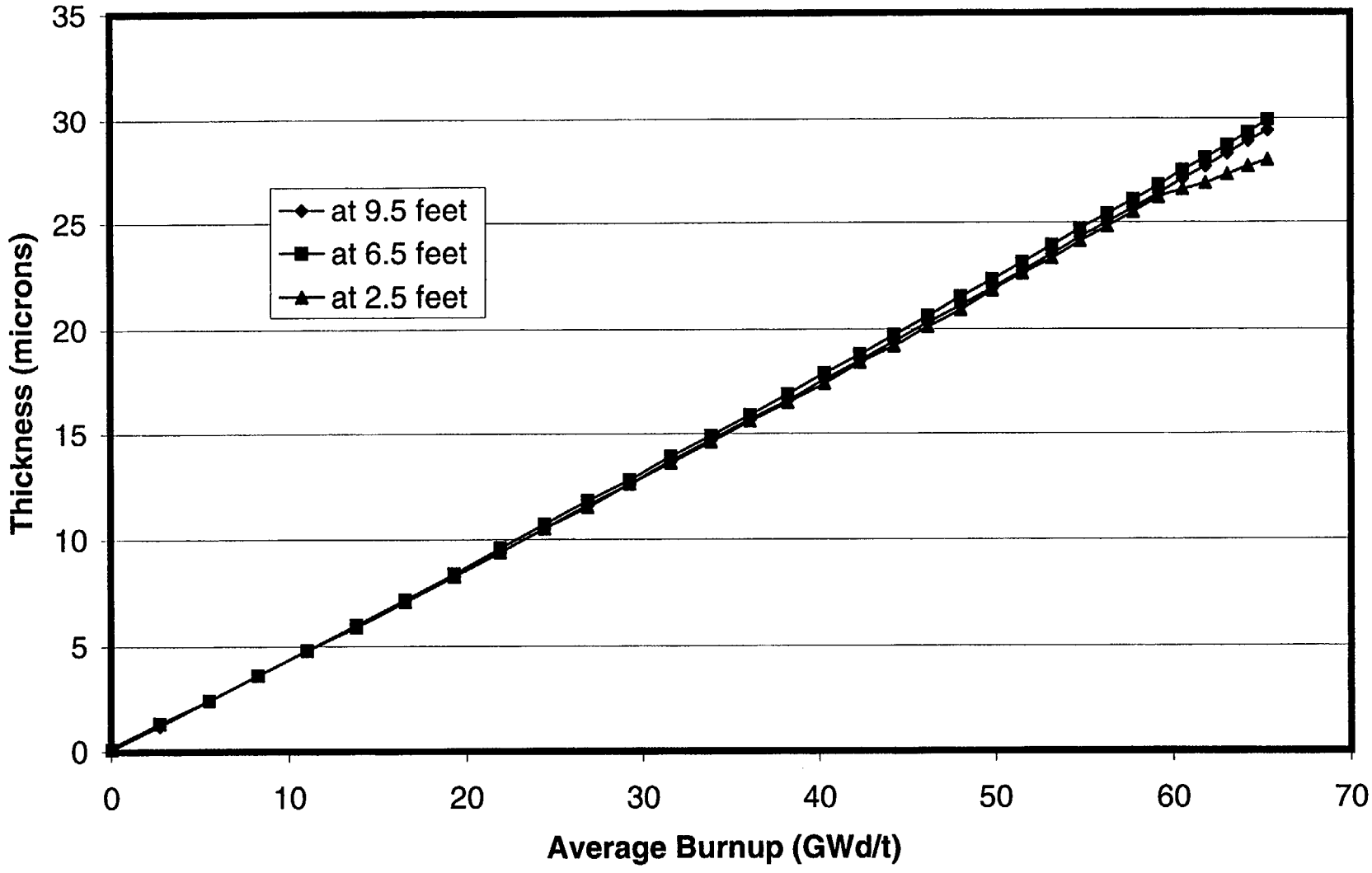

Fig. 6-23. Oxide thickness at three axial locations for a BWR 9x9 fuel rod with initial peak power of 12 kW/ft.

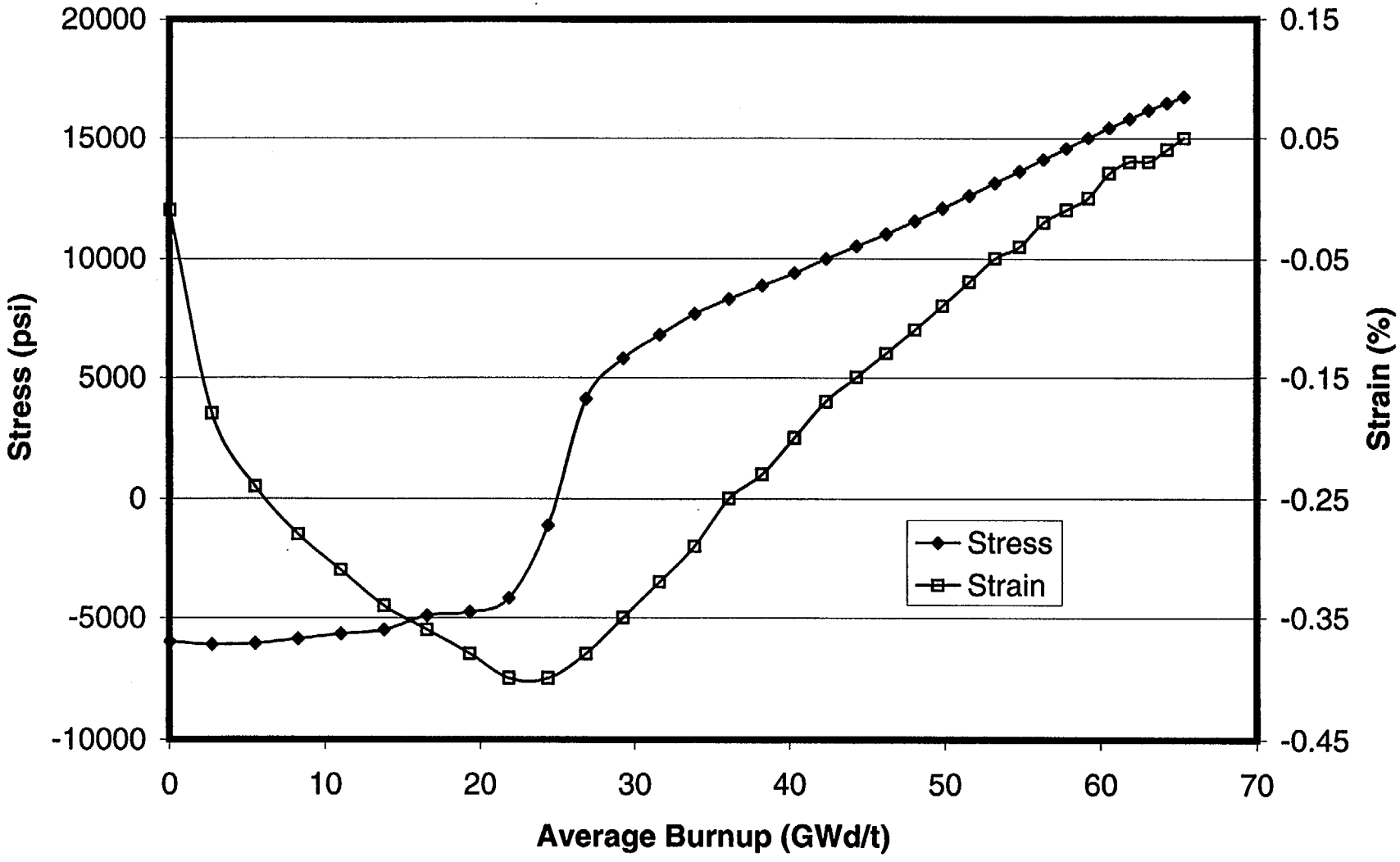

Fig. 6-24. Cladding hoop stress and hoop strain for a BWR 9x9 fuel rod with initial peak power of 12 kW/ft.

7. Calculations for BWR 10x10 Fuel

In the following figures, calculated values for BWR 10x10 fuel are plotted as a function of burnup for the parameters listed below:

Fuel centerline temperature
Average fuel temperature
Stored energy
Fuel O.D. temperature
Cladding I.D. temperature
Cladding O.D. temperature
Gap thickness
Gap conductance
Fission gas release
Rod internal gas pressure
Oxide thickness
Cladding hoop stress
Cladding hoop strain

Several general observations can be made about the calculated results:

- Within the first few GWd/t of burnup, a temperature peak is observed that is the result of fuel densification.

- Gap closure results in (a) the coming together of temperatures for fuel O.D. and cladding I.D. and (b) a sharp increase in gap conductance. The gap conductance increases again after a few time steps when the interaction between the pellet and cladding affects the contact conductance calculated for a closed gap. At this point there is also a large increase in stress, and the permanent strain changes directions.

- Some of the fission gas is released in spurts according to the Massih model in FRAPCON-3. This effect is apparent in many of the figures. Shorter time steps would produce slightly different looking curves, but the trend of gas release and the end-of-life gas release would be about the same.

- The burnup enhancement of fission gas release is readily seen in the lower power cases, but it is obscured in the highest power cases by the magnitude of prior gas release.

- Rod internal gas pressure increases with the accumulation of released fission gas. In the higher power PWR cases, as the power drops off near the end of life, the reduction in the plenum temperature offsets the increasing moles of fission gas.

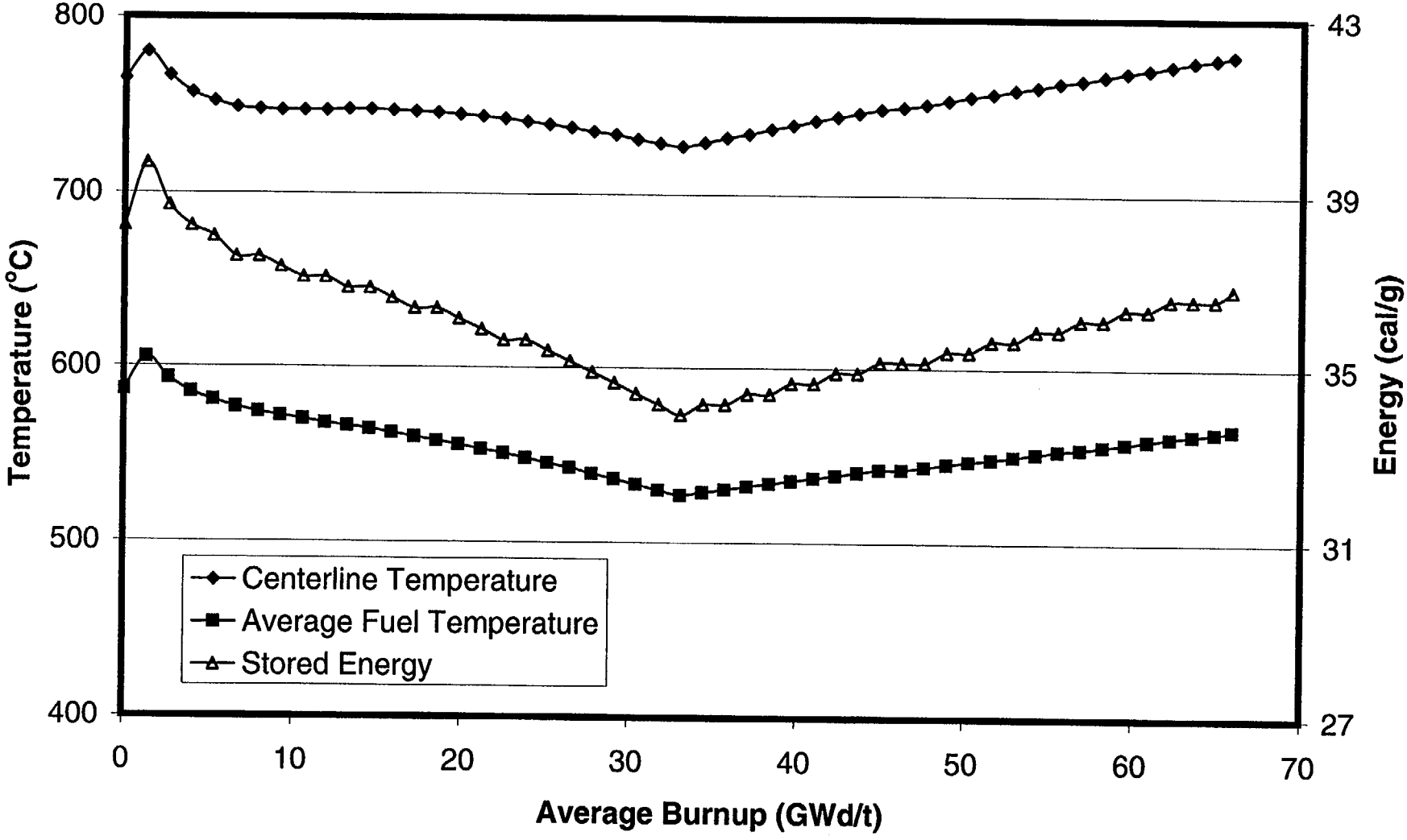

Fig. 7-1. Fuel temperatures and stored energy for a BWR 10x10 fuel rod with initial peak power of 5 kW/ft.

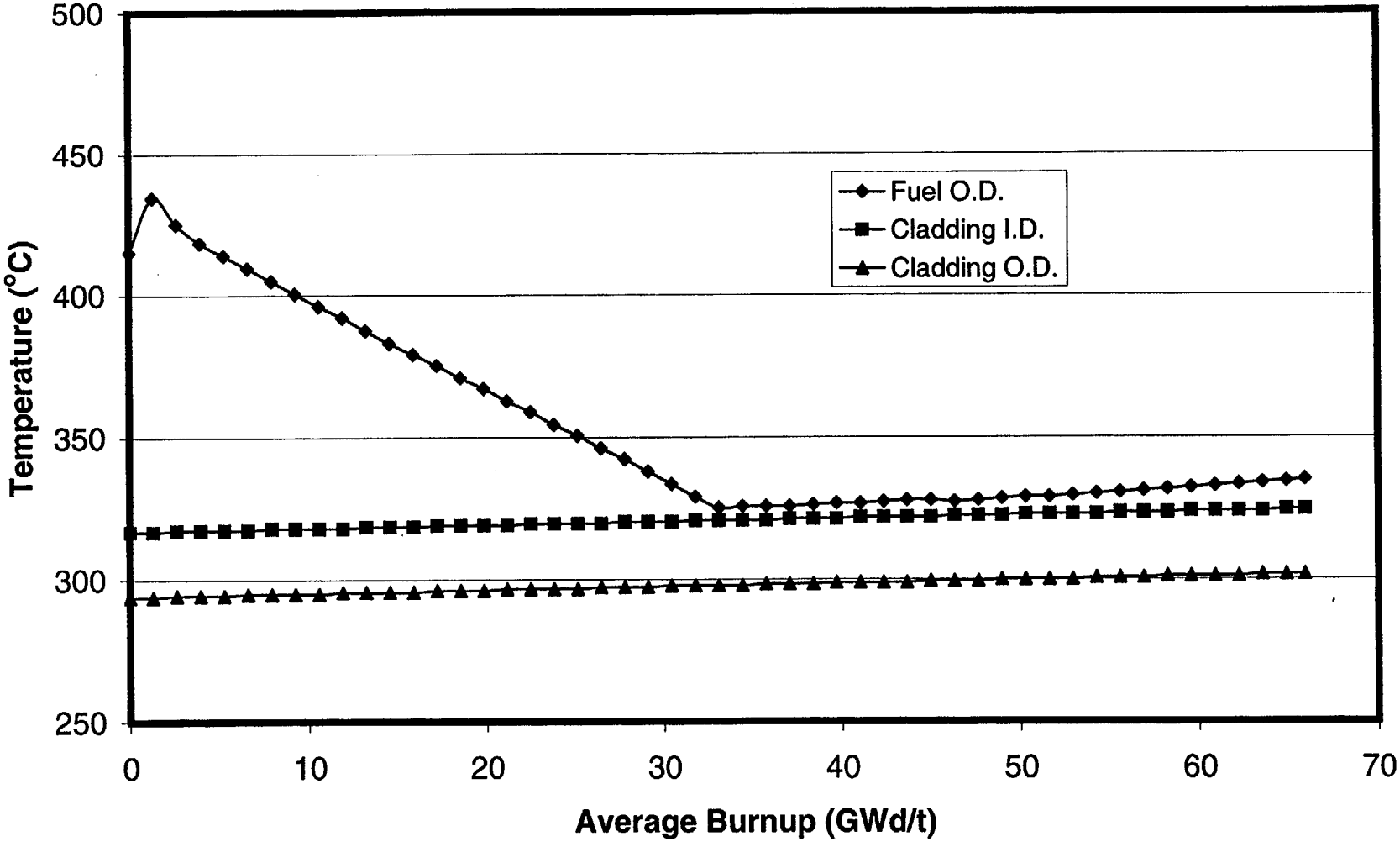

Fig. 7-2. Cladding temperatures and fuel surface temperature for a BWR 10x10 fuel rod with initial peak power of 5 kW/ft.

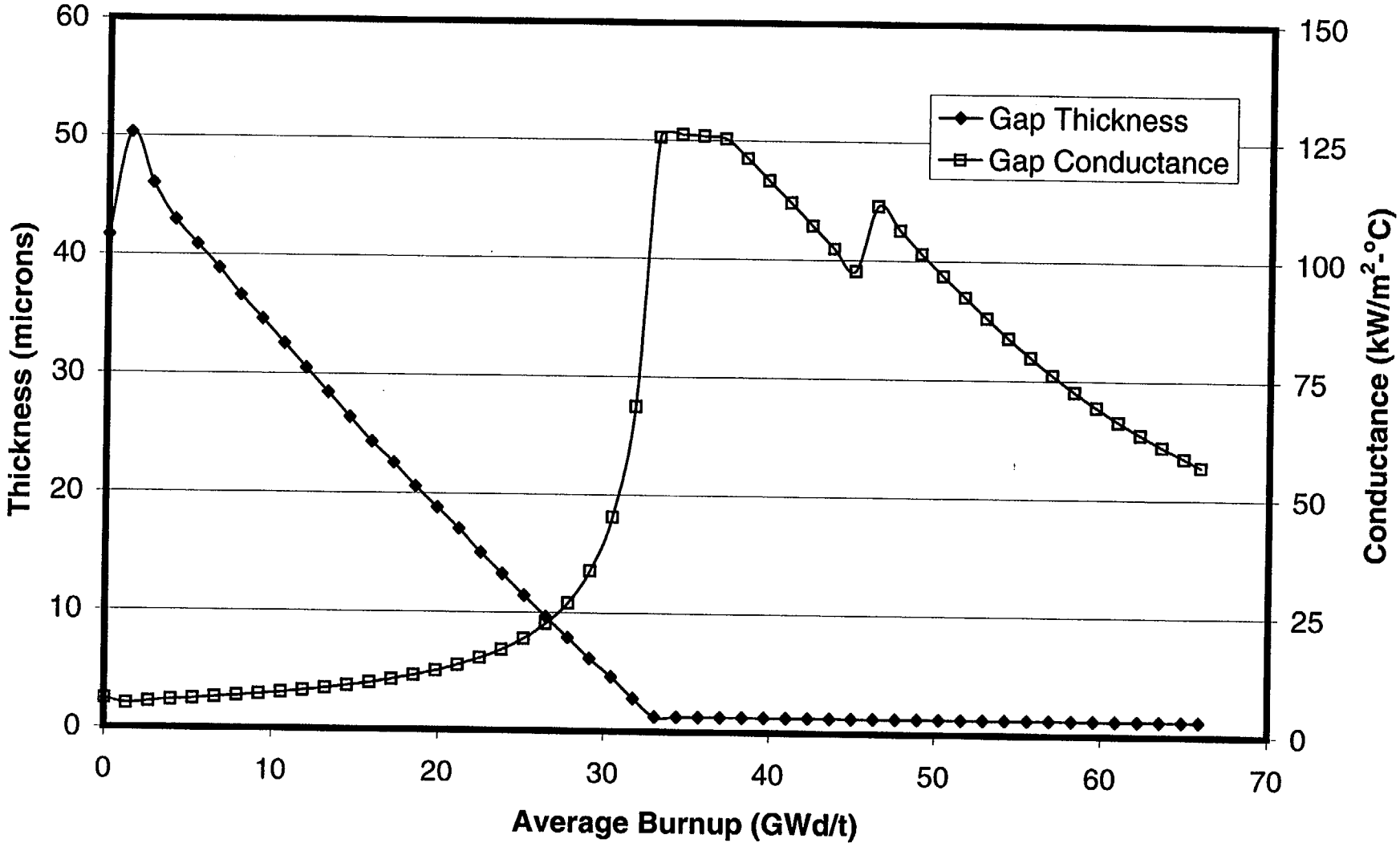

Fig. 7-3. Gap thickness and gap conductance for a BWR 10x10 fuel rod with initial peak power of 5 kW/ft.

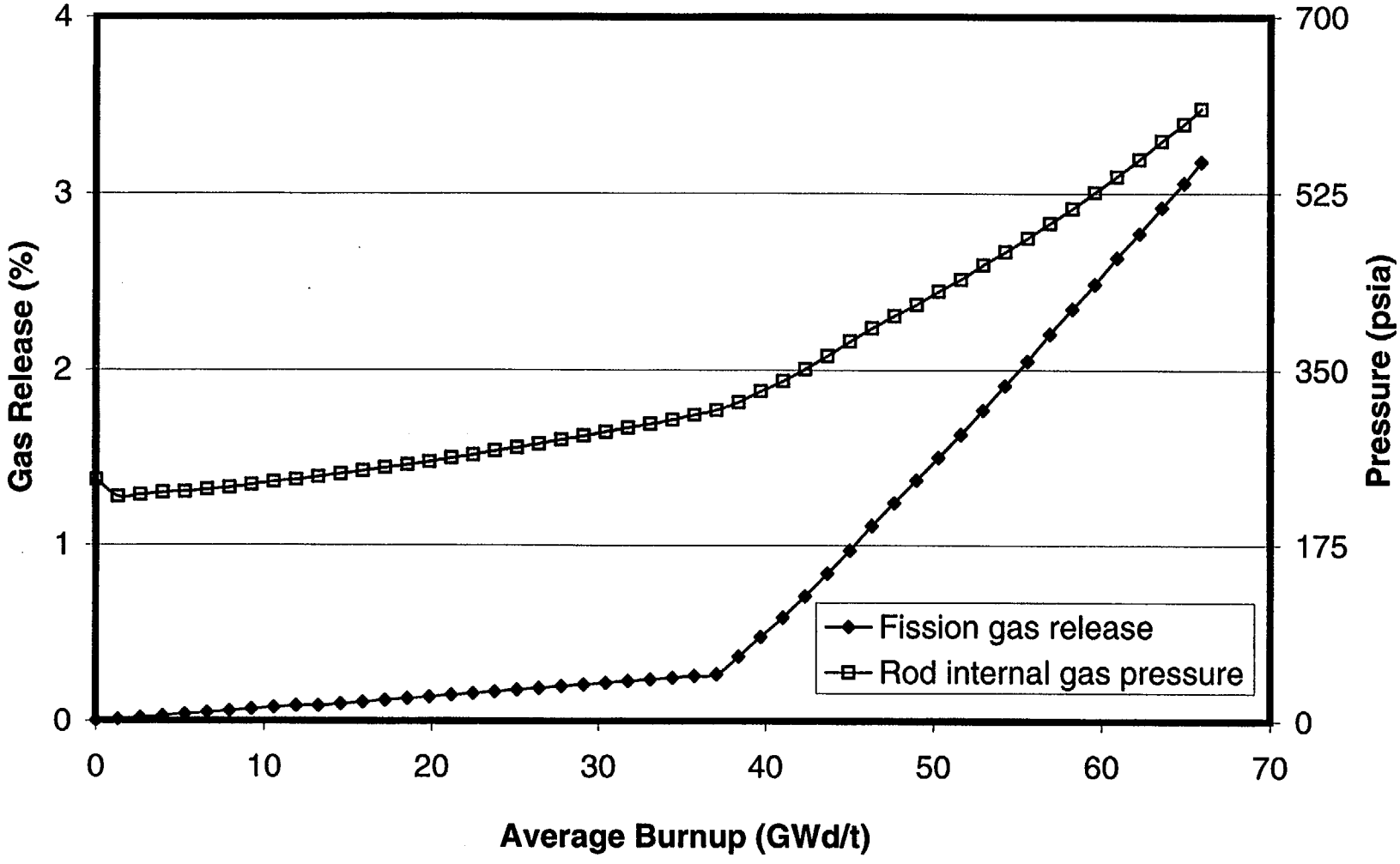

Fig. 7-4. Fission gas release and rod internal gas pressure for a BWR 10x10 fuel rod with initial peak power of 5 kW/ft.

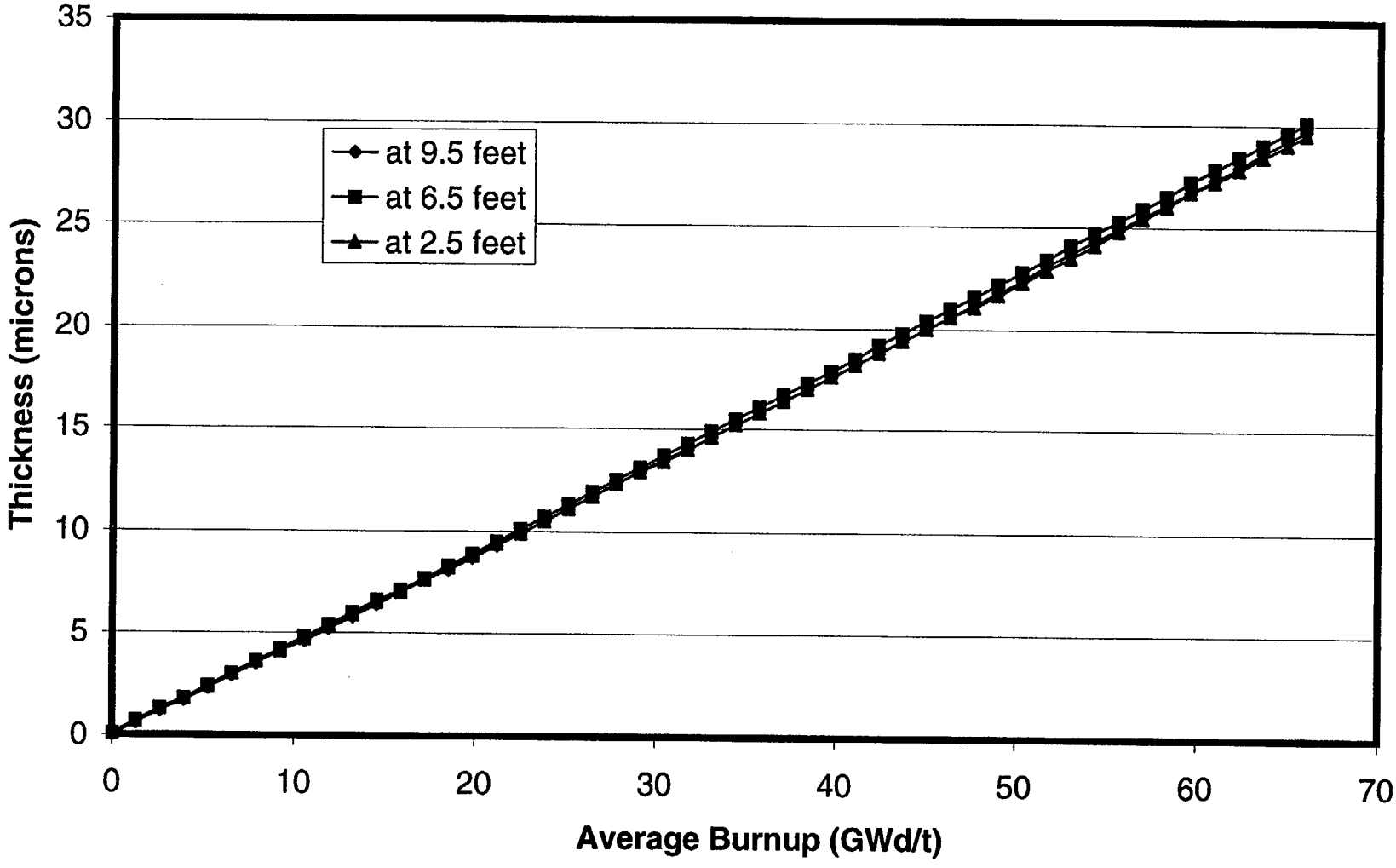

Fig. 7-5. Oxide thickness at three axial locations for a BWR 10x10 fuel rod with initial peak power of 5 kW/ft.

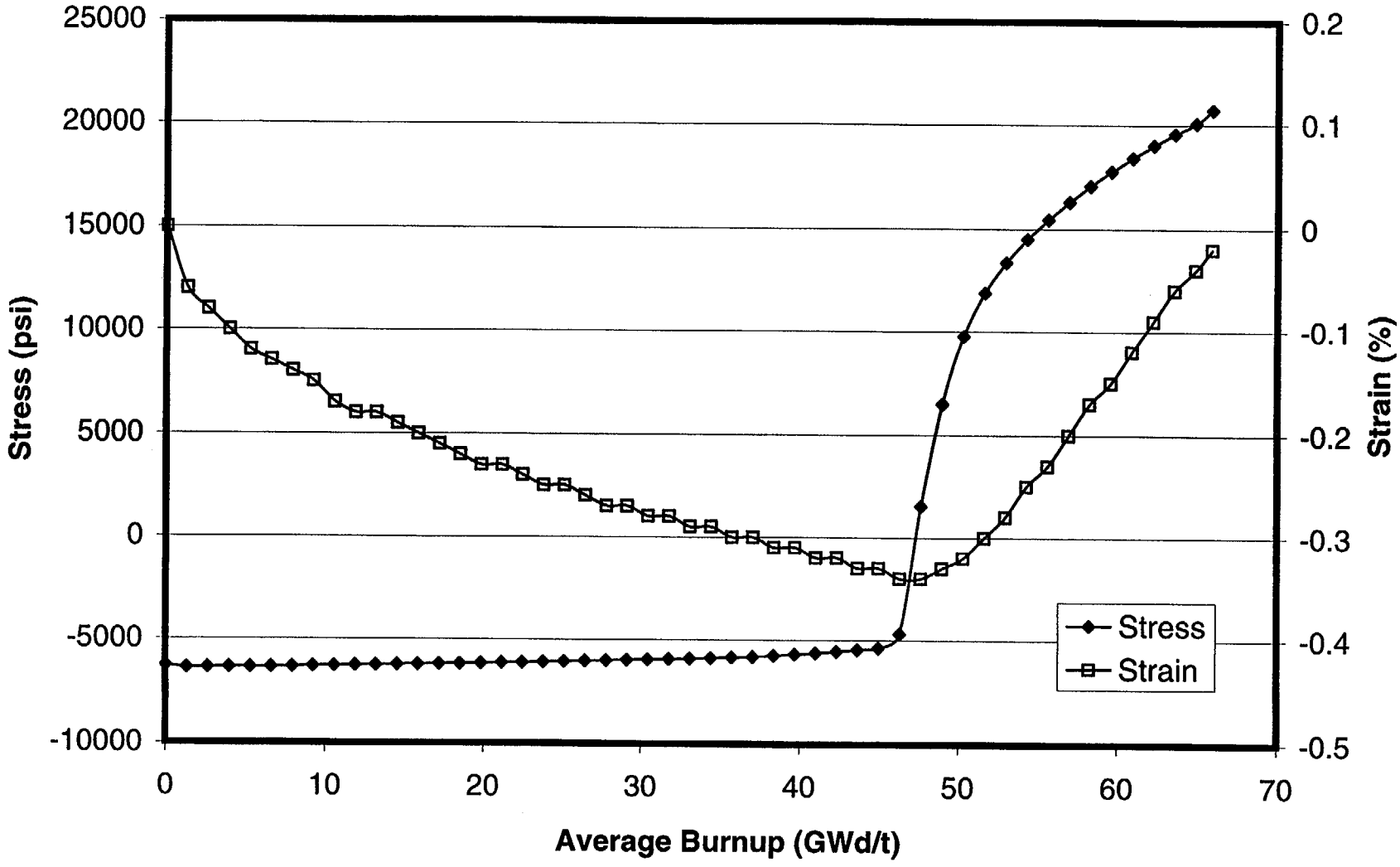

Fig. 7-6. Cladding hoop stress and hoop strain for a BWR 10x10 fuel rod with initial peak power of 5 kW/ft.

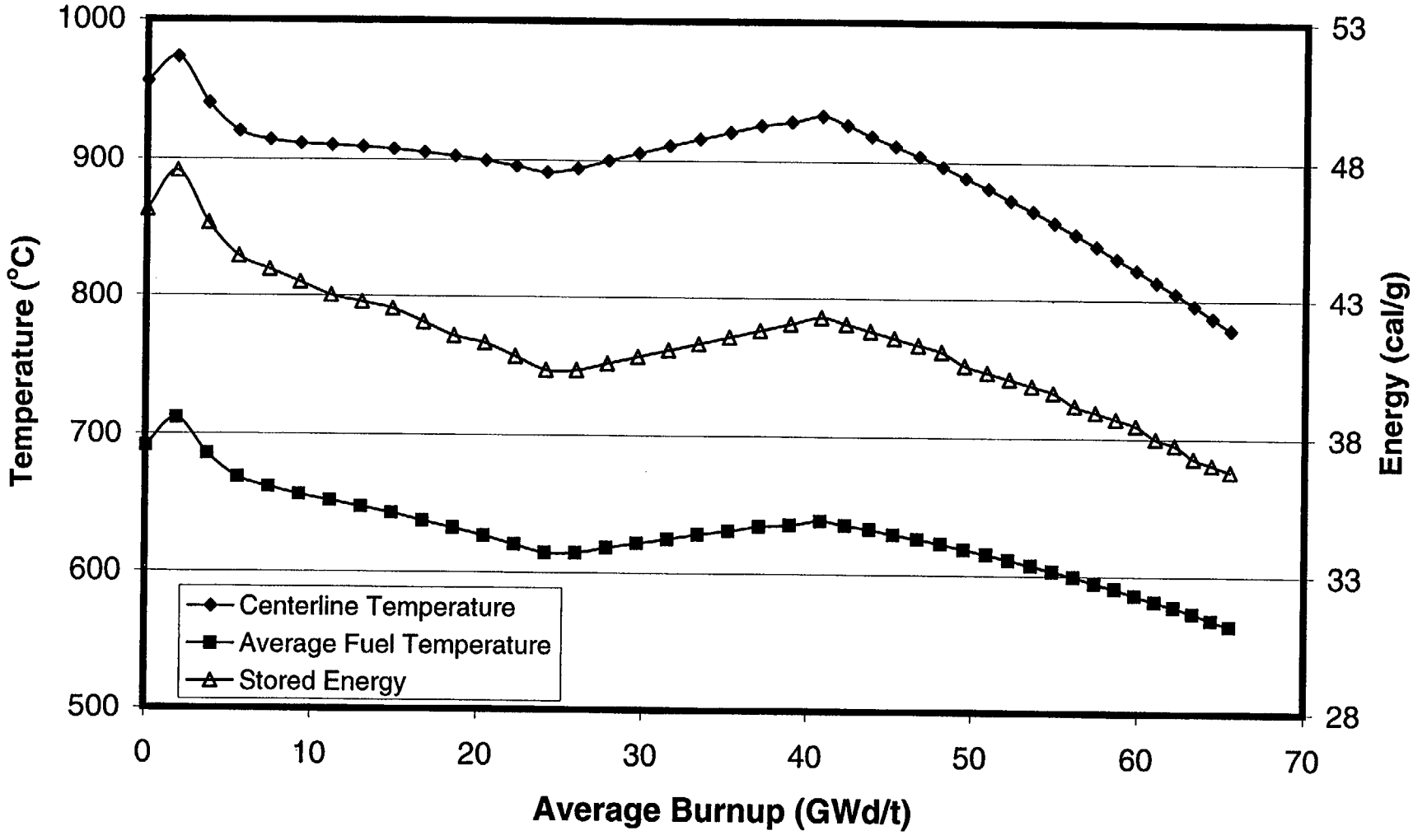

Fig. 7-7. Fuel temperatures and stored energy for a BWR 10x10 fuel rod with initial peak power of 7 kW/ft.

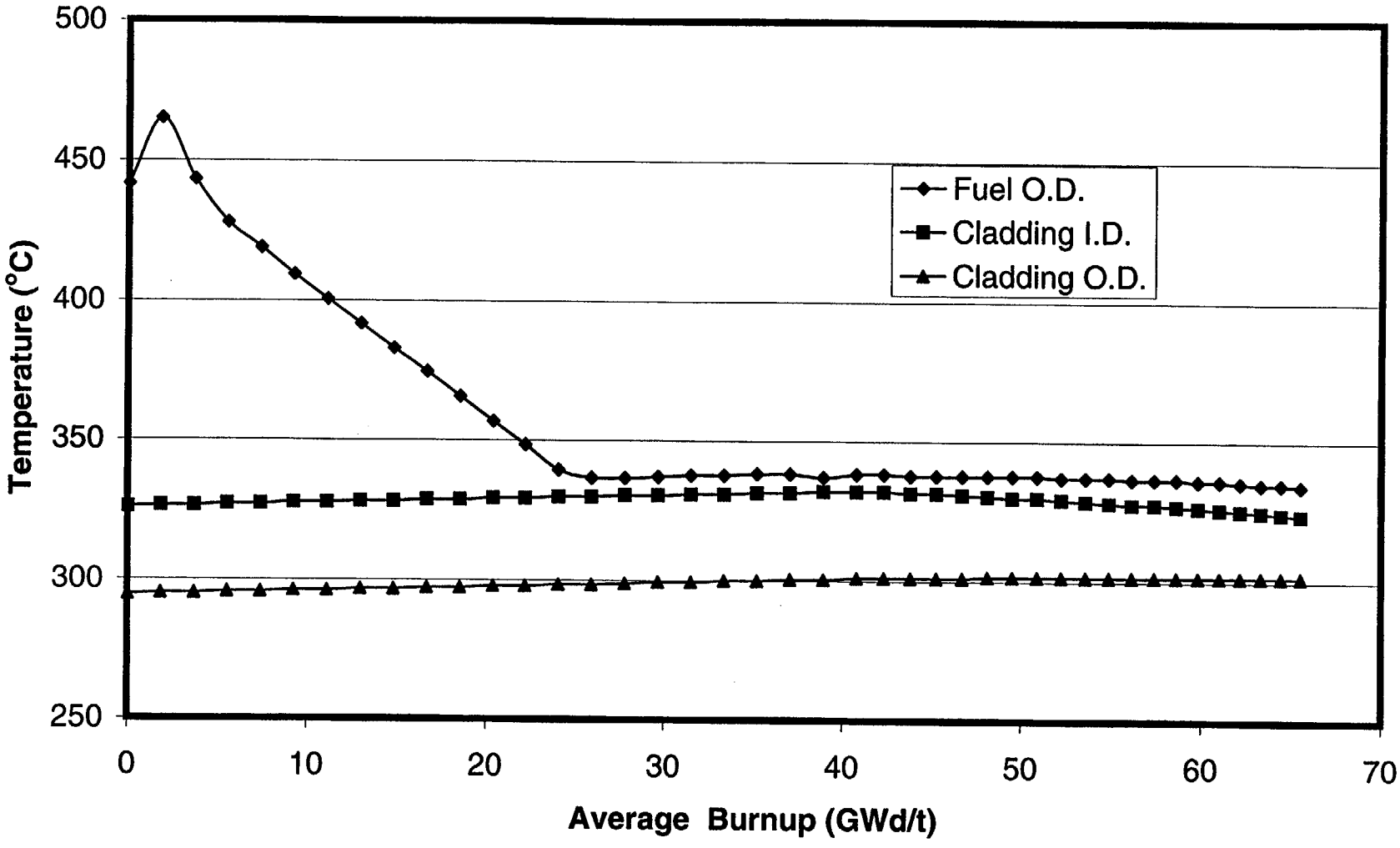

Fig. 7-8. Cladding temperatures and fuel surface temperature for a BWR 10x10 fuel rod with initial peak power of 7 kW/ft.

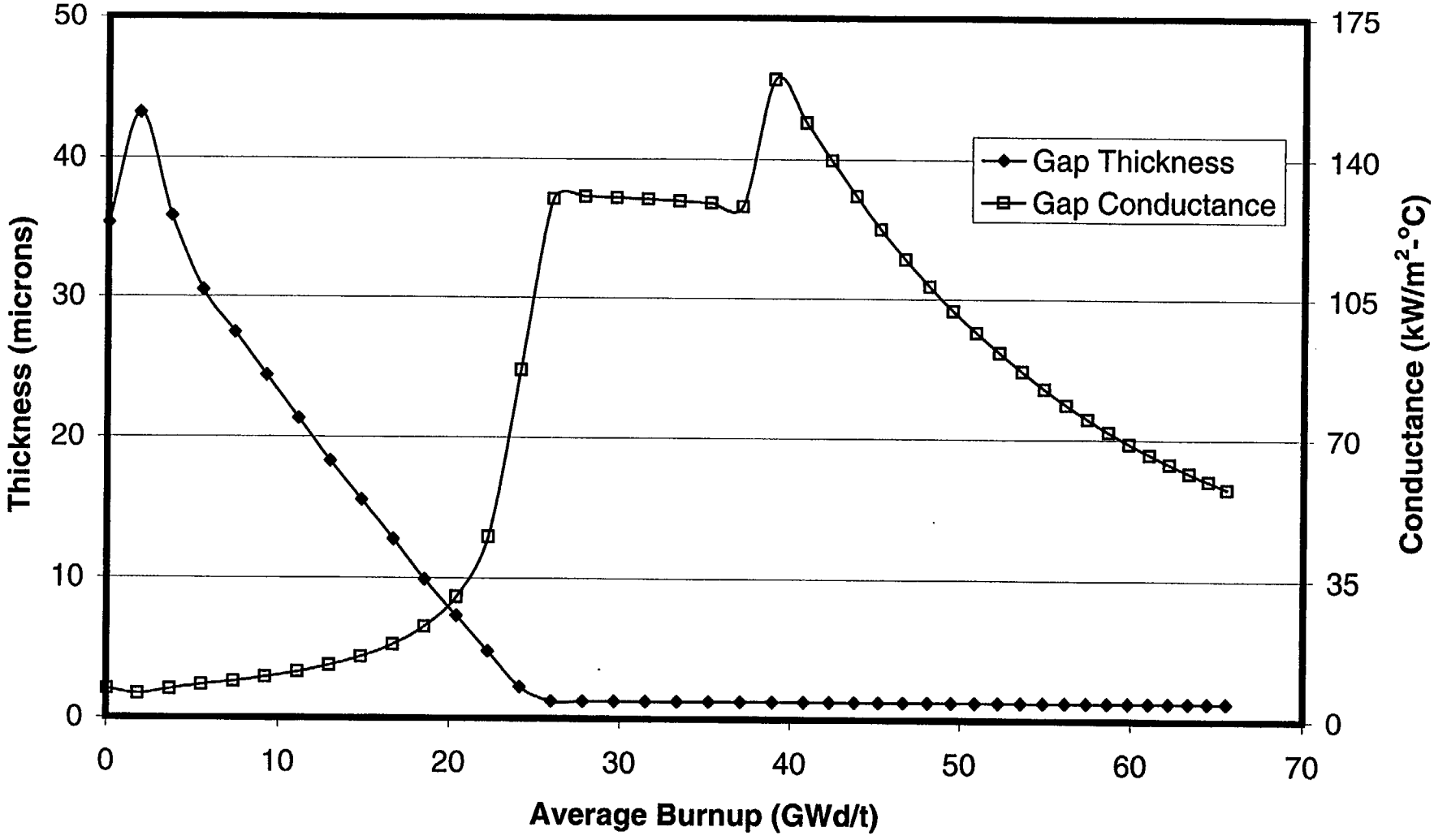

Fig. 7-9. Gap thickness and gap conductance for a BWR 10x10 fuel rod with initial peak power of 7 kW/ft.

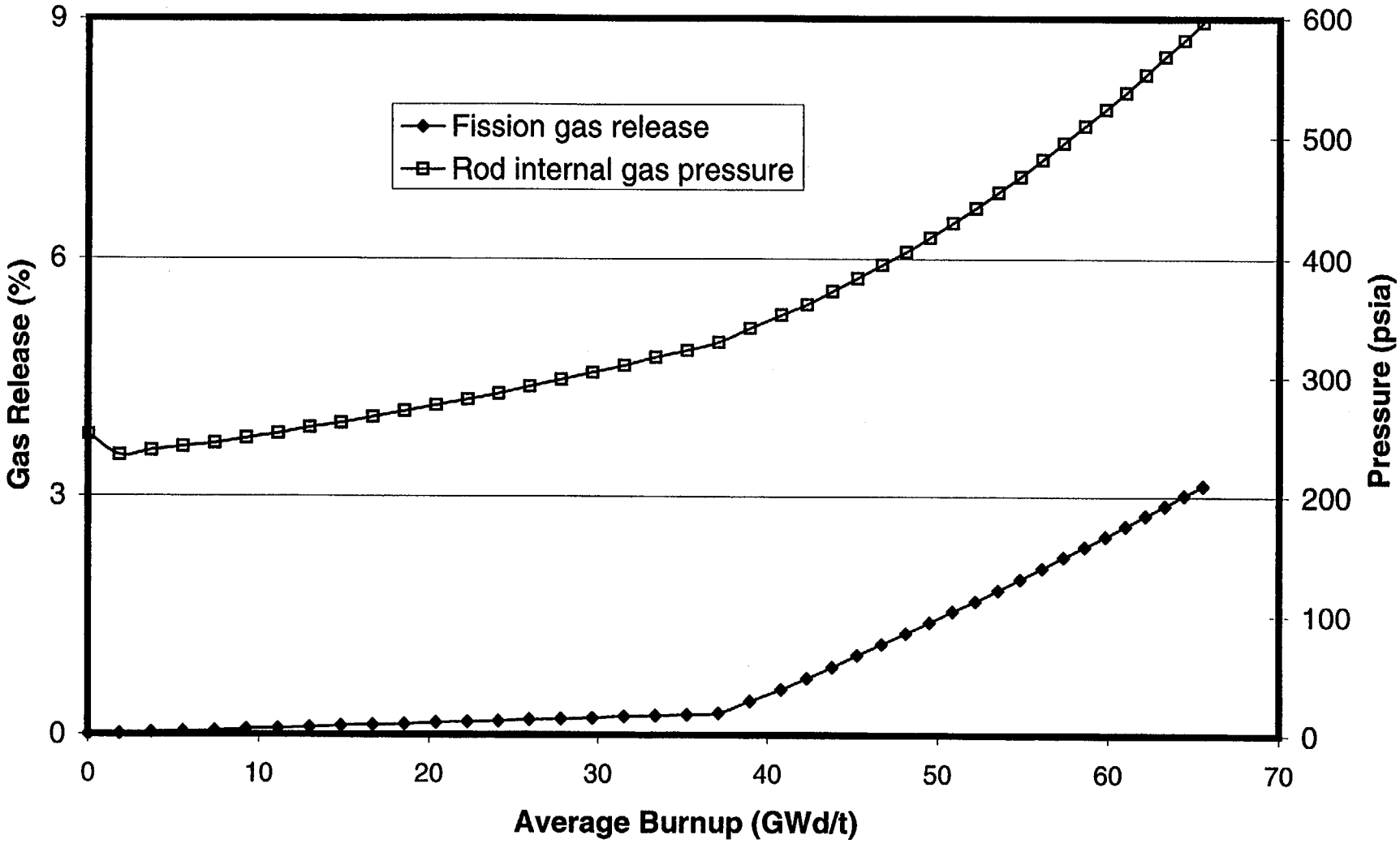

Fig. 7-10. Fission gas release and rod internal gas pressure for a BWR 10x10 fuel rod with initial peak power of 7 kW/ft.

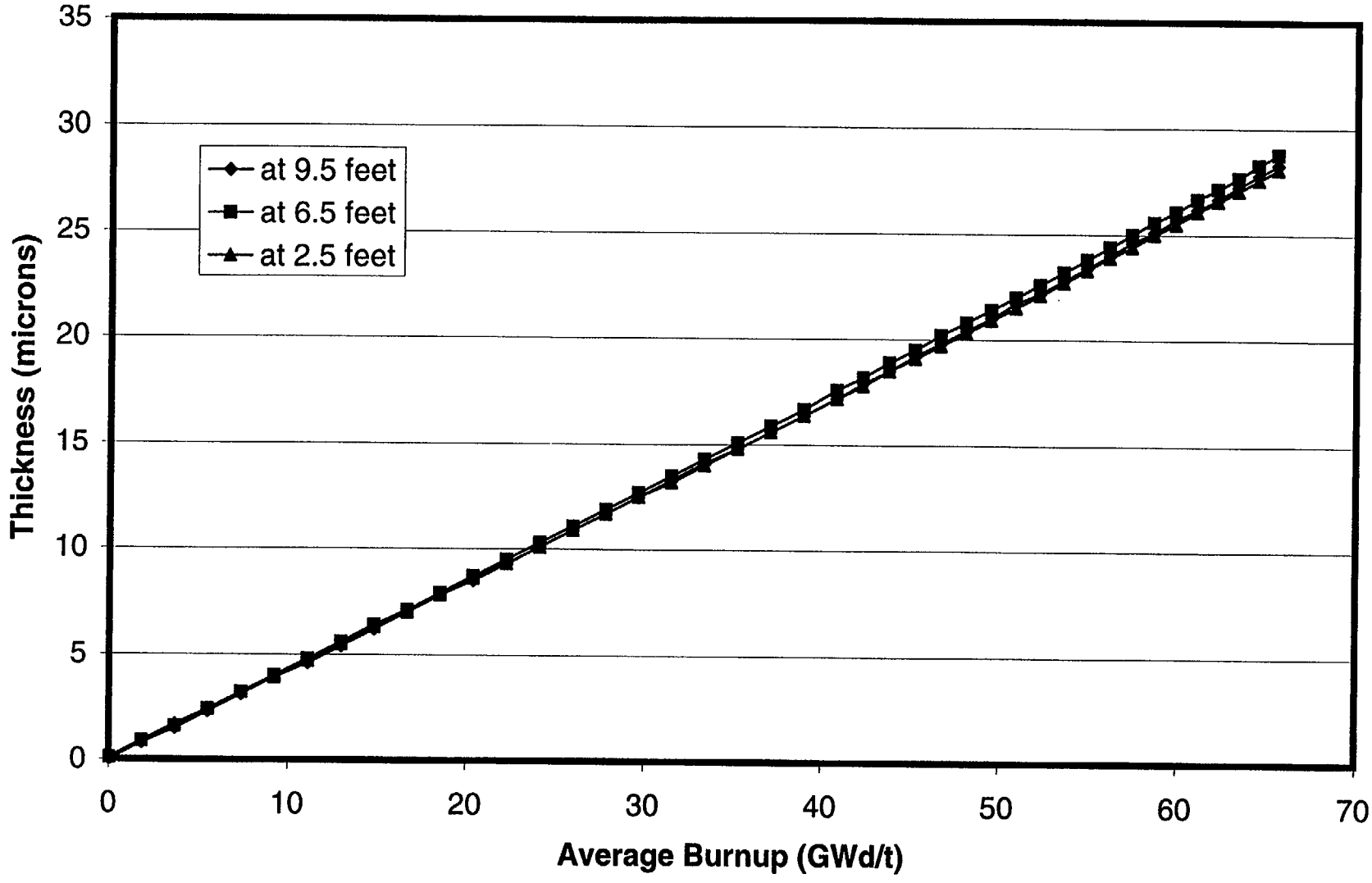

Fig. 7-11. Oxide thickness at three axial locations for a BWR 10x10 fuel rod with initial peak power of 7 kW/ft.

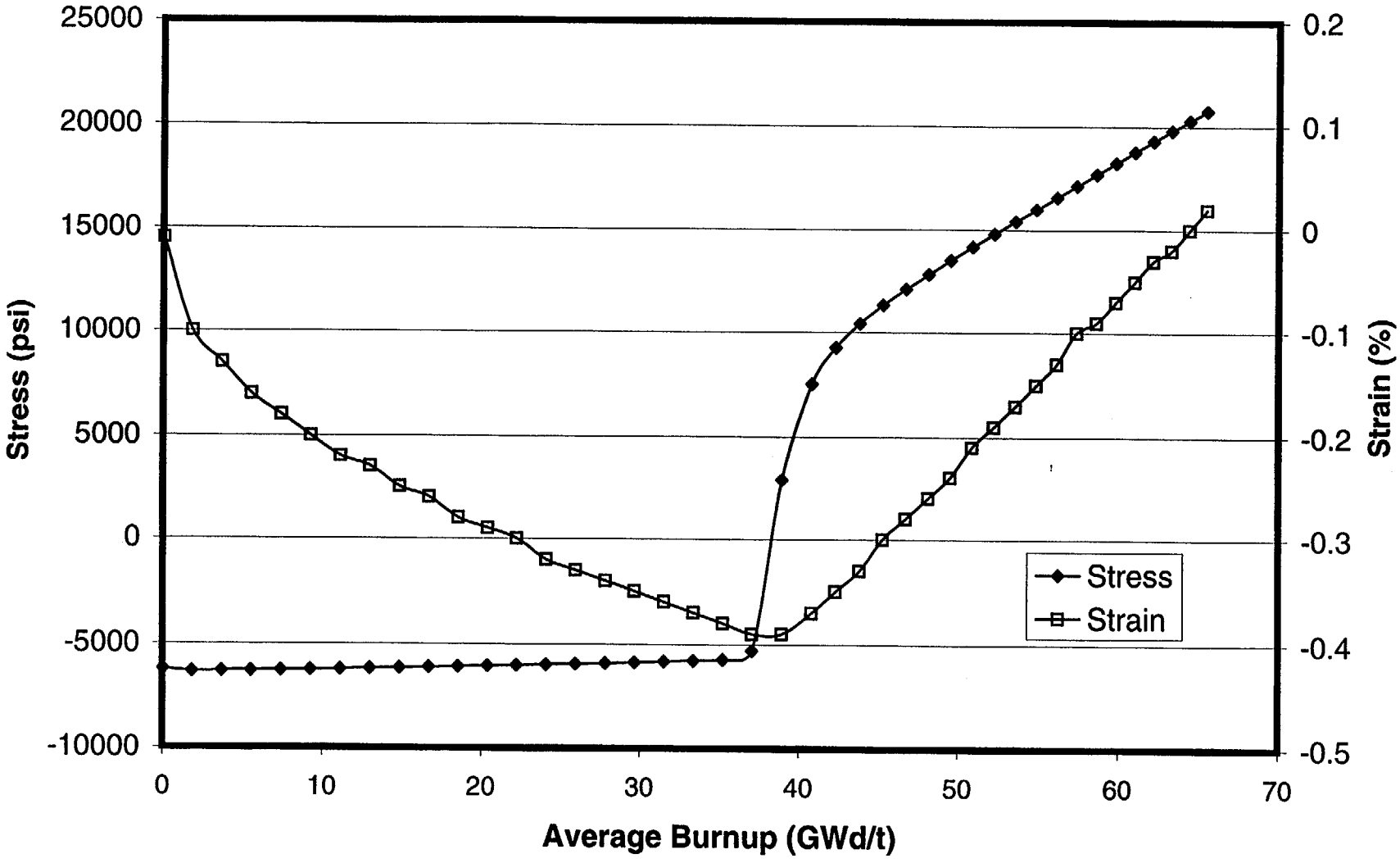

Fig. 7-12. Cladding hoop stress and hoop strain for a BWR 10x10 fuel rod with initial peak power of 7 kW/ft.

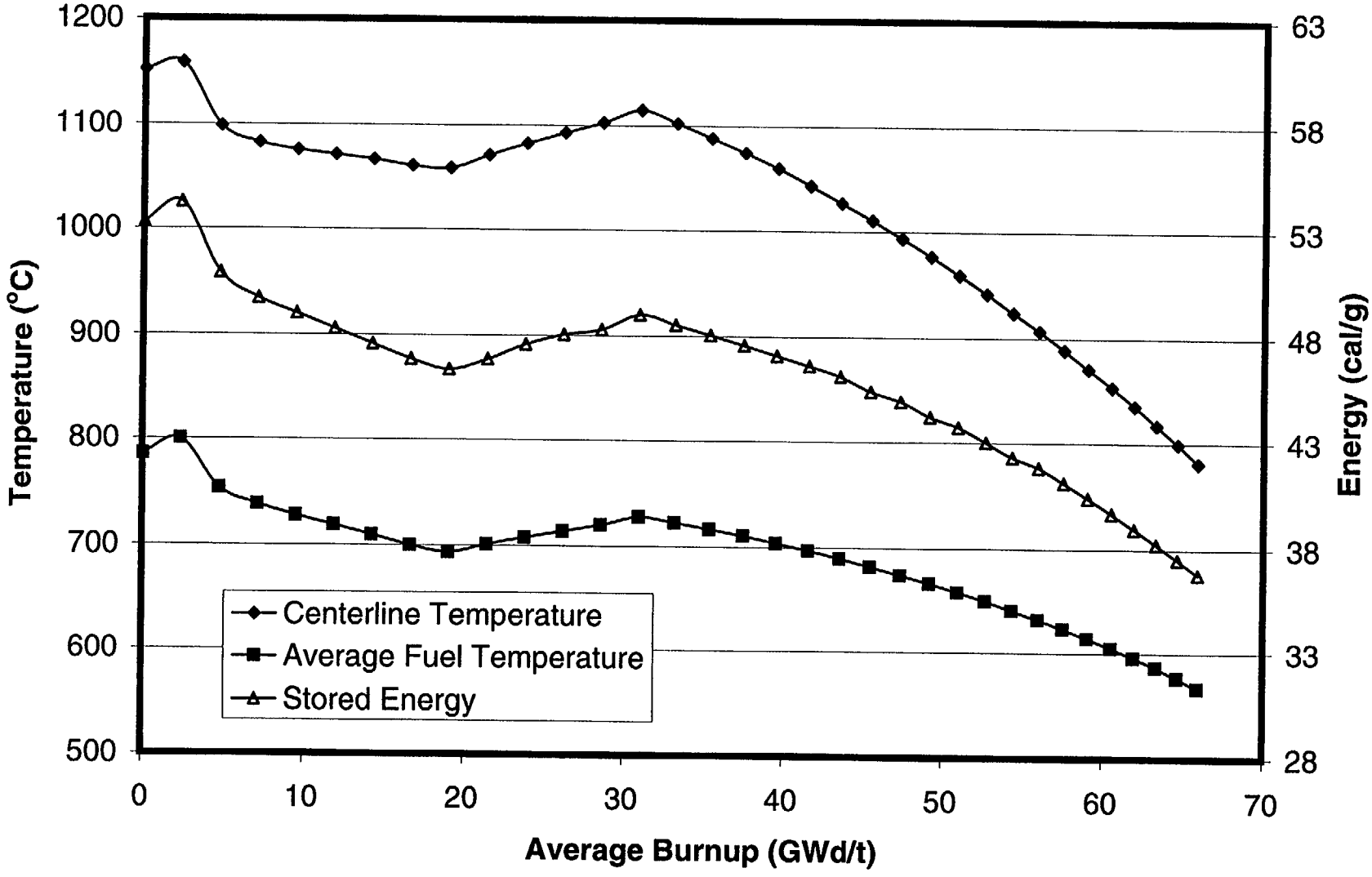

Fig. 7-13. Fuel temperatures and stored energy for a BWR 10x10 fuel rod with initial peak power of 9 kW/ft.

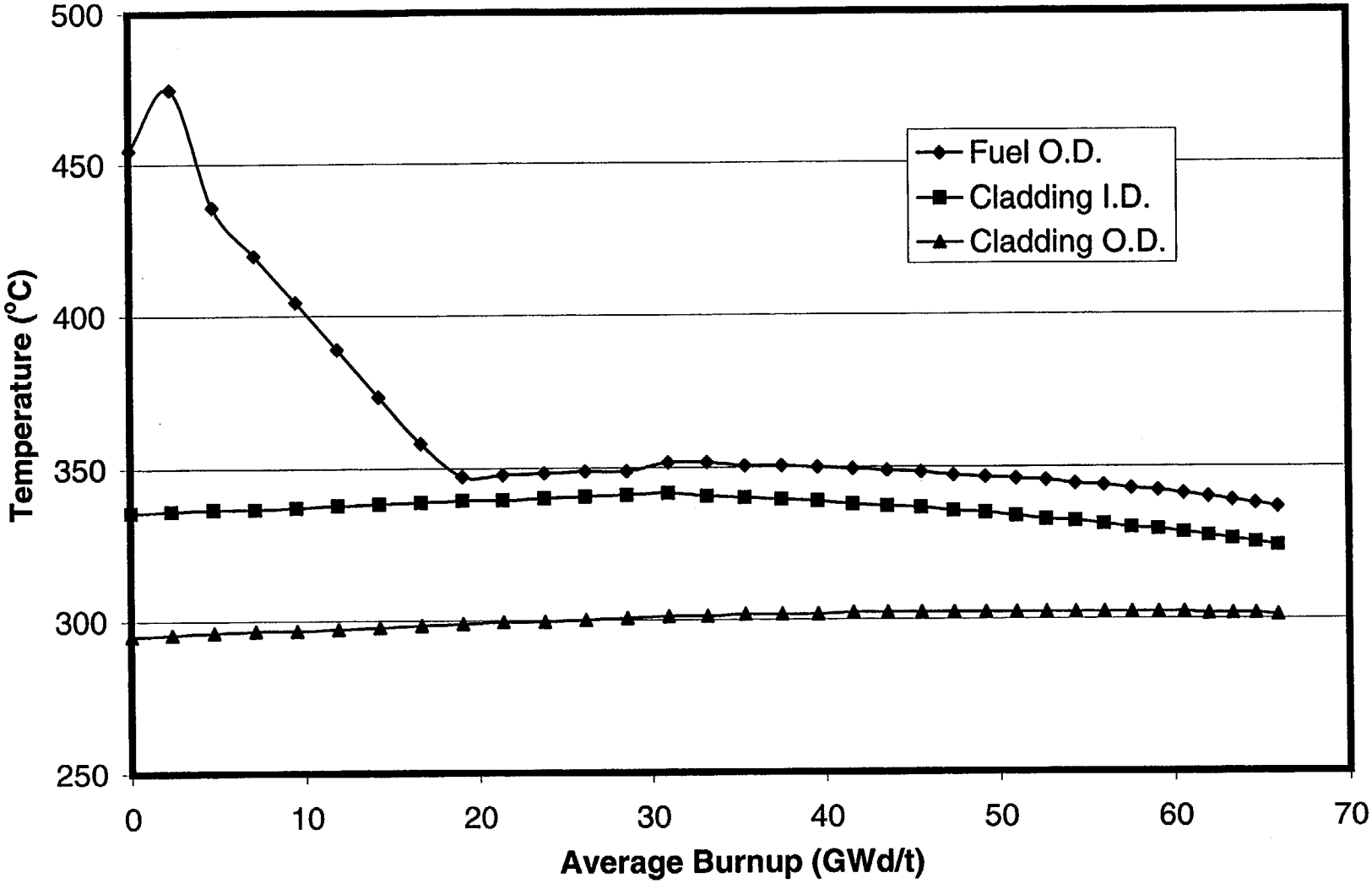

Fig. 7-14. Cladding temperatures and fuel surface temperature for a BWR 10x10 fuel rod with initial peak power of 9 kW/ft.

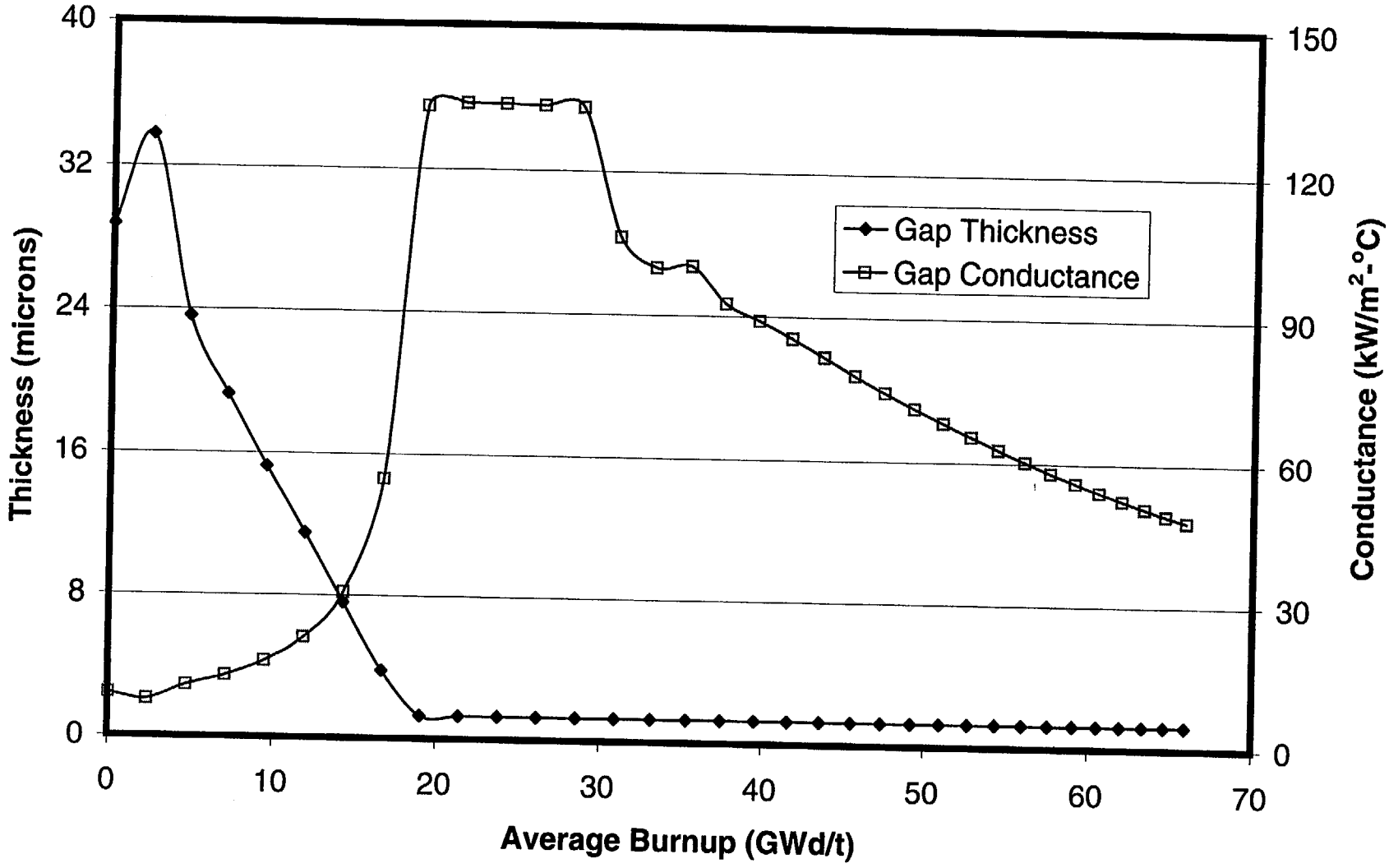

Fig. 7-15. Gap thickness and gap conductance for a BWR 10x10 fuel rod with initial peak power of 9 kW/ft.

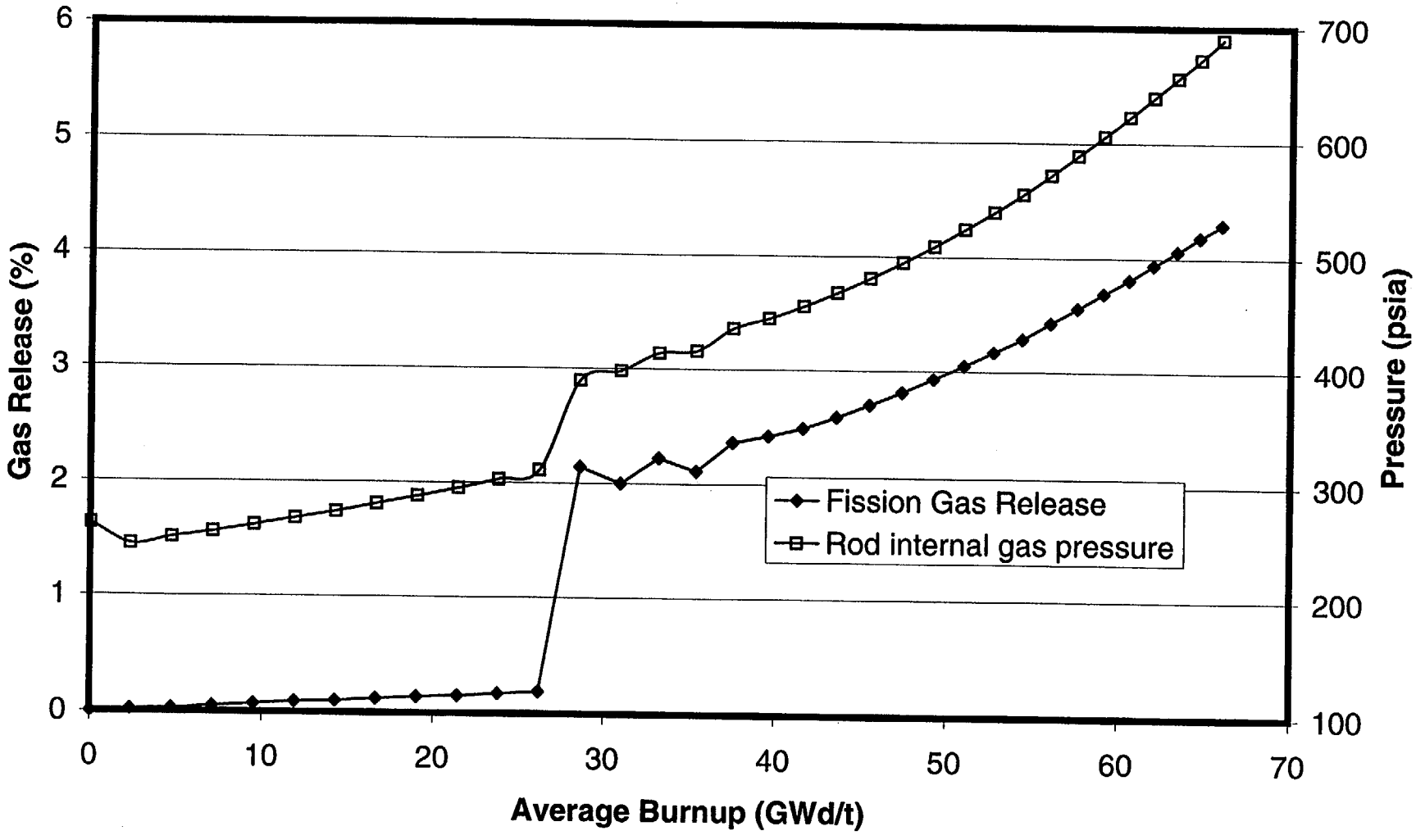

Fig. 7-16. Fission gas release and rod internal gas pressure for a BWR 10x10 fuel rod with initial peak power of 9 kW/ft.

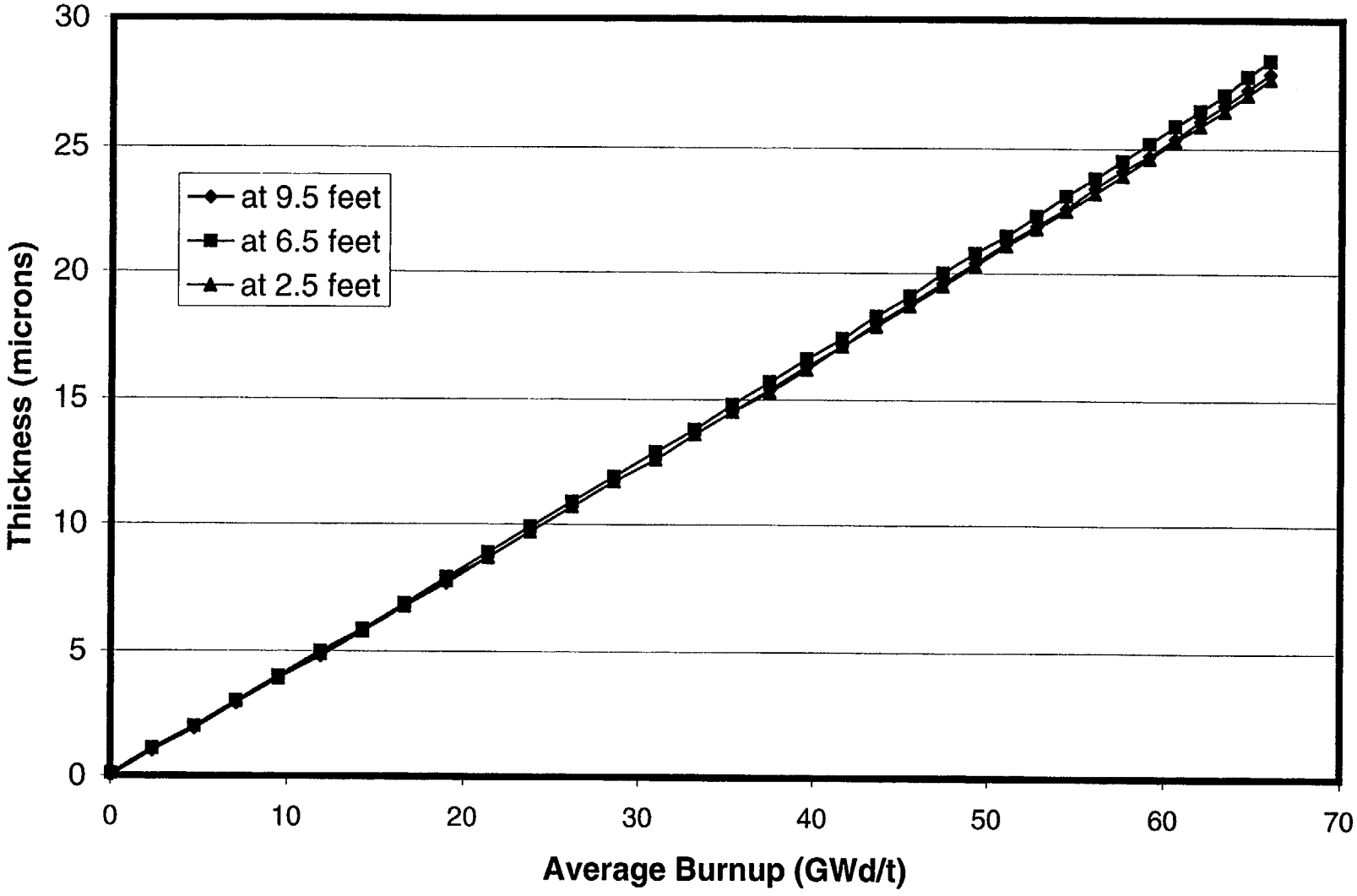

Fig. 7-17. Oxide thickness at three axial locations for a BWR 10x10 fuel rod with initial peak power of 9 kW/ft.

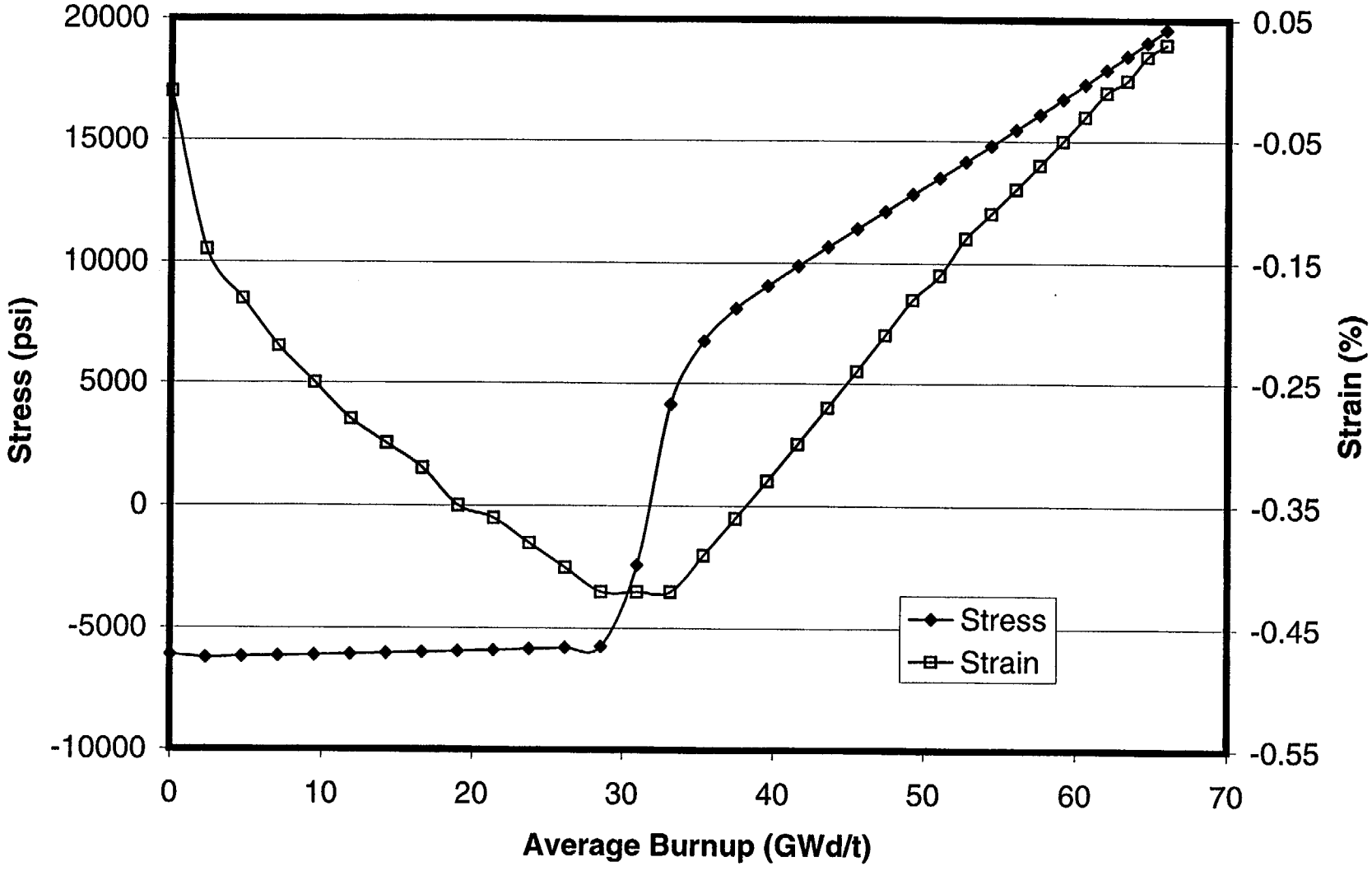

Fig. 7-18. Cladding hoop stress and hoop strain for a BWR 10x10 fuel rod with initial peak power of 9 kW/ft.

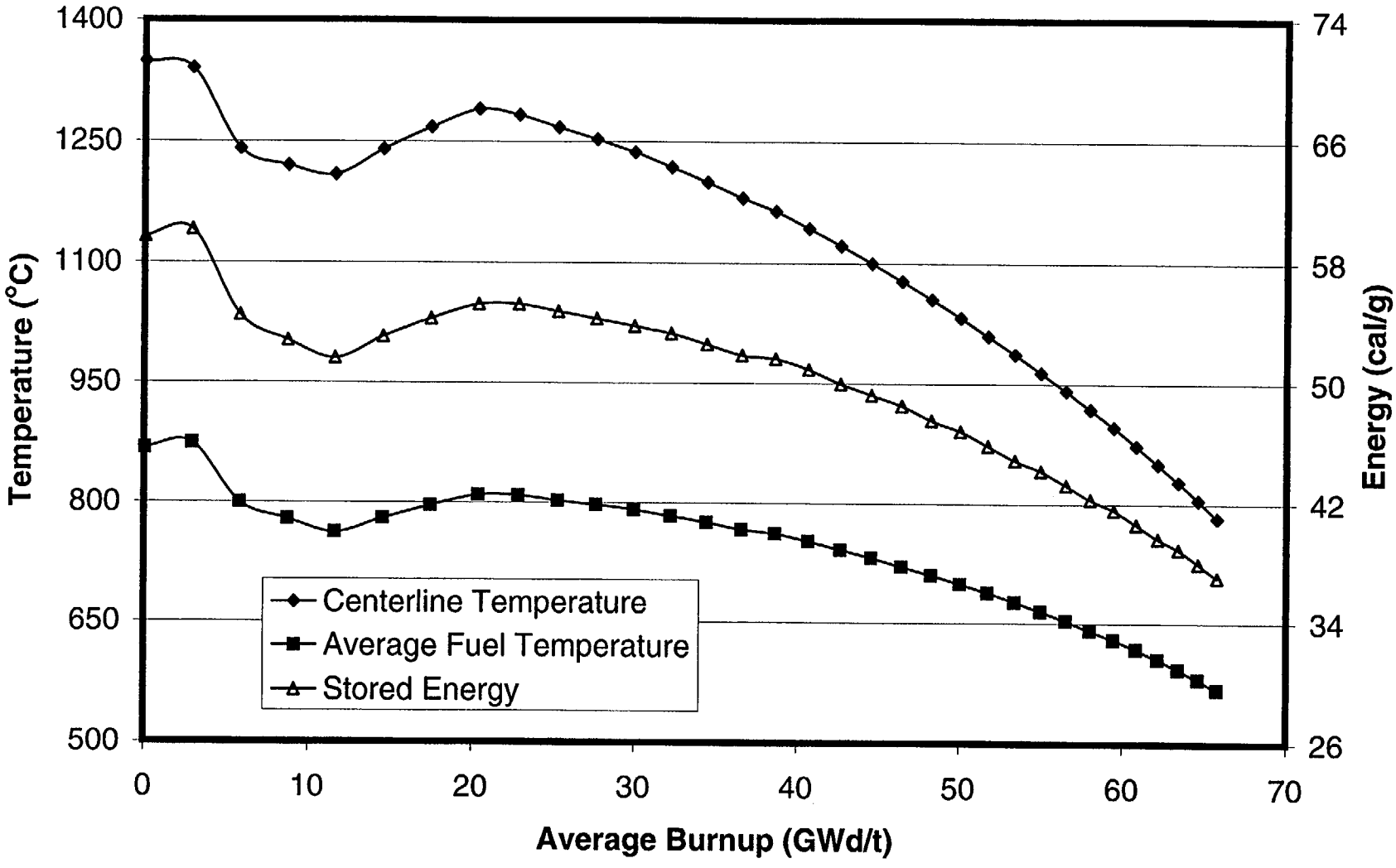

Fig. 7-19. Fuel Temperatures and stored energy for a BWR 10x10 fuel rod with initial peak power of 11 kW/ft.

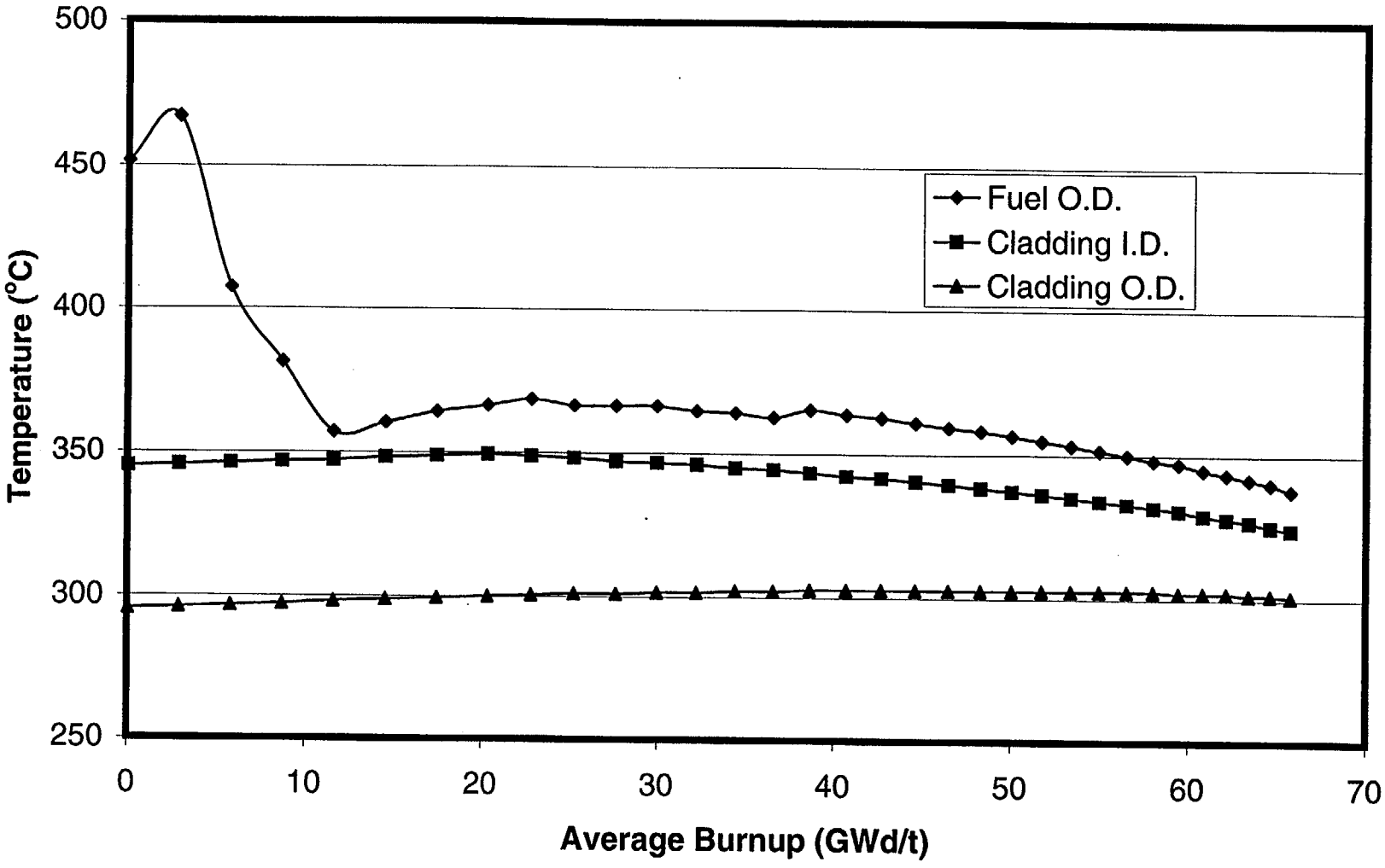

Fig. 7-20. Cladding temperatures and fuel surface temperature for a BWR 10x10 fuel rod with initial peak power of 11 kW/ft.

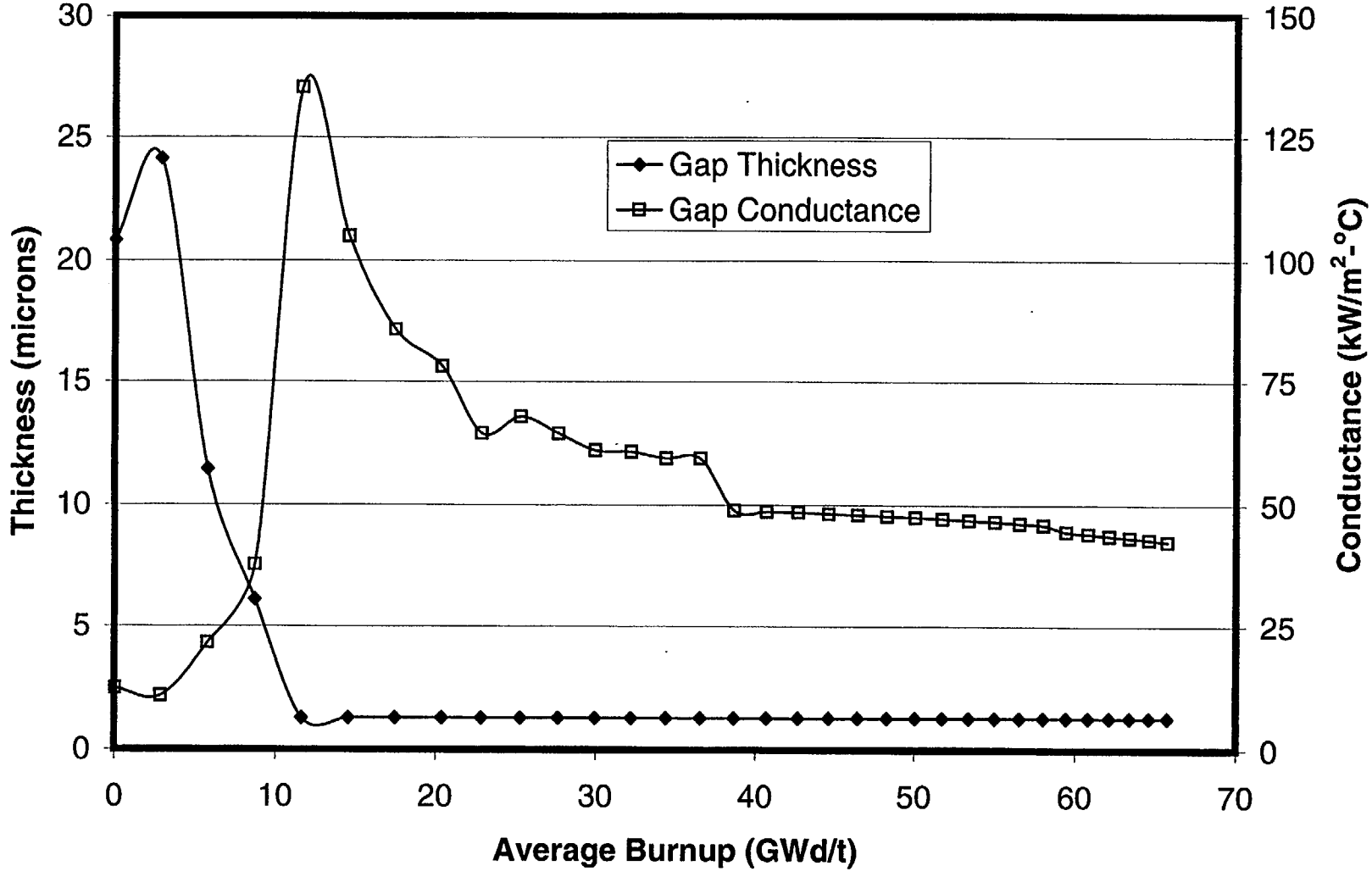

Fig. 7-21. Gap thickness and gap conductance for a BWR 10x10 fuel rod with initial peak power of 11 kW/ft.

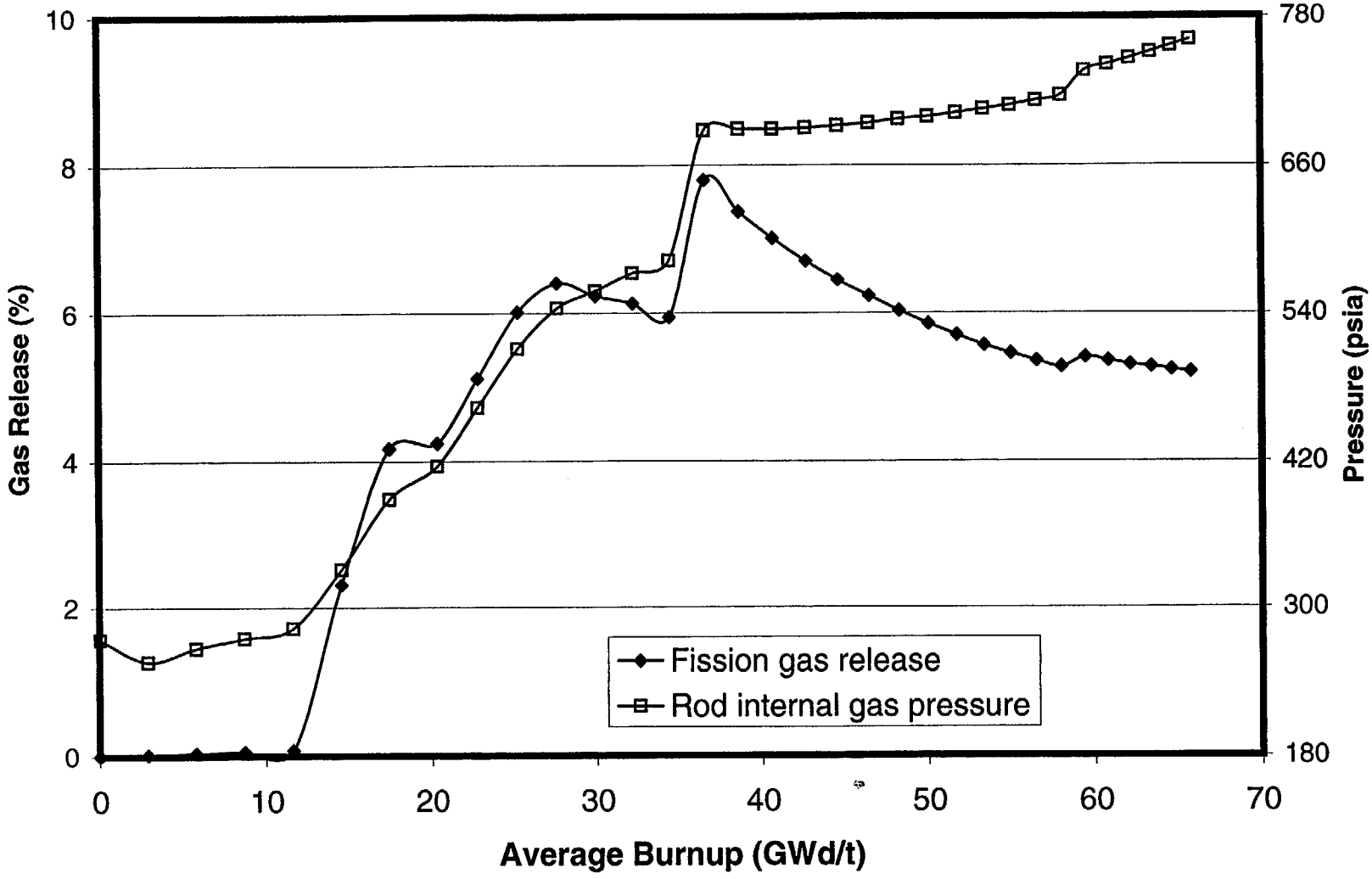

Fig. 7-22. Fission gas release and rod internal gas pressure for a BWR 10x10 fuel rod with initial peak power of 11 kW/ft.

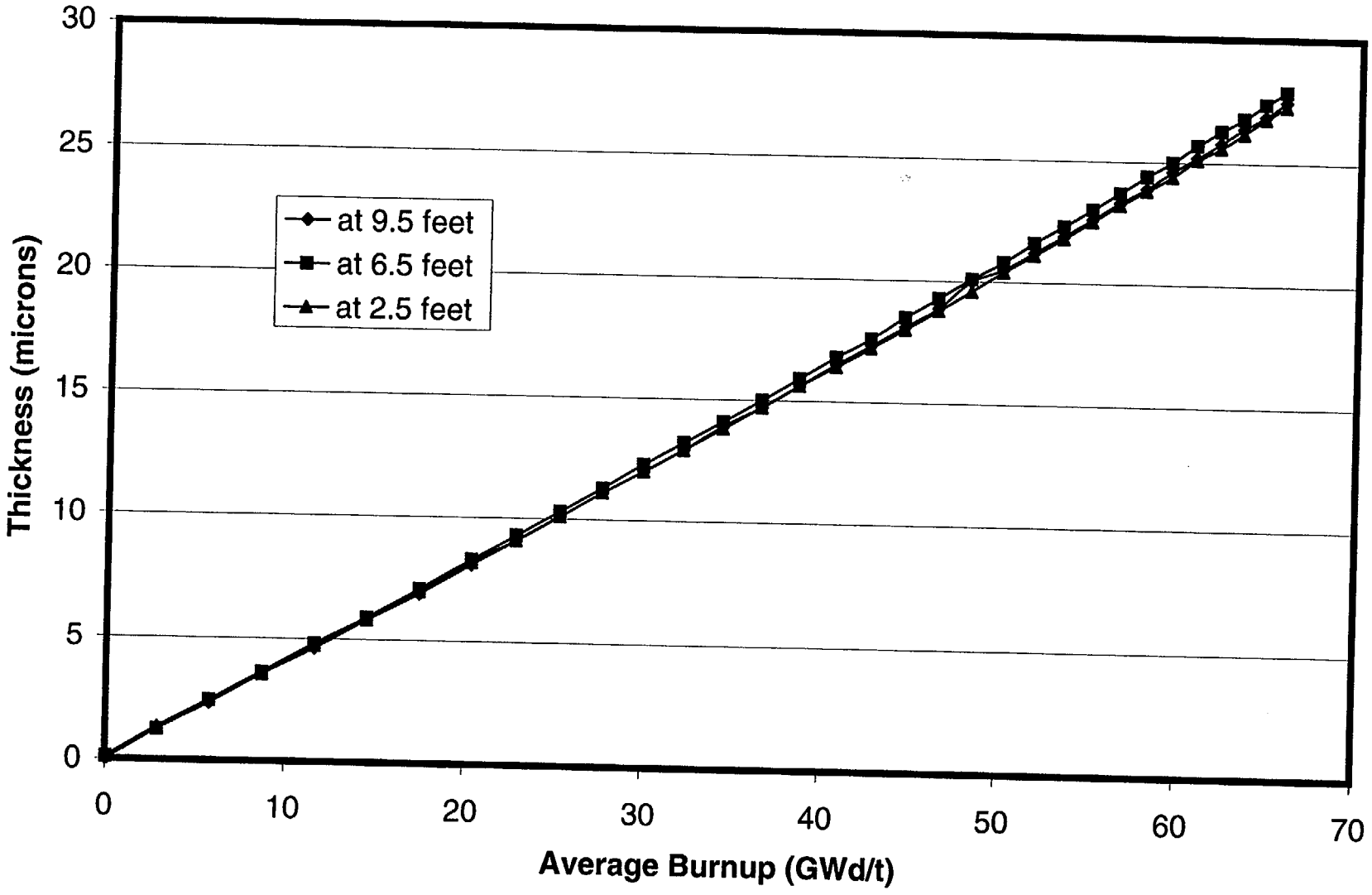

Fig. 7-23. Oxide thickness at three axial locations for a BWR 10x10 fuel rod with initial peak power of 11 kW/ft.

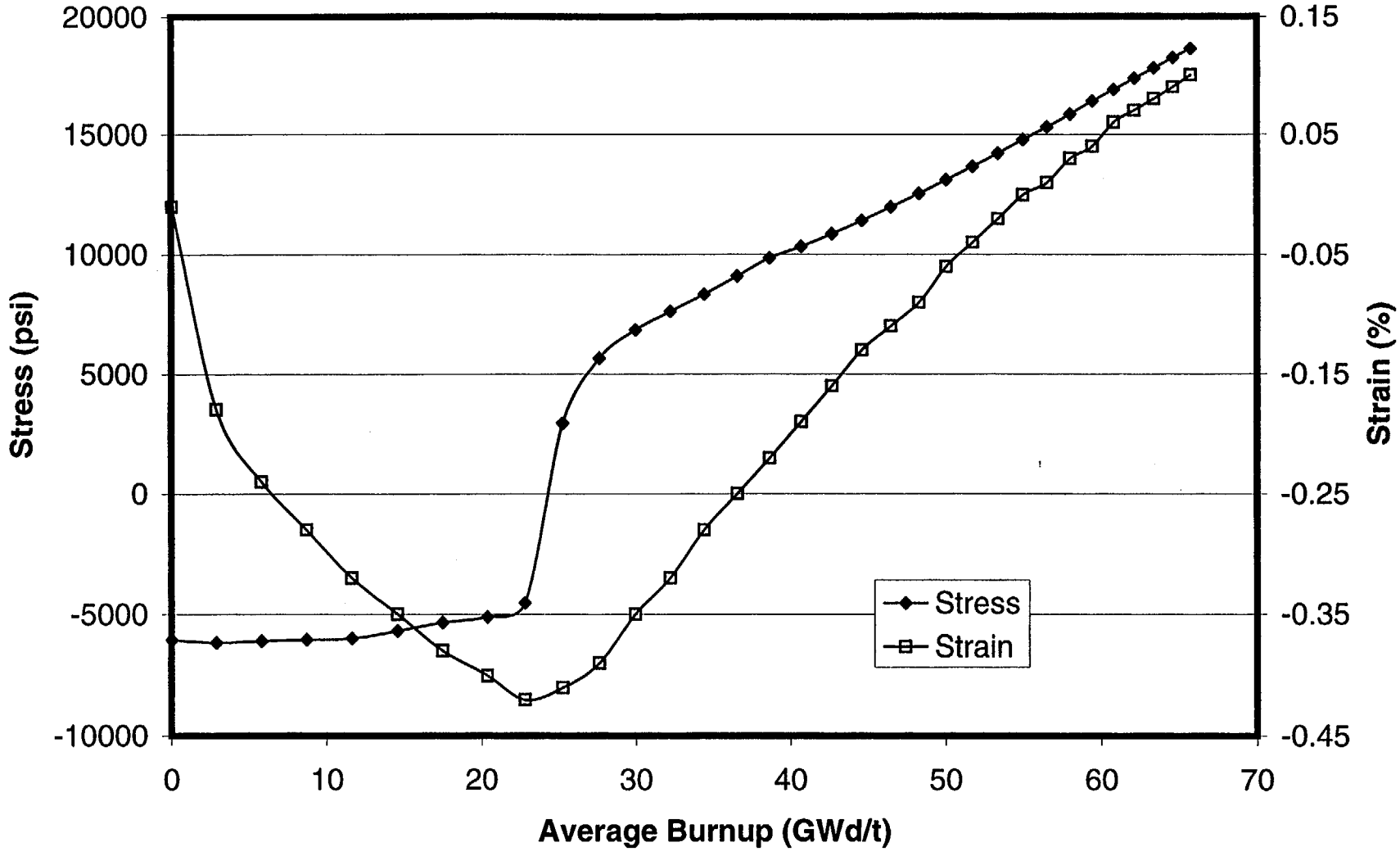

Fig. 7-24. Cladding hoop stress and hoop strain for a BWR 10x10 fuel rod with initial peak power of 11 kW/ft.

8. Calculations for PWR 14X14 Fuel

In the following figures, calculated values for PWR 14X14 fuel are plotted as a function of burnup for the parameters listed below:

Fuel centerline temperature
Average fuel temperature
Stored energy
Fuel O.D. temperature
Cladding I.D. temperature
Cladding O.D. temperature
Gap thickness
Gap conductance
Fission gas release
Rod internal gas pressure
Oxide thickness
Cladding hoop stress
Cladding hoop strain

Several general observations can be made about the calculated results:

- Within the first few GWd/t of burnup, a temperature peak is observed that is the result of fuel densification.

- Gap closure results in (a) the coming together of temperatures for fuel O.D. and cladding I.D. and (b) a sharp increase in gap conductance. The gap conductance increases again after a few time steps when the interaction between the pellet and cladding affects the contact conductance calculated for a closed gap. At this point there is also a large increase in stress, and the permanent strain changes directions.

- Some of the fission gas is released in spurts according to the Massih model in FRAPCON-3. This effect is apparent in many of the figures. Shorter time steps would produce slightly different looking curves, but the trend of gas release and the end-of-life gas release would be about the same.

- The burnup enhancement of fission gas release is readily seen in the lower power cases, but it is obscured in the highest power cases by the magnitude of prior gas release.

- Rod internal gas pressure increases with the accumulation of released fission gas. In the higher power PWR cases, as the power drops off near the end of life, the reduction in the plenum temperature offsets the increasing moles of fission gas.

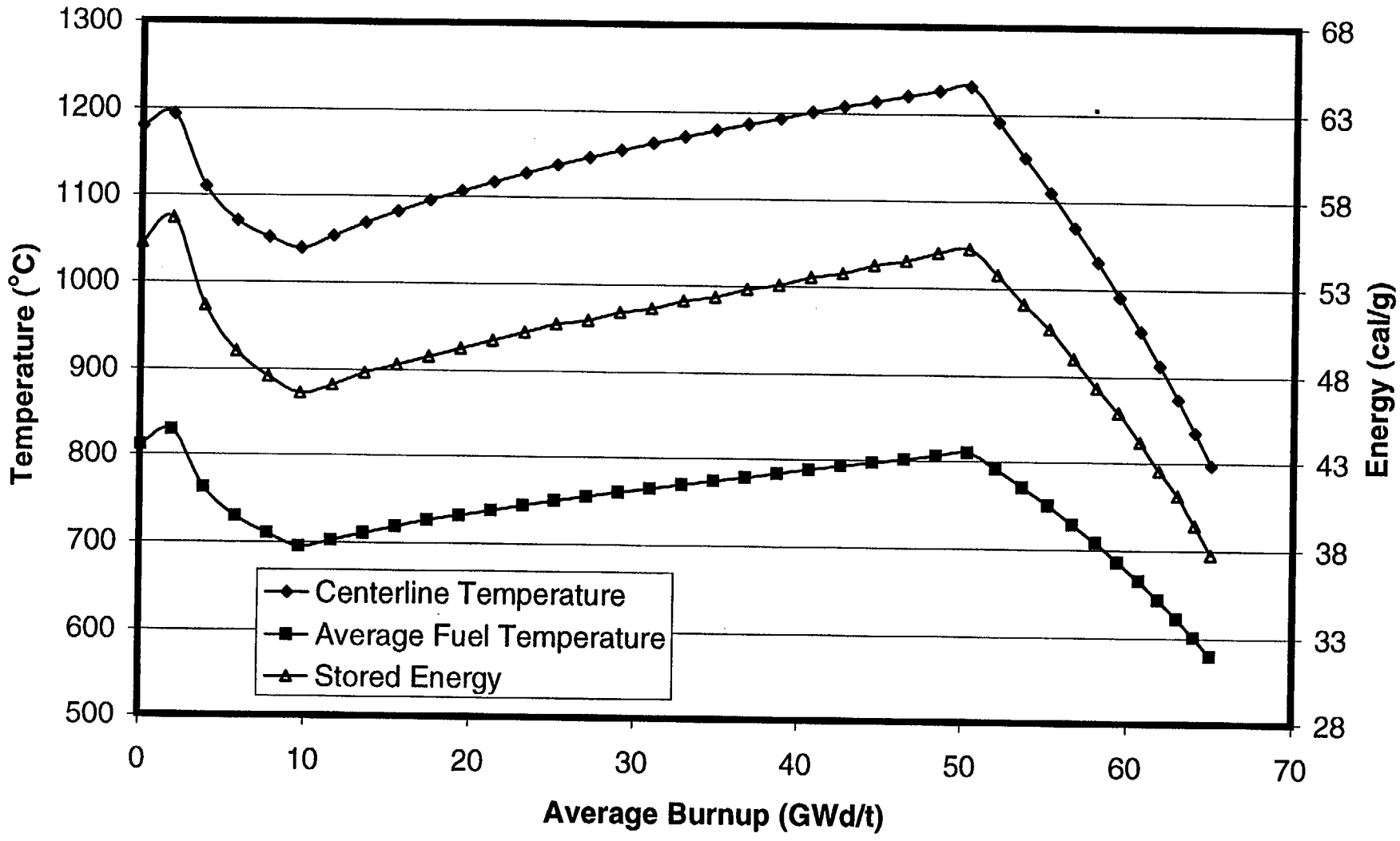

Fig. 8-1. Fuel temperatures and stored energy for a PWR 14x14 fuel rod with initial peak power of 9 kW/ft.

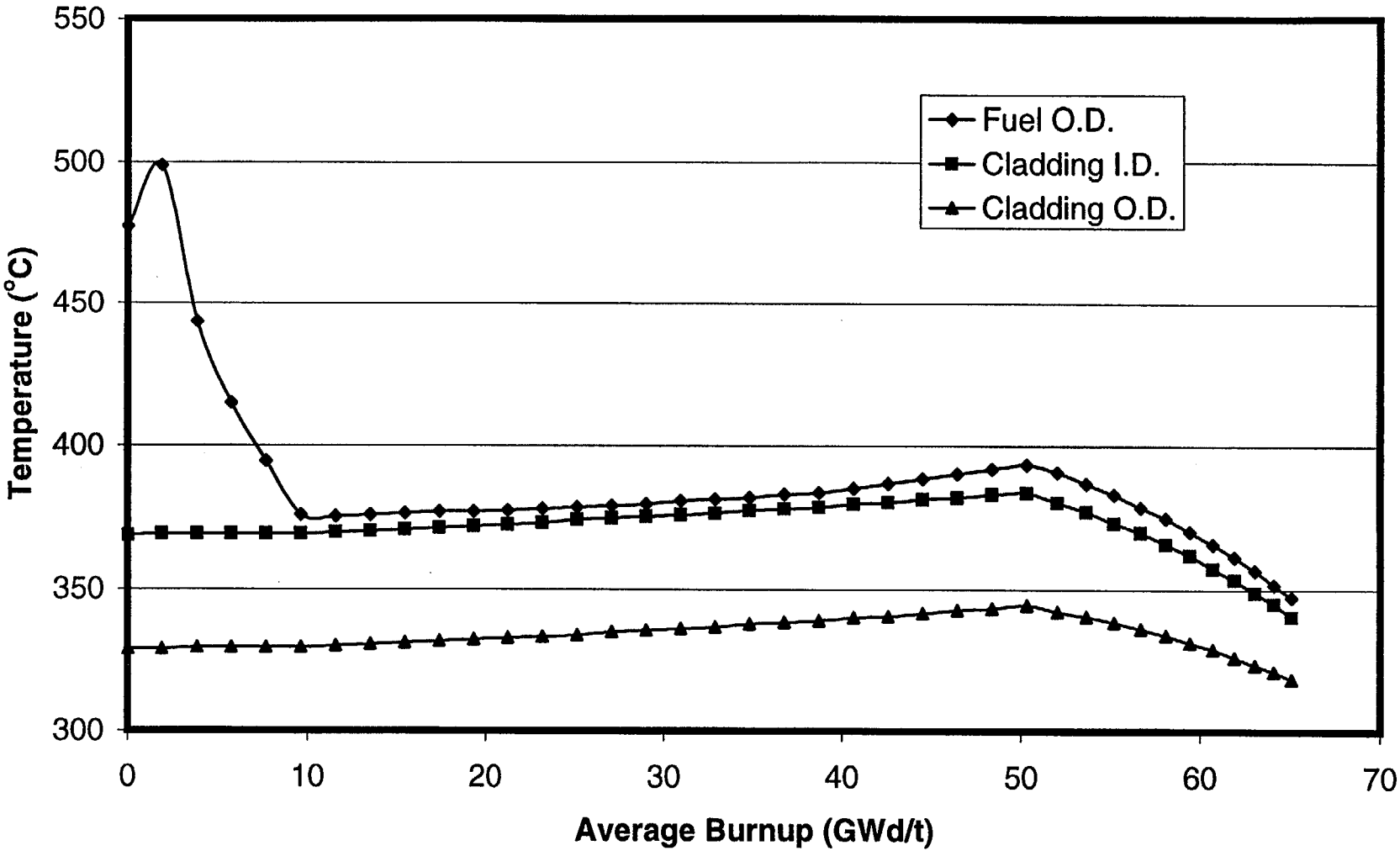

Fig. 8-2. Cladding temperatures and fuel surface temperature for a PWR 14x14 fuel rod with initial peak power of 9 kW/ft.

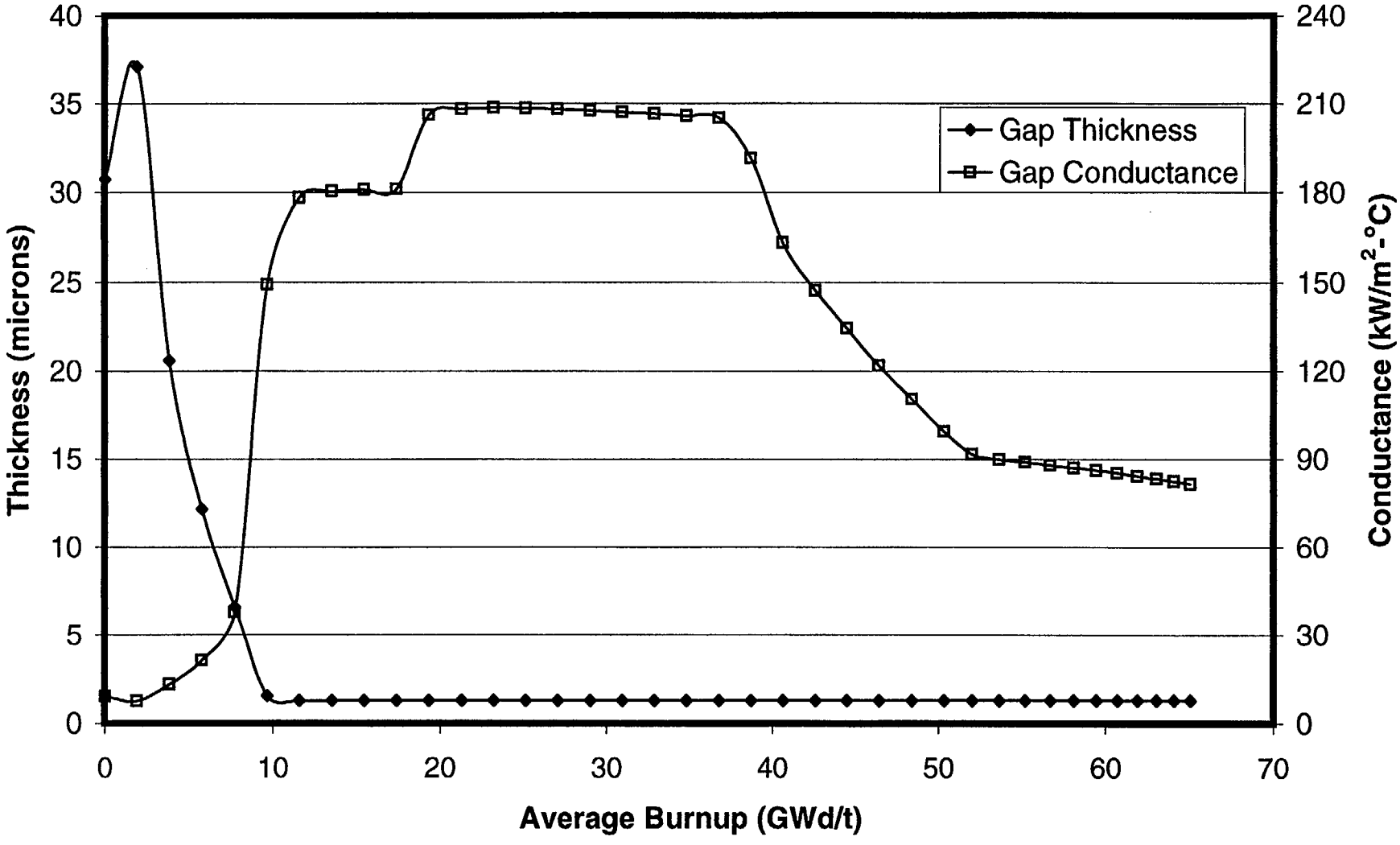

Fig. 8-3. Gap thickness and gap conductance for a PWR 14x14 fuel rod with initial peak power of 9 kW/ft.

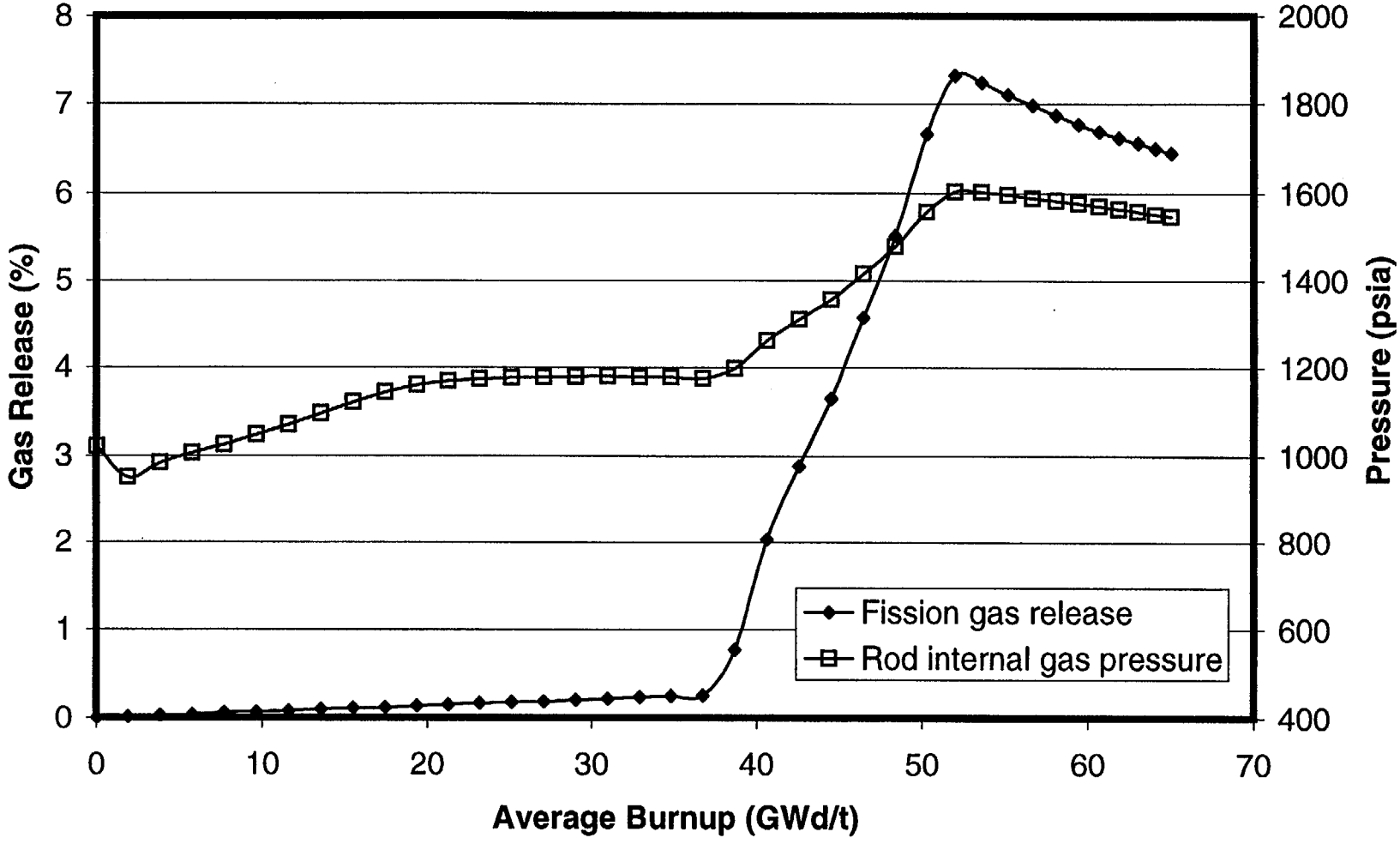

Fig. 8-4. Fission gas release and rod internal gas pressure for a PWR 14x14 fuel rod with initial peak power of 9 kW/ft.

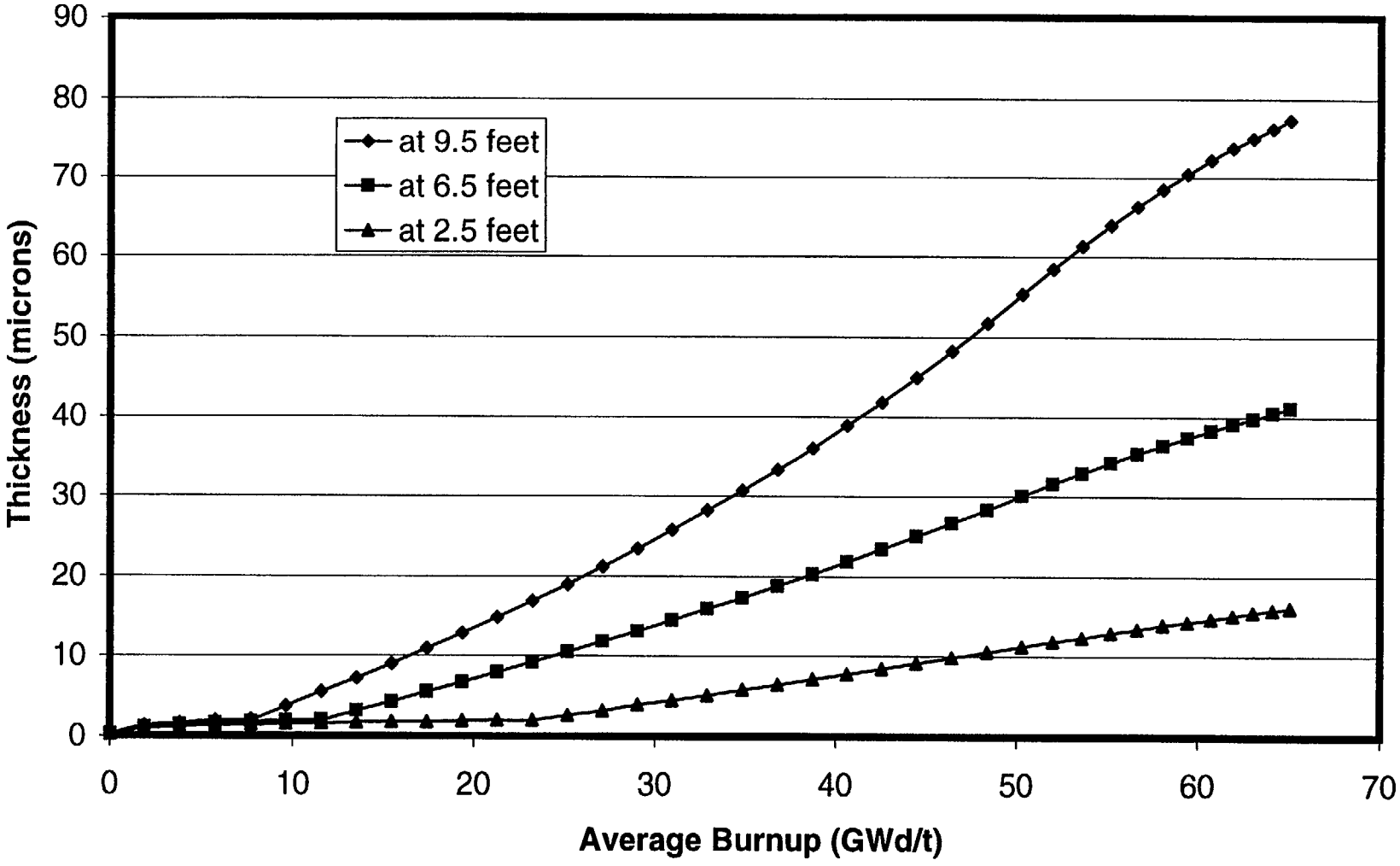

Fig. 8-5. Oxide thickness at three axial locations for a PWR 14x14 fuel rod with initial peak power of 9 kW/ft.

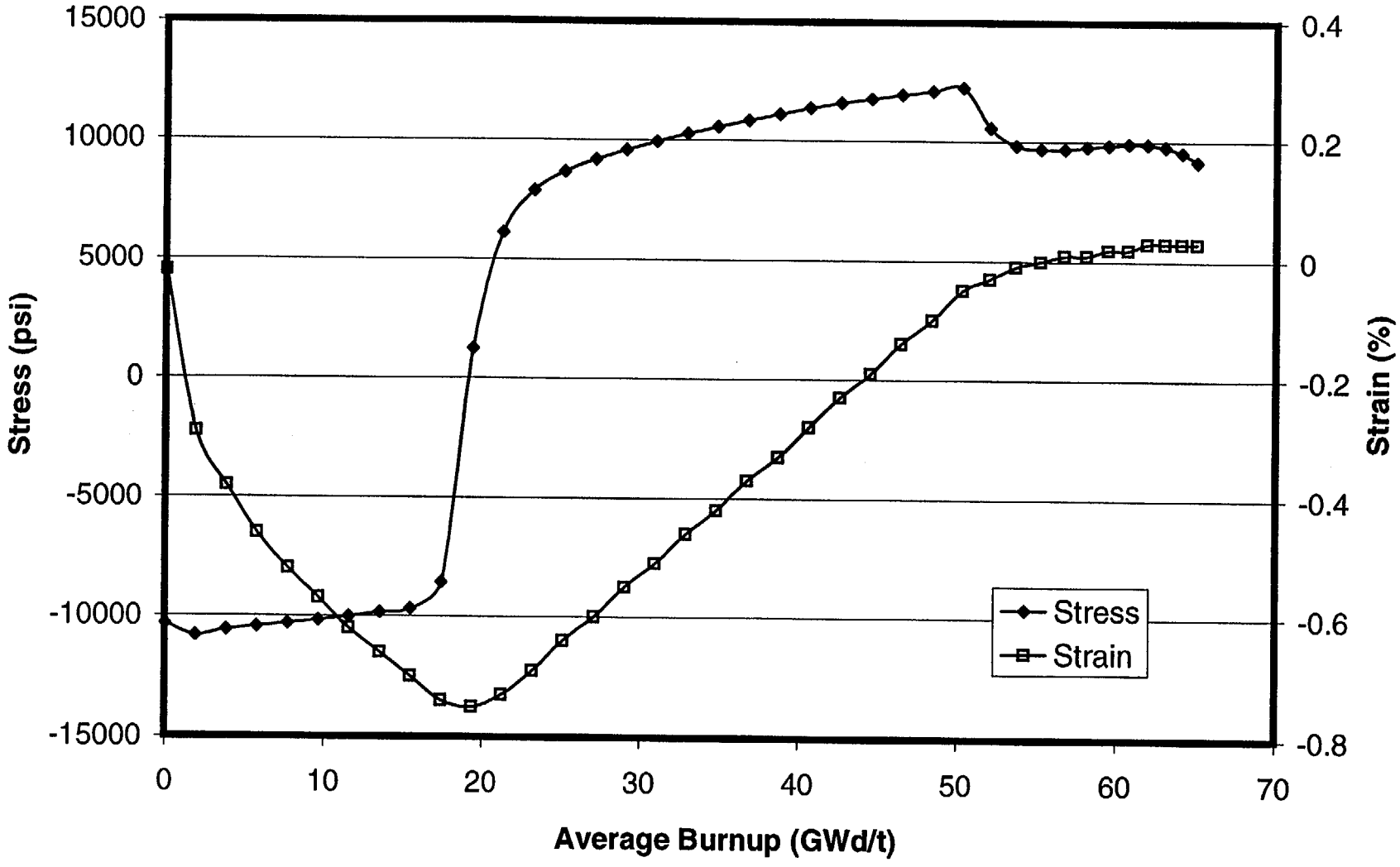

Fig. 8-6. Cladding hoop stress and hoop strain for a PWR 14x14 fuel rod with initial peak power of 9 kW/ft.

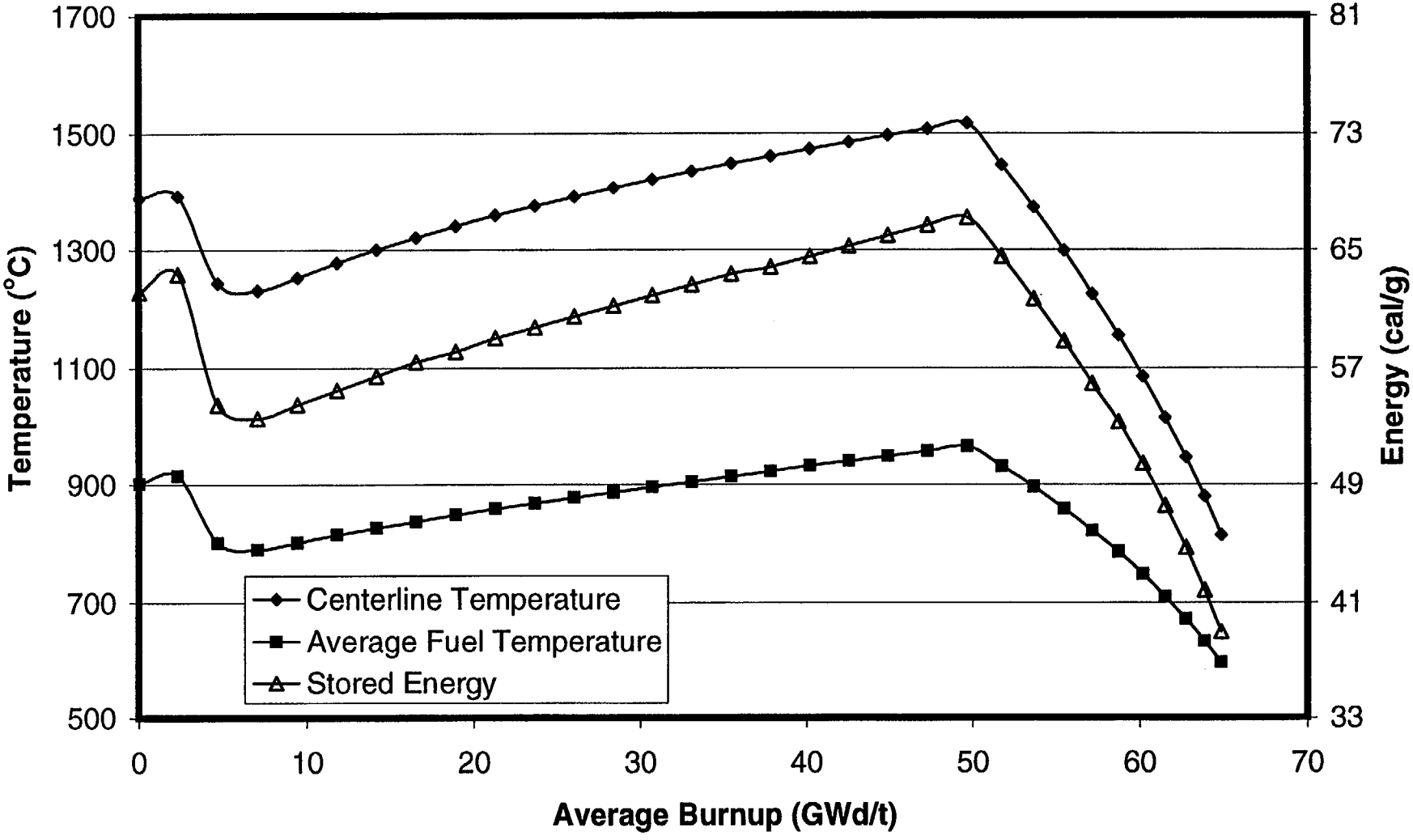

Fig. 8-7. Fuel temperatures and stored energy for a PWR 14x14 fuel rod with initial peak power of 11 kW/ft.

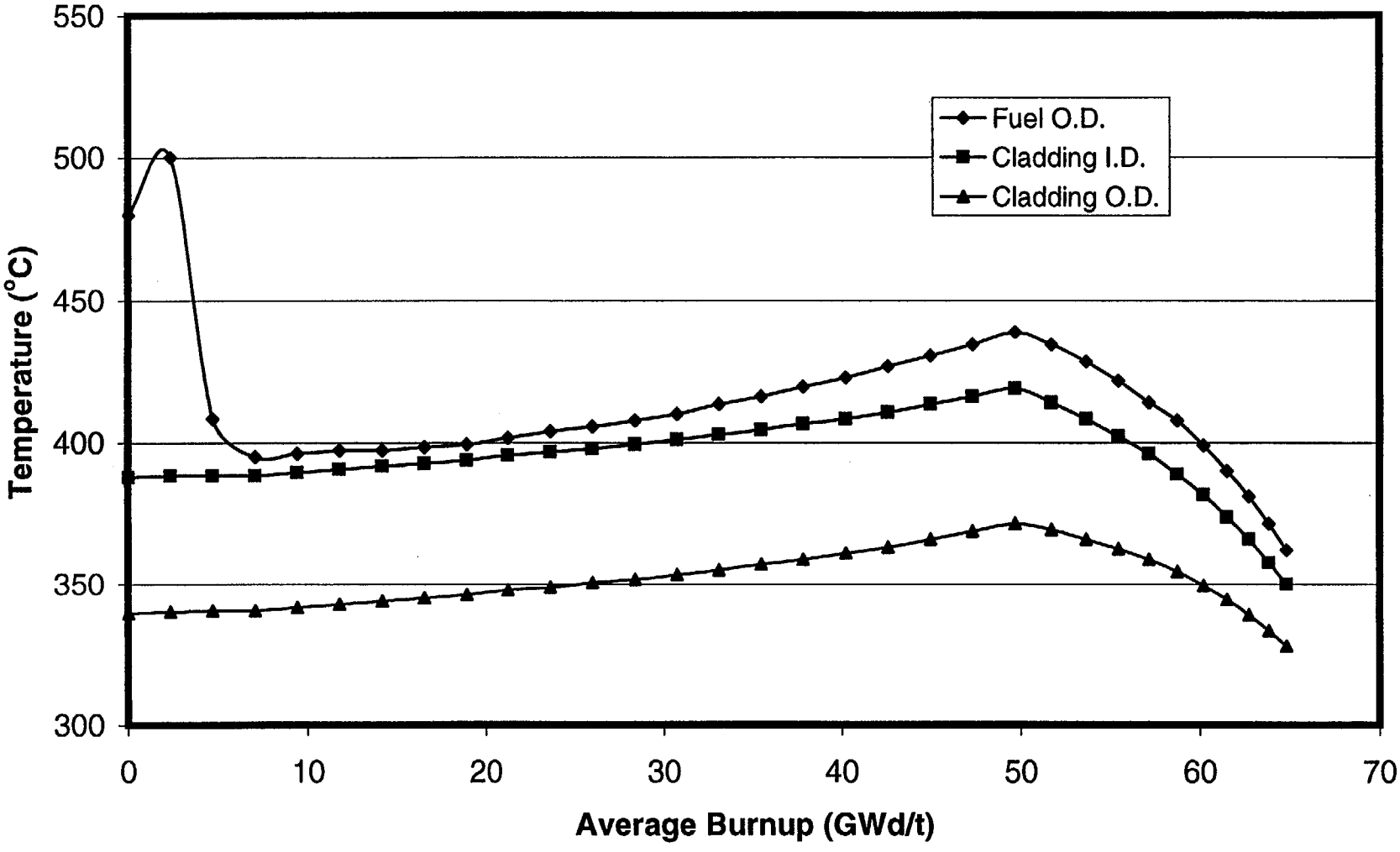

Fig. 8-8. Cladding temperatures and fuel surface temperature for a PWR 14x14 fuel rod with initial peak power of 11 kW/ft.

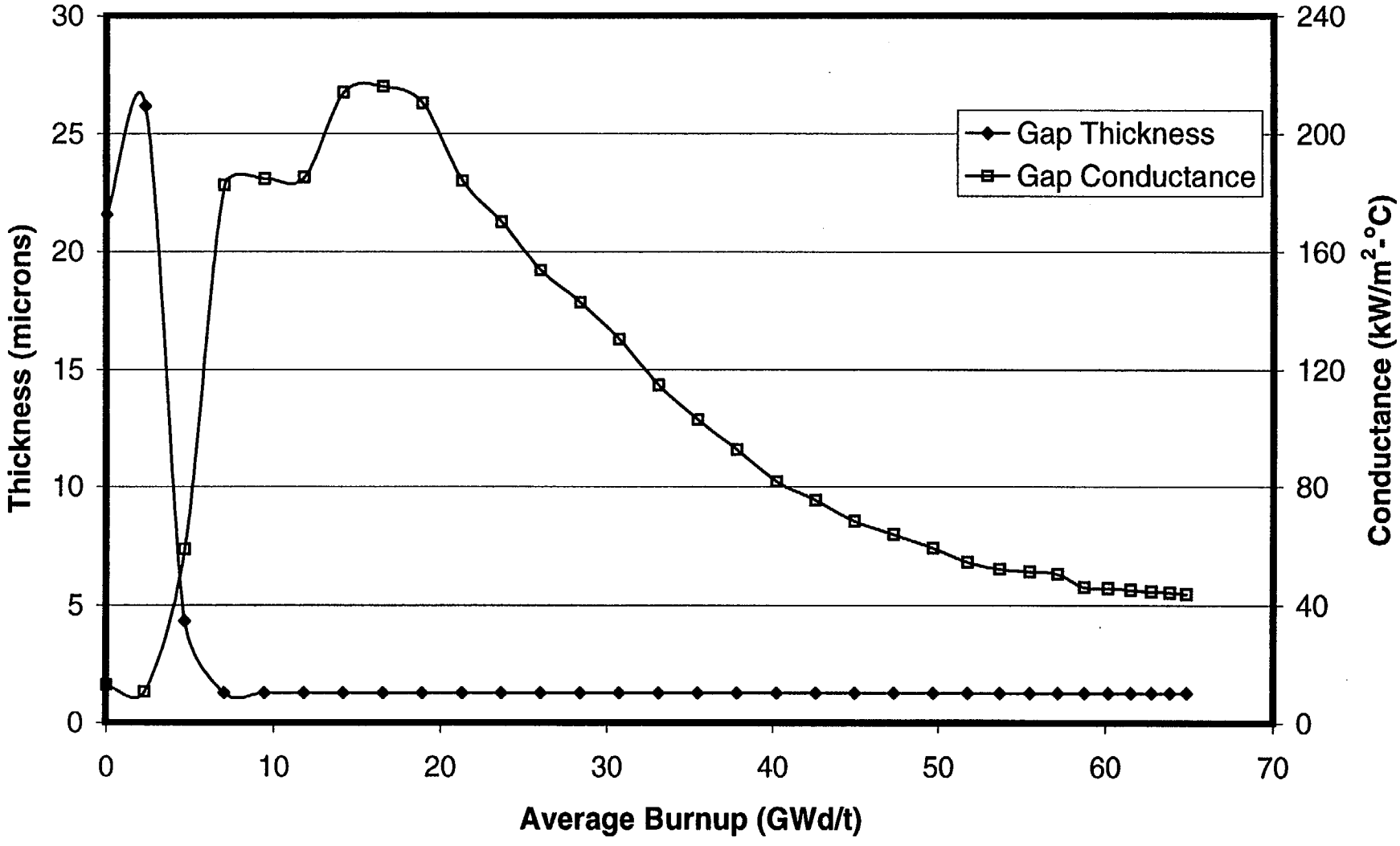

Fig. 8-9. Gap thickness and gap conductance for a PWR 14x14 fuel rod with initial peak power of 11 kW/ft.

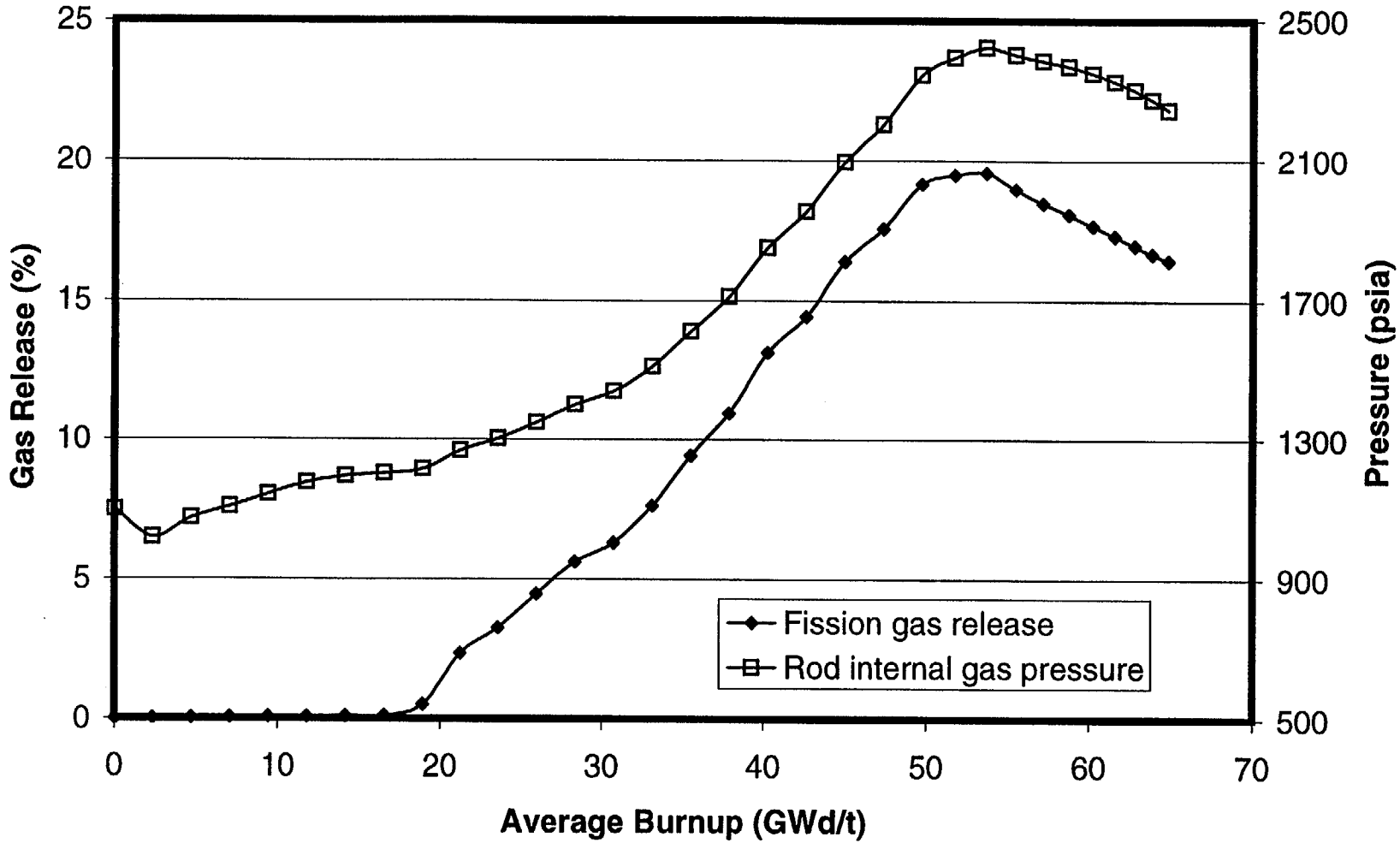

Fig. 8-10. Fission gas release and rod internal gas pressure in a PWR 14x14 fuel rod with initial peak power of 11 kW/ft.

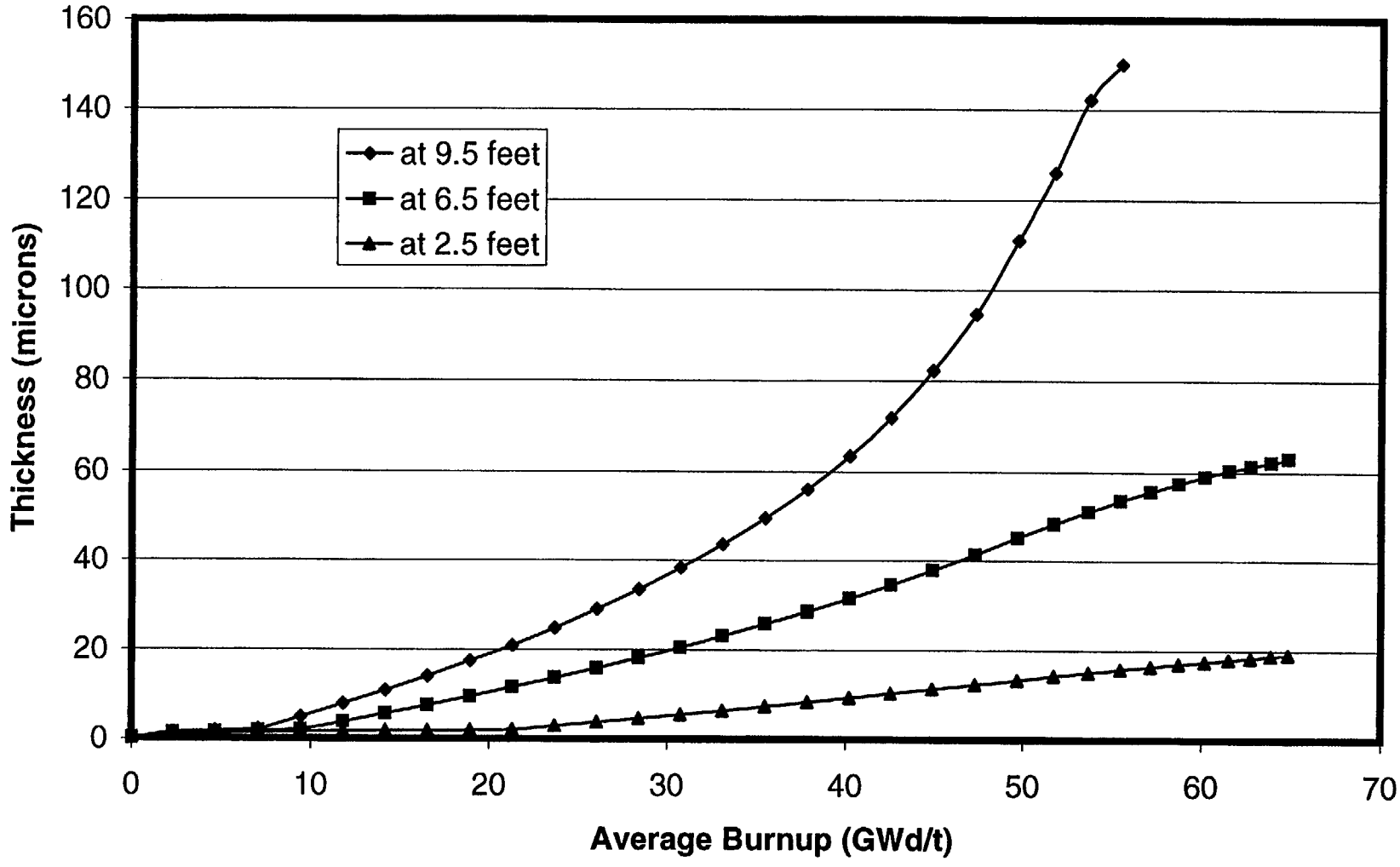

Fig. 8-11. Oxide thickness at three axial locations for a PWR 14x14 fuel rod with initial peak power of 11 kW/ft.

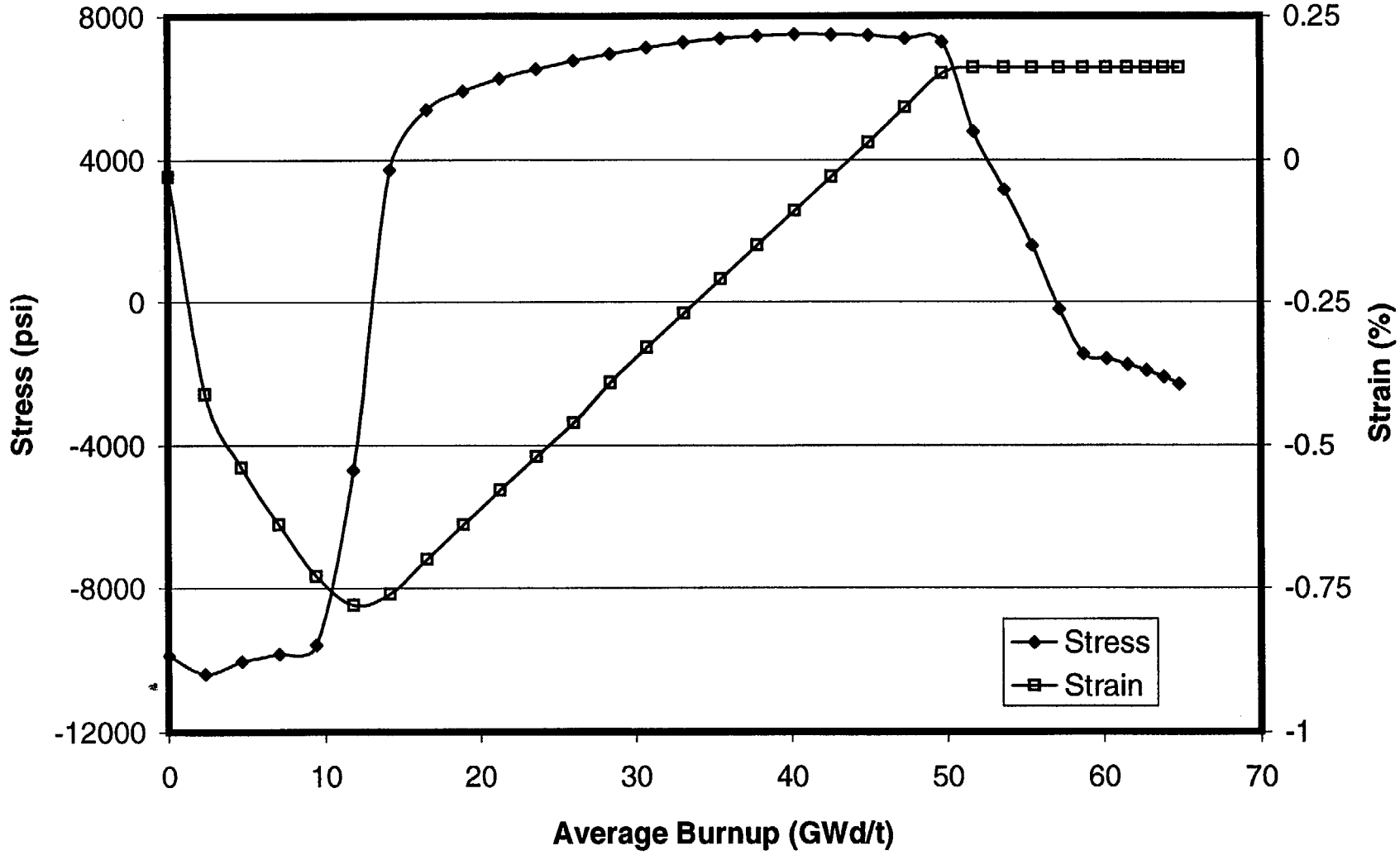

Fig. 8-12. Cladding hoop stress and hoop strain for a PWR 14x14 fuel rod with initial peak power of 11 kW/ft.

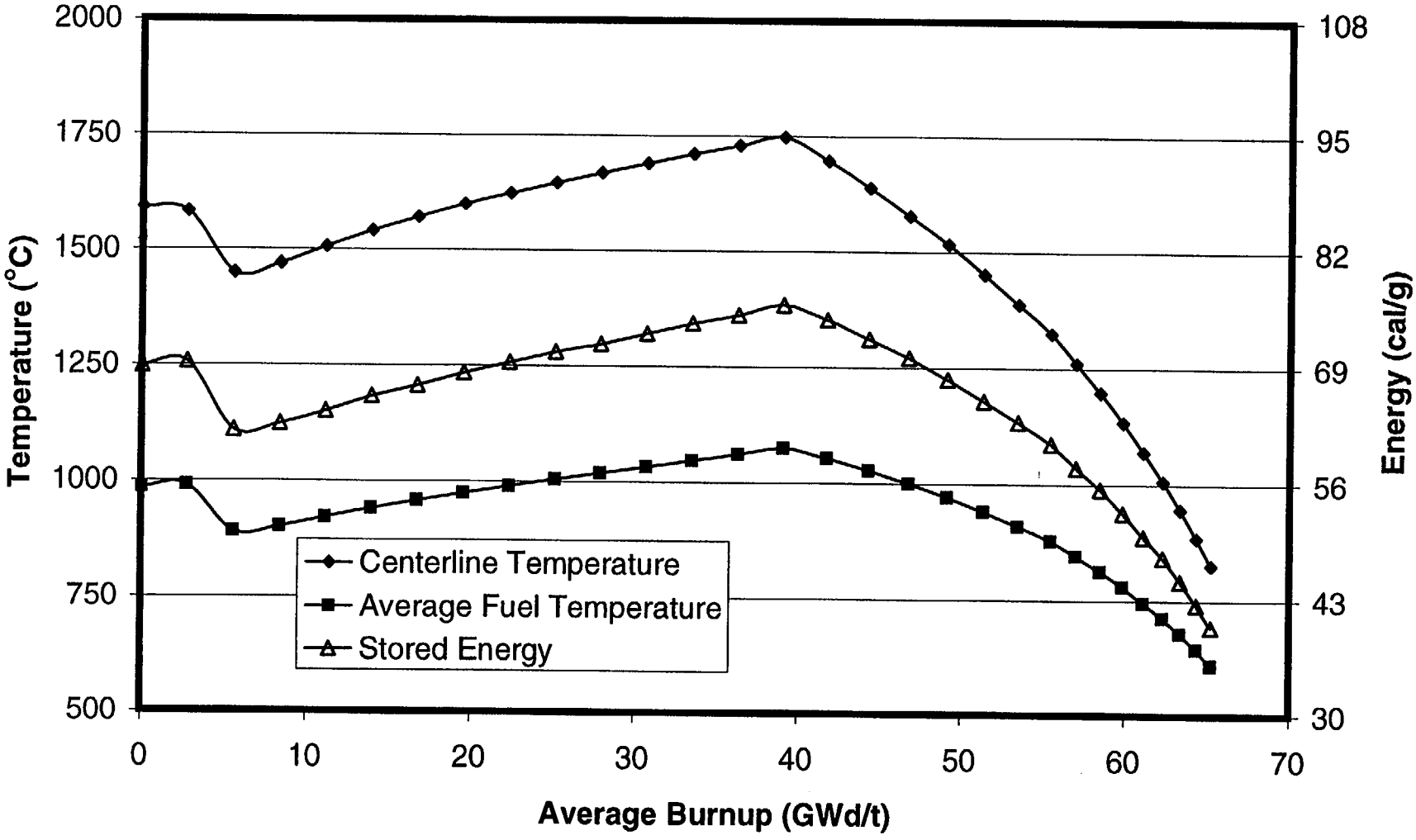

Fig. 8-13. Fuel temperatures and stored energy for a PWR 14x14 fuel rod with initial peak power of 13 kW/ft.

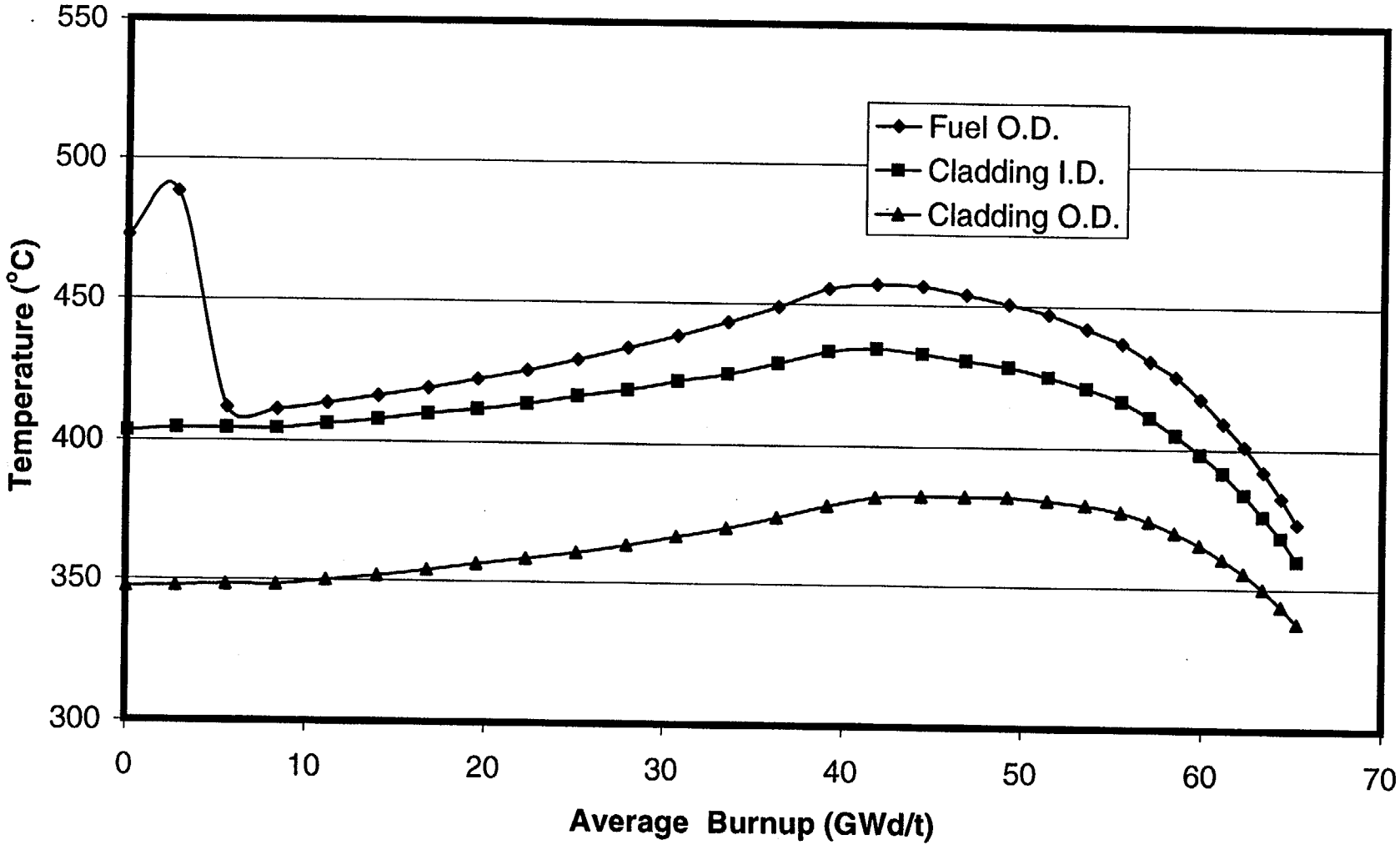

Fig. 8-14. Cladding temperatures and fuel surface temperature for a PWR 14x14 fuel rod with initial peak power of 13 kW/ft.

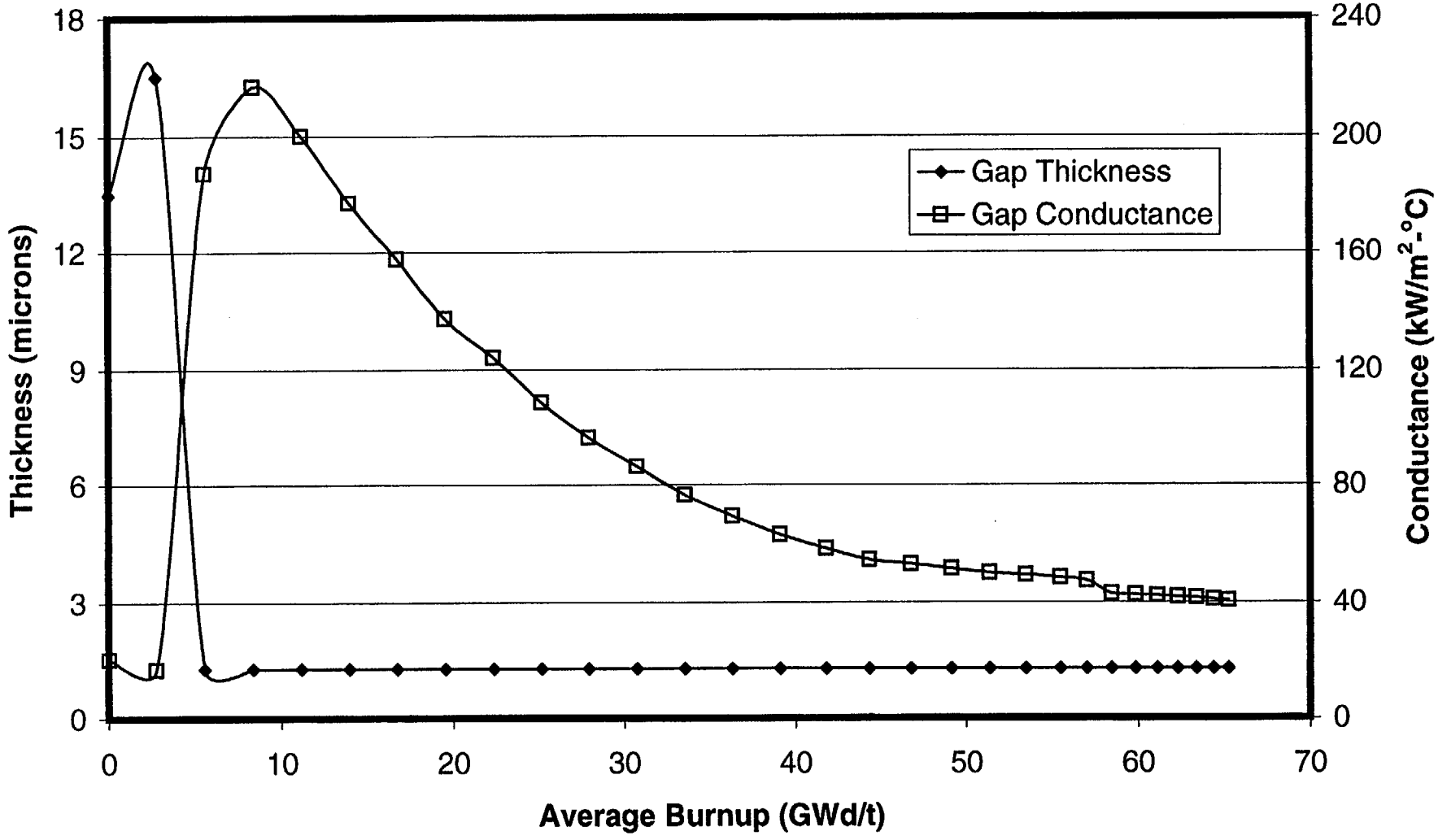

Fig. 8-15. Gap thickness and gap conductance for a PWR 14x14 fuel rod with initial peak power of 13 kW/ft.

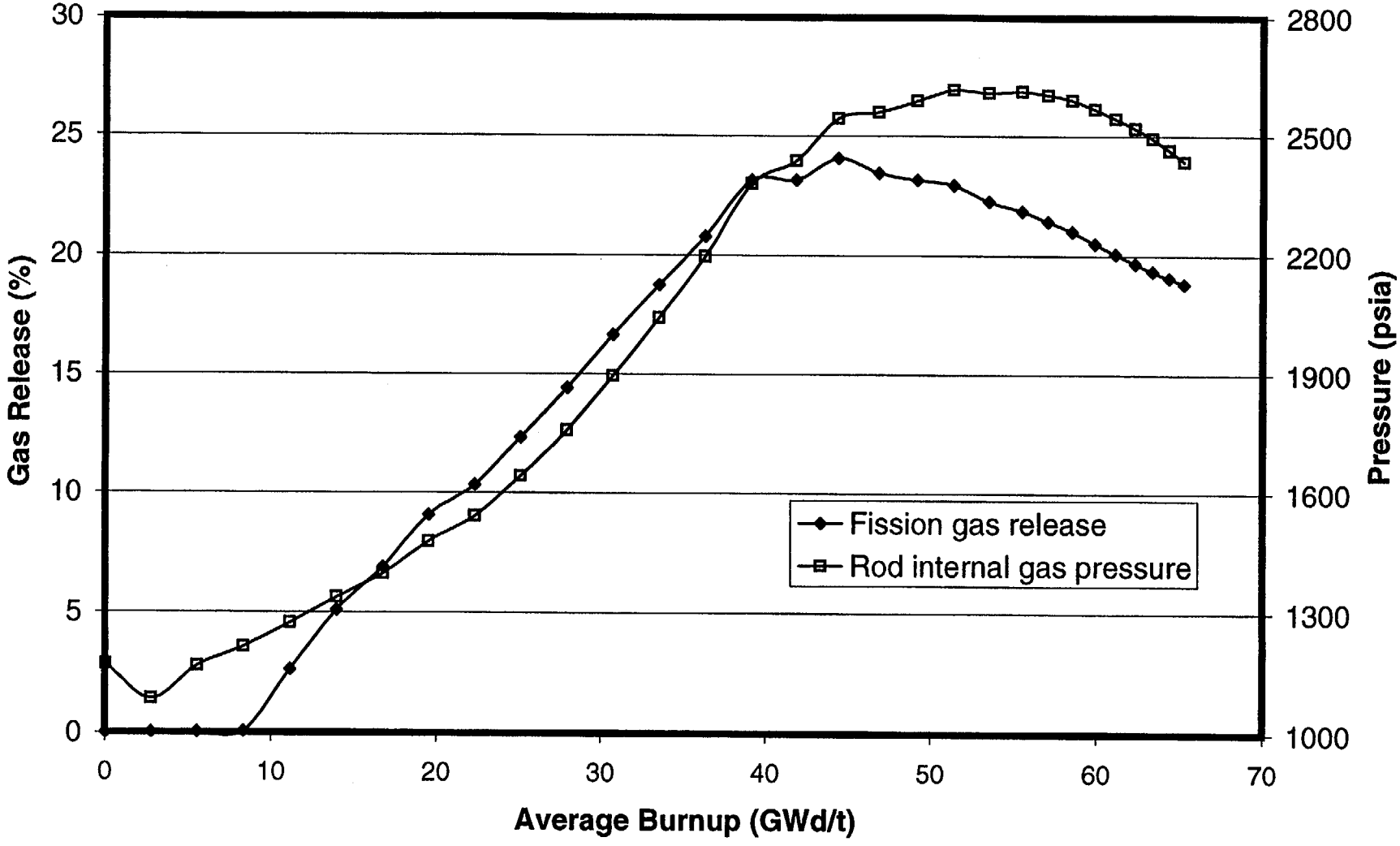

Fig. 8-16. Fission gas release and rod internal gas pressure for a PWR 14x14 fuel rod with initial peak power of 13 kW/ft.

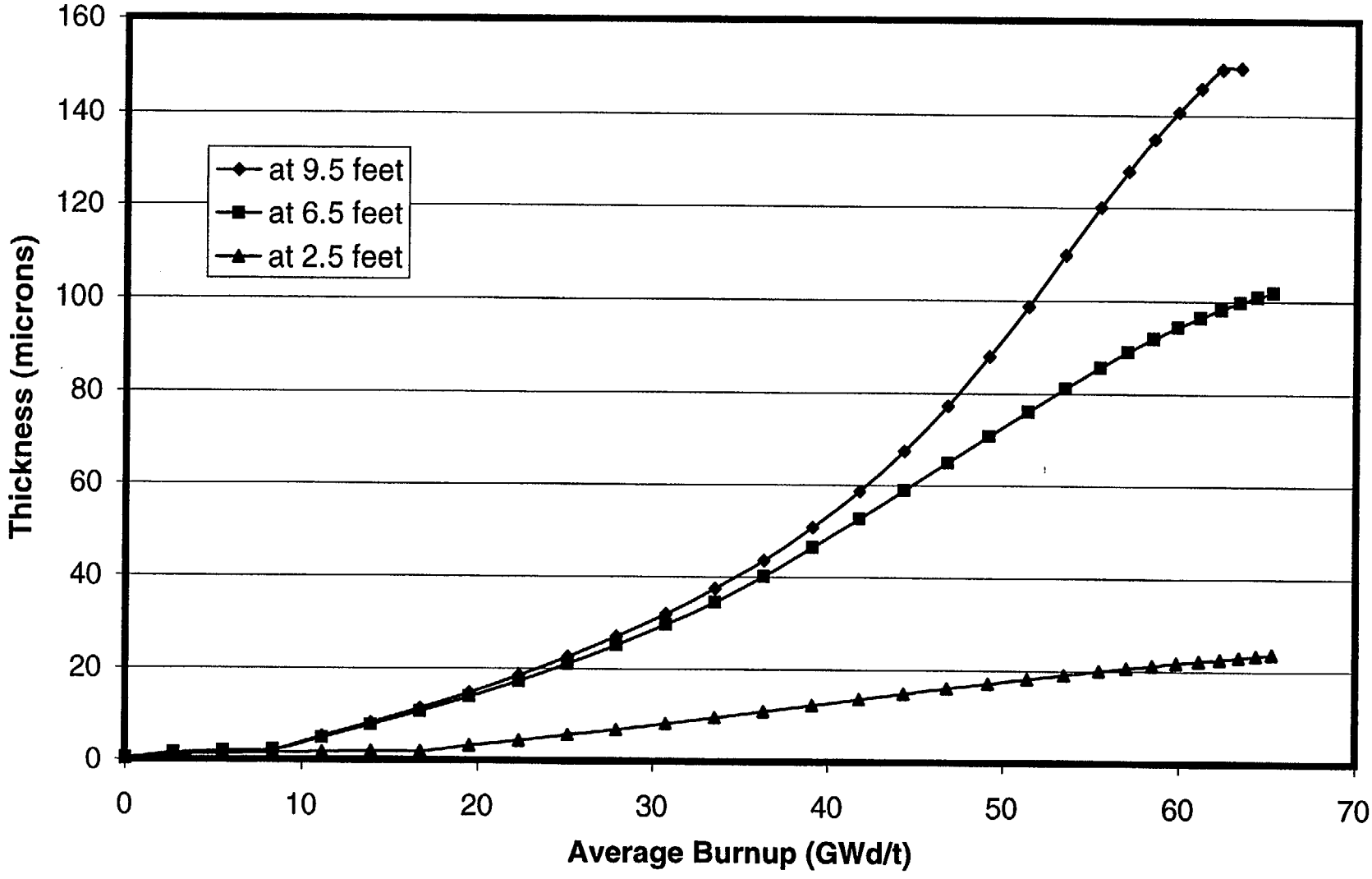

Fig. 8-17. Oxide thickness at three axial locations for a PWR 14x14 fuel rod with initial peak power of 13 kW/ft.

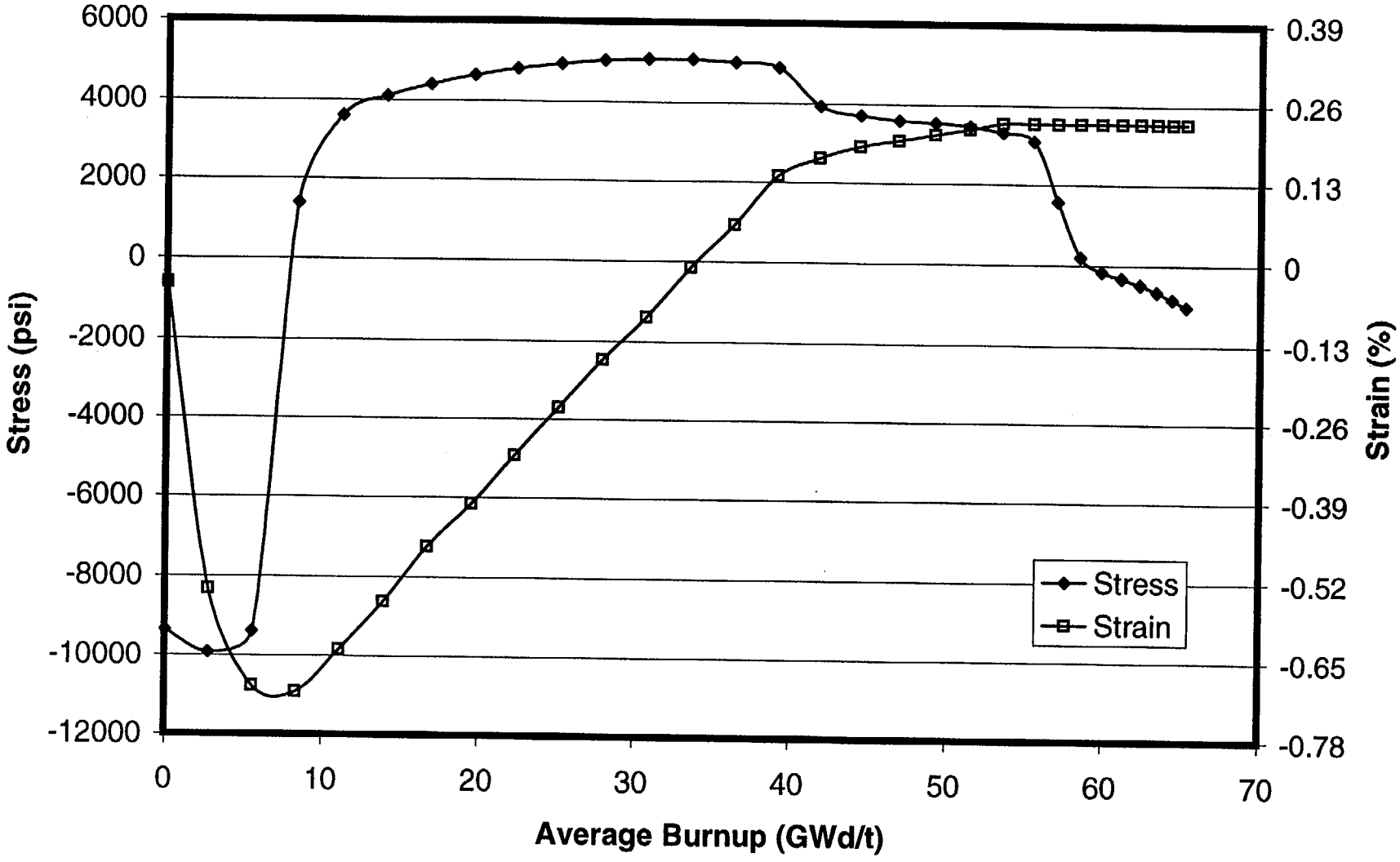

Fig. 8-18. Cladding hoop stress and hoop strain for a PWR 14x14 fuel rod with initial peak power of 13 kW/ft.

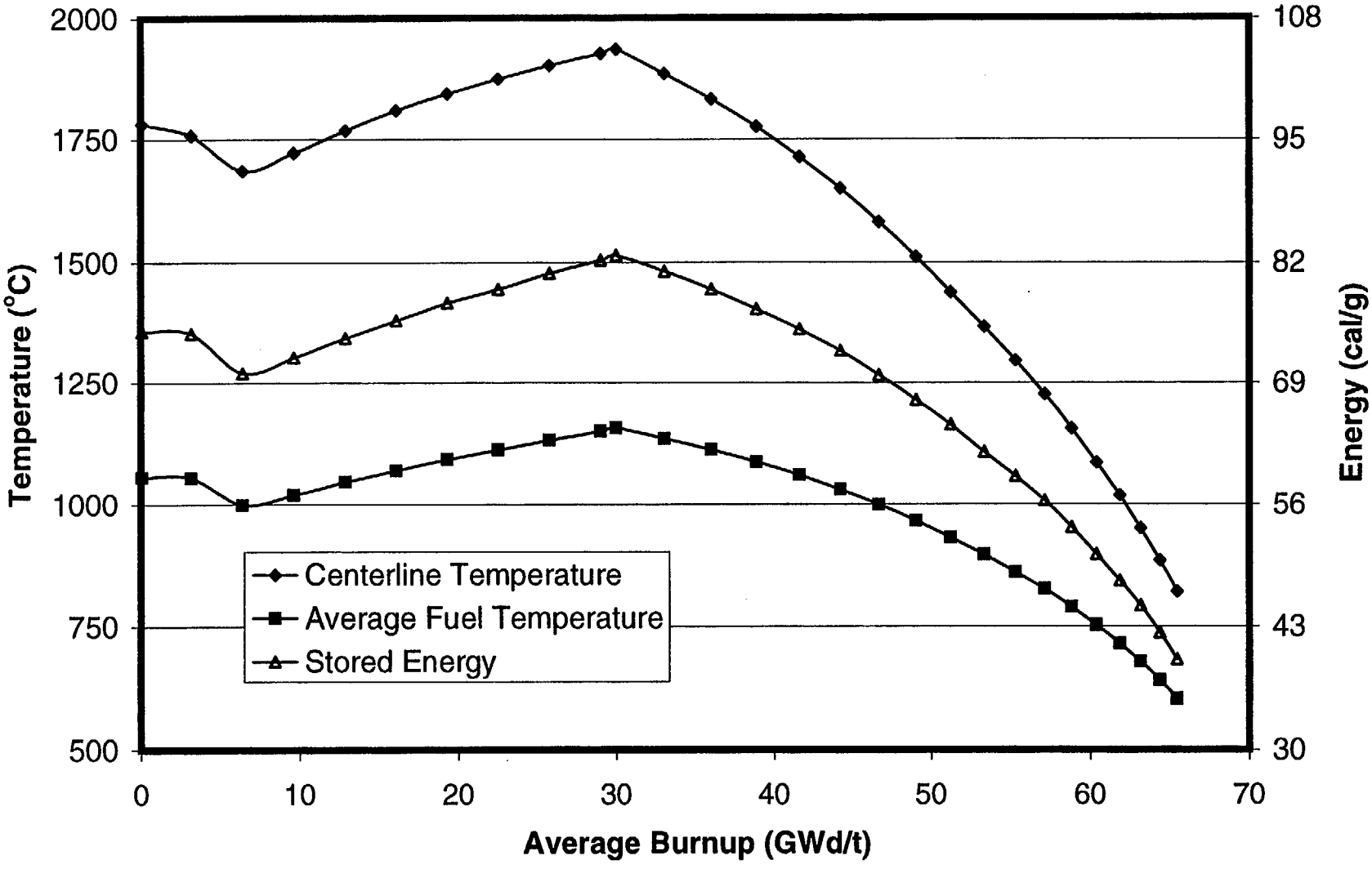

Fig. 8-19. Fuel temperatures and stored energy for a PWR 14x14 fuel rod with initial peak power of 15 kW/ft.

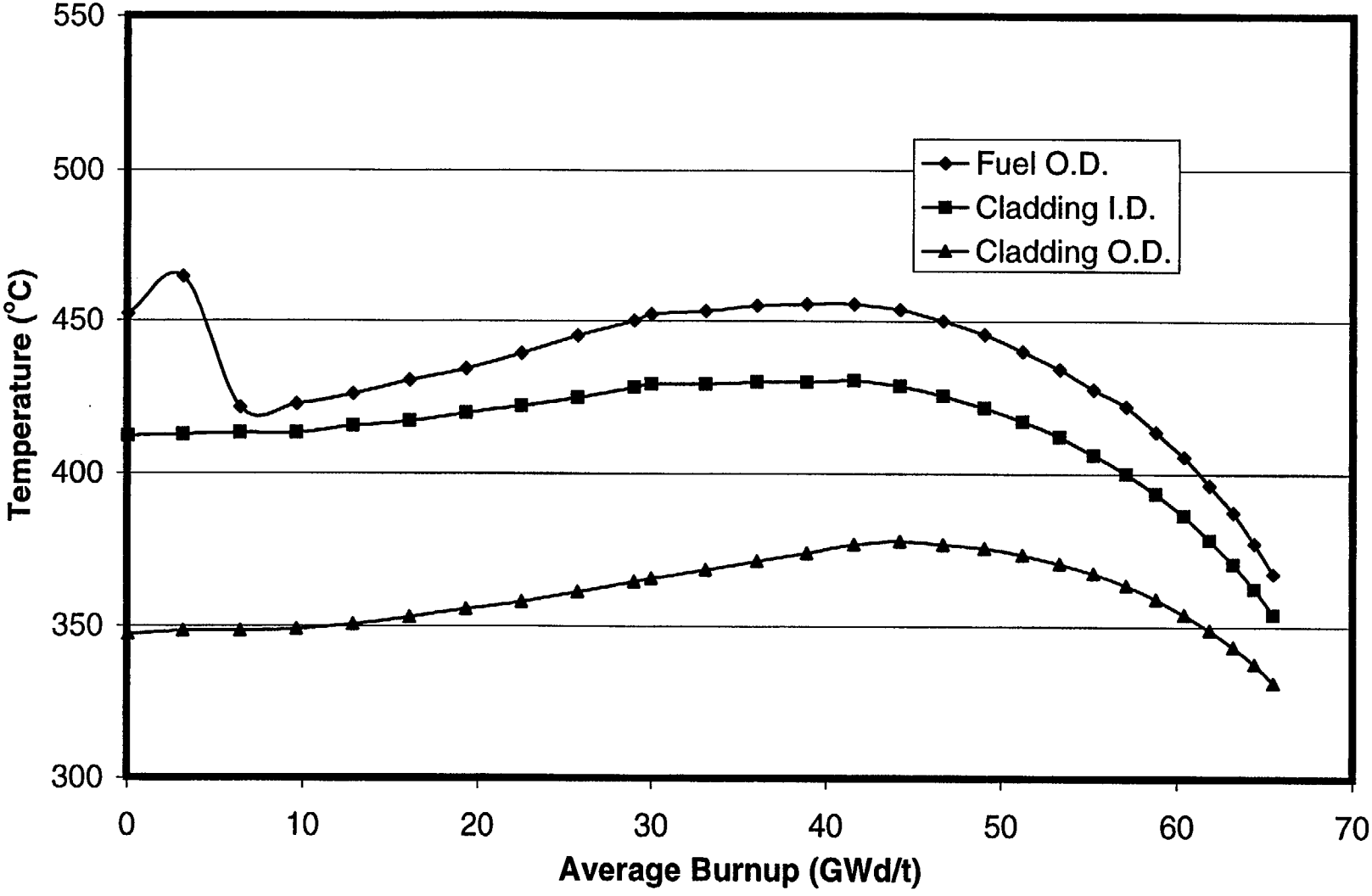

Fig. 8-20. Cladding temperatures and fuel surface temperature for a PWR 14x14 fuel rod with initial peak power of 15 kW/ft.

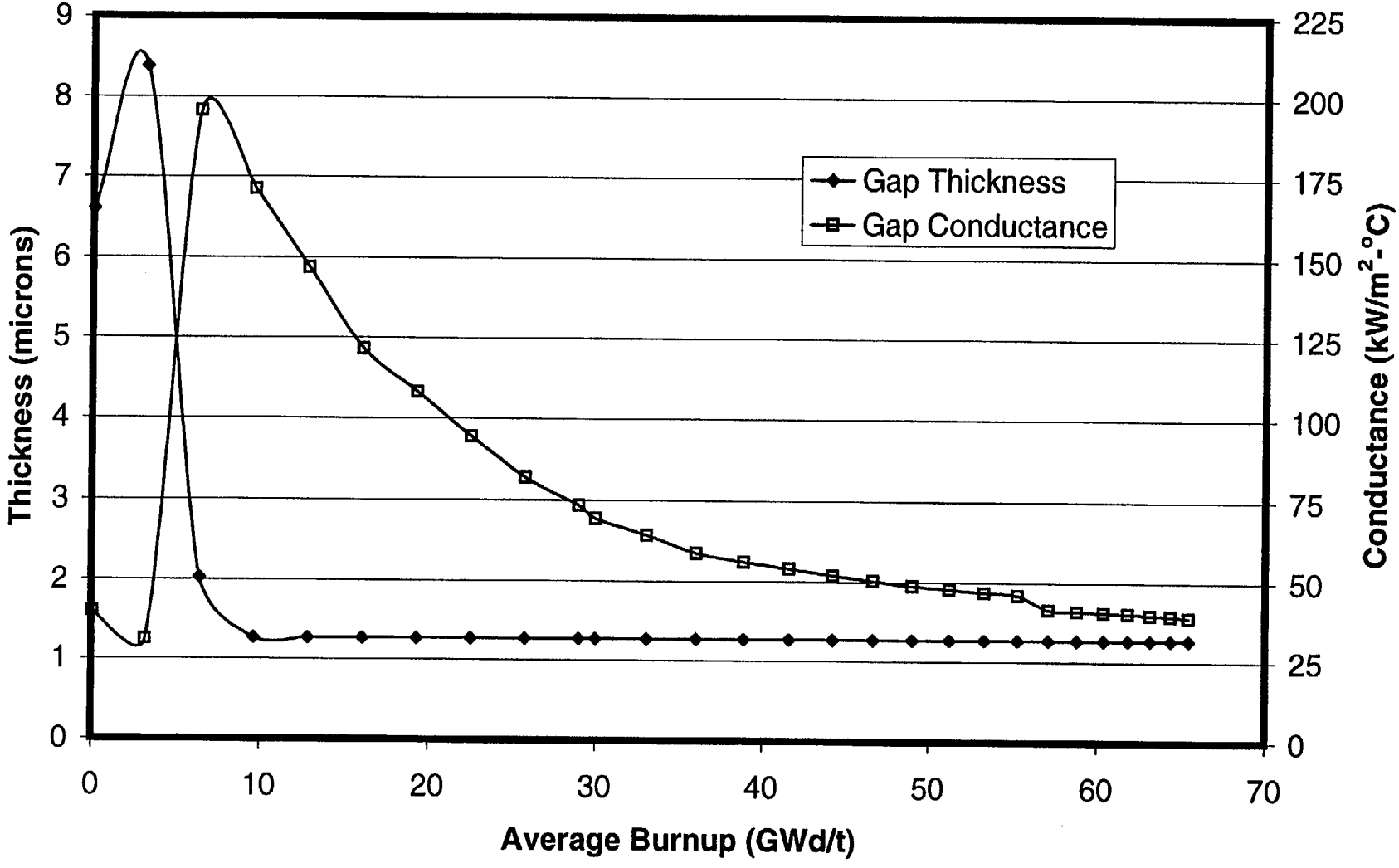

Fig. 8-21. Gap thickness and gap conductance for a PWR 14x14 fuel rod with initial peak power of 15 kW/ft.

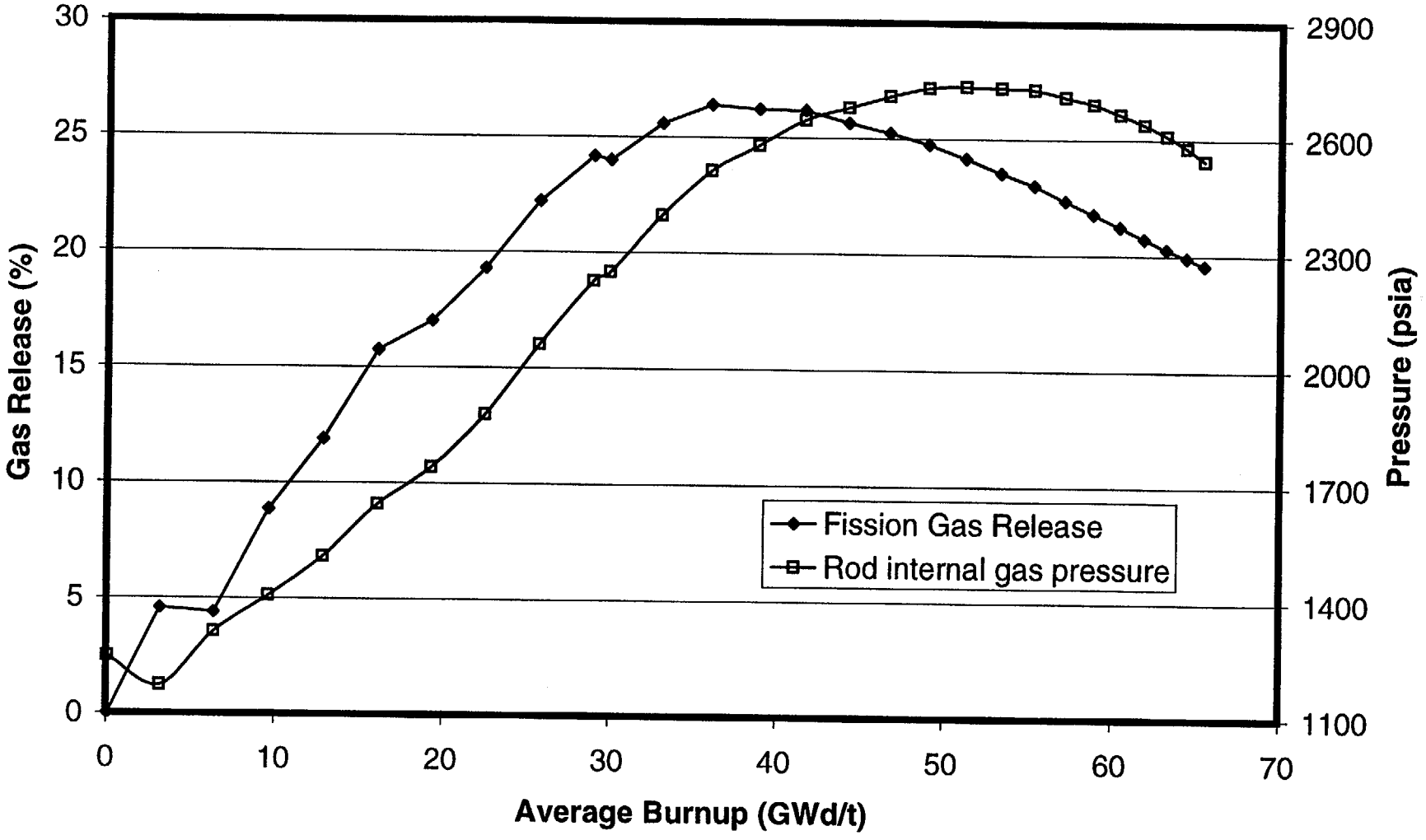

Fig. 8-22. Fission gas release and rod internal gas pressure in a PWR 14x14 fuel rod with initial peak power of 15 kW/ft.

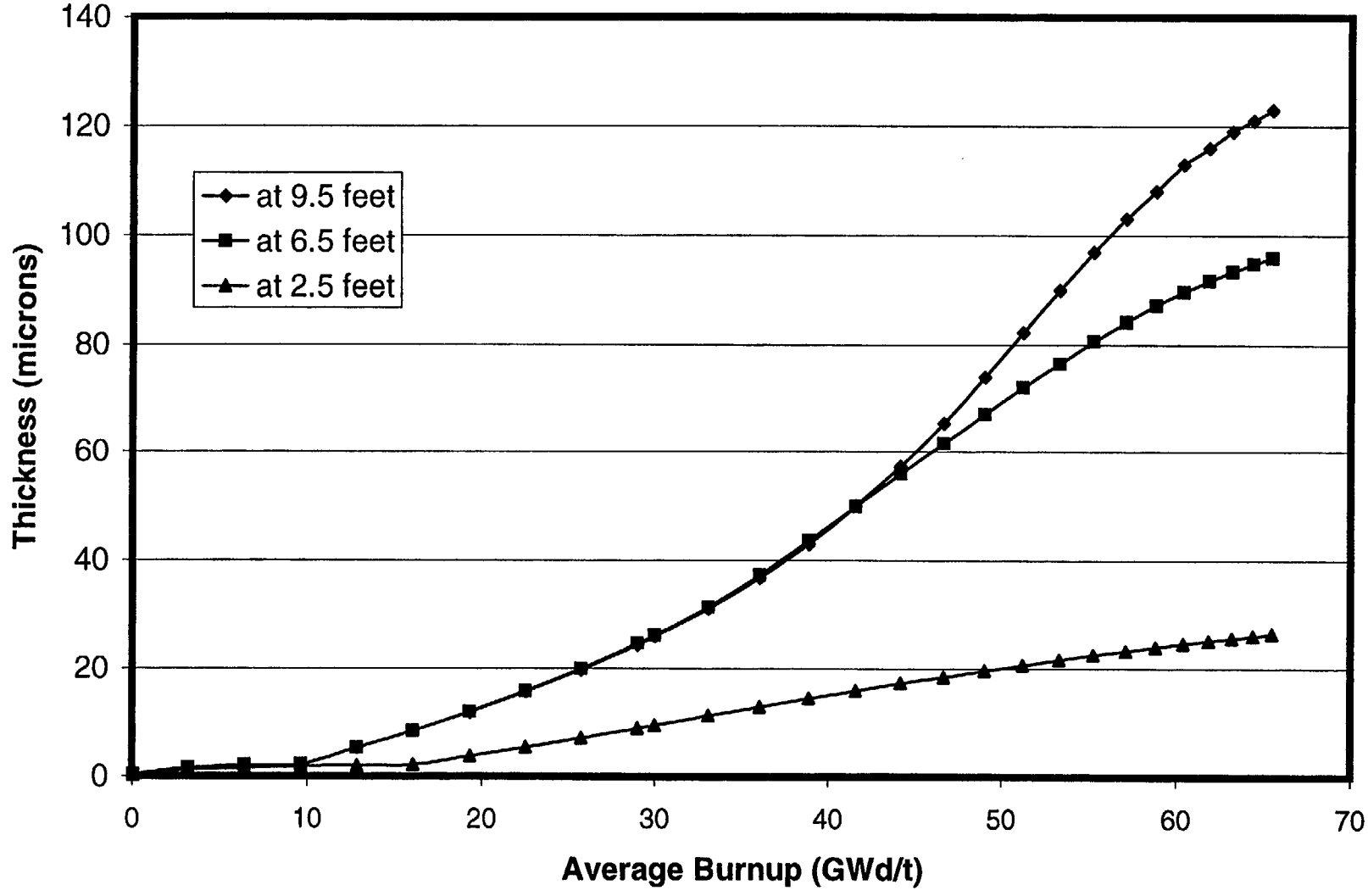

Fig. 8-23. Oxide thickness at three axial locations for a PWR 14x14 fuel rod with initial peak power of 15 kW/ft.

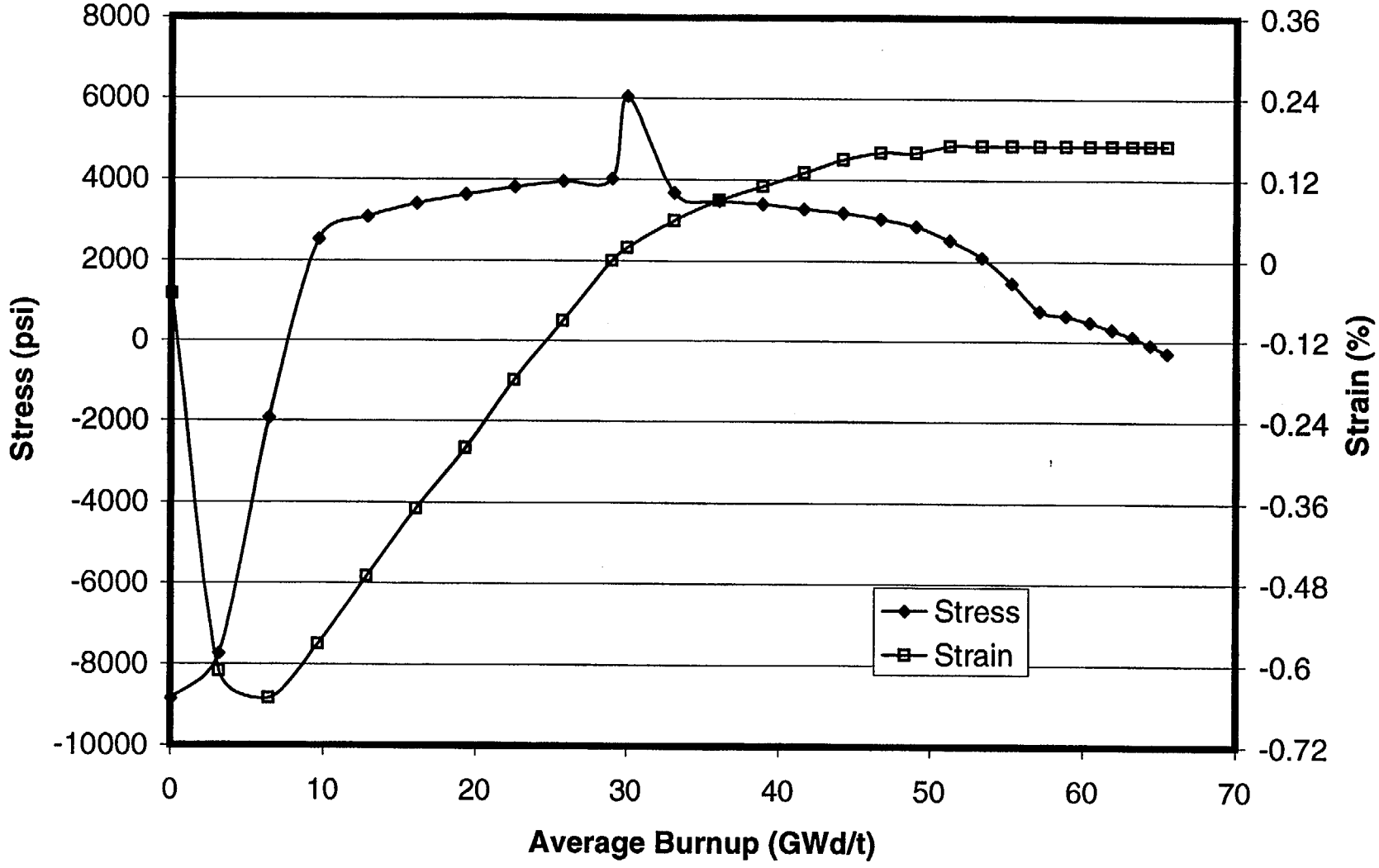

Fig. 8-24. Cladding hoop stress and hoop strain for a PWR 14x14 fuel rod with initial peak power of 15 kW/ft.

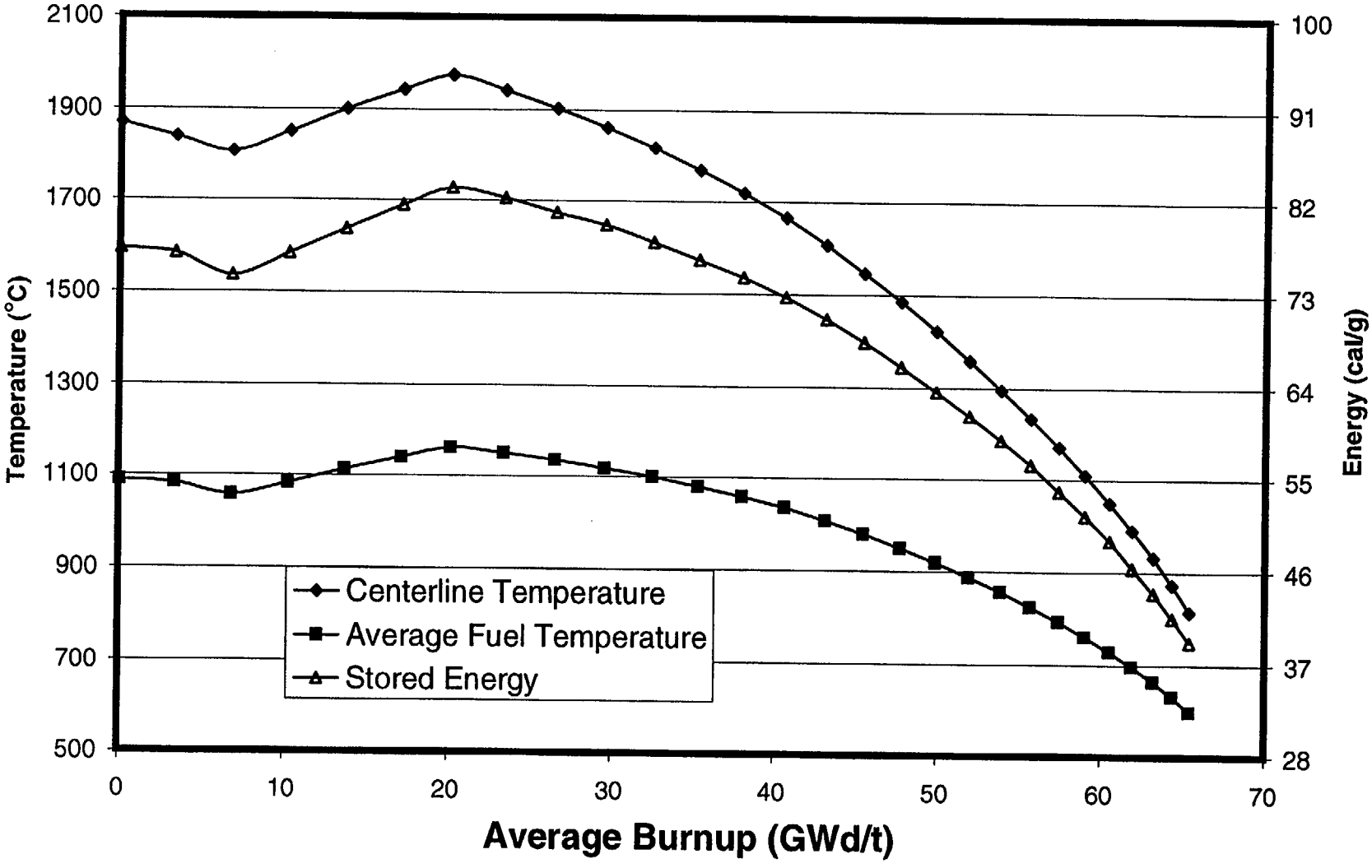

Fig. 8-25. Fuel Temperatures and stored energy for a PWR 14x14 fuel rod with initial peak power of 16 kW/ft.

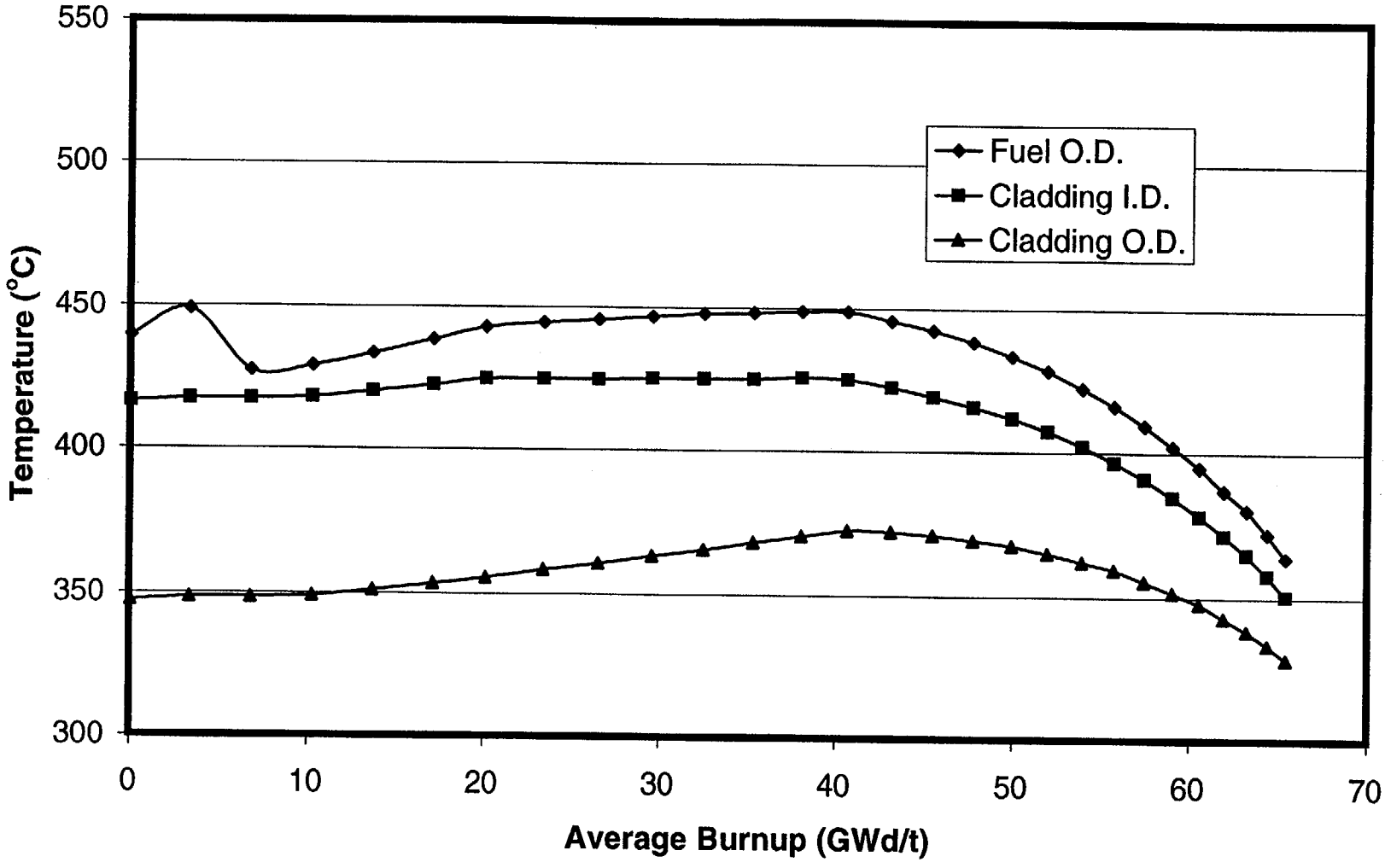

Fig. 8-26. Cladding temperatures and fuel surface temperature for a PWR 14x14 fuel rod with initial peak power of 16 kW/ft.

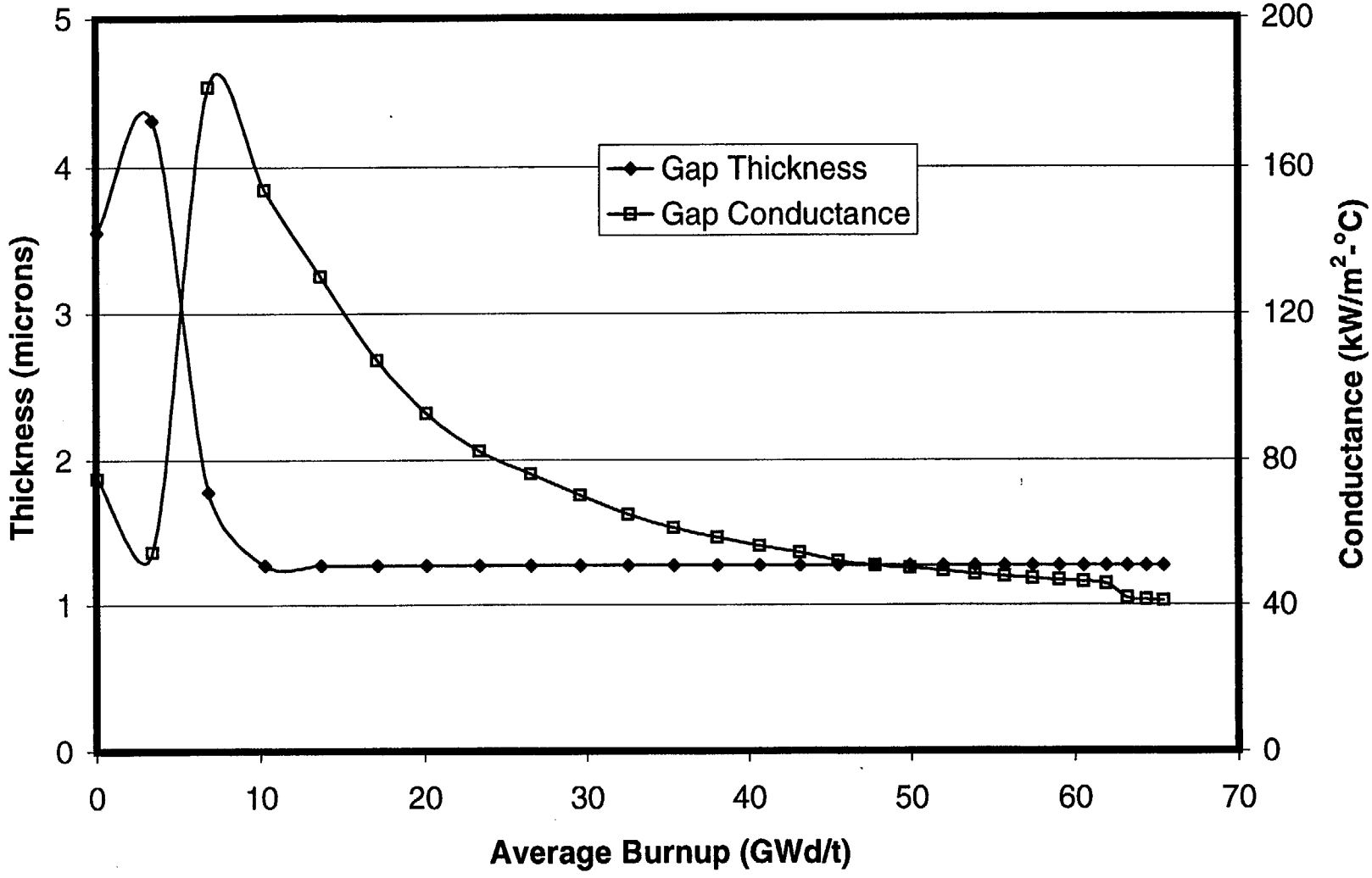

Fig. 8-27. Gap thickness and gap conductance for a PWR 14x14 fuel rod with initial peak power of 16 kW/ft.

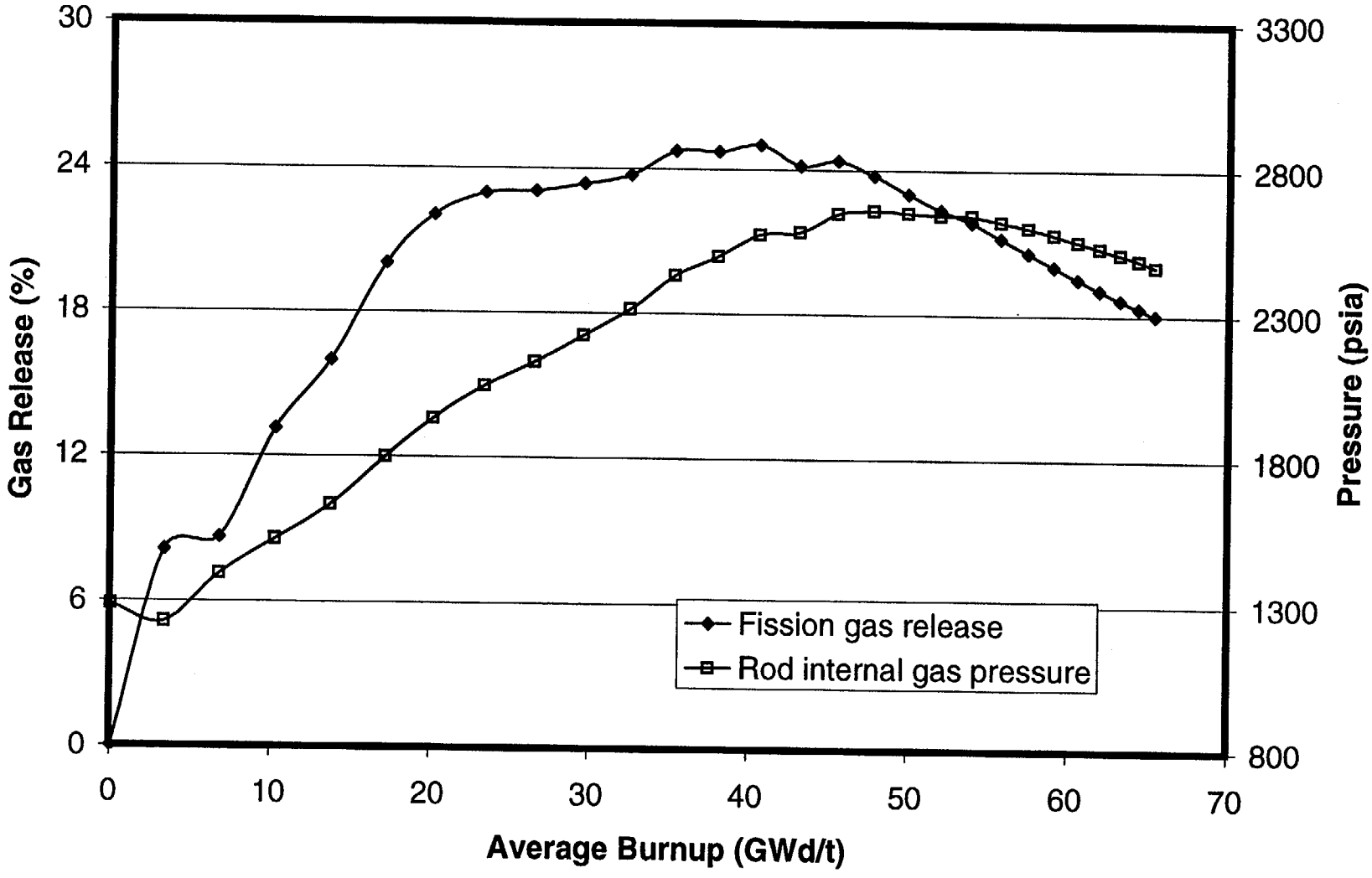

Fig. 8-28. Fission gas release and rod internal gas pressure for a PWR 14x14 fuel rod with initial peak power of 16 kW/ft.

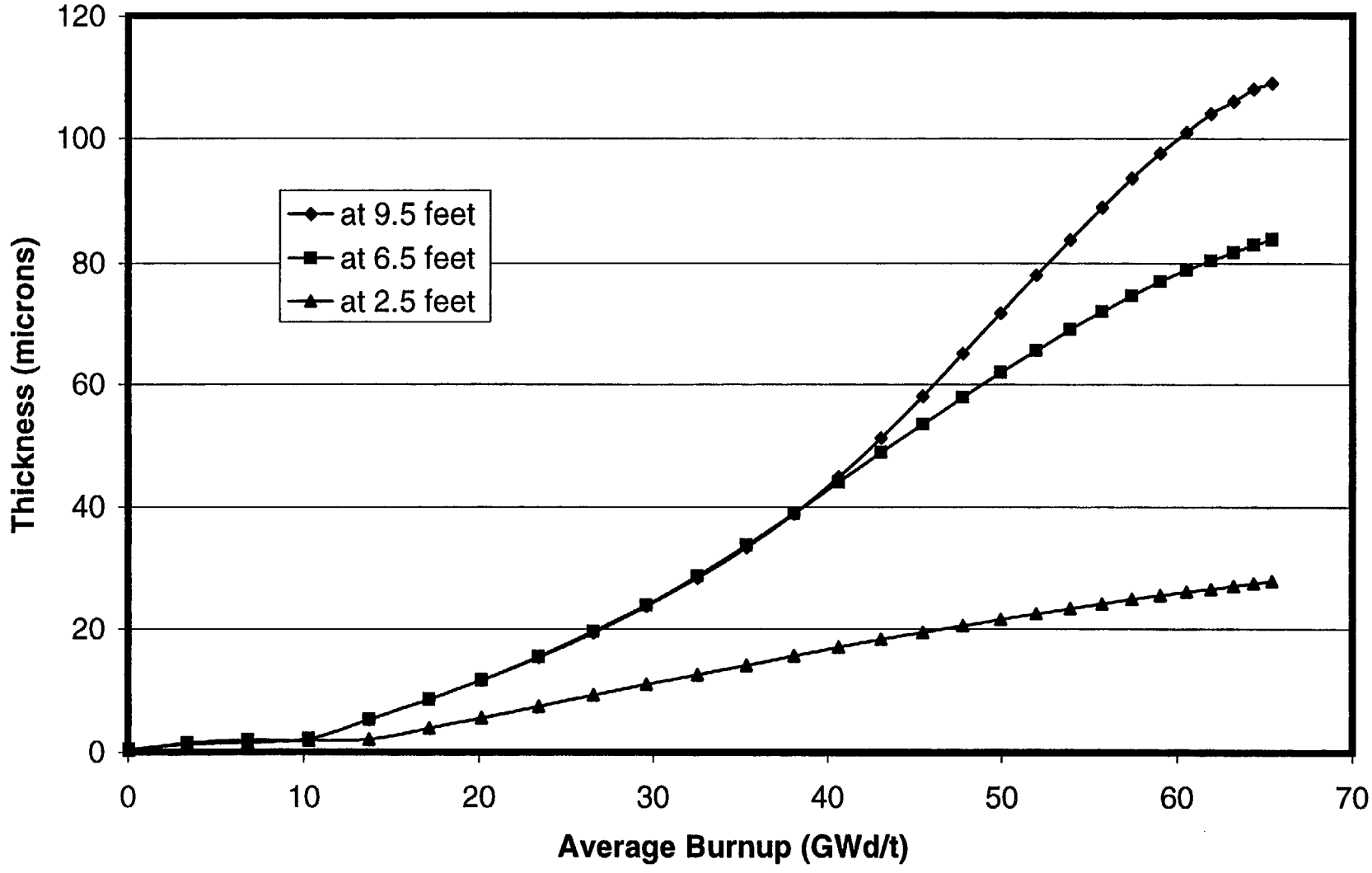

Fig. 8-29. Oxide thickness at three axial locations for a PWR 14x14 fuel rod with initial peak power of 16 kW/ft.

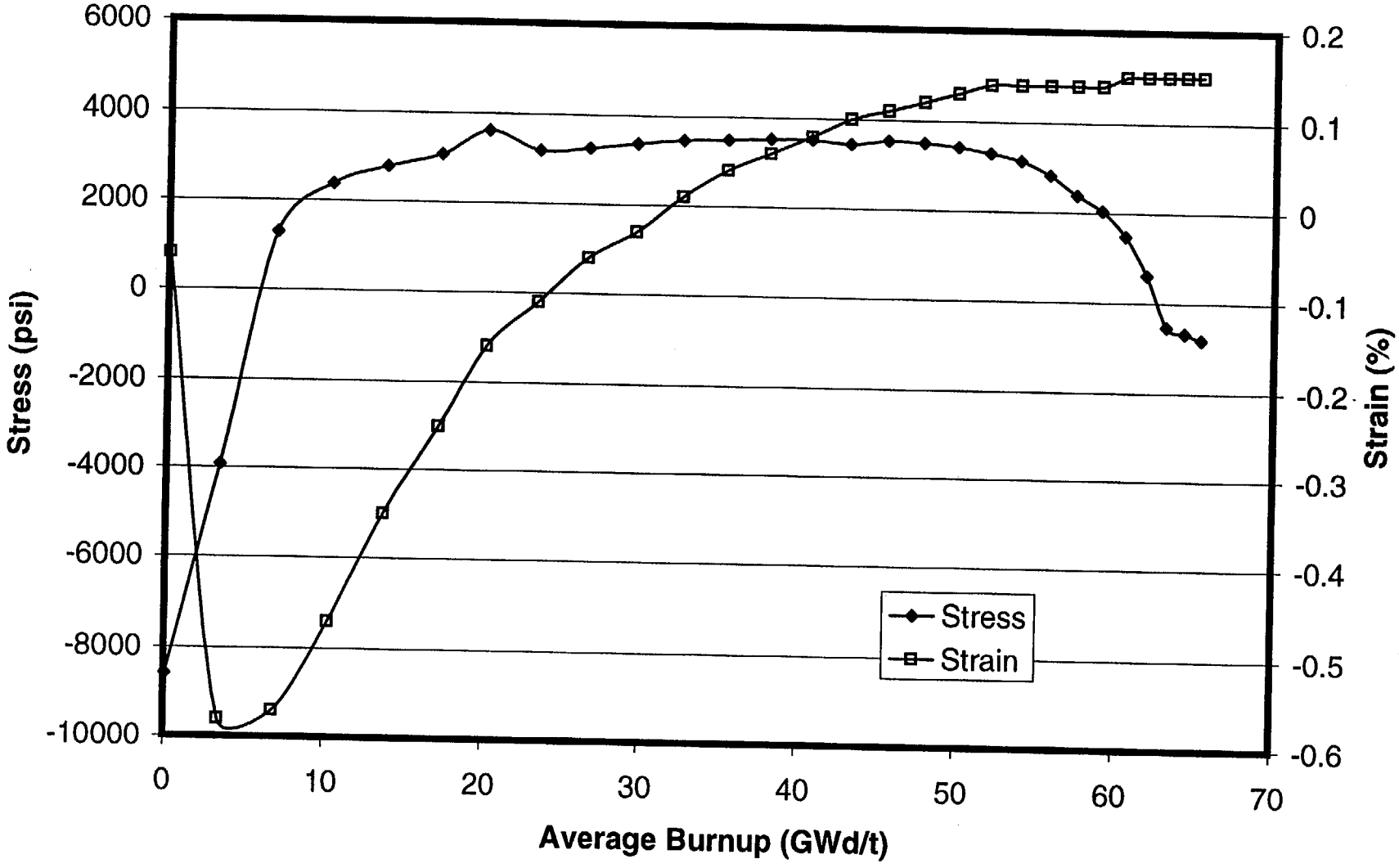

Fig. 8-30. Cladding hoop stress and hoop strain for a PWR 14x14 fuel rod with initial peak power of 16 kW/ft.

9. Calculations for PWR 15X15 Fuel

In the following figures, calculated values for PWR 15X15 fuel are plotted as a function of burnup for the parameters listed below:

Fuel centerline temperature
Average fuel temperature
Stored energy
Fuel O.D. temperature
Cladding I.D. temperature
Cladding O.D. temperature
Gap thickness
Gap conductance
Fission gas release
Rod internal gas pressure
Oxide thickness
Cladding hoop stress
Cladding hoop strain

Several general observations can be made about the calculated results:

- Within the first few GWd/t of burnup, a temperature peak is observed that is the result of fuel densification.

- Gap closure results in (a) the coming together of temperatures for fuel O.D. and cladding I.D. and (b) a sharp increase in gap conductance. The gap conductance increases again after a few time steps when the interaction between the pellet and cladding affects the contact conductance calculated for a closed gap. At this point there is also a large increase in stress, and the permanent strain changes directions.

- Some of the fission gas is released in spurts according to the Massih model in FRAPCON-3. This effect is apparent in many of the figures. Shorter time steps would produce slightly different looking curves, but the trend of gas release and the end-of-life gas release would be about the same.

- The burnup enhancement of fission gas release is readily seen in the lower power cases, but it is obscured in the highest power cases by the magnitude of prior gas release.

- Rod internal gas pressure increases with the accumulation of released fission gas. In the higher power PWR cases, as the power drops off near the end of life, the reduction in the plenum temperature offsets the increasing moles of fission gas.

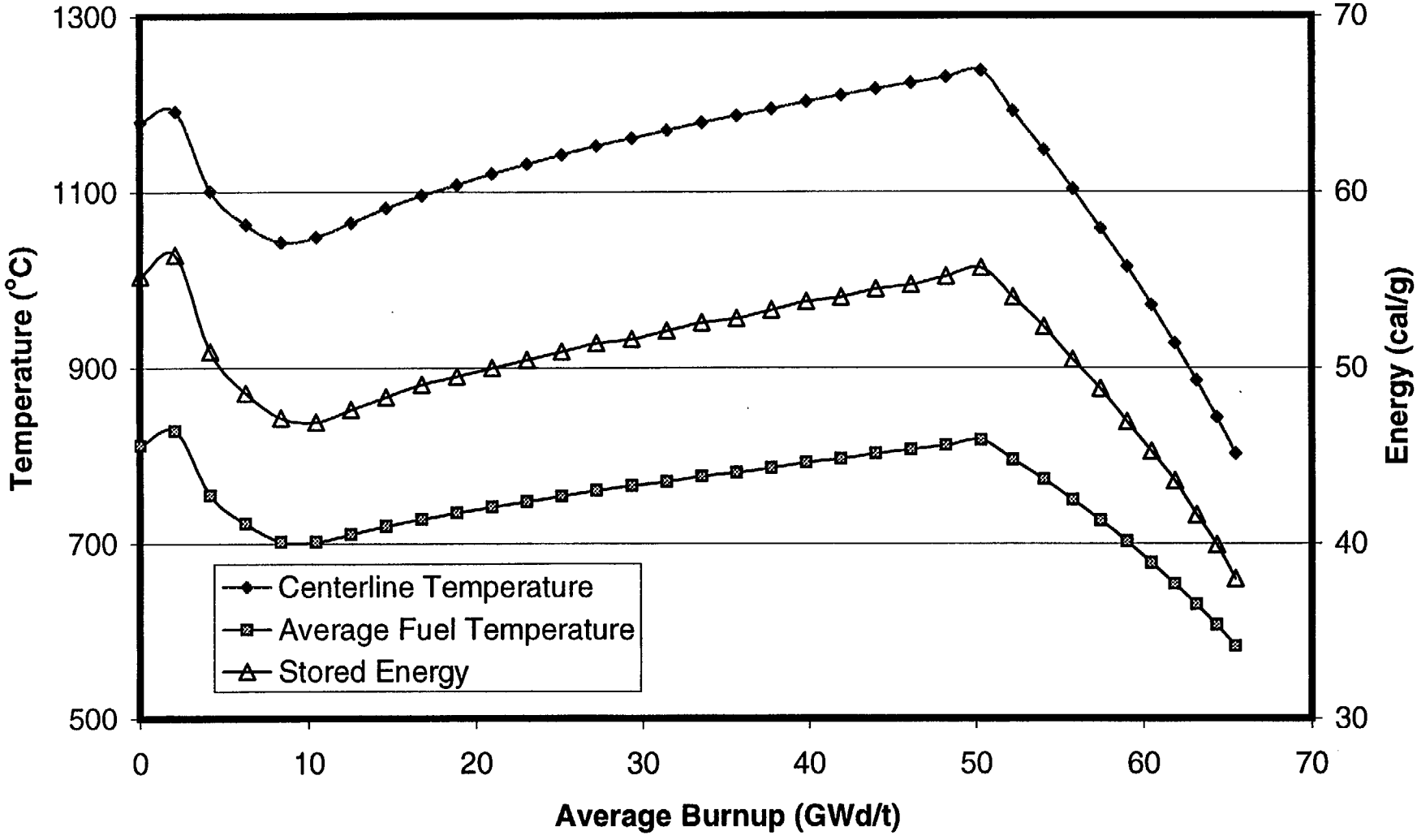

Fig. 9-1. Fuel temperatures and stored energy for a PWR 15x15 fuel rod with initial peak power of 9 kW/ft.

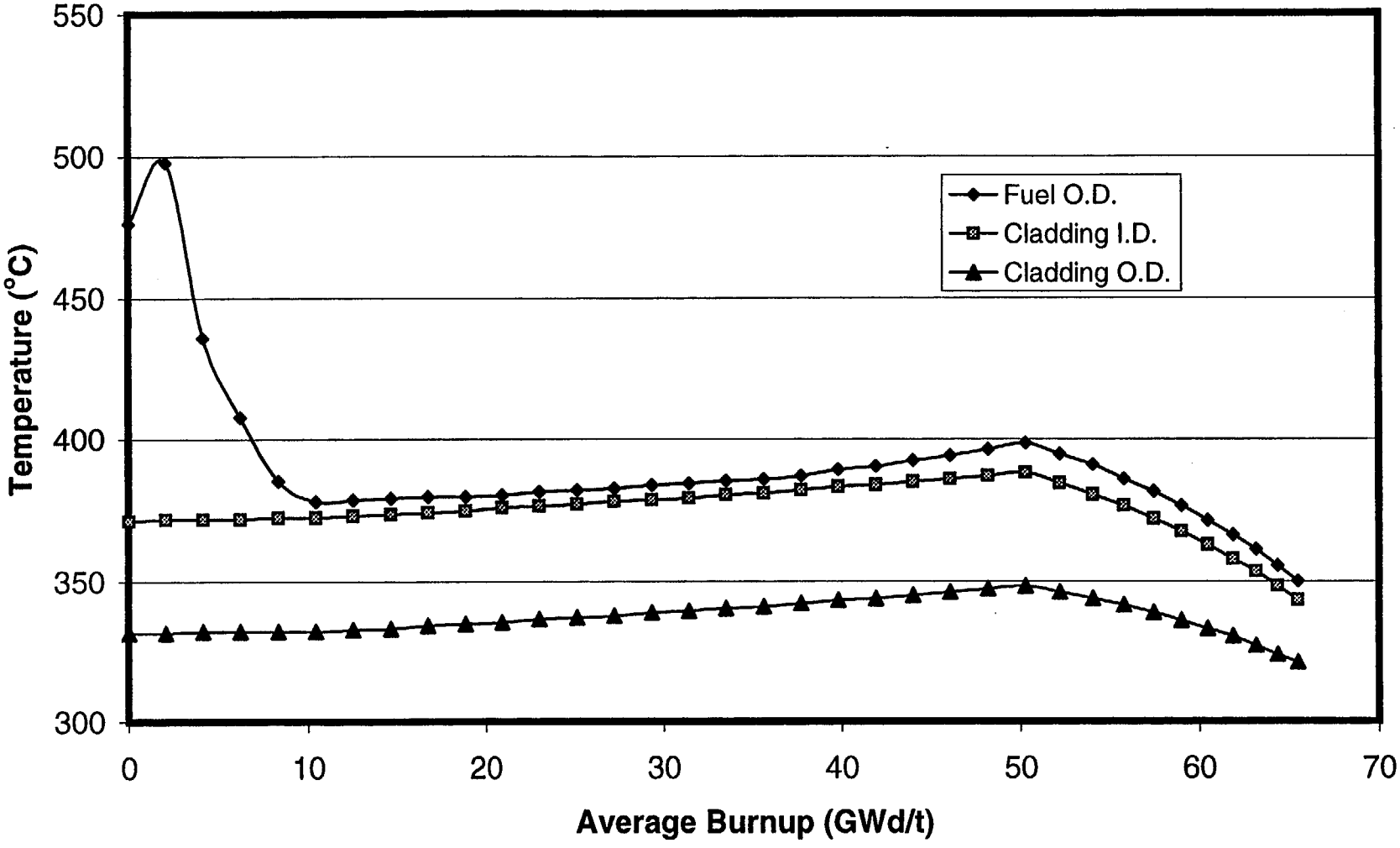

Fig. 9-2. Cladding temperatures and fuel surface temperature for a PWR 15x15 fuel rod with initial peak power of 9 kW/ft.

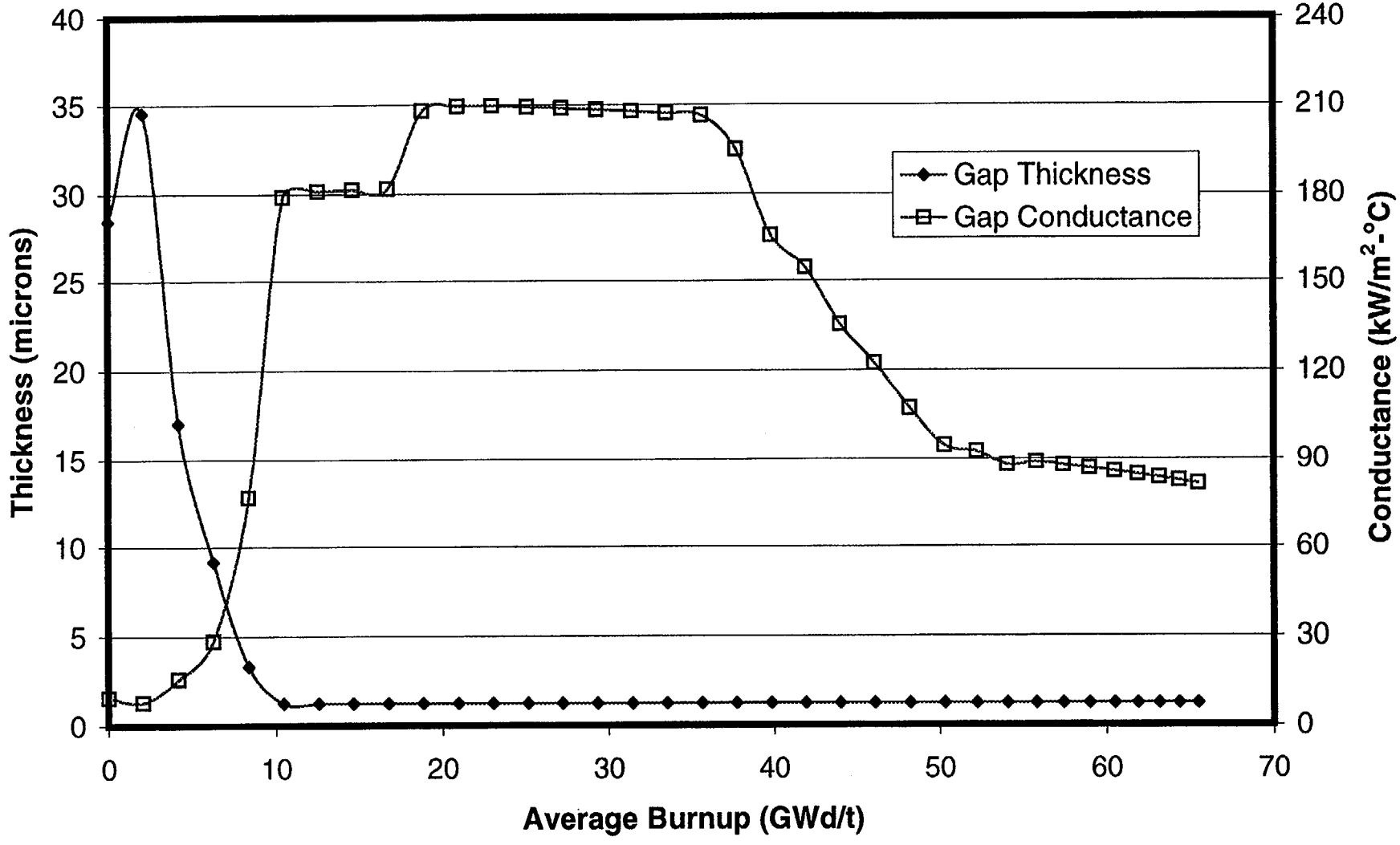

Fig. 9-3. Gap thickness and gap conductance for a PWR 15x15 fuel rod with initial peak power of 9 kW/ft.

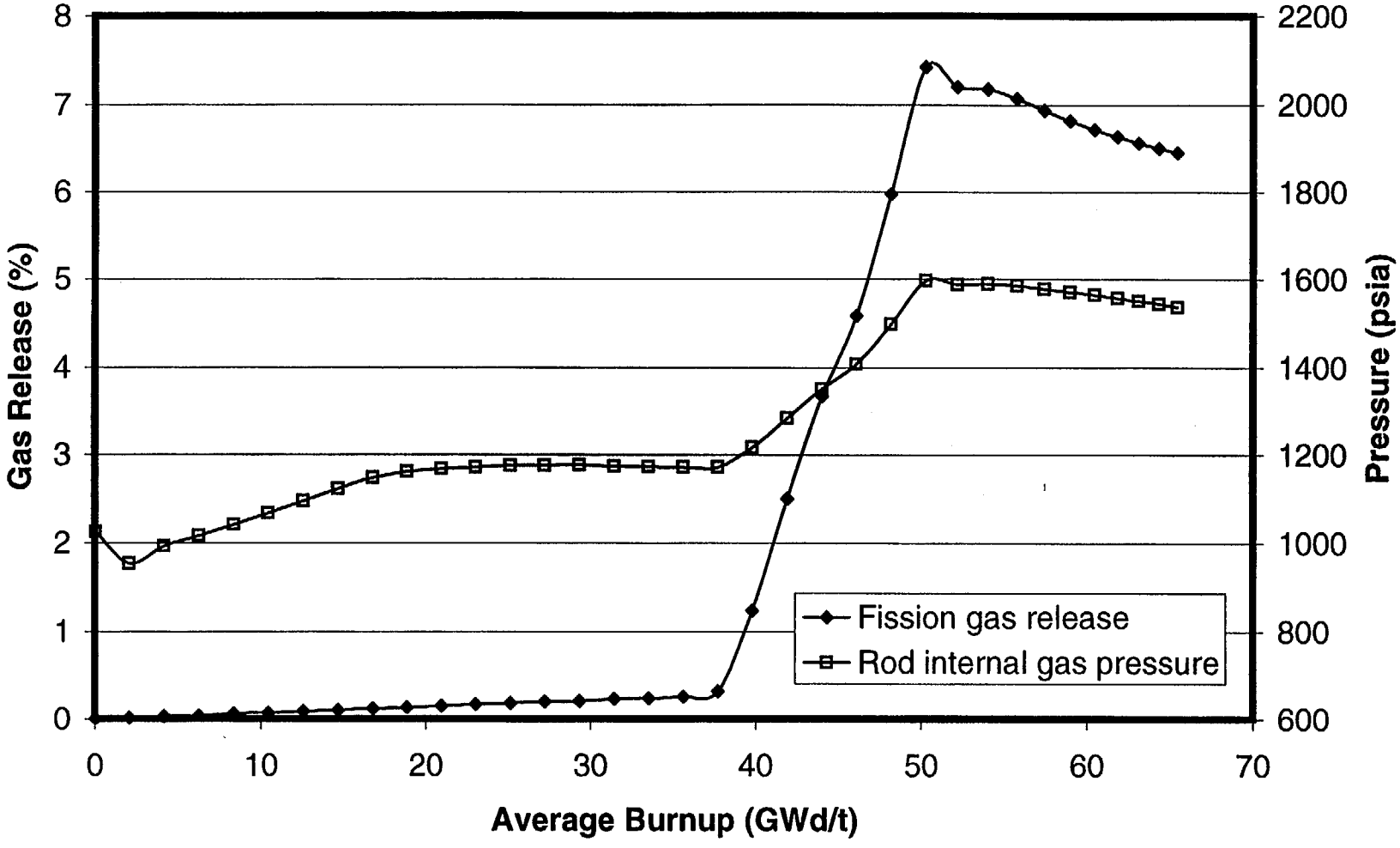

Fig. 9-4. Fission gas release and rod internal gas pressure for a PWR 15x15 fuel rod with initial peak power of 9 kW/ft.

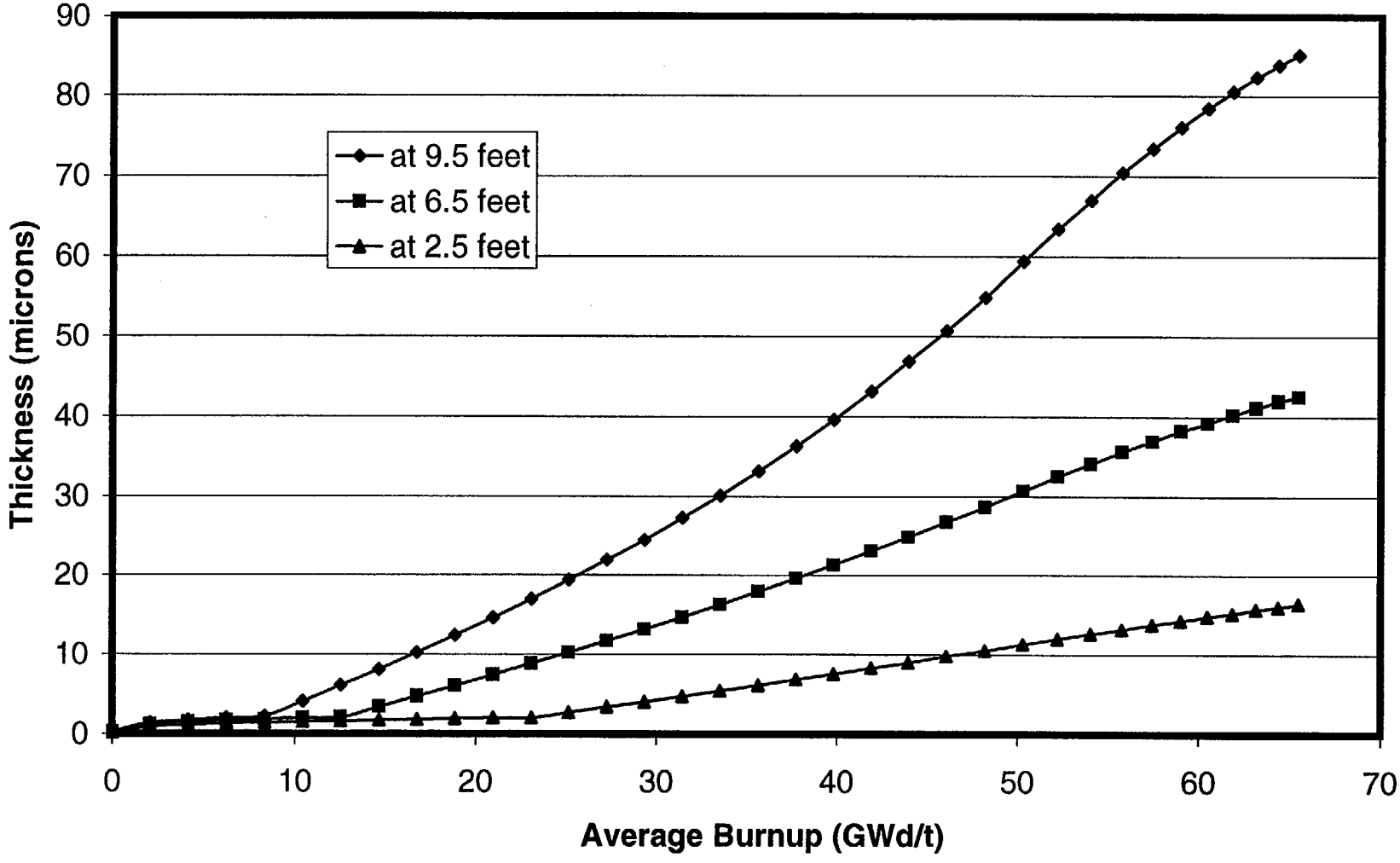

Fig. 9-5. Oxide thickness at three axial locations for a PWR 15x15 fuel rod with initial peak power of 9 kW/ft.

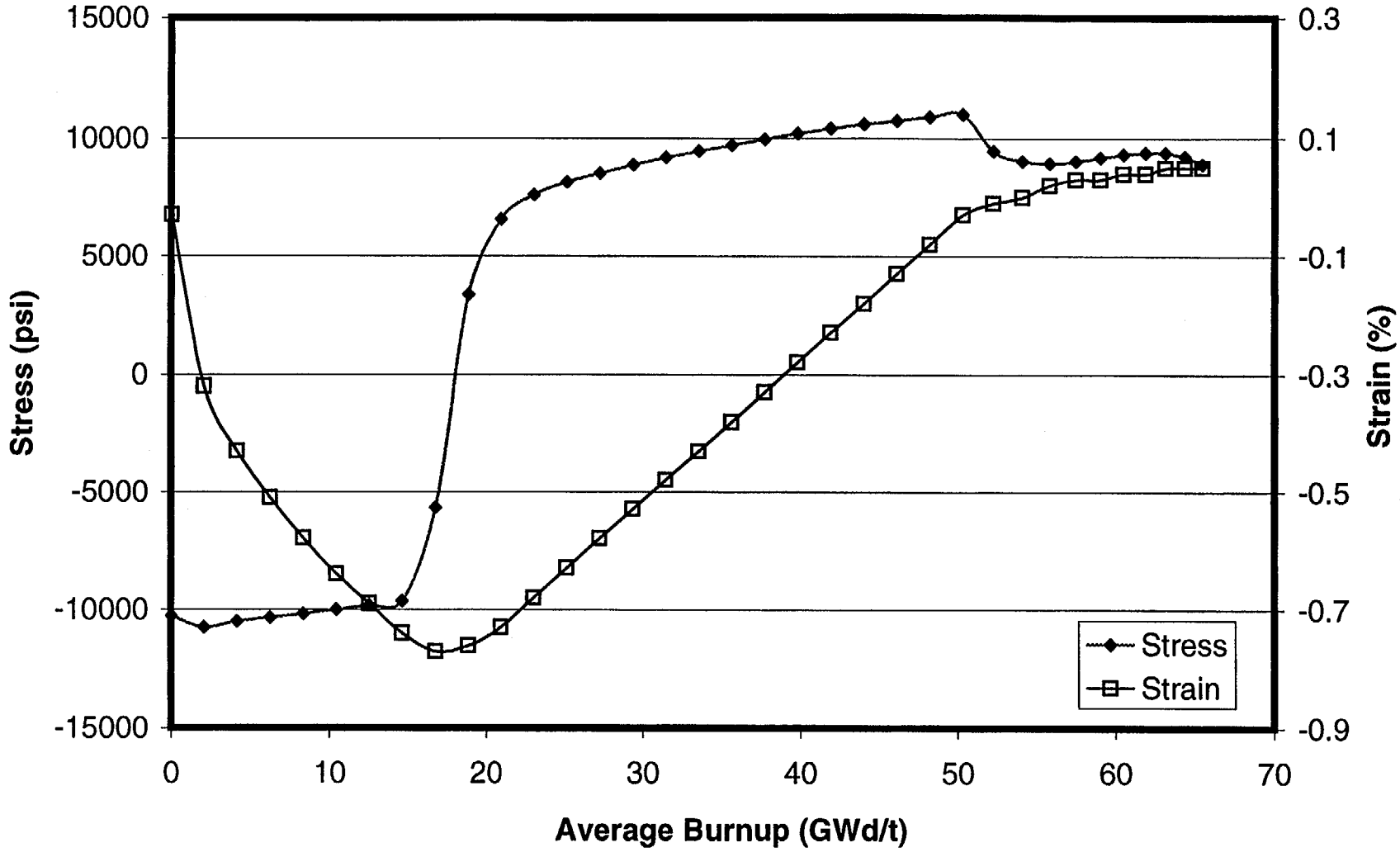

Fig. 9-6. Cladding hoop stress and hoop strain for a PWR 15x15 fuel rod with initial peak power of 9 kW/ft.

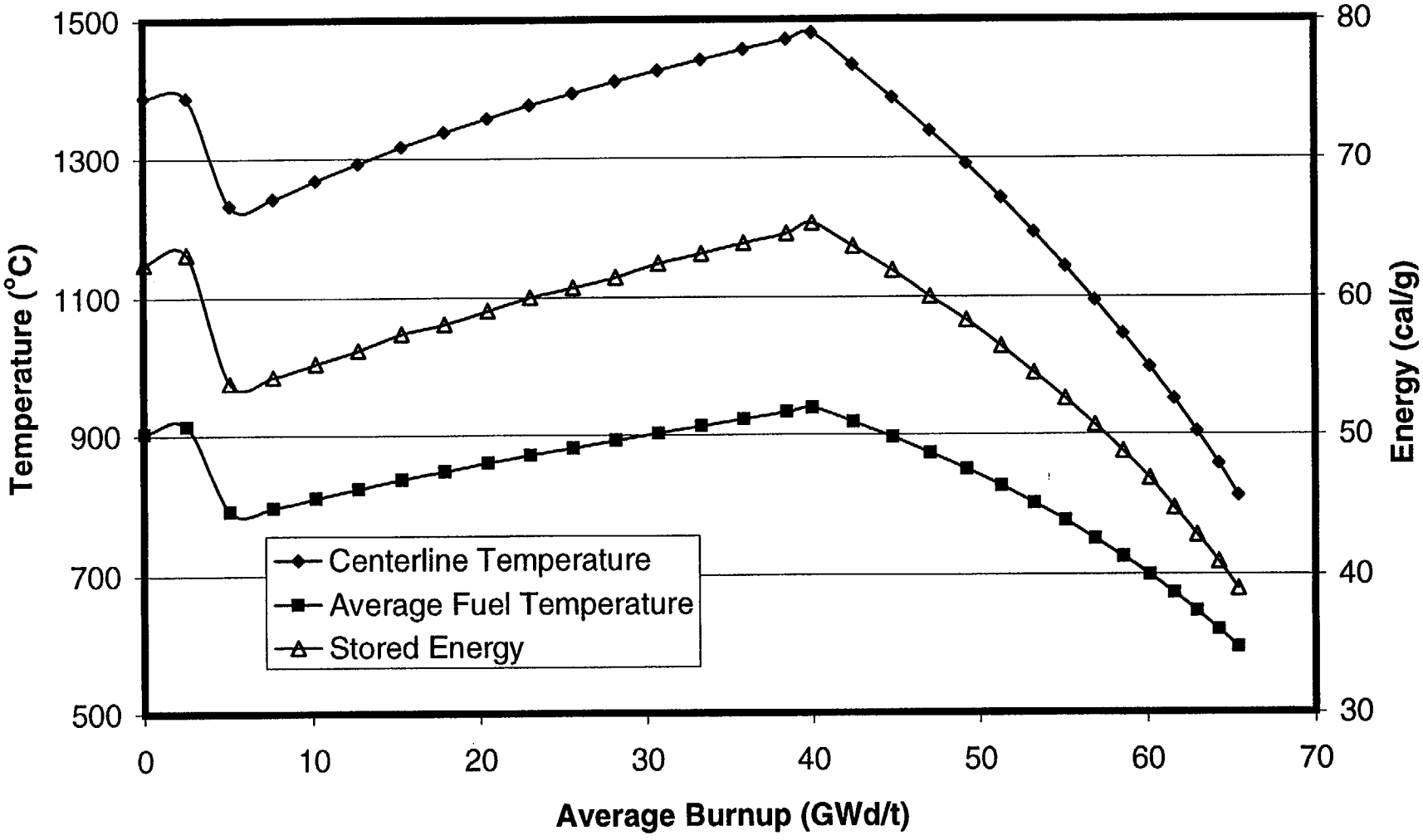

Fig. 9-7. Fuel temperatures and stored energy for a PWR 15x15 fuel rod with initial peak power of 11 kW/ft.

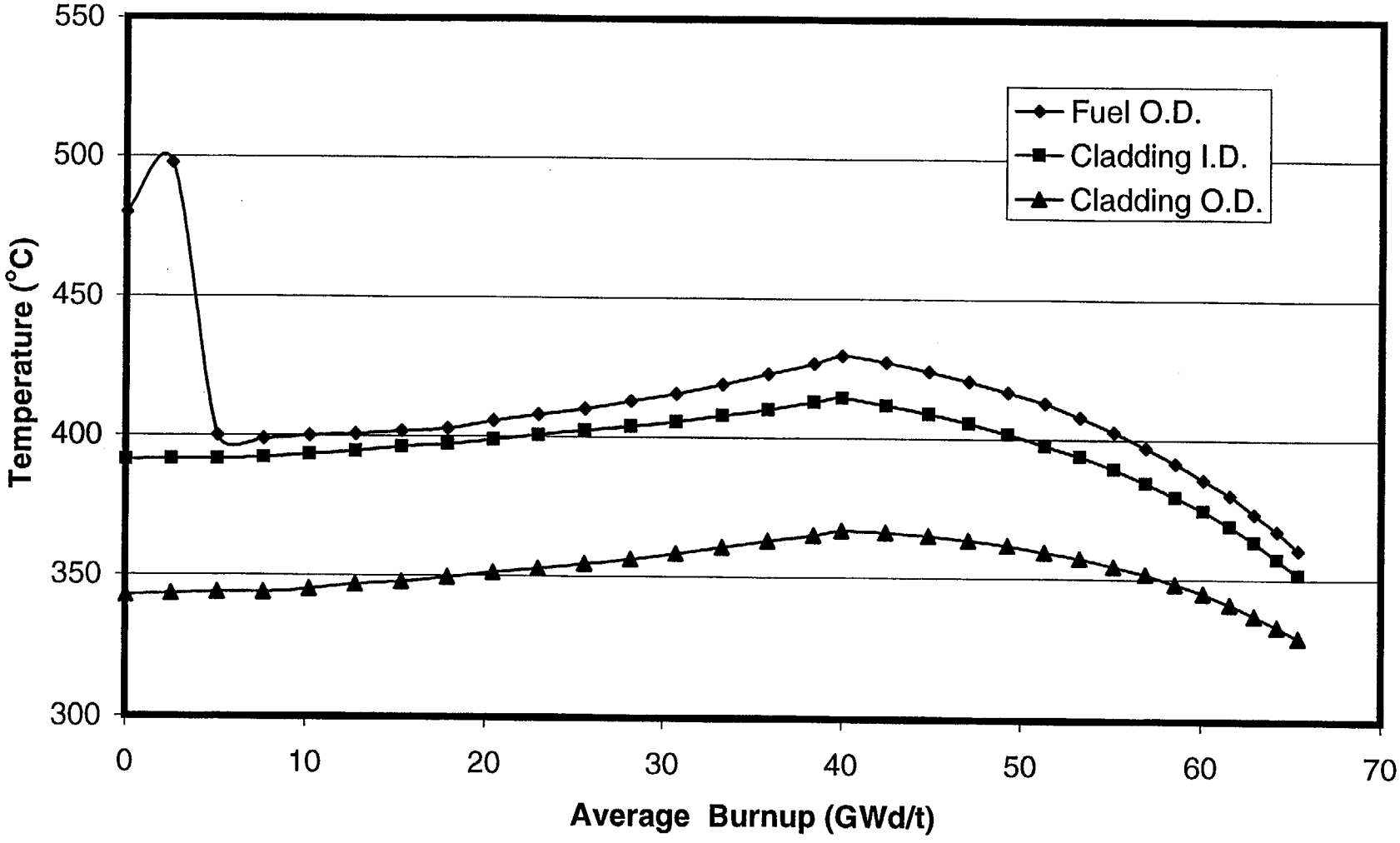

Fig. 9-8. Cladding temperatures and fuel surface temperature for a PWR 15x15 fuel rod with initial peak power of 11 kW/ft.

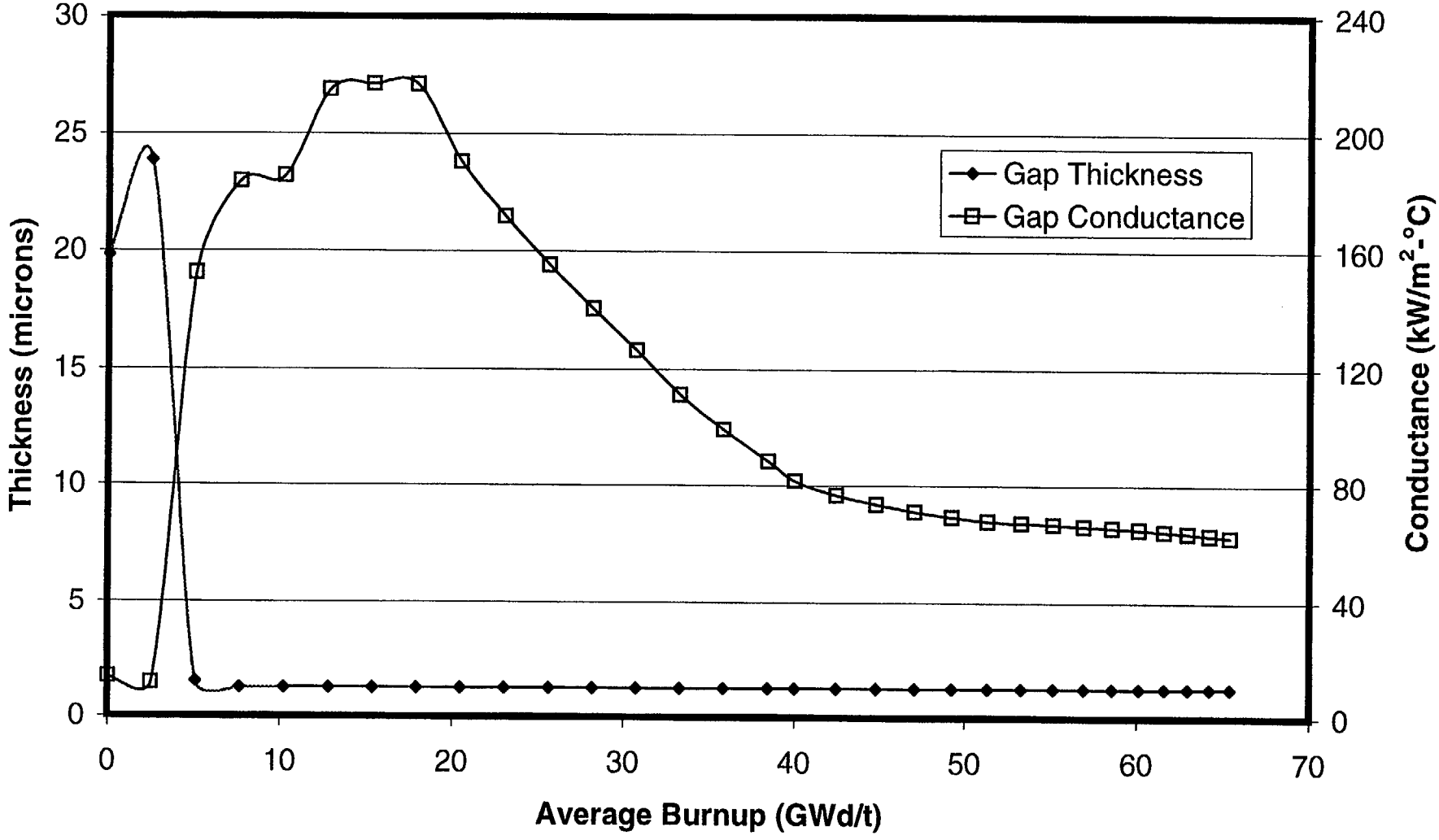

Fig. 9-9. Gap thickness and gap conductance for a PWR 15x15 fuel rod with initial peak power of 11 kW/ft.

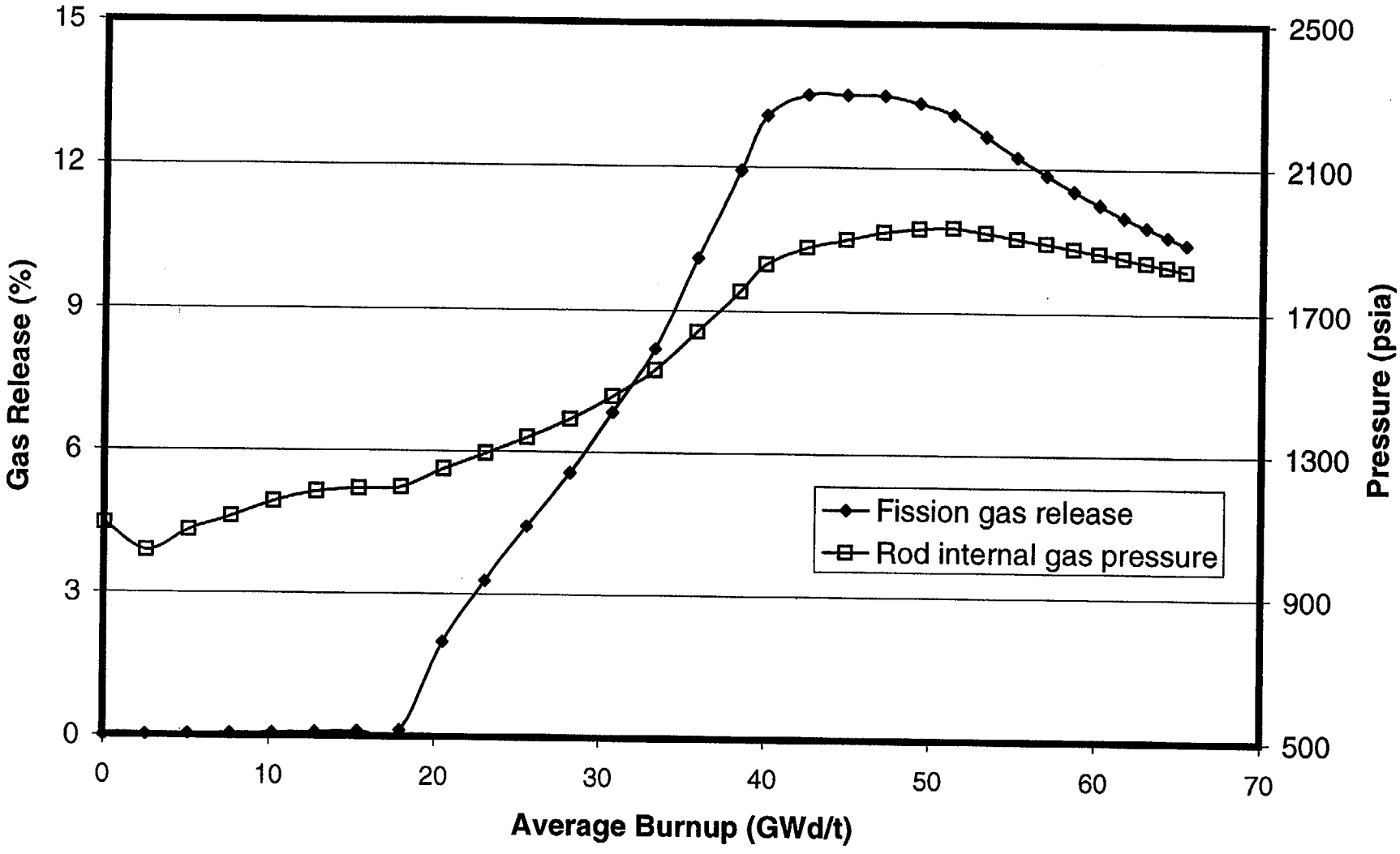

Fig. 9-10. Fission gas release and rod internal gas pressure for a PWR 15x15 fuel rod with initial peak power of 11 kW/ft.

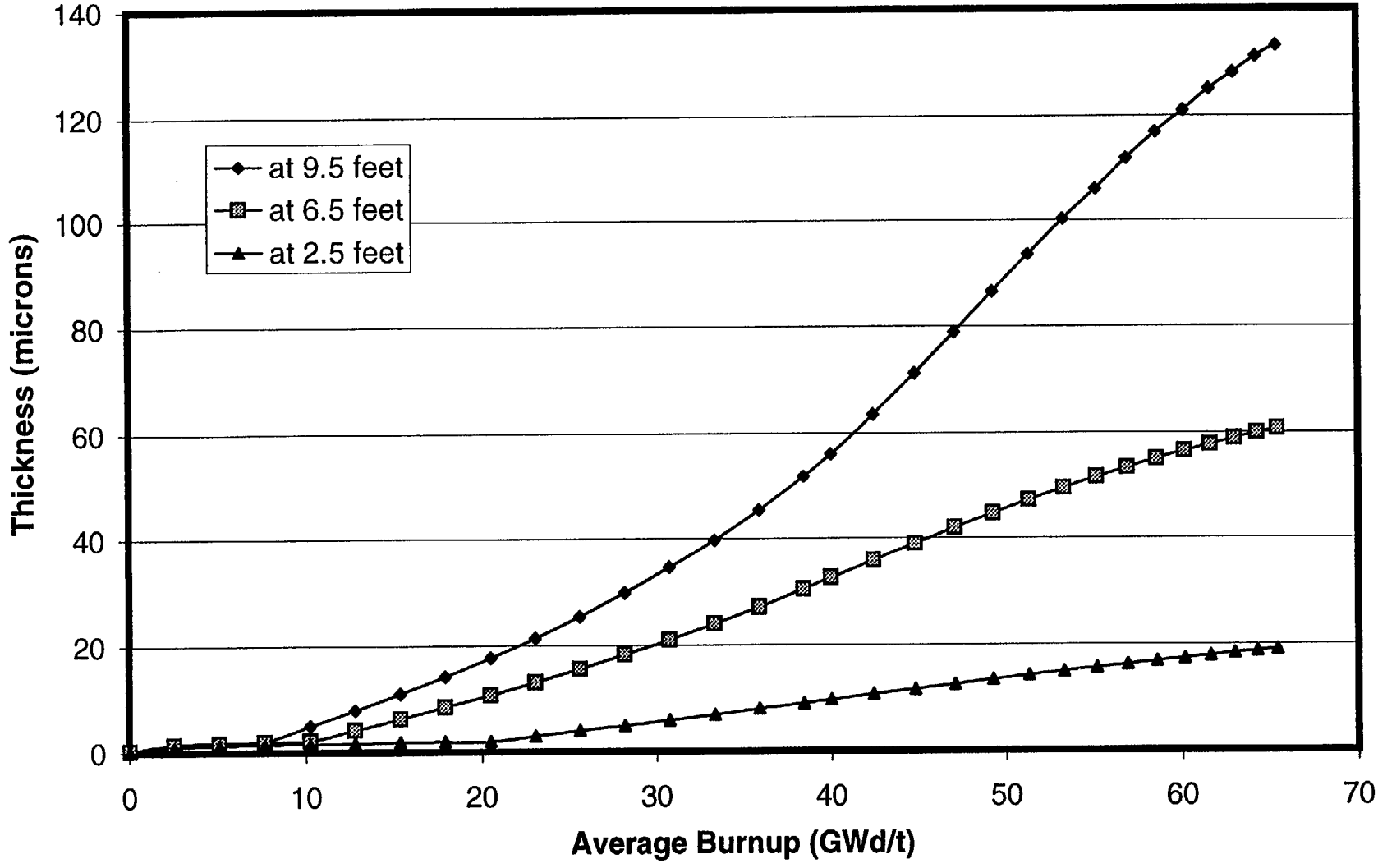

Fig. 9-11. Oxide thickness at three axial locations for a PWR 15x15 fuel rod with initial peak power of 11 kW/ft.

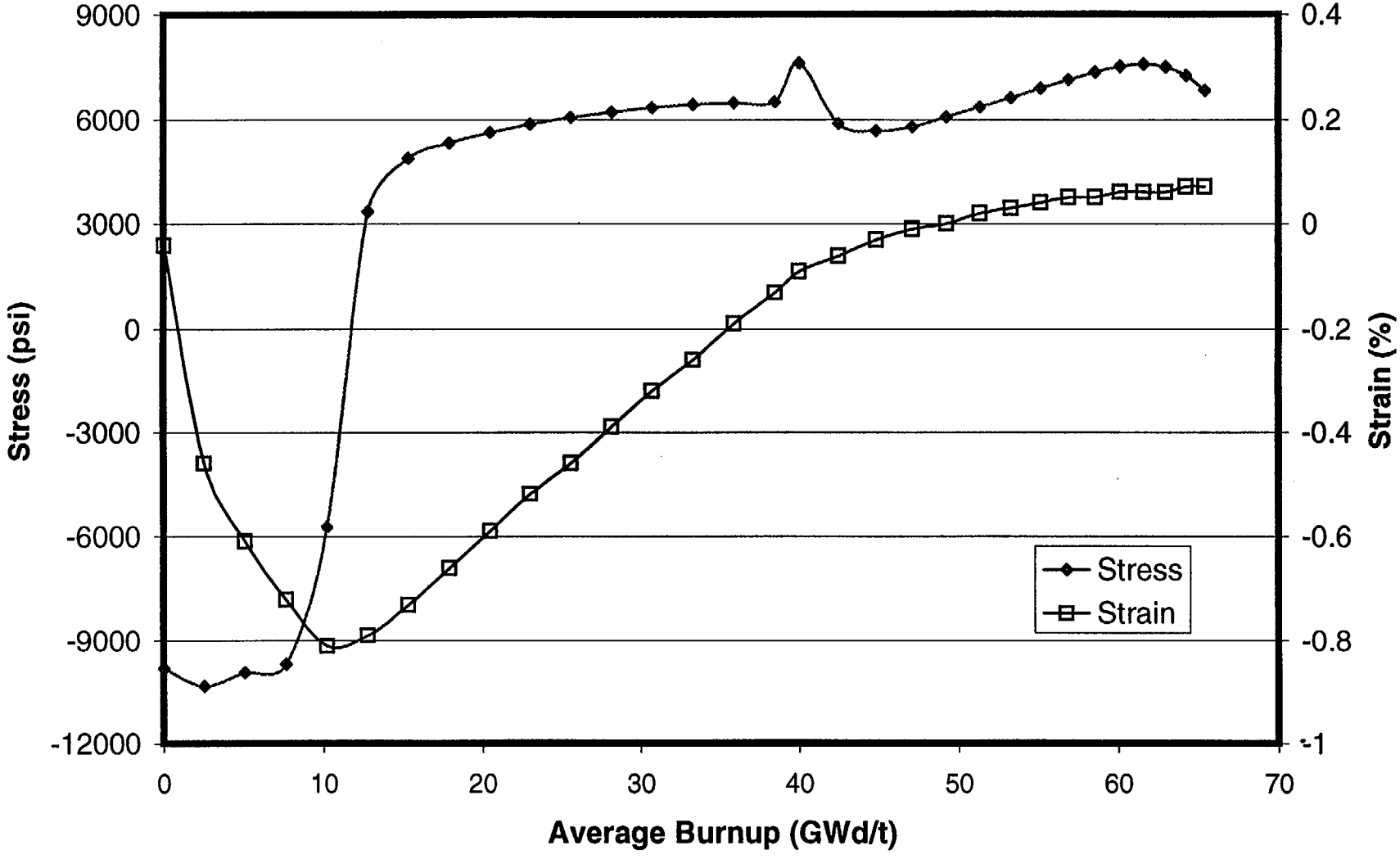

Fig. 9-12. Cladding hoop stress and hoop strain for a PWR 15x15 fuel rod with initial peak power of 11 kW/ft.

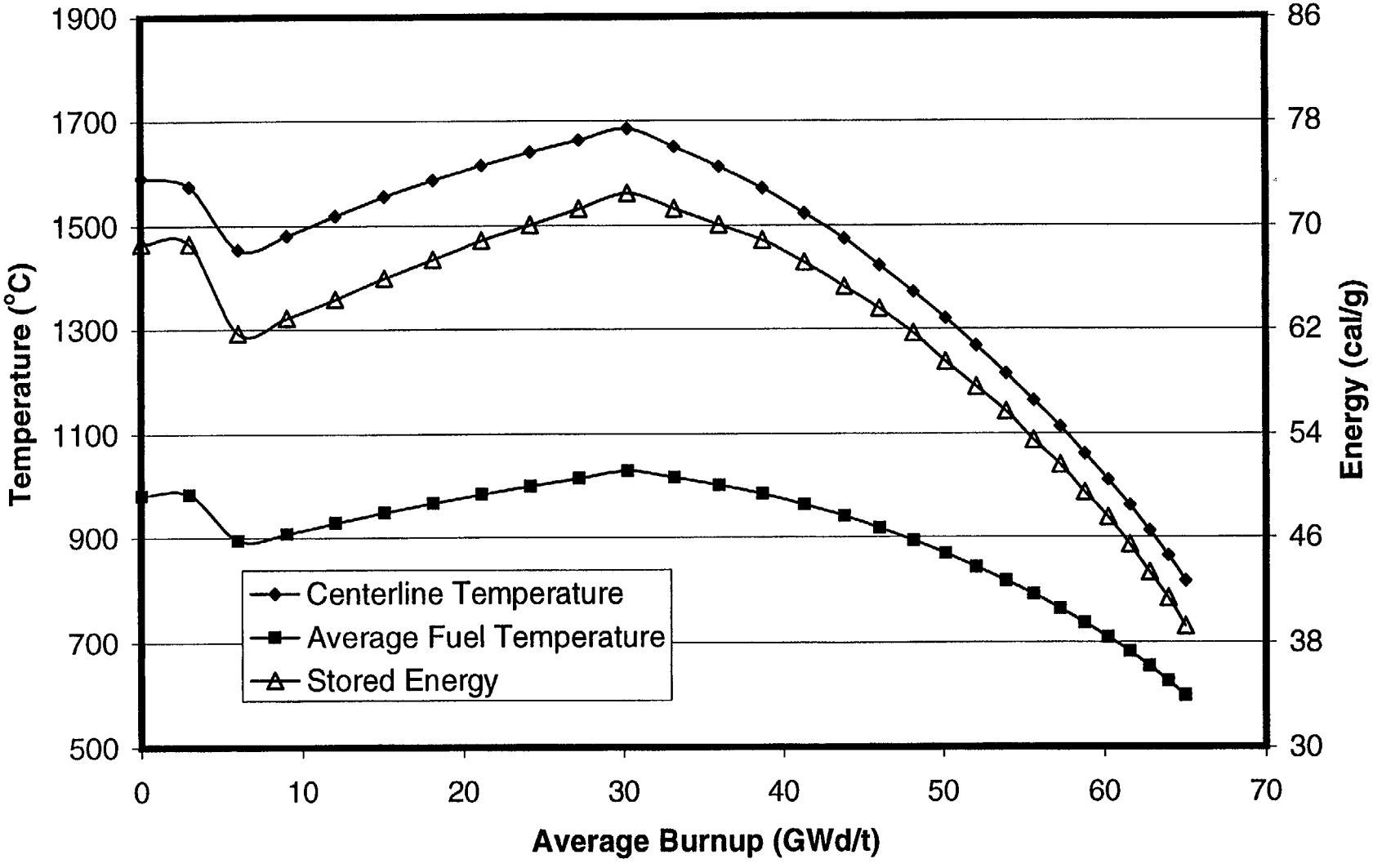

Fig. 9-13. Fuel temperatures and stored energy for a PWR 15x15 fuel rod with initial peak power of 13 kW/ft.

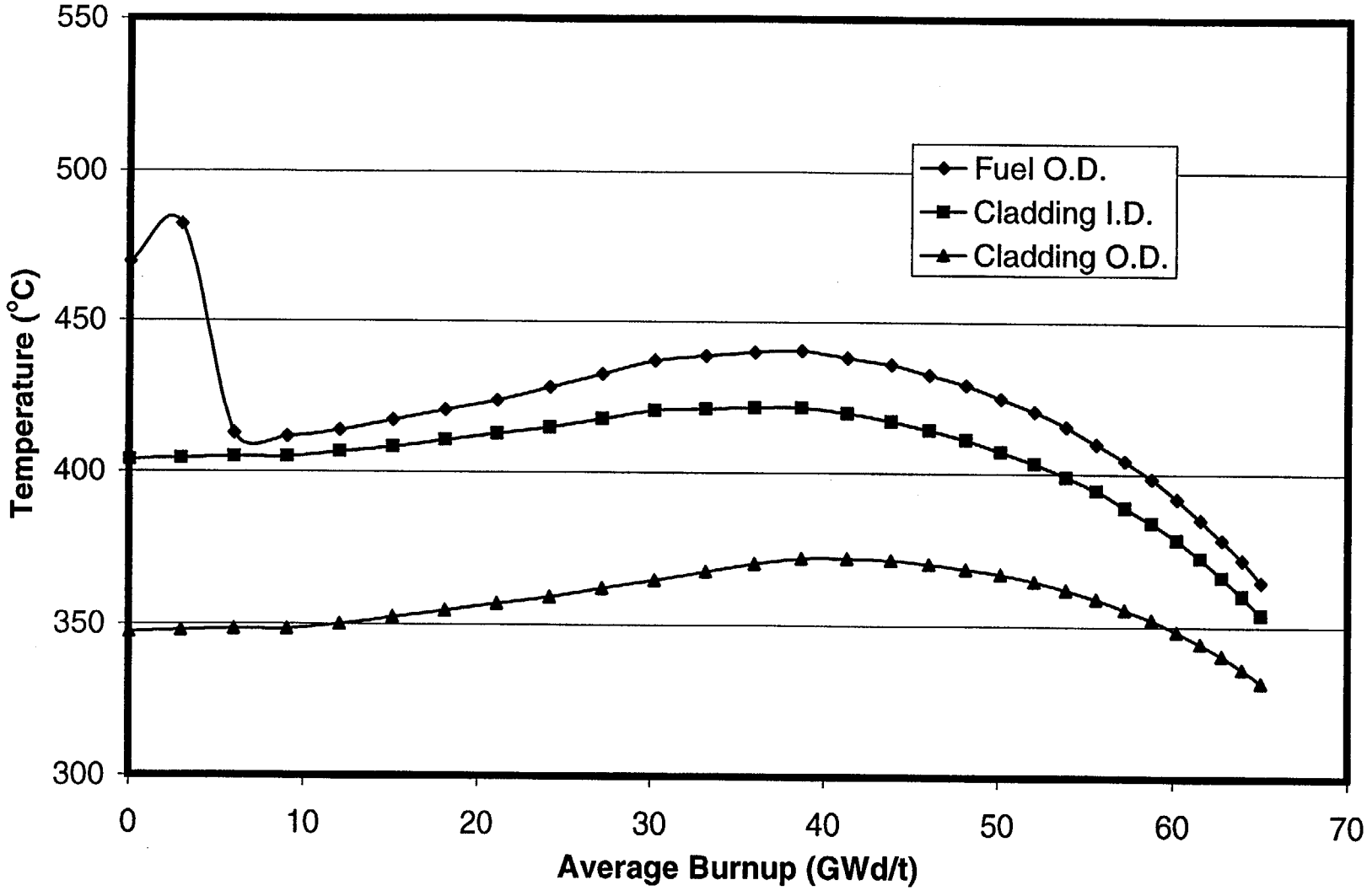

Fig. 9-14. Cladding temperatures and fuel surface temperature for a PWR 15x15 fuel rod with initial peak power of 13 kW/ft.

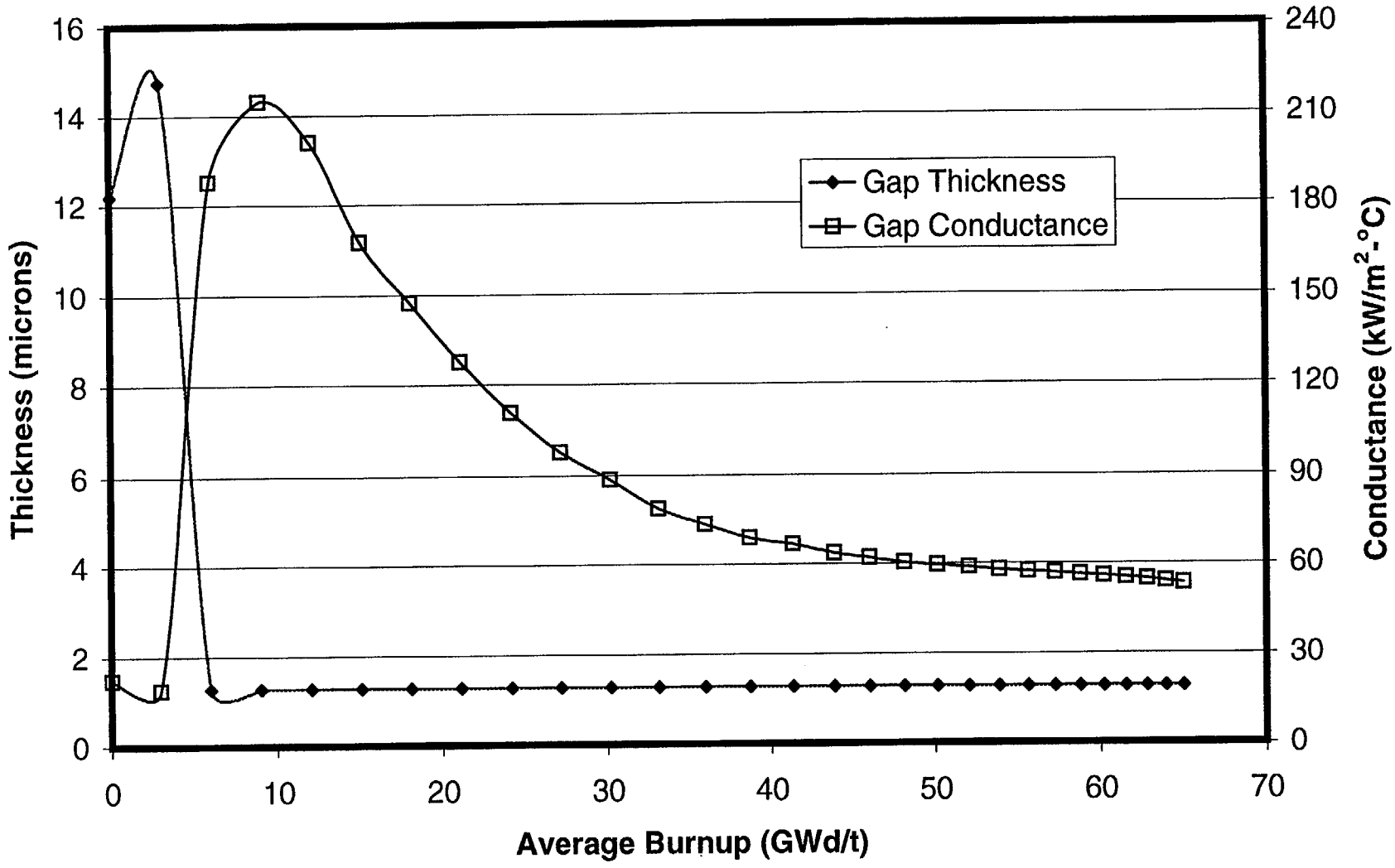

Fig. 9-15. Gap thickness and gap conductance for a PWR 15x15 fuel rod with initial peak power of 13 kW/ft.

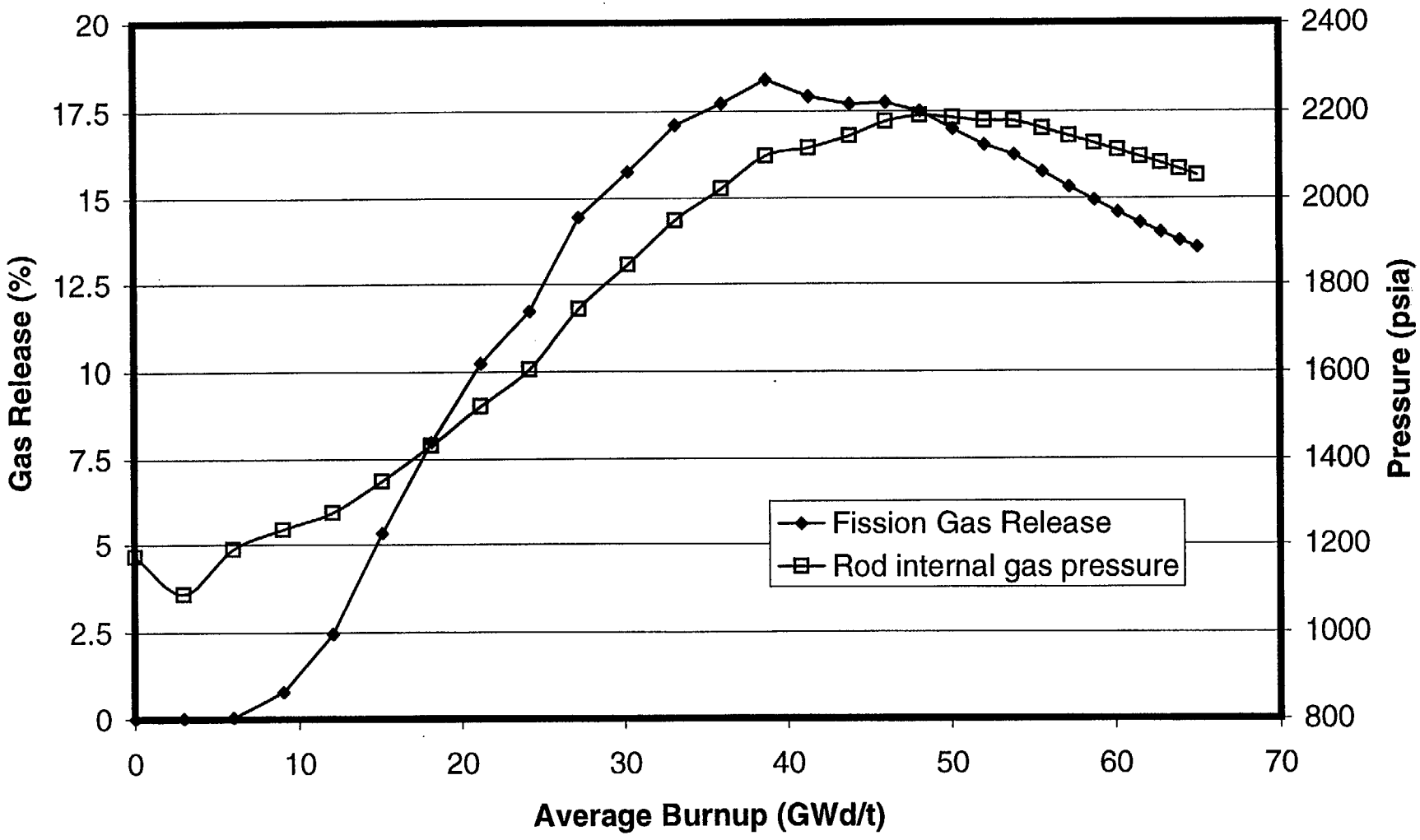

Fig. 9-16. Fission gas release and rod internal gas pressure for a PWR 15x15 fuel rod with initial peak power of 13 kW/ft.

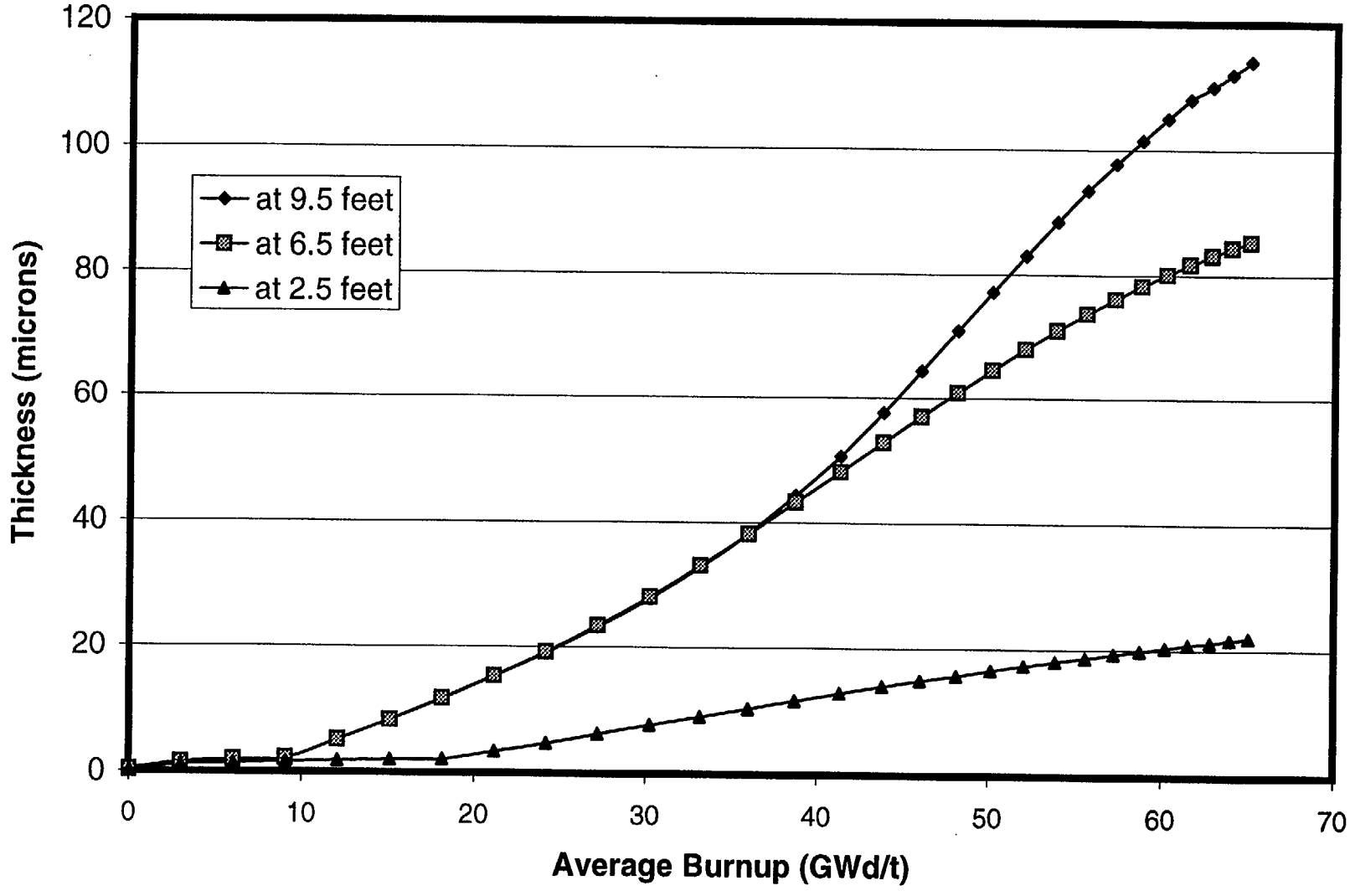

Fig. 9-17. Oxide thickness at three axial locations for a PWR 15x15 fuel rod with initial peak power of 13 kW/ft.

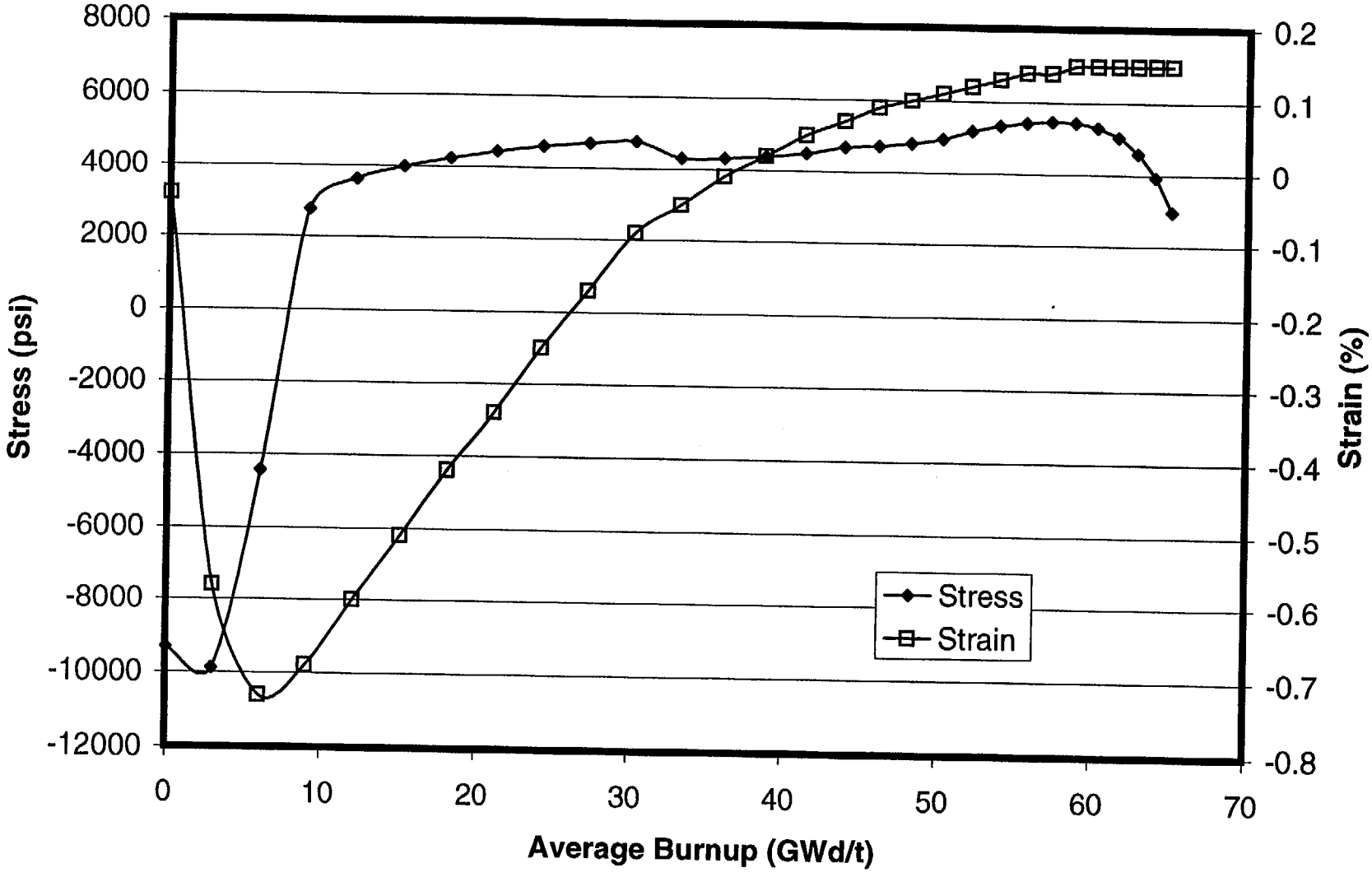

Fig. 9-18. Cladding hoop stress and hoop strain for a PWR 15x15 fuel rod with initial peak power of 13 kW/ft.

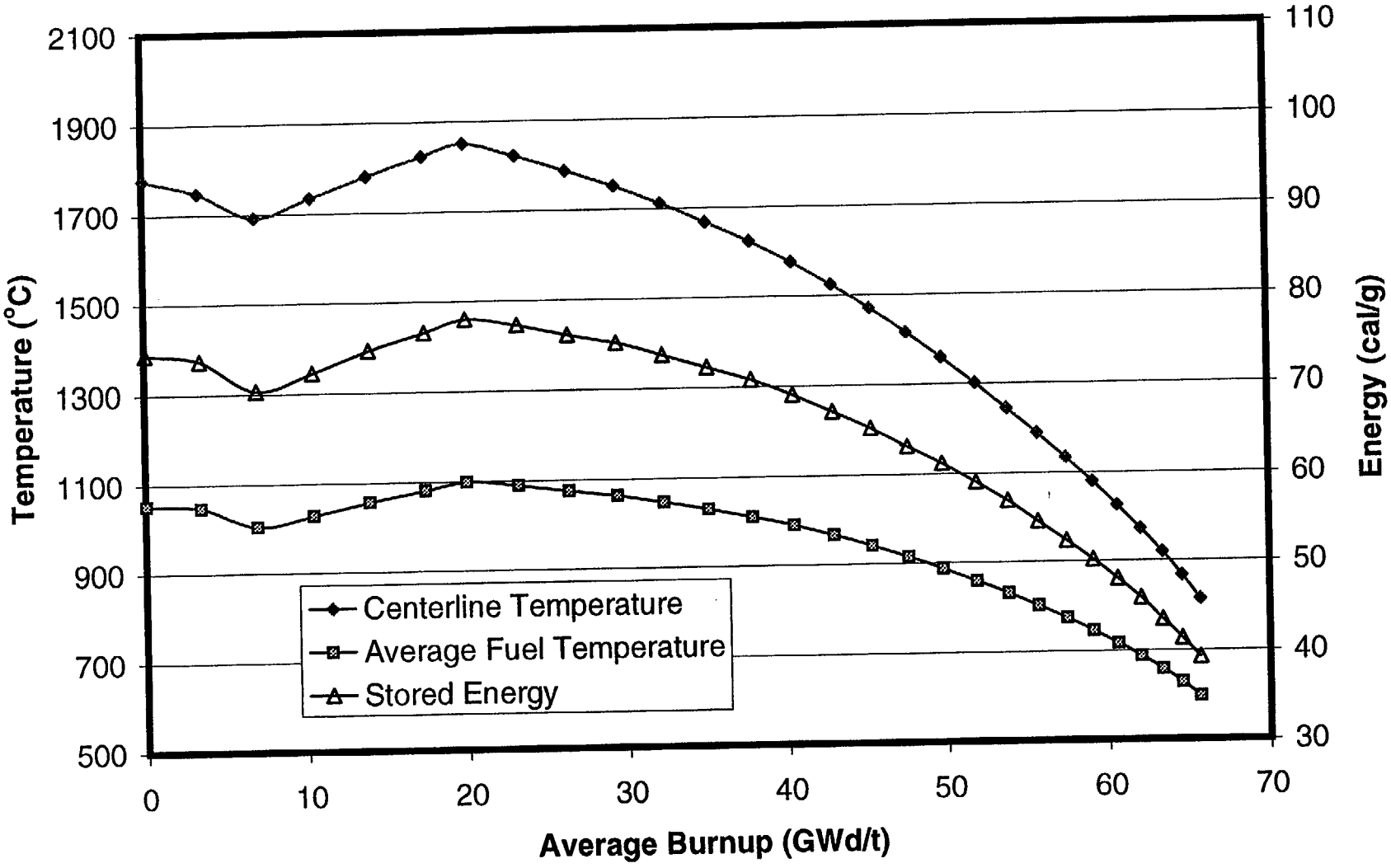

Fig. 9-19. Fuel Temperatures and stored energy for a PWR 15x15 fuel rod with initial peak power of 15 kW/ft.

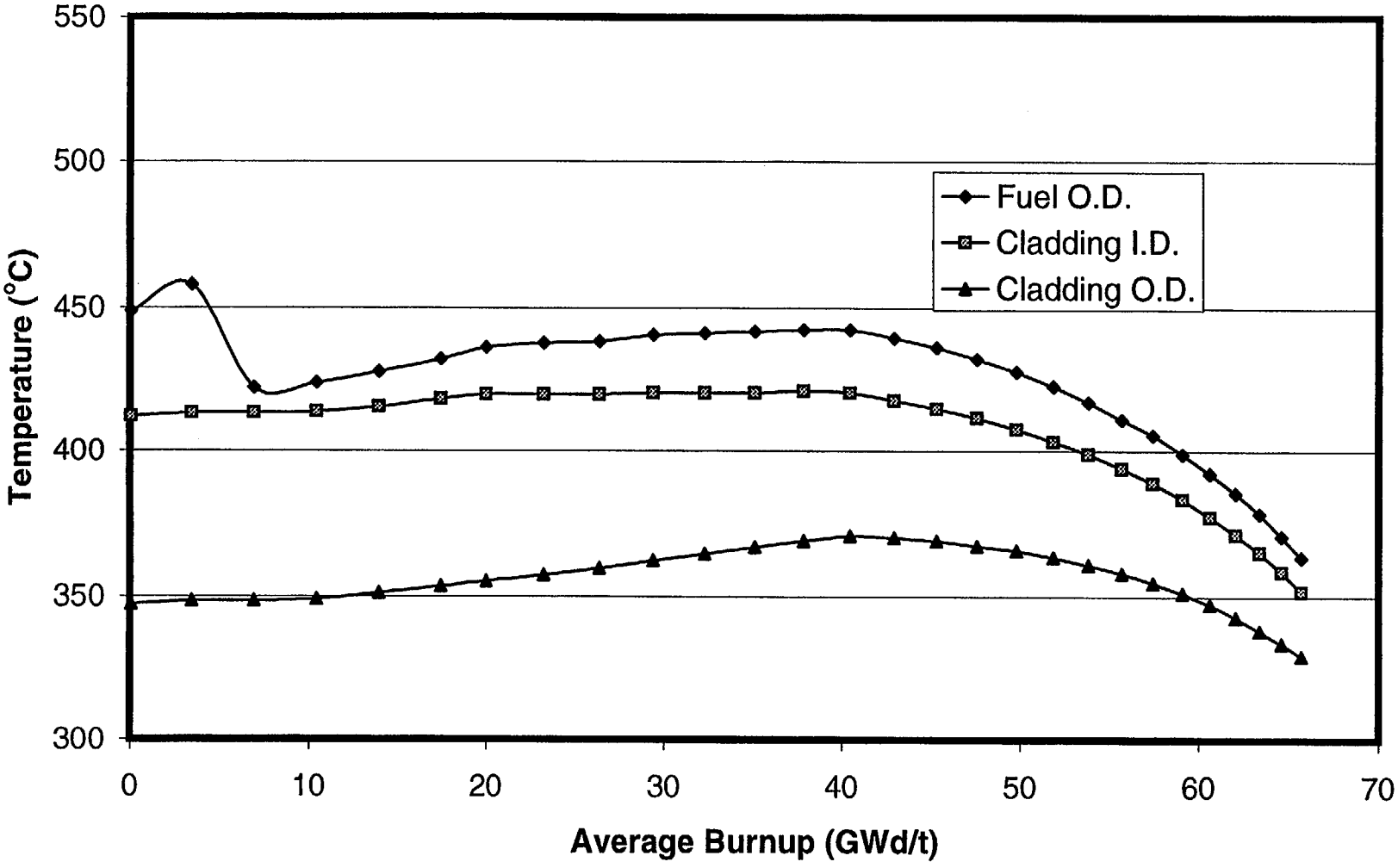

Fig. 9-20. Cladding temperatures and fuel surface temperature for a PWR 15x15 fuel rod with initial peak power of 15 kW/ft.

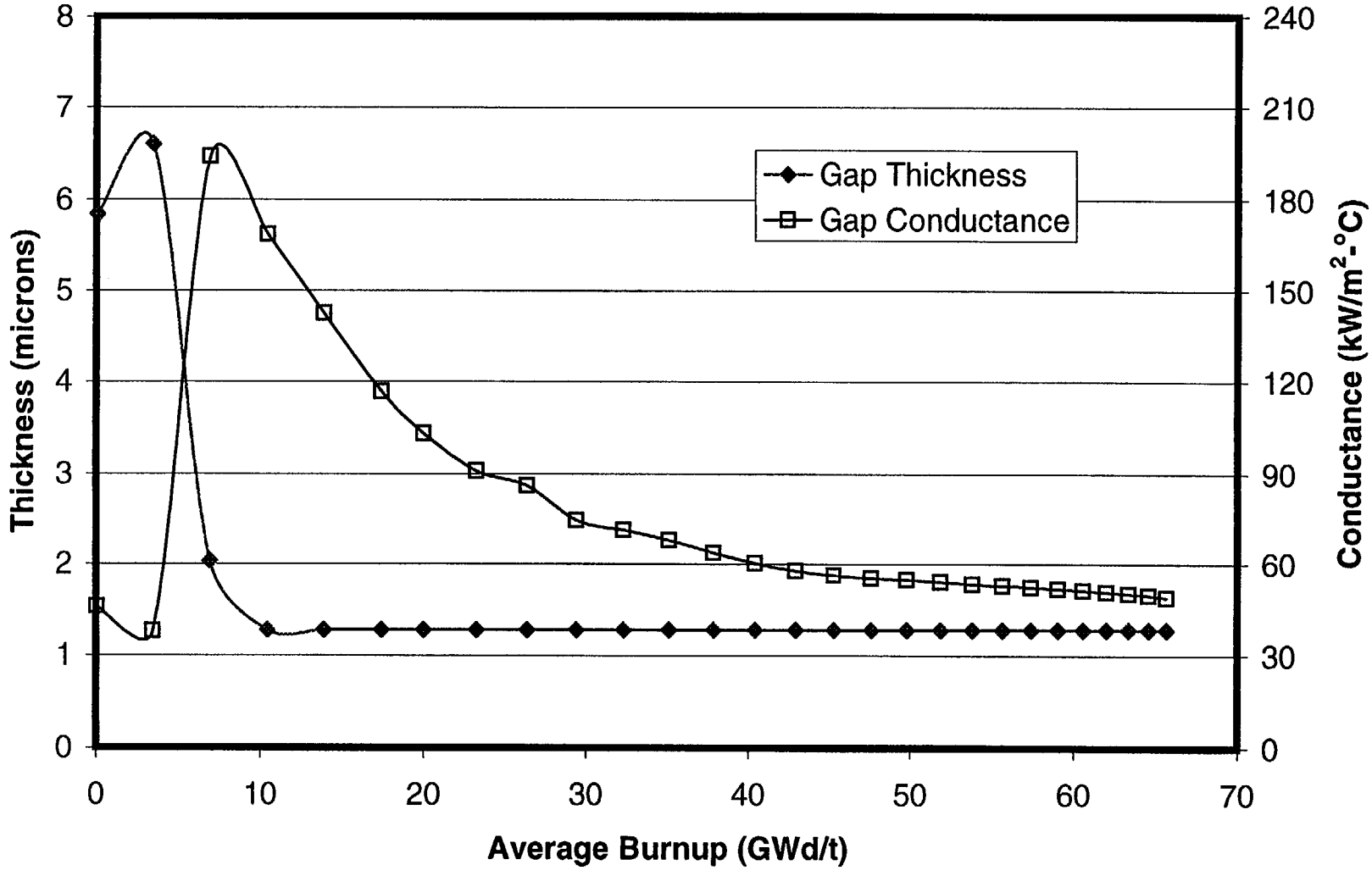

Fig. 9-21. Gap thickness and gap conductance for a PWR 15x15 fuel rod with initial peak power of 15 kW/ft.

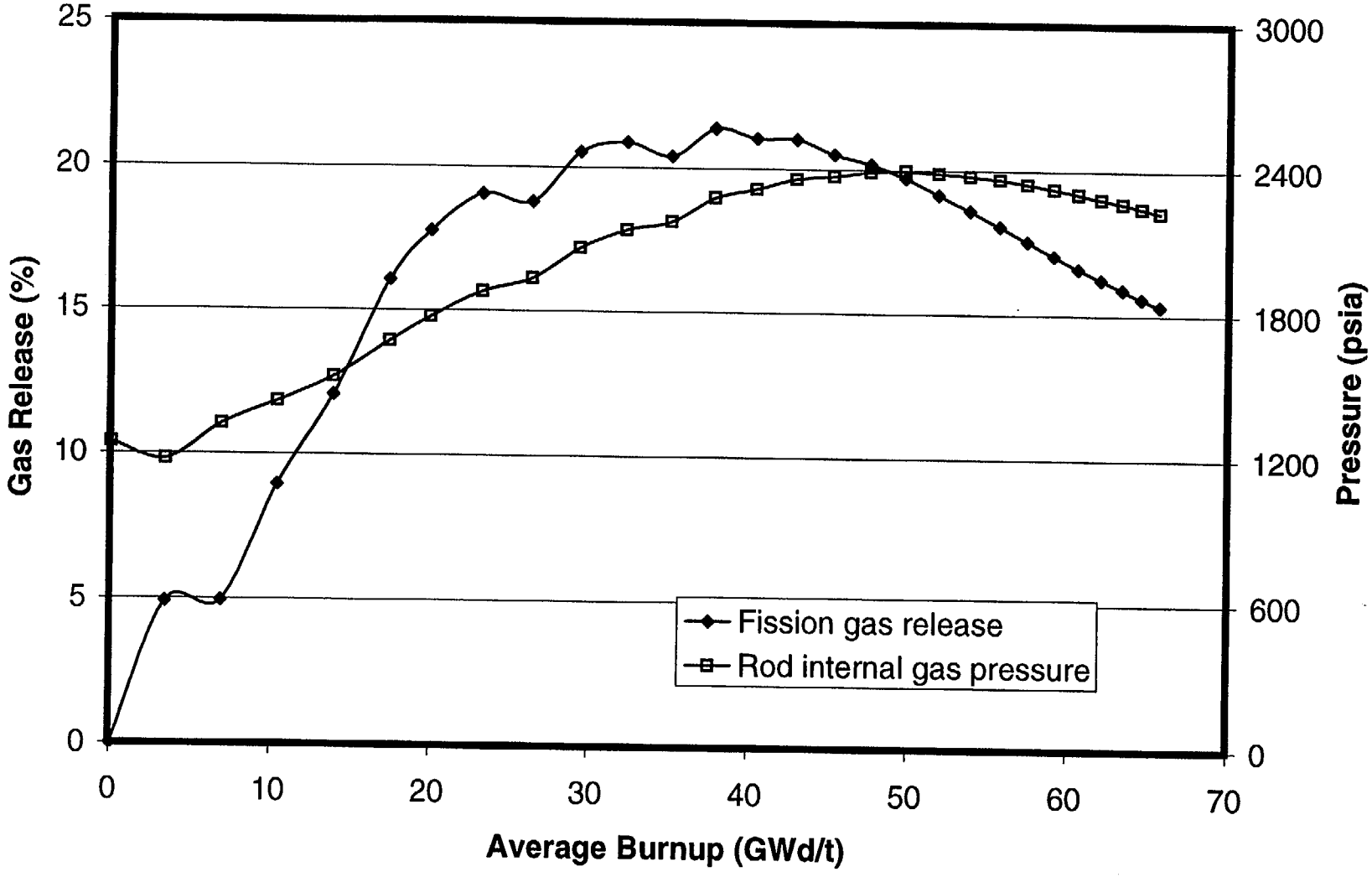

Fig. 9-22. Fission gas release and rod internal gas pressure for a PWR 15x15 fuel rod with initial peak power of 15 kW/ft.

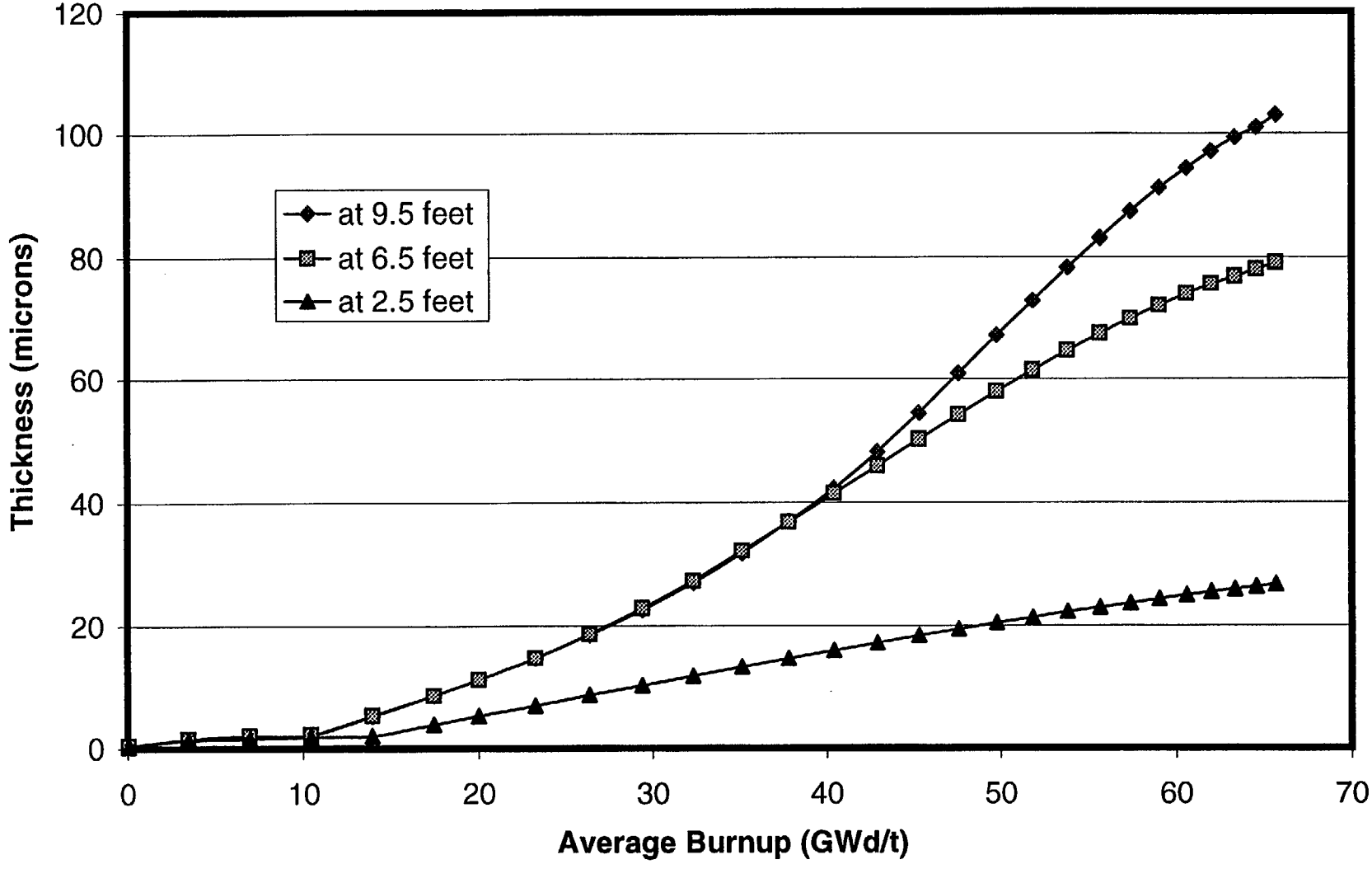

Fig. 9-23. Oxide thickness at three axial locations for a PWR 15x15 fuel rod with initial peak power of 15 kW/ft.

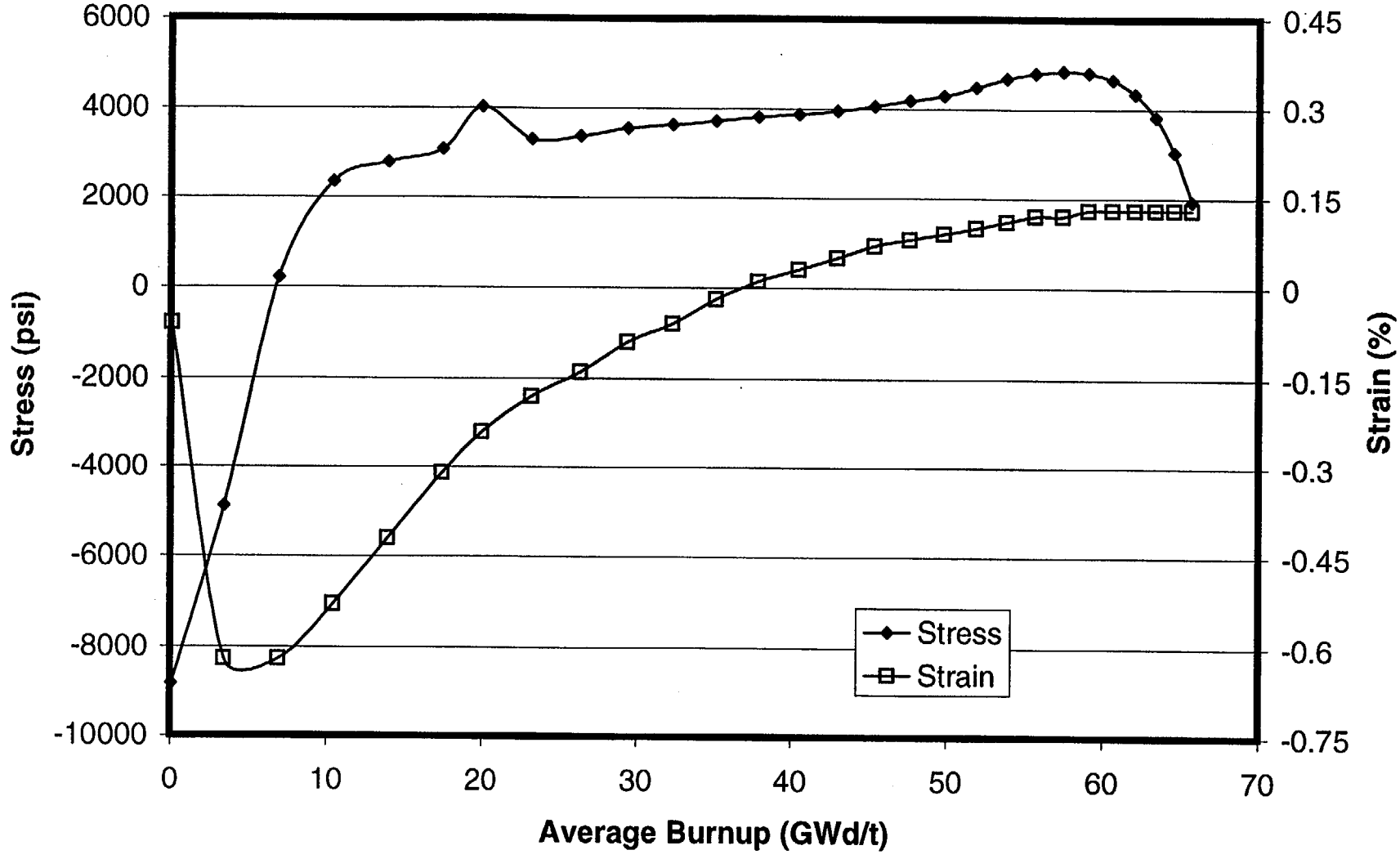

Fig. 9-24. Cladding hoop stress and hoop strain for a PWR 15x15 fuel rod with initial peak power of 15 kW/ft.

10. Calculations for PWR 16X16 Fuel

In the following figures, calculated values for PWR 16X16 fuel are plotted as a function of burnup for the parameters listed below:

Fuel centerline temperature
Average fuel temperature
Stored energy
Fuel O.D. temperature
Cladding I.D. temperature
Cladding O.D. temperature
Gap thickness
Gap conductance
Fission gas release
Rod internal gas pressure
Oxide thickness
Cladding hoop stress
Cladding hoop strain

Several general observations can be made about the calculated results:

- Within the first few GWd/t of burnup, a temperature peak is observed that is the result of fuel densification.

- Gap closure results in (a) the coming together of temperatures for fuel O.D. and cladding I.D. and (b) a sharp increase in gap conductance. The gap conductance increases again after a few time steps when the interaction between the pellet and cladding affects the contact conductance calculated for a closed gap. At this point there is also a large increase in stress, and the permanent strain changes directions.

- Some of the fission gas is released in spurts according to the Massih model in FRAPCON-3. This effect is apparent in many of the figures. Shorter time steps would produce slightly different looking curves, but the trend of gas release and the end-of-life gas release would be about the same.

- The burnup enhancement of fission gas release is readily seen in the lower power cases, but it is obscured in the highest power cases by the magnitude of prior gas release.

- Rod internal gas pressure increases with the accumulation of released fission gas. In the higher power PWR cases, as the power drops off near the end of life, the reduction in the plenum temperature offsets the increasing moles of fission gas.

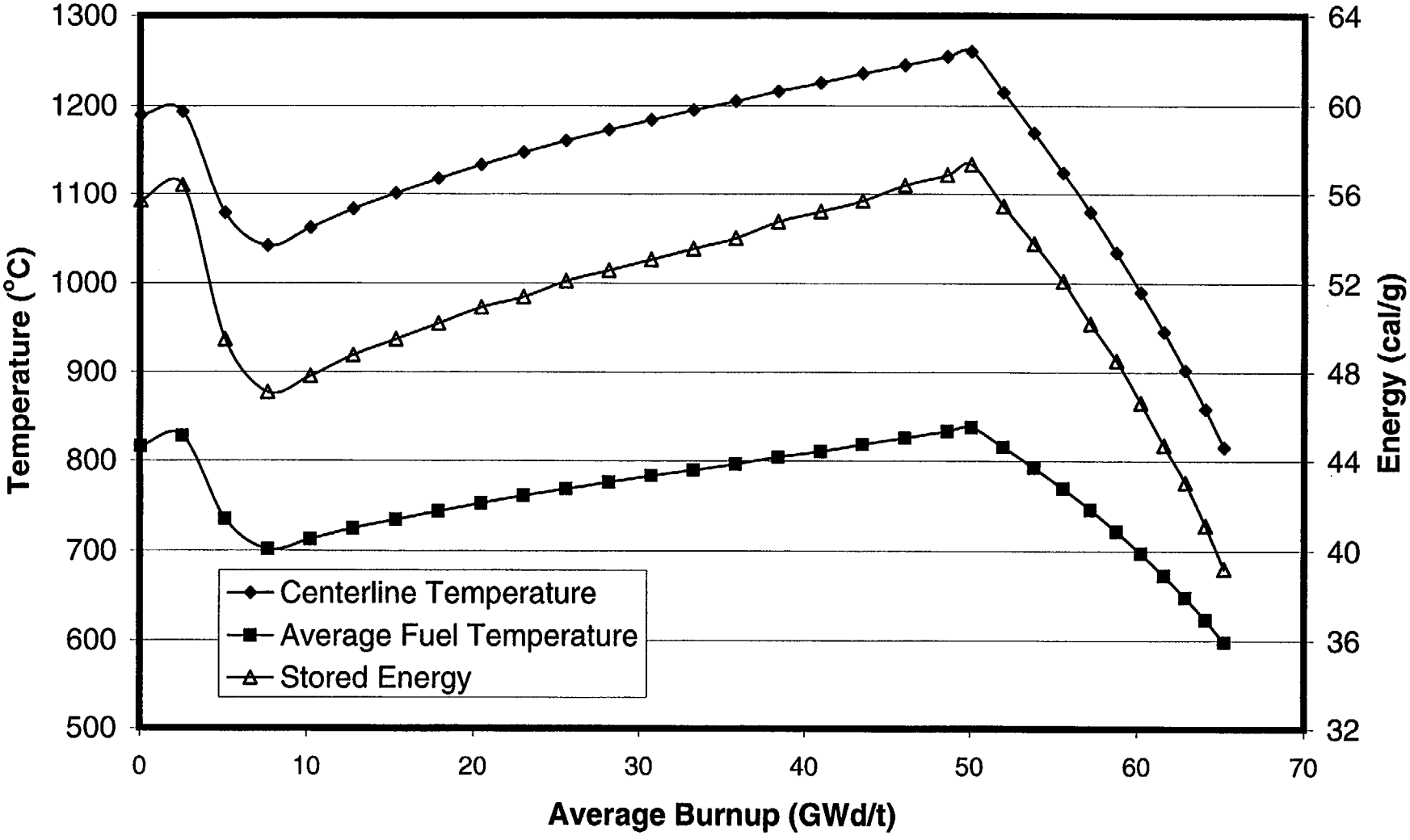

Fig. 10-1. Fuel temperatures and stored energy for a PWR 16x16 fuel rod with initial peak power of 9 kW/ft.

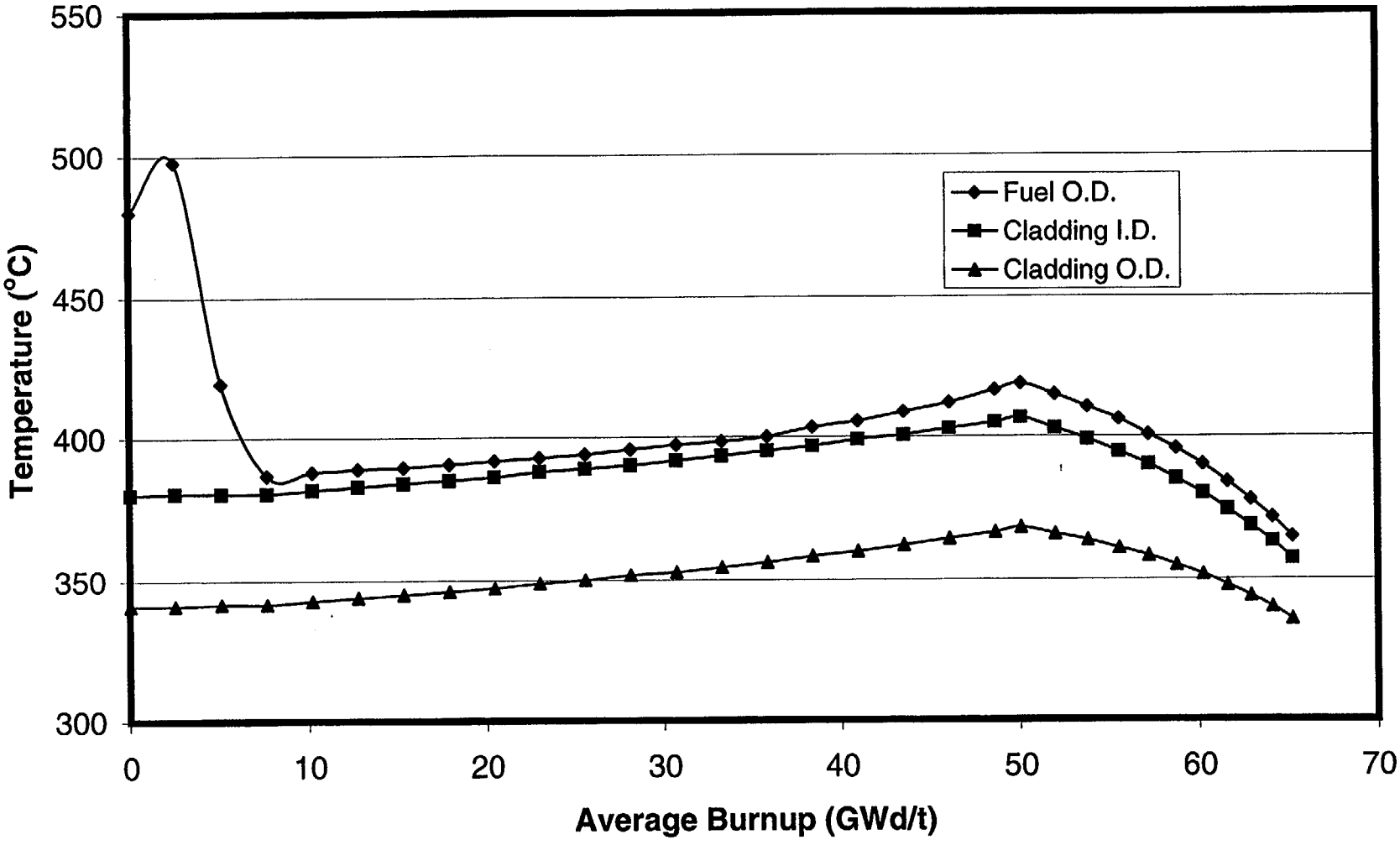

Fig. 10-2. Cladding temperatures and fuel surface temperature for a PWR 16x16 fuel rod with initial peak power of 9 kW/ft.

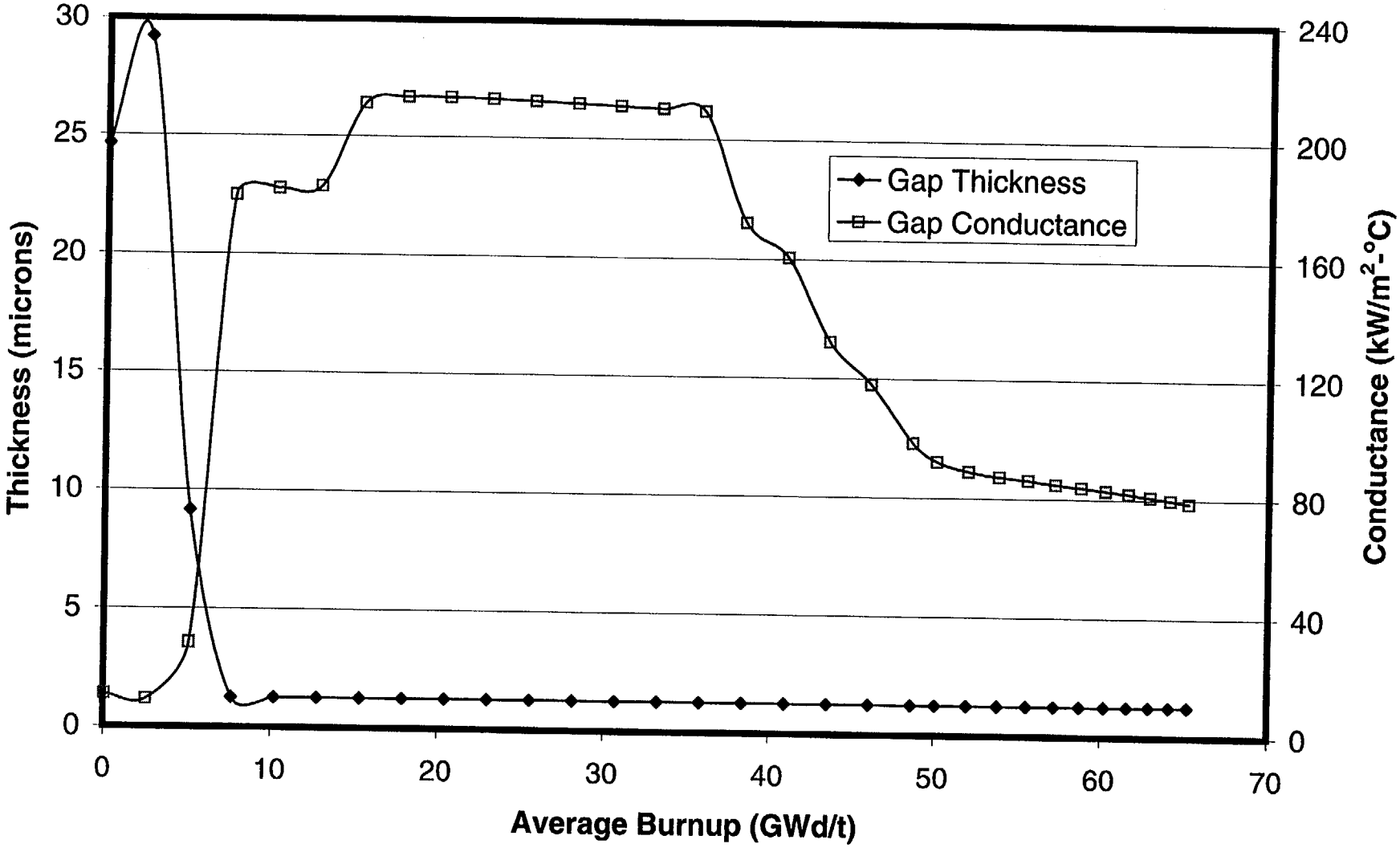

Fig. 10-3. Gap thickness and gap conductance for a PWR 16x16 fuel rod with initial peak power of 9 kW/ft.

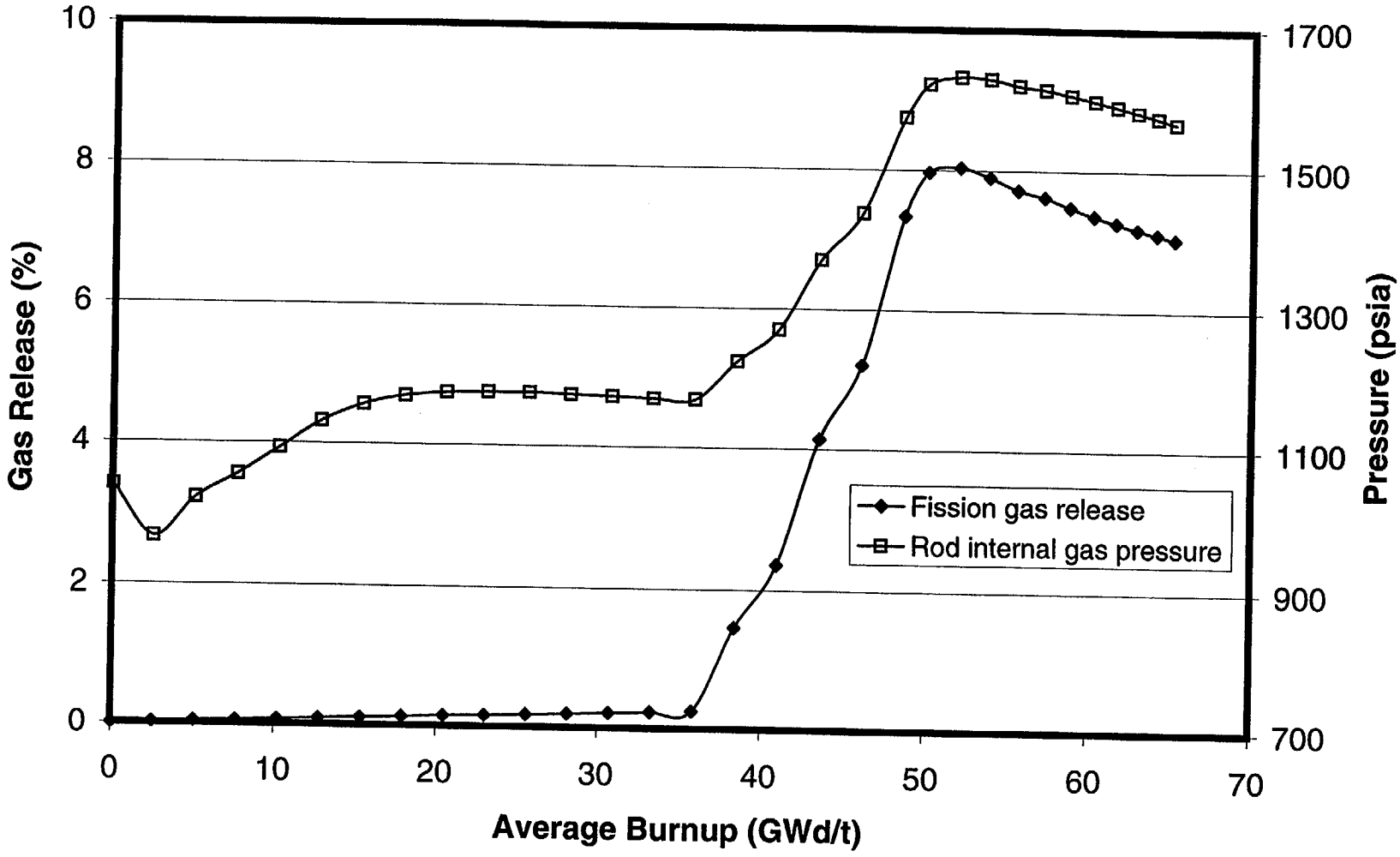

Fig. 10-4. Fission gas release and rod internal gas pressure for a PWR 16x16 fuel rod with initial peak power of 9 kW/ft.

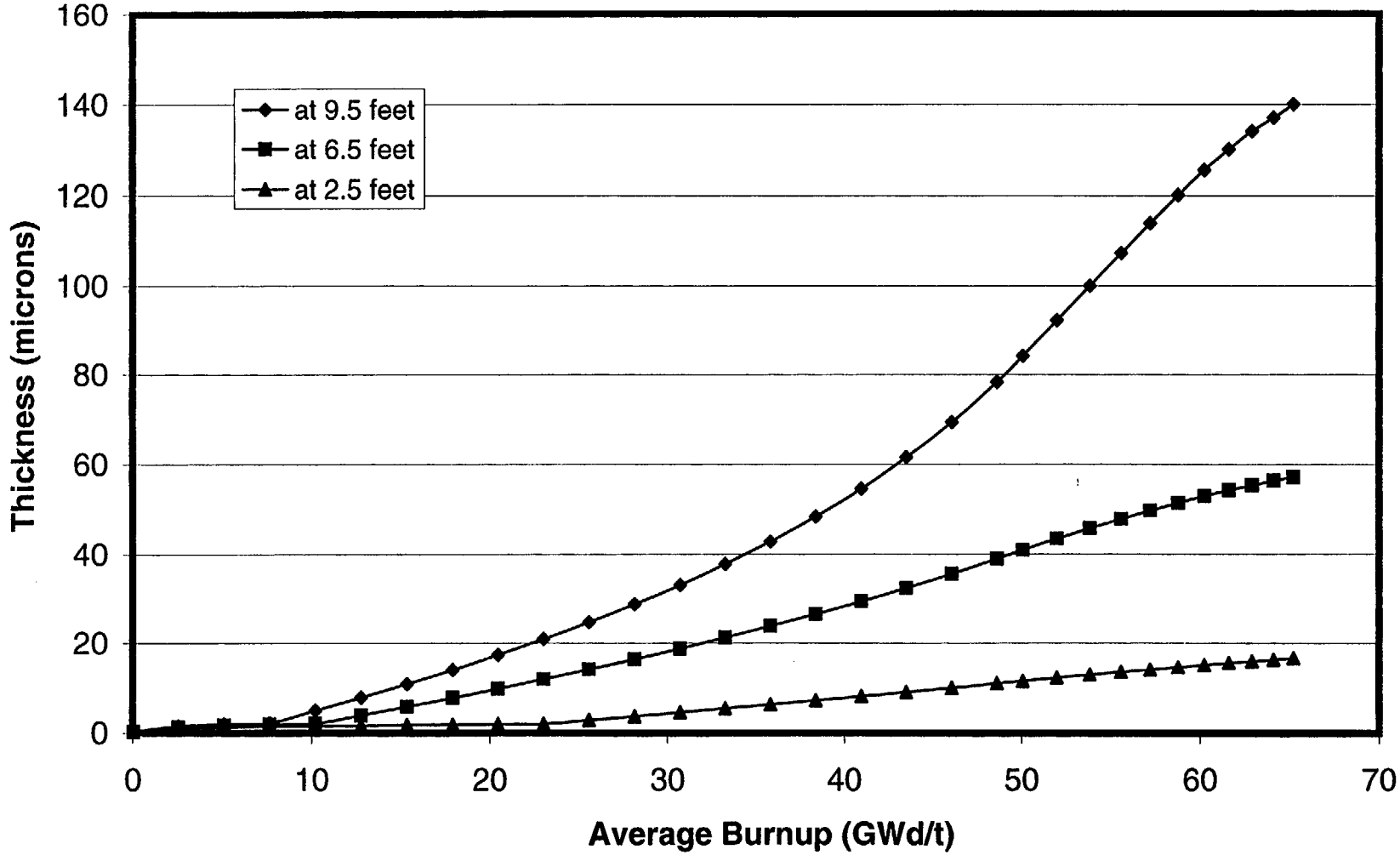

Fig. 10-5. Oxide thickness at three axial locations for a PWR 16x16 fuel rod with initial peak power of 9 kW/ft.

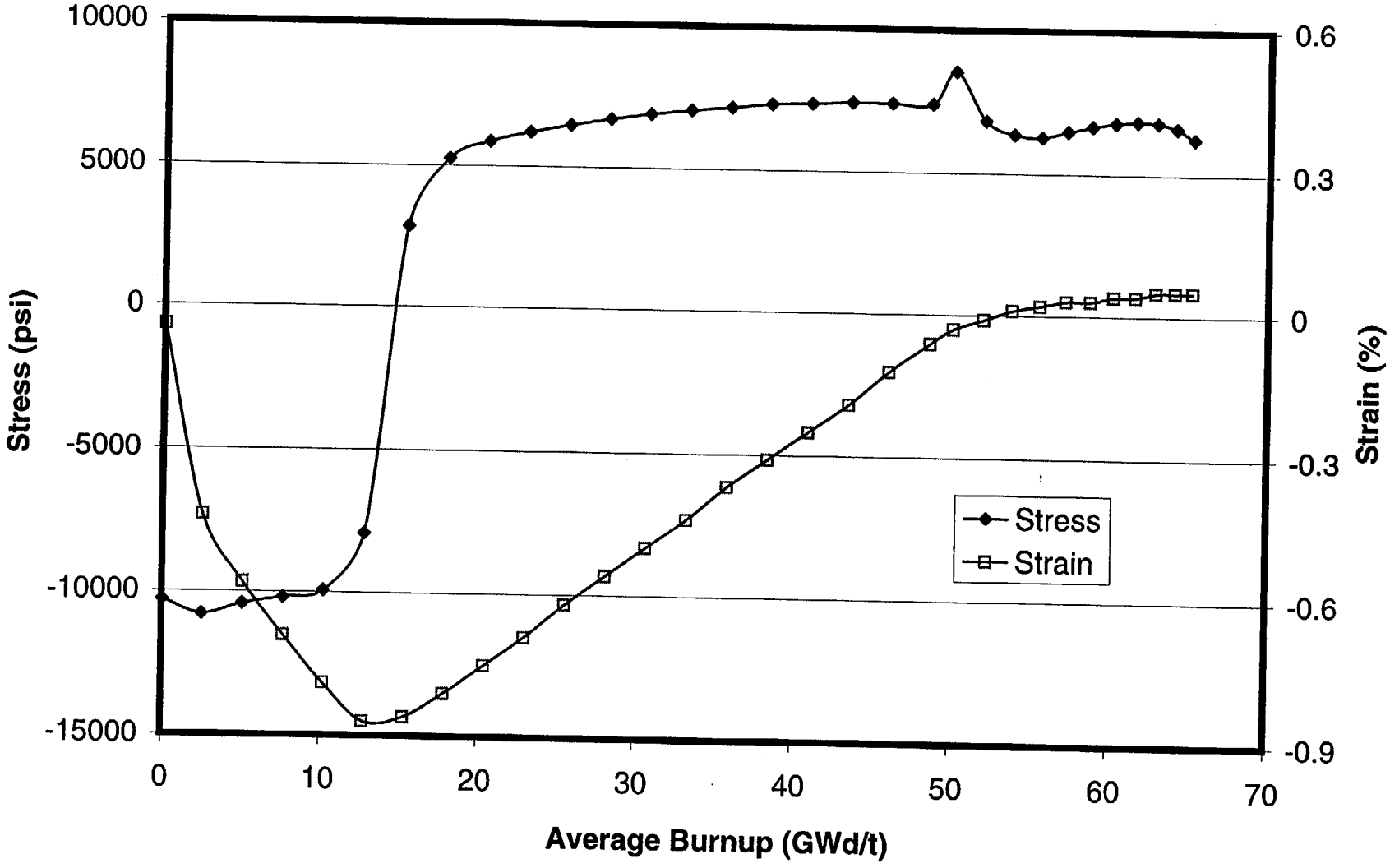

Fig. 10-6. Cladding hoop stress and hoop strain for a PWR 16x16 fuel rod with initial peak power of 9 kW/ft.

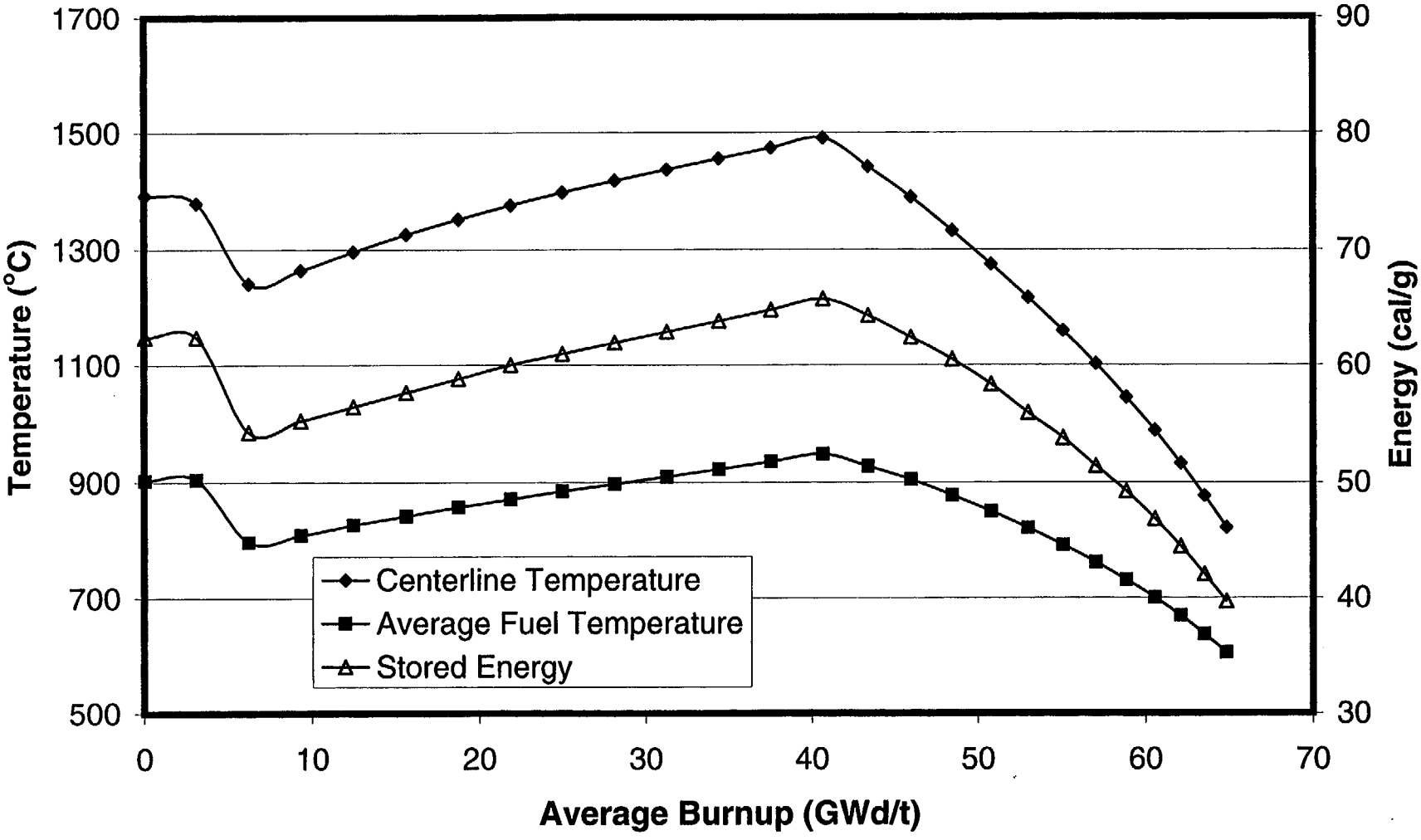

Fig. 10-7. Fuel temperatures and stored energy for a PWR 16x16 fuel rod with initial peak power of 11 kW/ft.

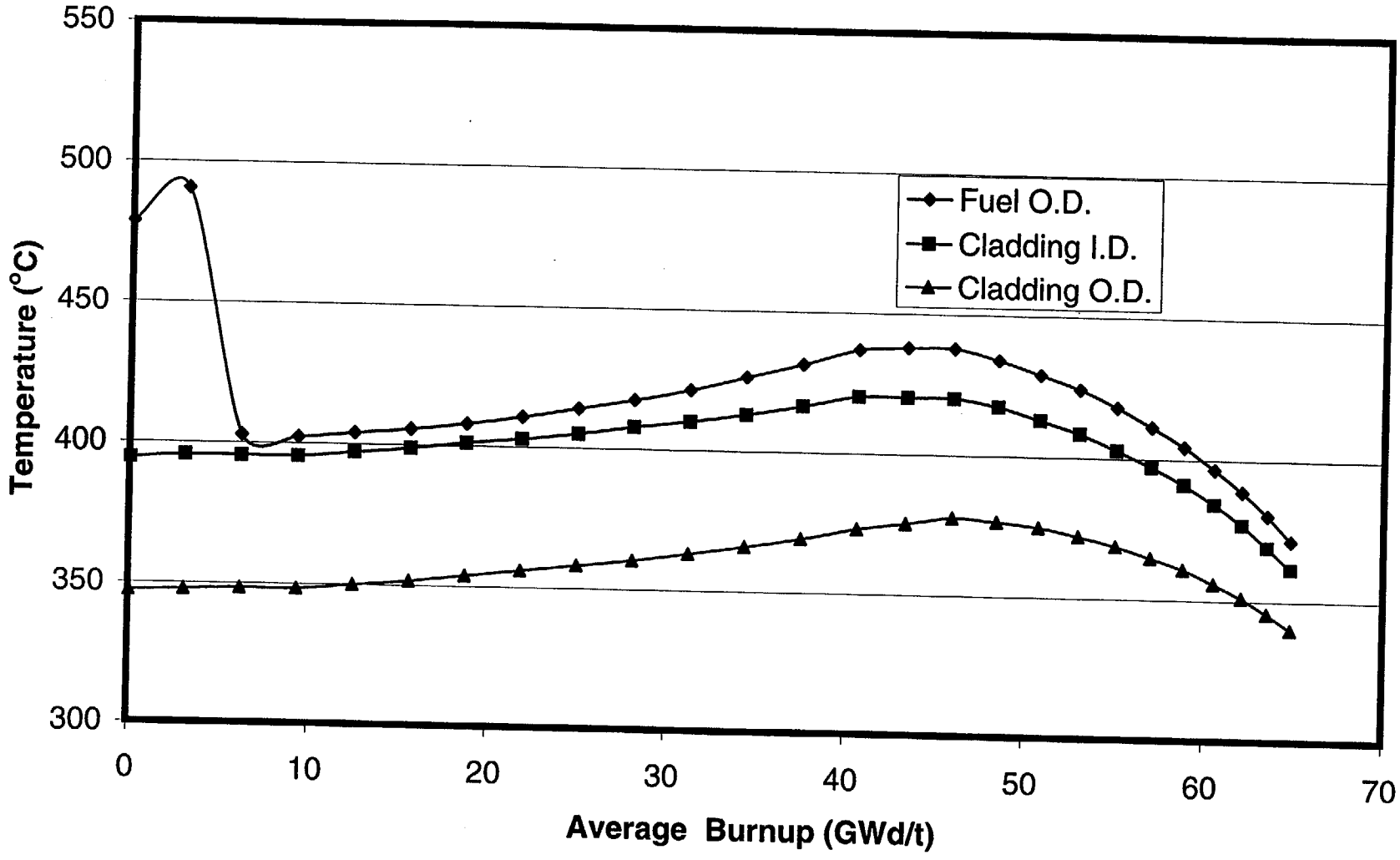

Fig. 10-8. Cladding temperatures and fuel surface temperature for a PWR 16x16 fuel rod with initial peak power of 11 kW/ft.

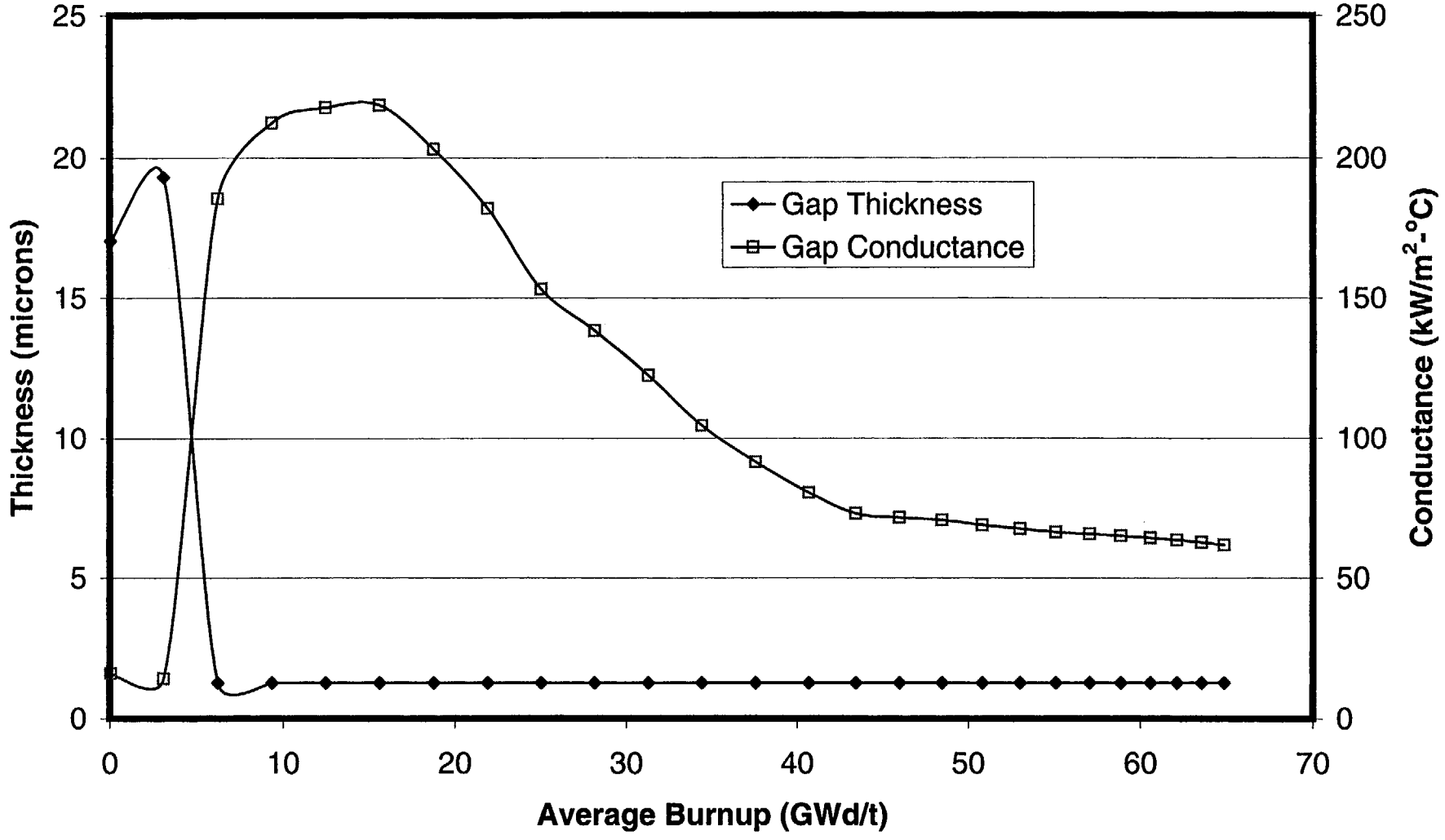

Fig. 10-9. Gap thickness and gap conductance for a PWR 16x16 fuel rod with initial peak power of 11 kW/ft.

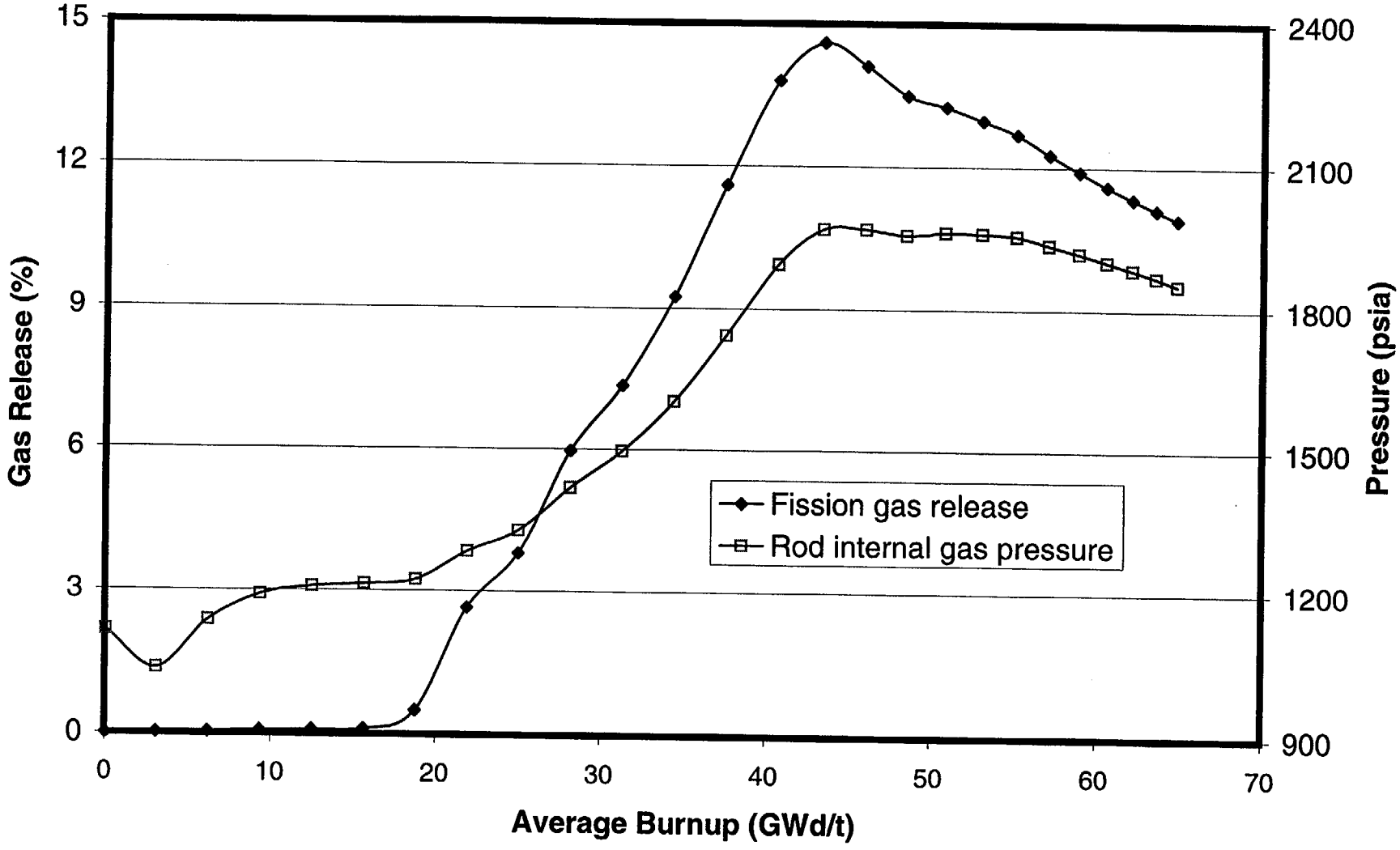

Fig. 10-10. Fission gas release and rod internal gas pressure for a PWR 16x16 fuel rod with initial peak power of 11 kW/ft.

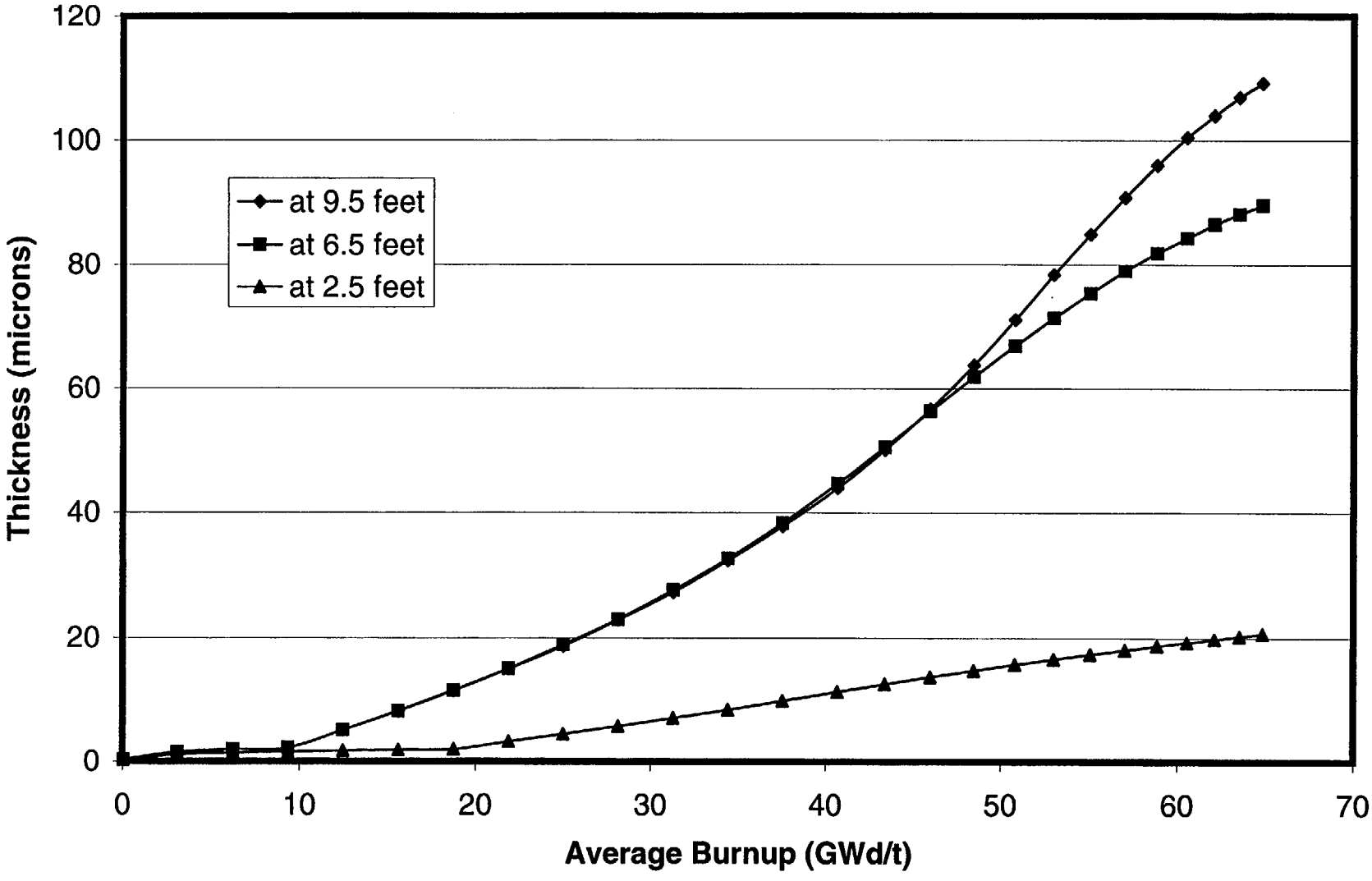

Fig. 10-11. Oxide thickness at three axial locations for a PWR 16x16 fuel rod with initial peak power of 11 kW/ft.

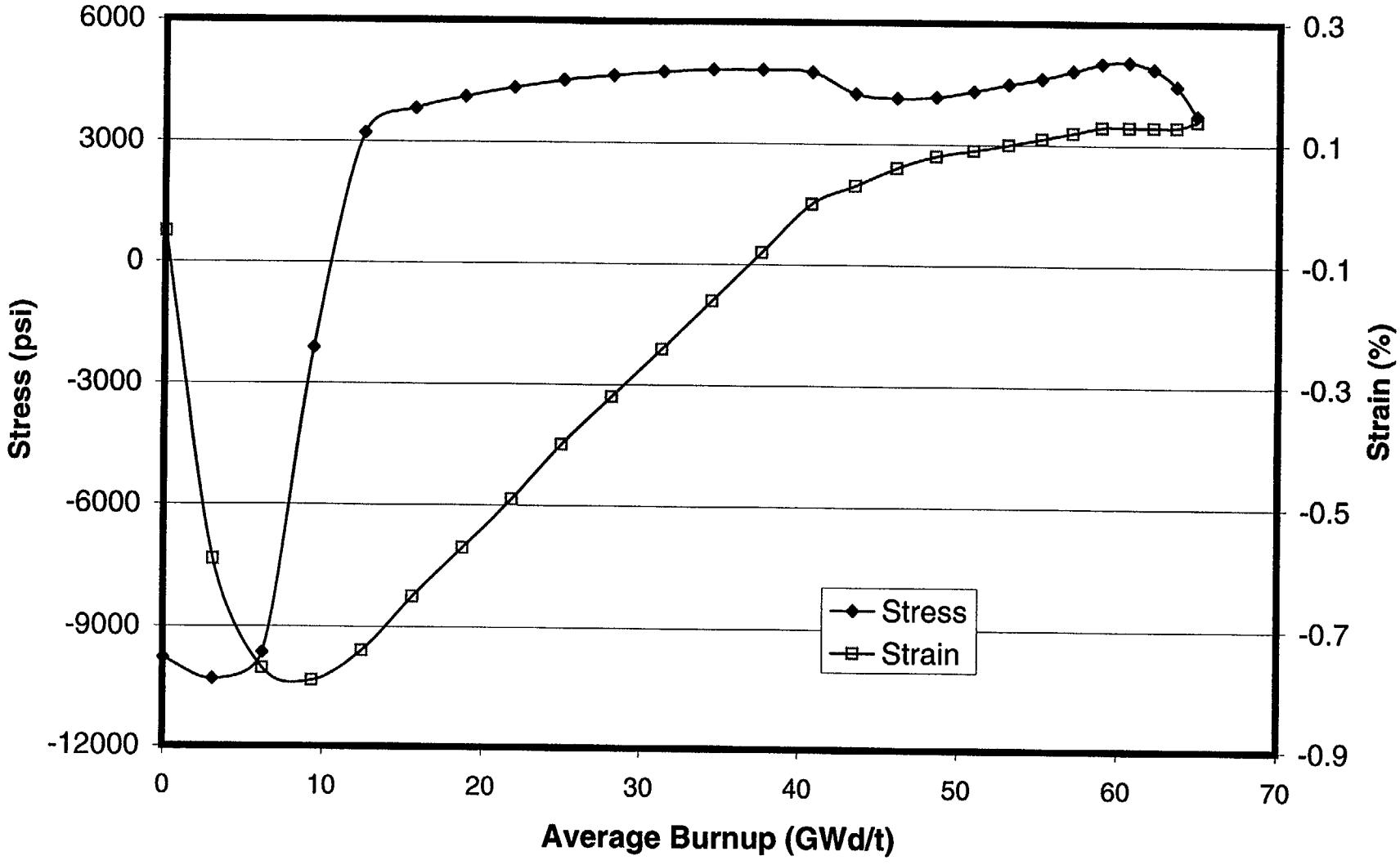

Fig. 10-12. Cladding hoop stress and hoop strain for a PWR 16x16 fuel rod with initial peak power of 11 kW/ft.

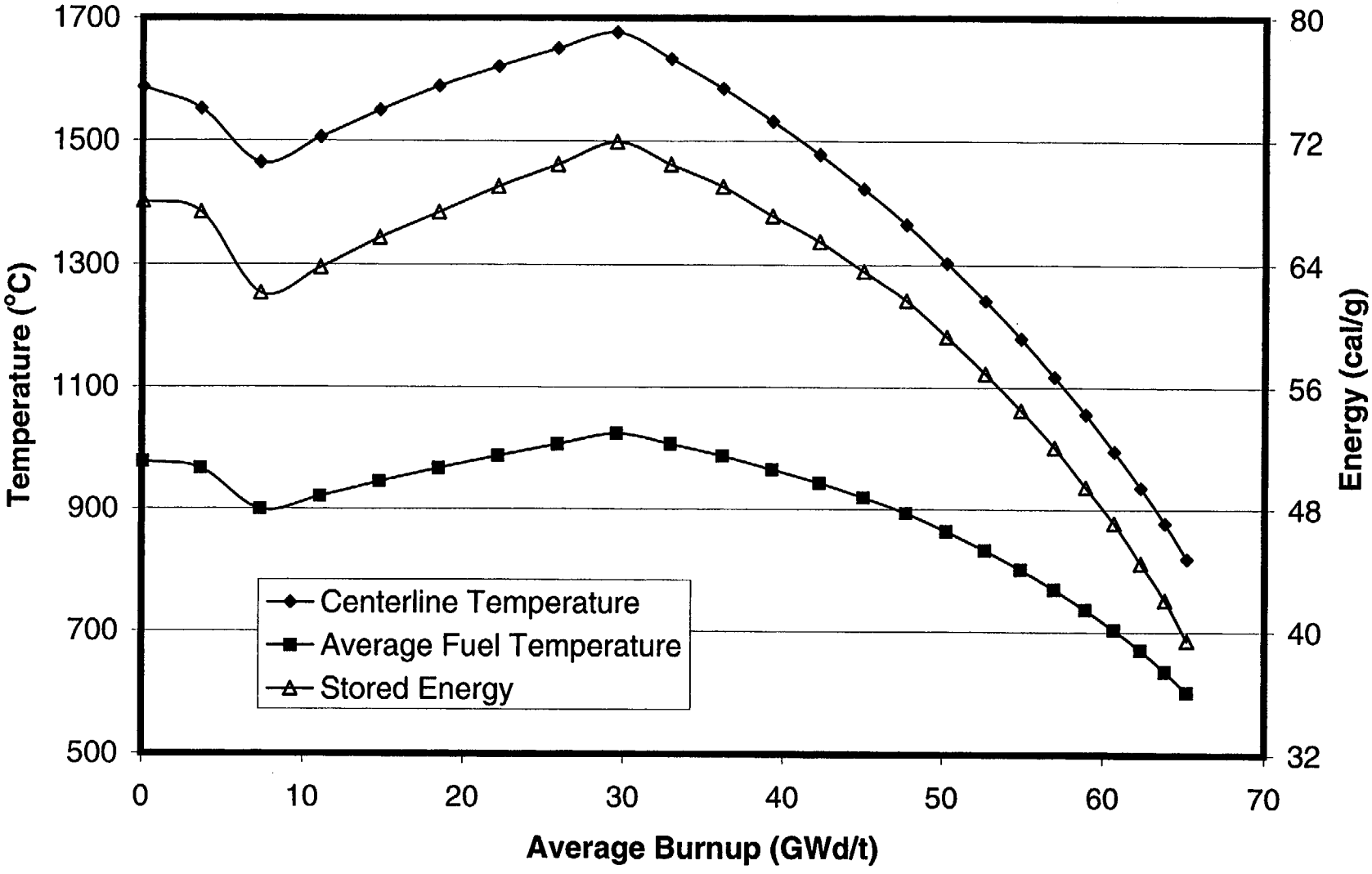

Fig. 10-13. Fuel temperatures and stored energy for a PWR 16x16 fuel rod with initial peak power of 13 kW/ft.

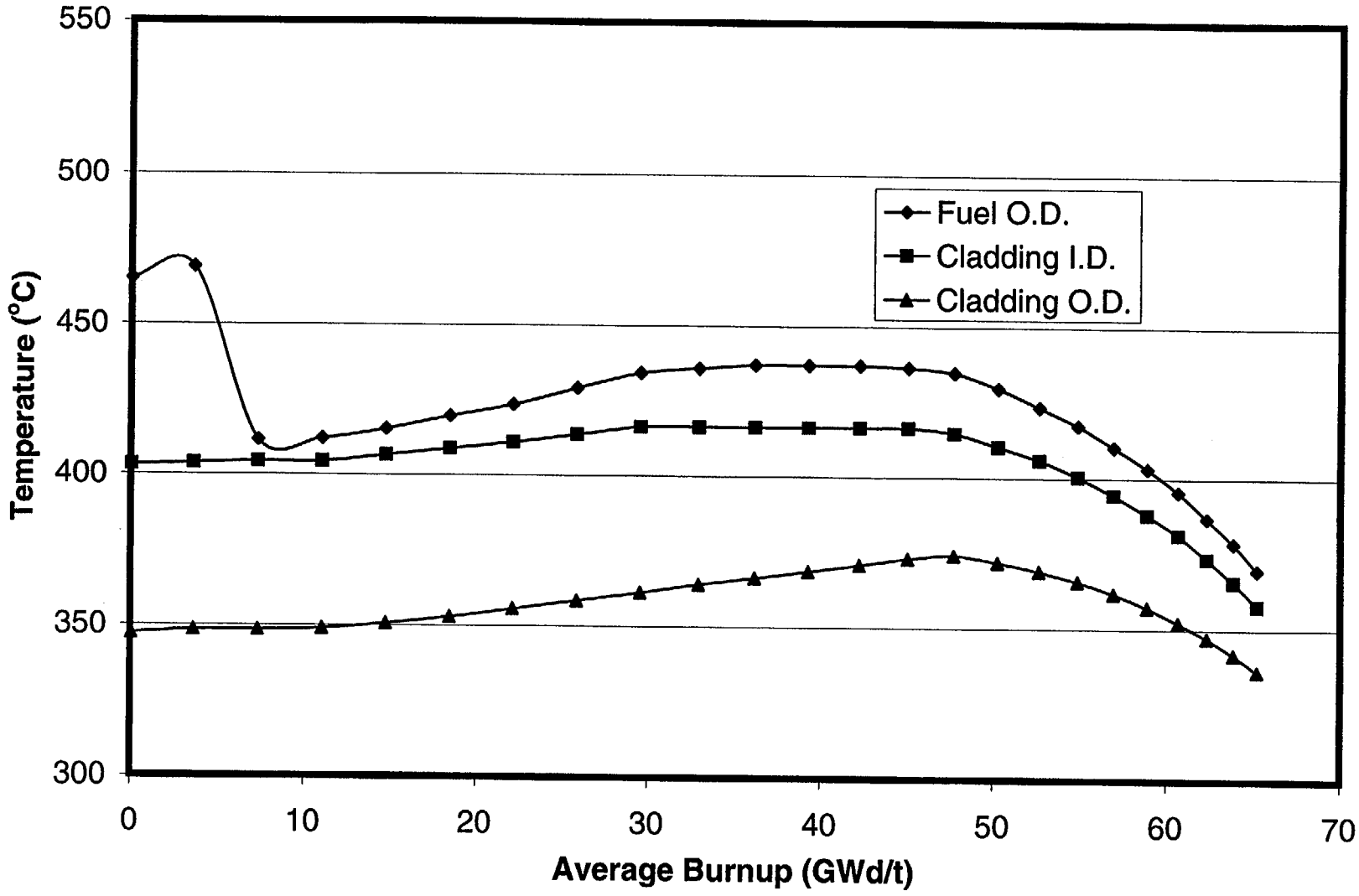

Fig. 10-14. Cladding temperatures and fuel surface temperature for a PWR 16x16 fuel rod with initial peak power of 13 kW/ft.

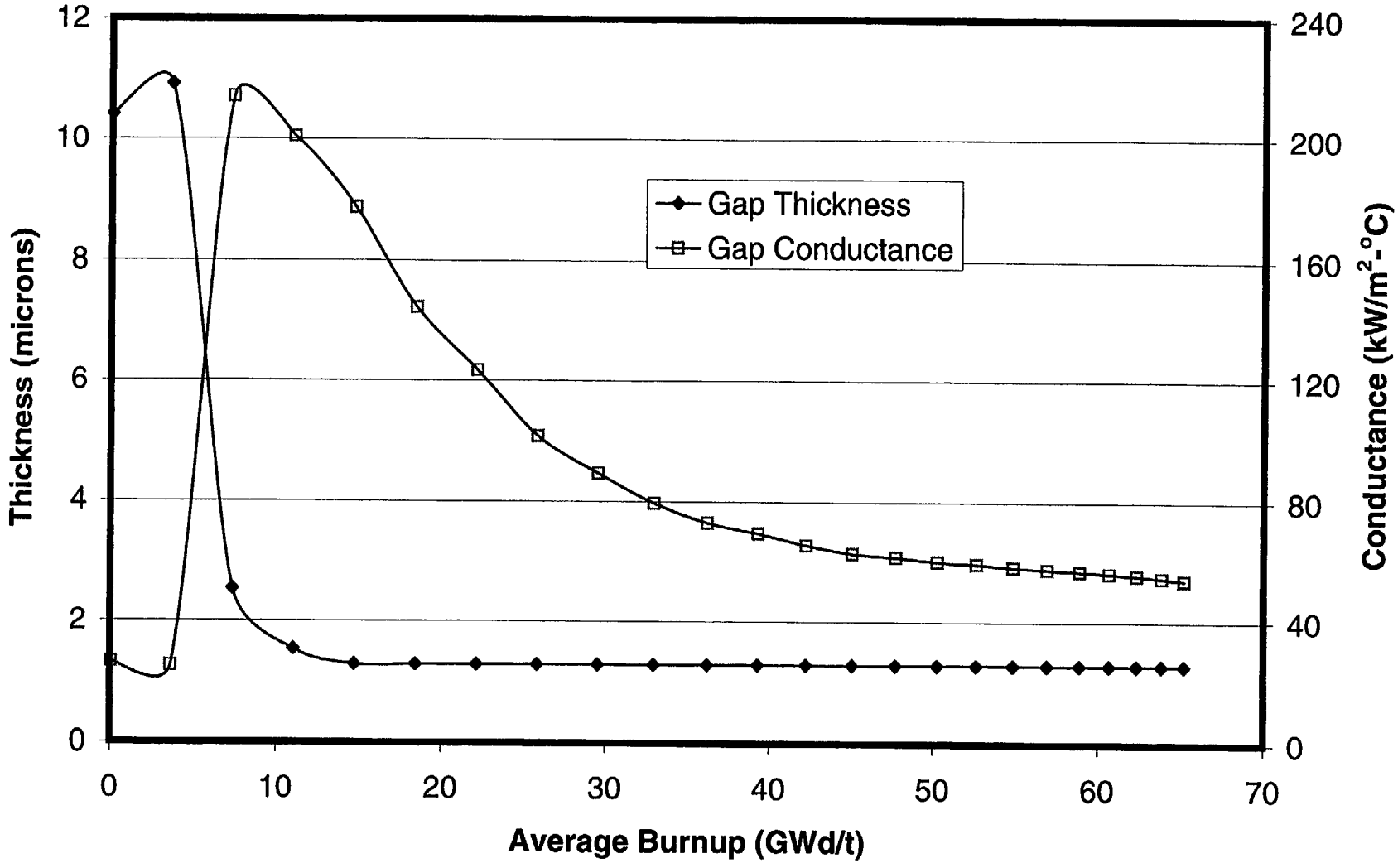

Fig. 10-15. Gap thickness and gap conductance for a PWR 16x16 fuel rod with initial peak power of 13 kW/ft.

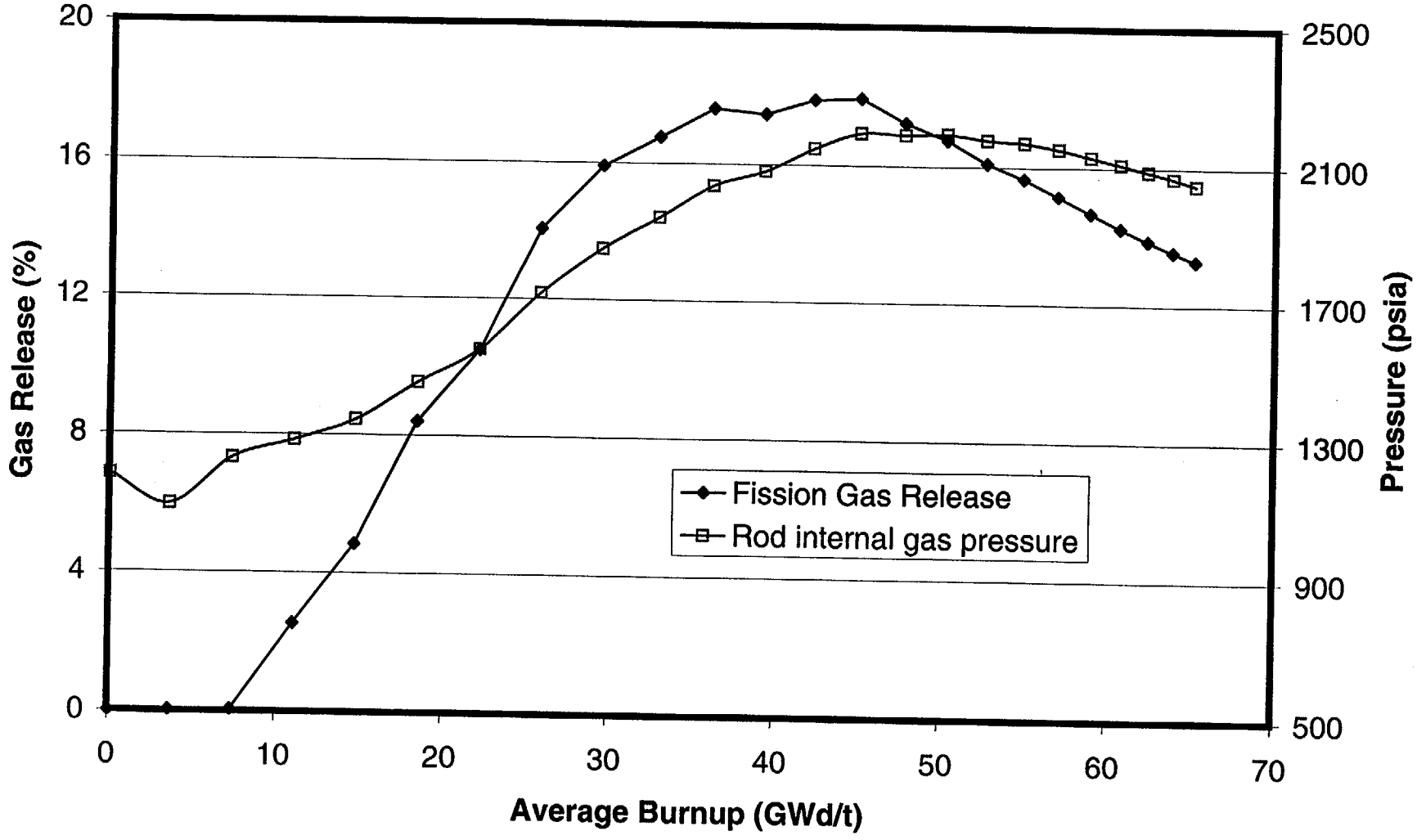

Fig. 10-16. Fission gas release and rod internal gas pressure for a PWR 16x16 fuel rod with initial peak power of 13 kW/ft.

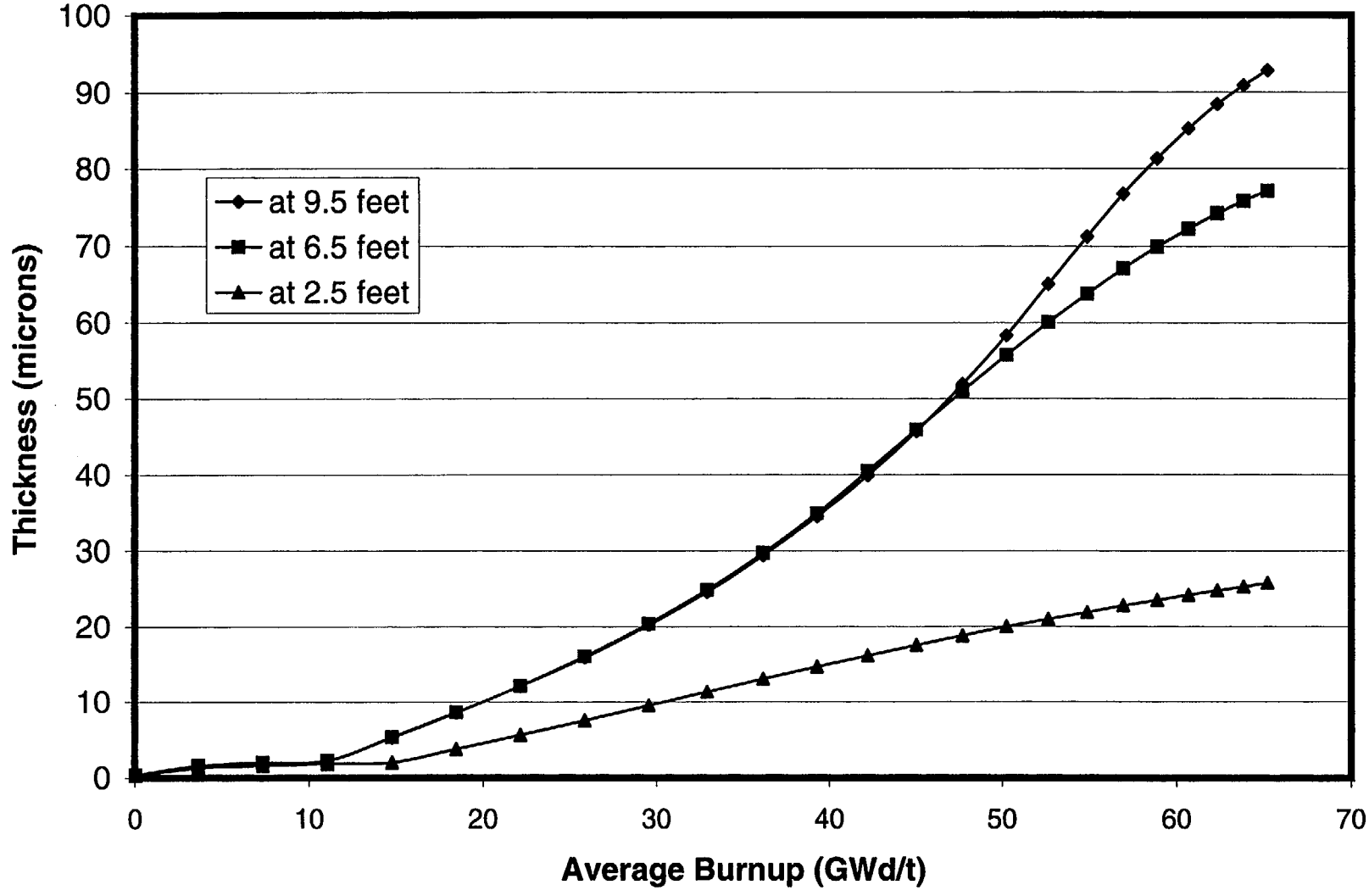

Fig. 10-17. Oxide thickness at three axial locations for a PWR 16x16 fuel rod with initial peak power of 13 kW/ft.

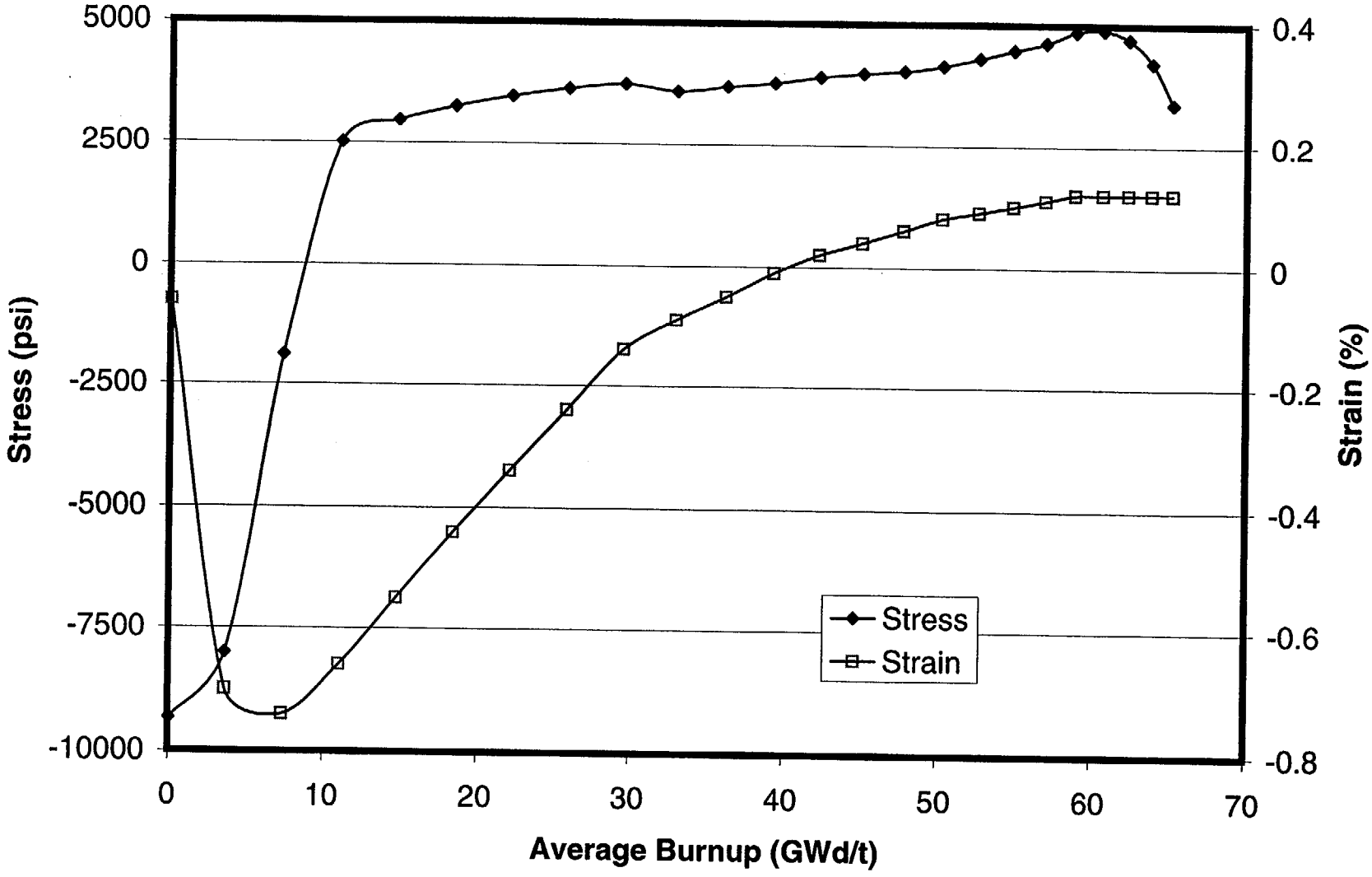

Fig. 10-18. Cladding hoop stress and hoop strain for a PWR 16x16 fuel rod with initial peak power of 13 kW/ft.

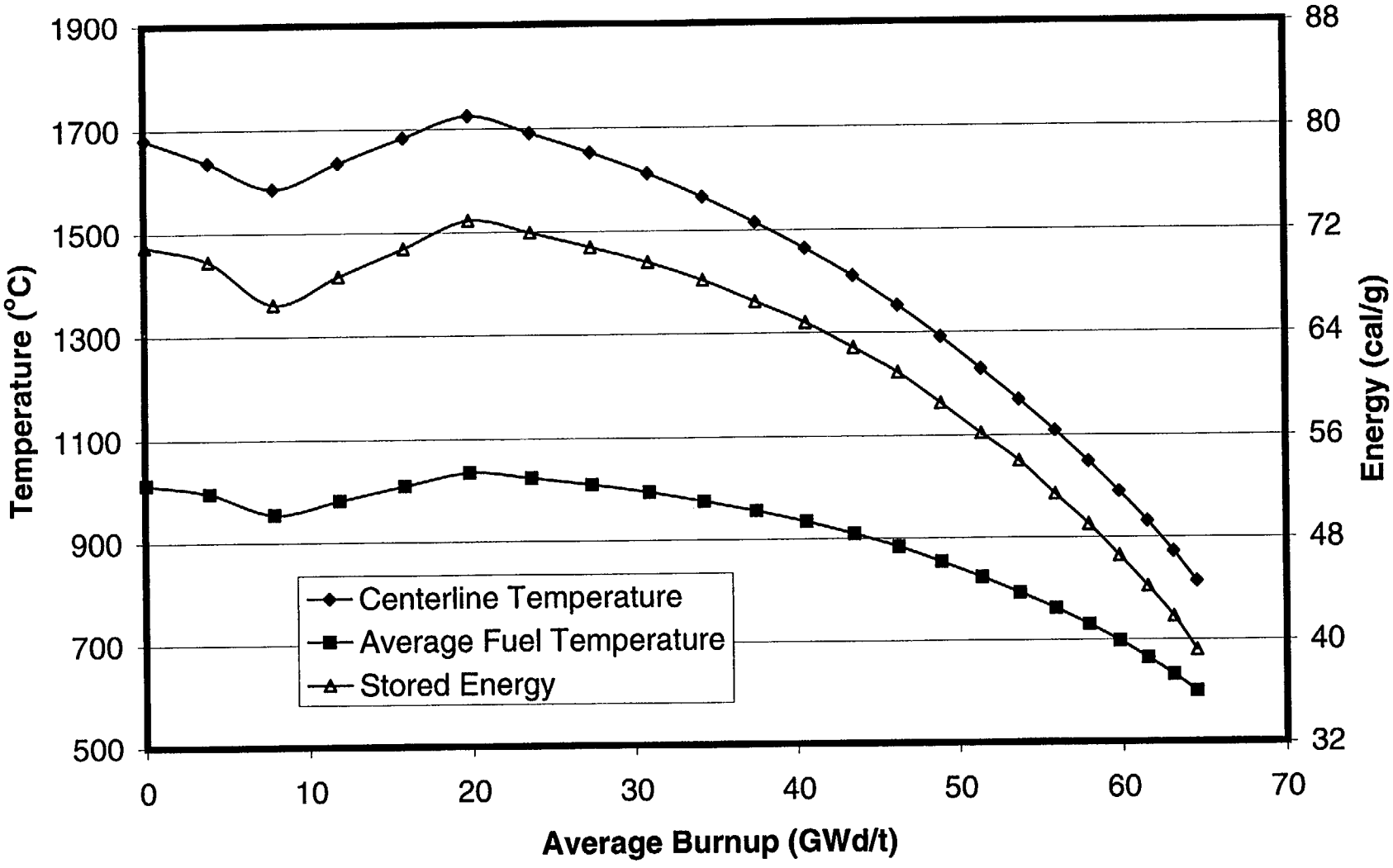

Fig. 10-19. Fuel Temperatures and stored energy for a PWR 16x16 fuel rod with initial peak power of 14 kW/ft.

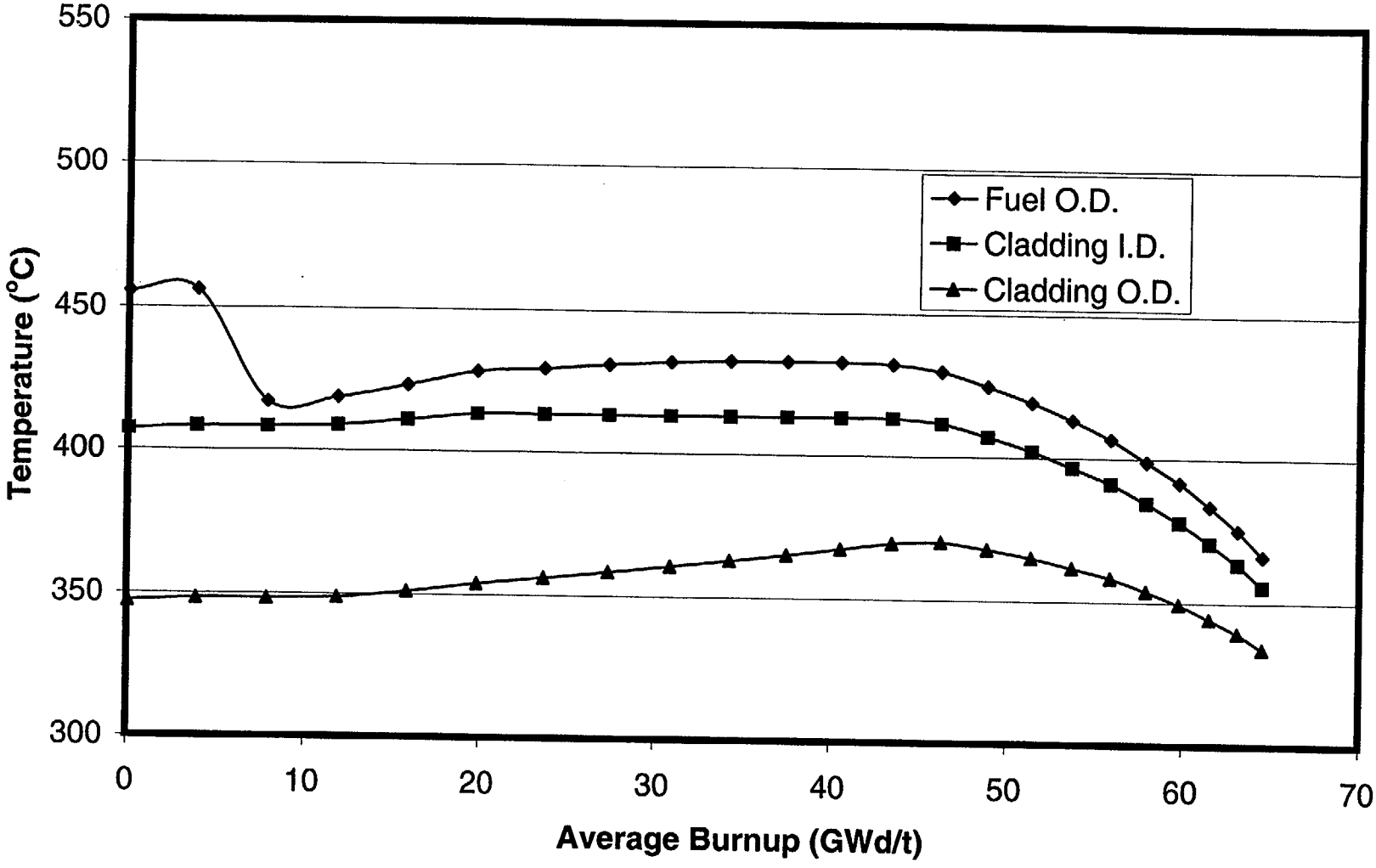

Fig. 10-20. Cladding temperatures and fuel surface temperature for a PWR 16x16 fuel rod with initial peak power of 14 kW/ft.

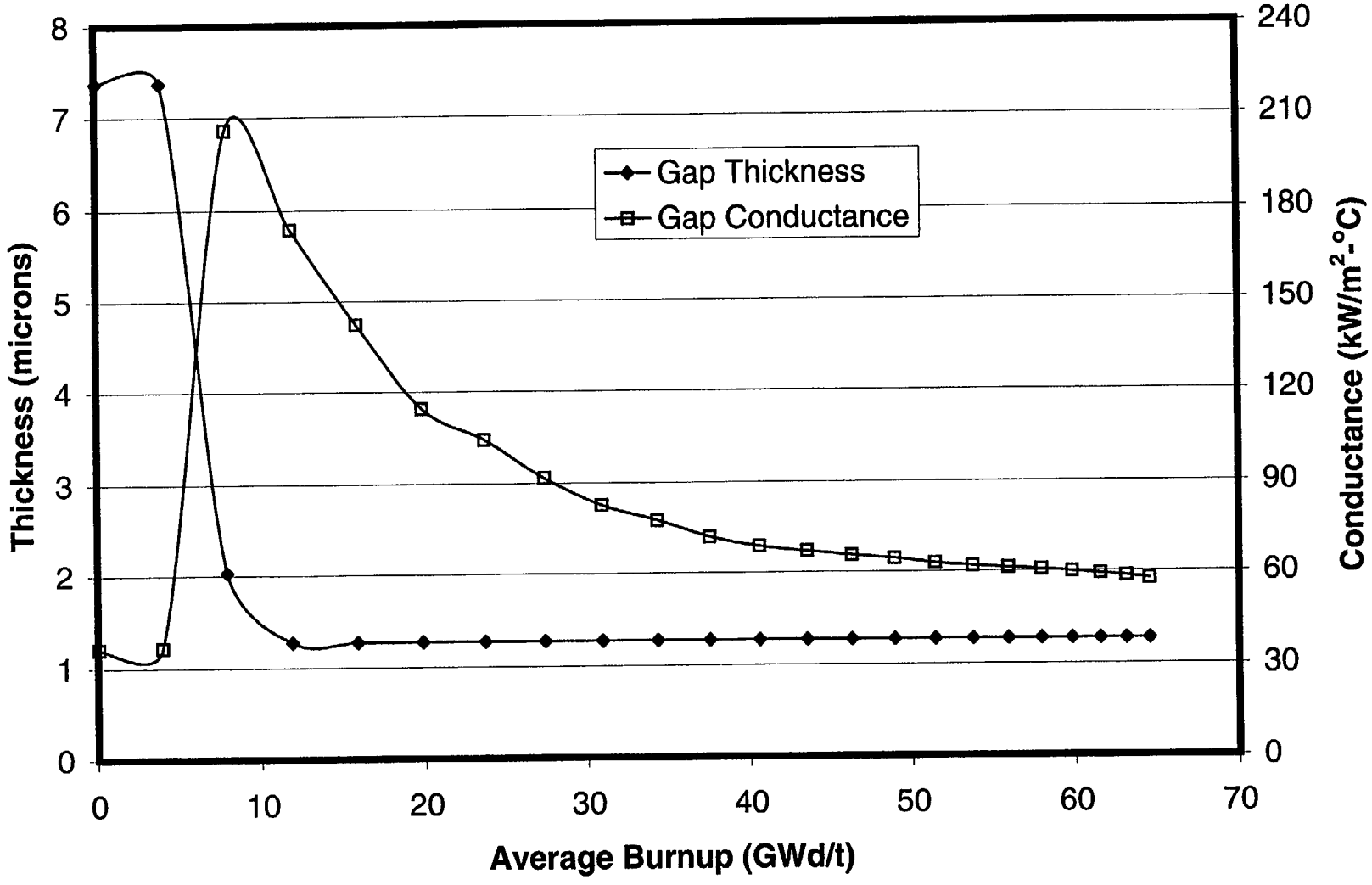

Fig. 10-21. Gap thickness and gap conductance for a PWR 16x16 fuel rod with initial peak power of 14 kW/ft.

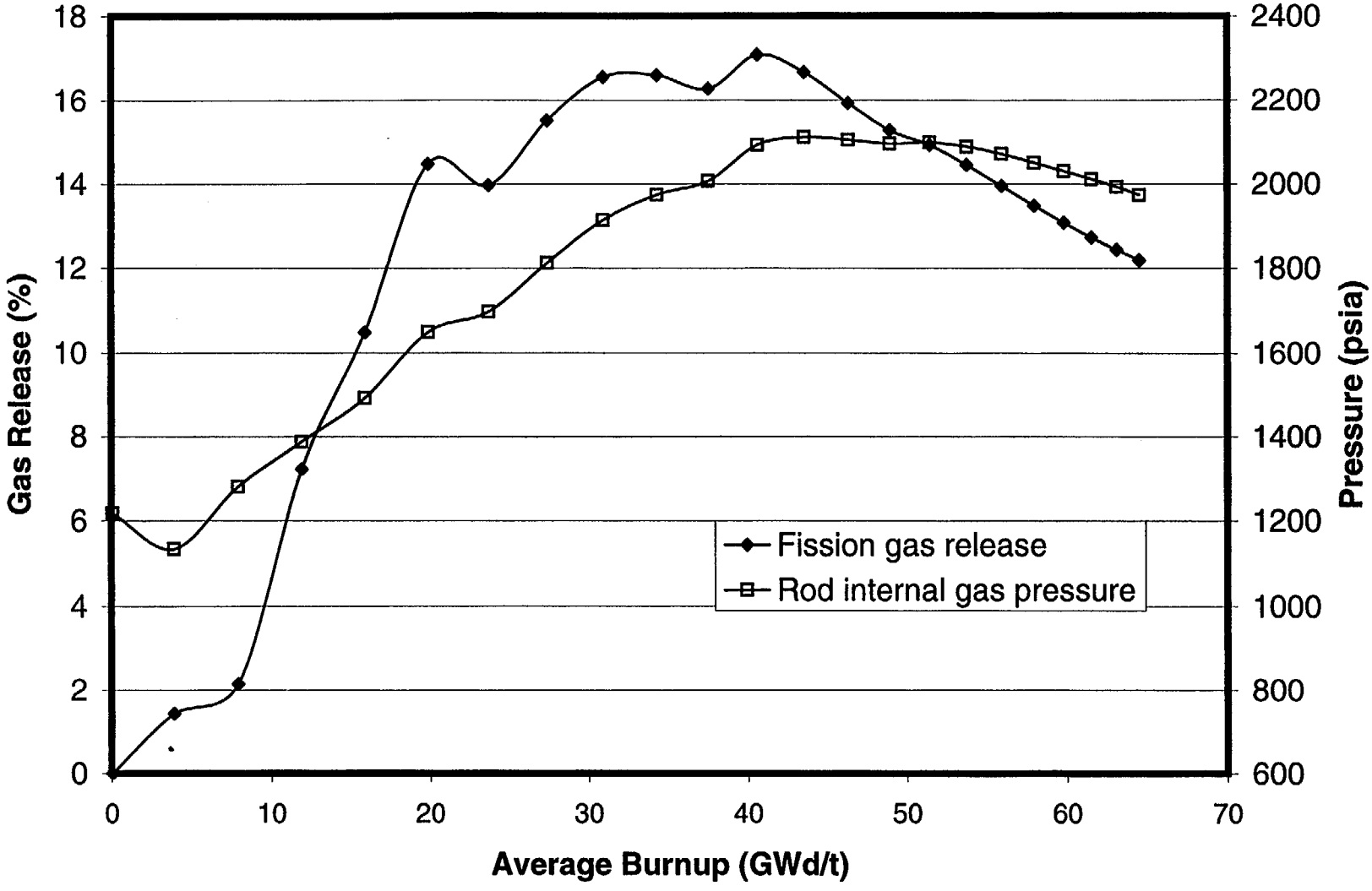

Fig. 10-22. Fission gas release and rod internal gas pressure for a PWR 16x16 fuel rod with initial peak power of 14 kW/ft.

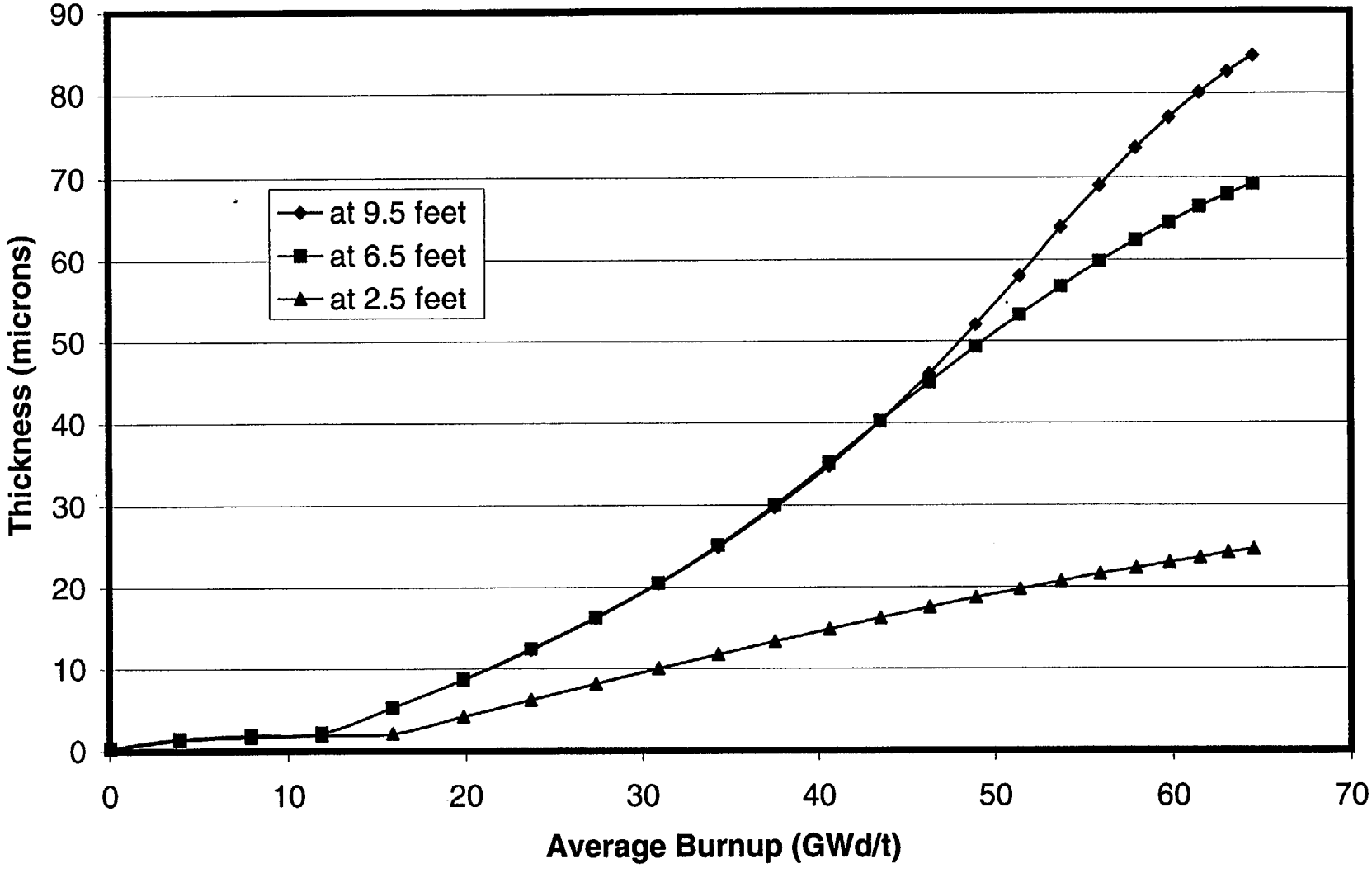

Fig. 10-23. Oxide thickness at three axial locations for a PWR 16x16 fuel rod with initial peak power of 14 kW/ft.

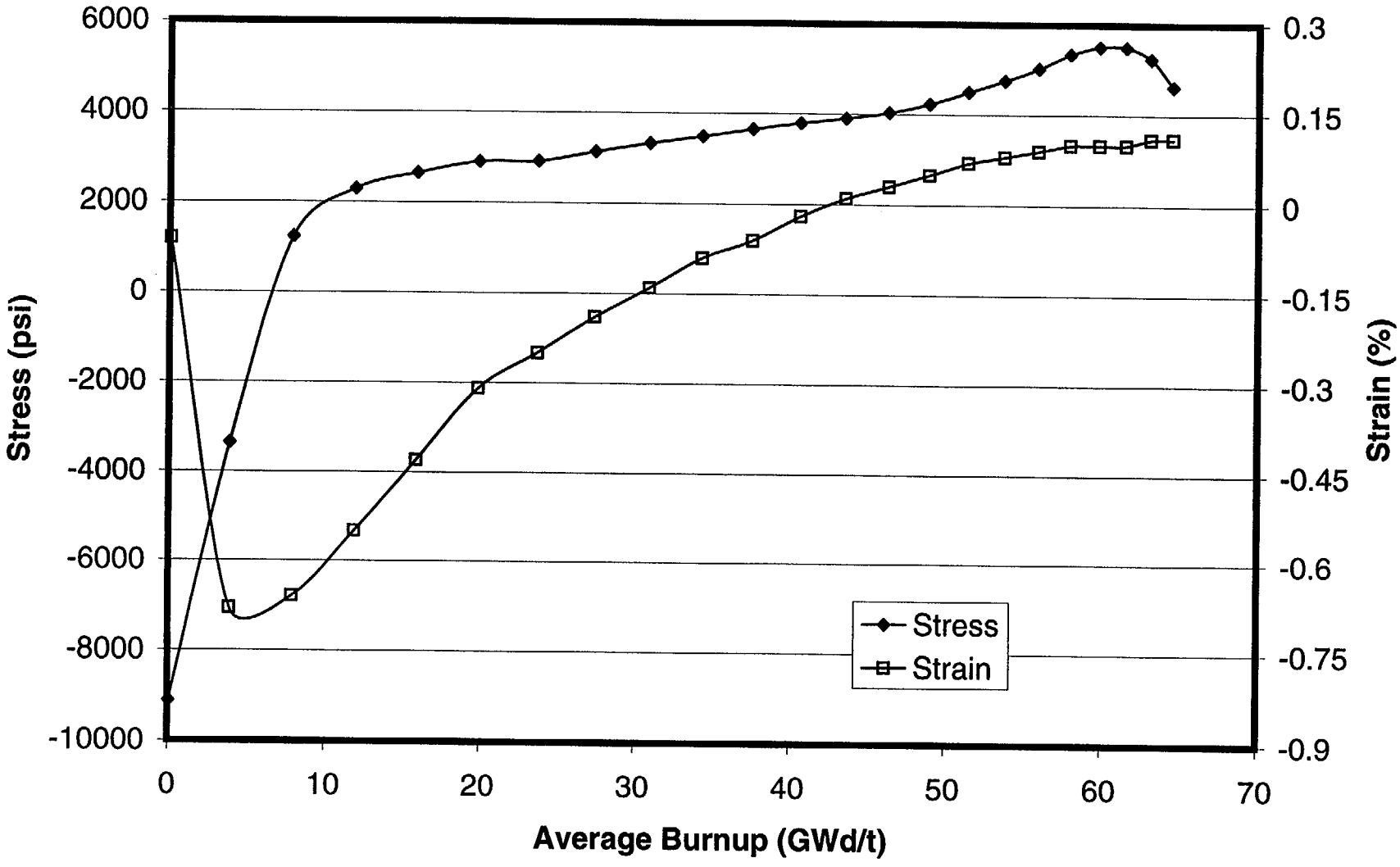

Fig. 10-24. Cladding hoop stress and hoop strain for a PWR 16x16 fuel rod with initial peak power of 14 kW/ft.

11. Calculations for PWR 17X17 Fuel

In the following figures, calculated values for PWR 17X17 fuel are plotted as a function of burnup for the parameters listed below:

Fuel centerline temperature
Average fuel temperature
Stored energy
Fuel O.D. temperature
Cladding I.D. temperature
Cladding O.D. temperature
Gap thickness
Gap conductance
Fission gas release
Rod internal gas pressure
Oxide thickness
Cladding hoop stress
Cladding hoop strain

Several general observations can be made about the calculated results:

- Within the first few GWd/t of burnup, a temperature peak is observed that is the result of fuel densification.

- Gap closure results in (a) the coming together of temperatures for fuel O.D. and cladding I.D. and (b) a sharp increase in gap conductance. The gap conductance increases again after a few time steps when the interaction between the pellet and cladding affects the contact conductance calculated for a closed gap. At this point there is also a large increase in stress, and the permanent strain changes directions.

- Some of the fission gas is released in spurts according to the Massih model in FRAPCON-3. This effect is apparent in many of the figures. Shorter time steps would produce slightly different looking curves, but the trend of gas release and the end-of-life gas release would be about the same.

- The burnup enhancement of fission gas release is readily seen in the lower power cases, but it is obscured in the highest power cases by the magnitude of prior gas release.

- Rod internal gas pressure increases with the accumulation of released fission gas. In the higher power PWR cases, as the power drops off near the end of life, the reduction in the plenum temperature offsets the increasing moles of fission gas.

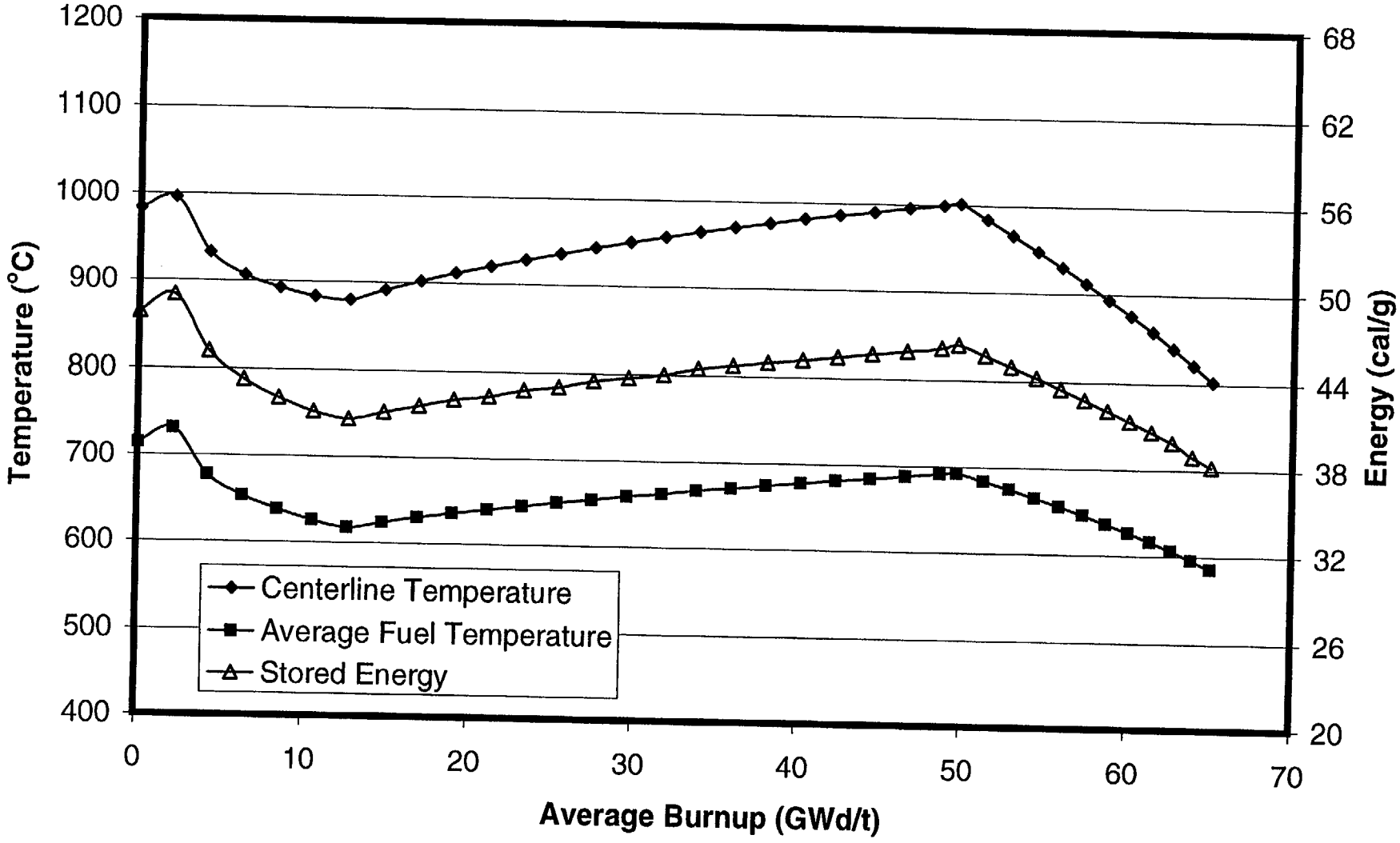

Fig. 11-1. Fuel temperatures and stored energy for a PWR 17x17 fuel rod with initial peak power of 7 kW/ft.

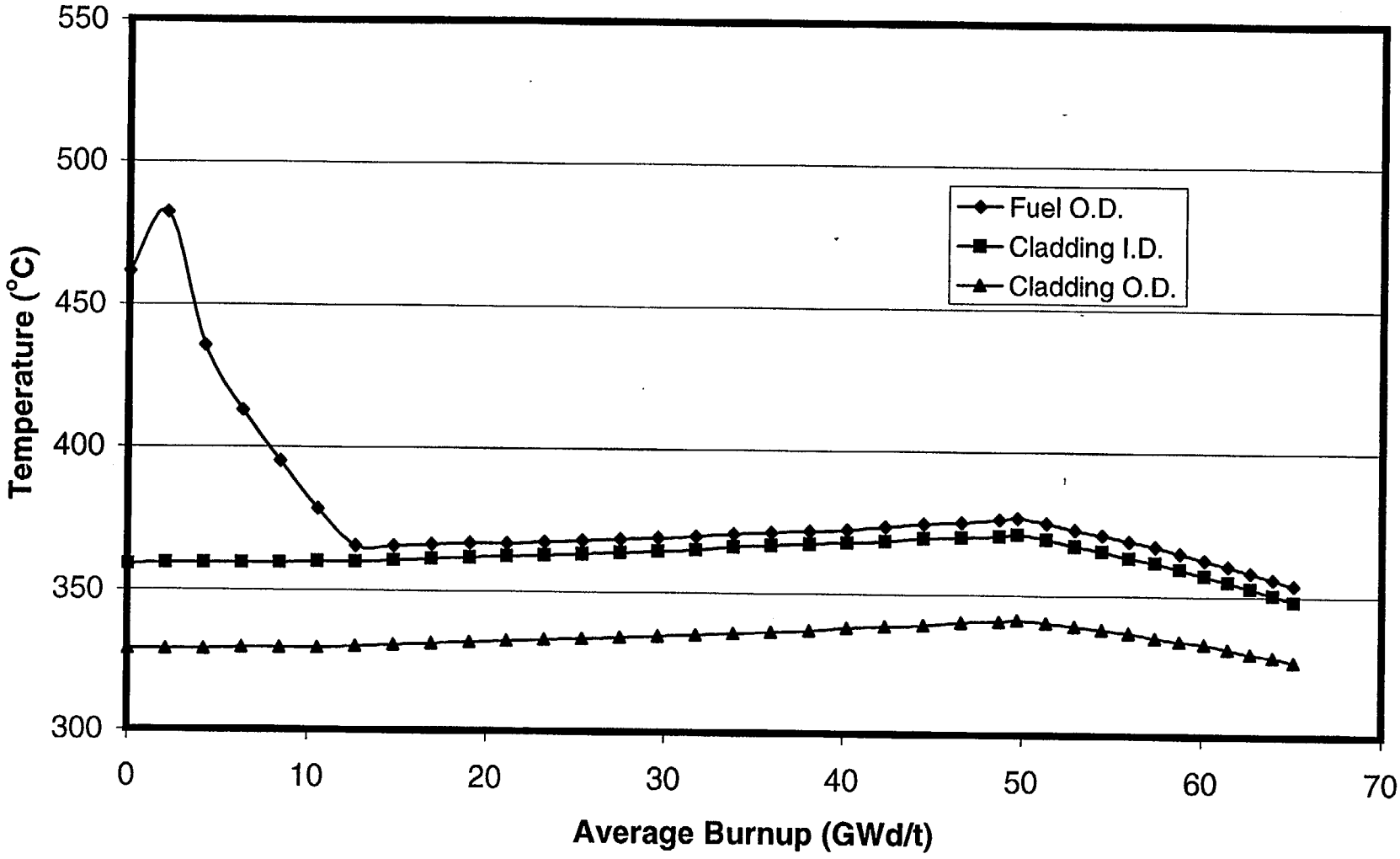

Fig. 11-2. Cladding temperatures and fuel surface temperature for a PWR 17x17 fuel rod with initial peak power of 7 kW/ft.

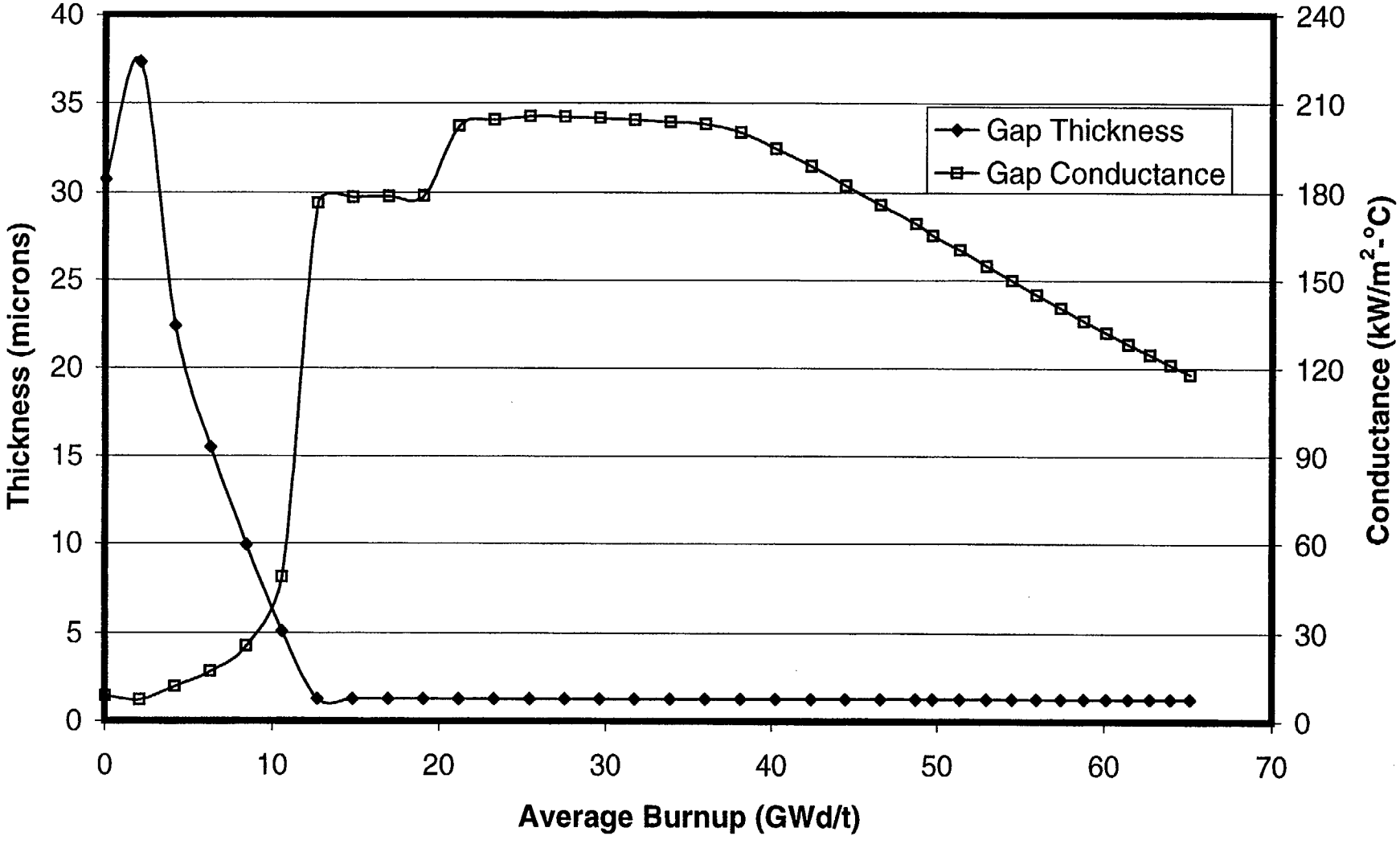

Fig. 11-3. Gap thickness and gap conductance for a PWR 17x17 fuel rod with initial peak power of 7 kW/ft.

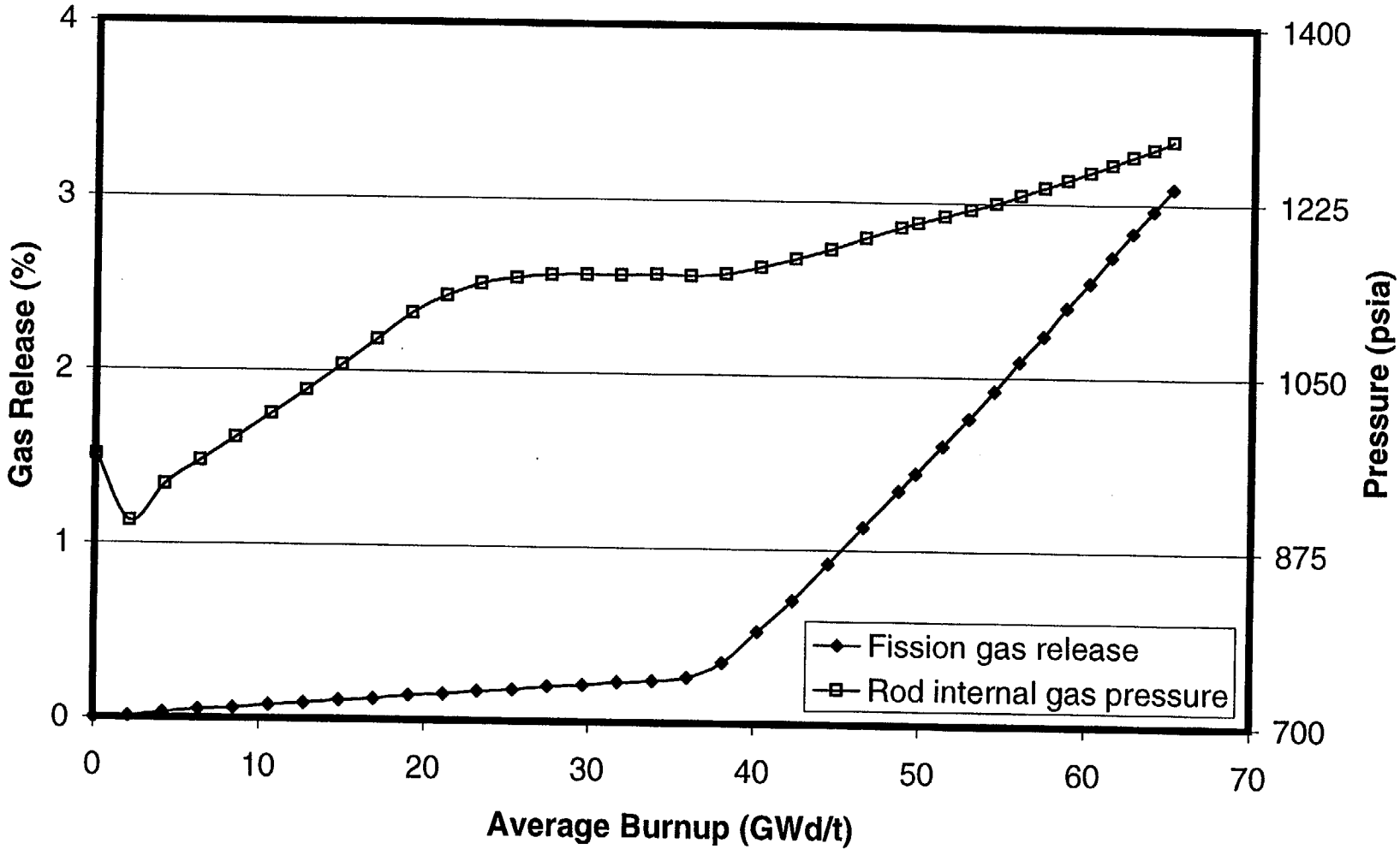

Fig. 11-4. Fission gas release and rod internal gas pressure for a PWR 17x17 fuel rod with initial peak power of 7 kW/ft.

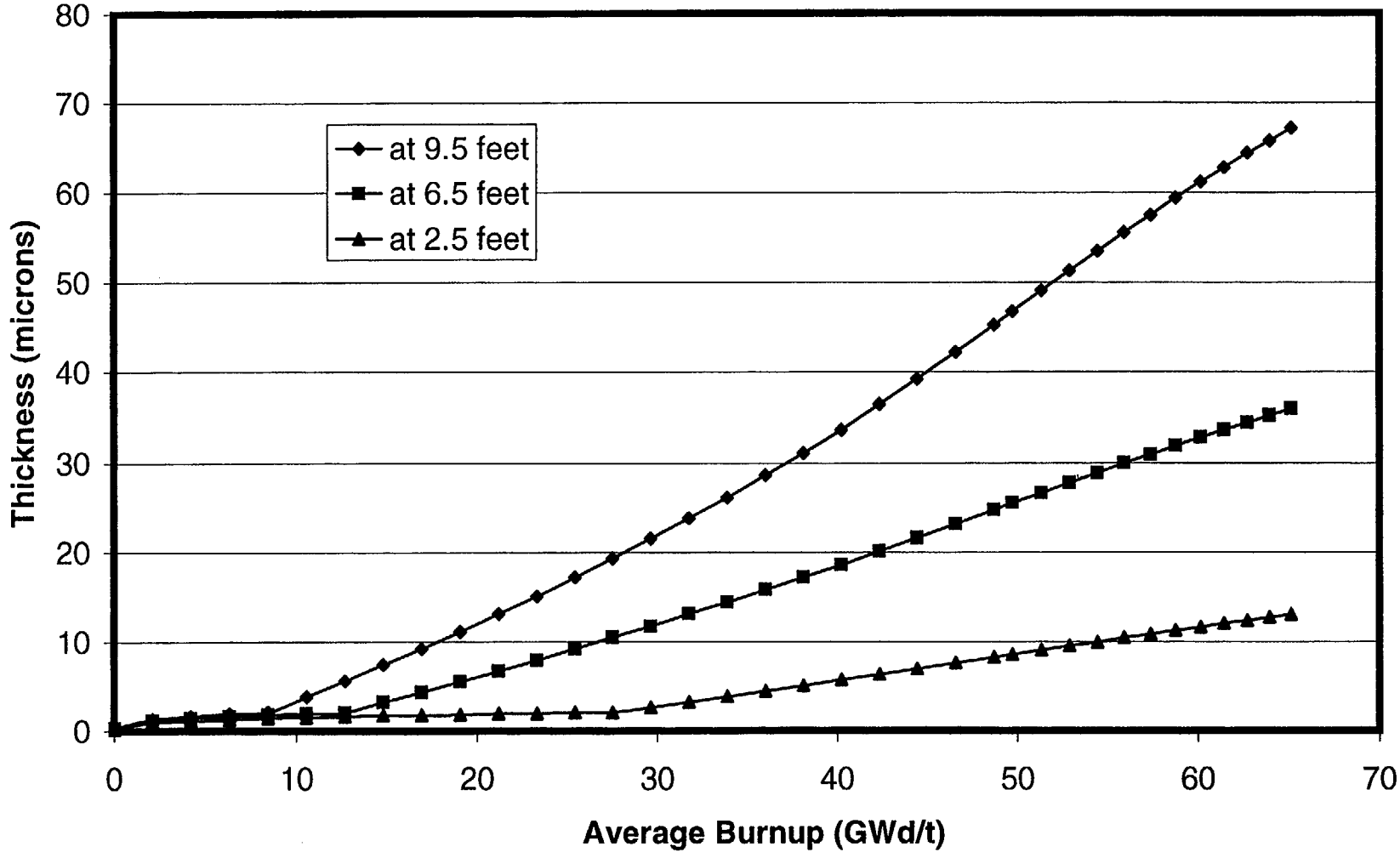

Fig. 11-5. Oxide thickness at three axial locations for a PWR 17x17 fuel rod with initial peak power of 7 kW/ft.

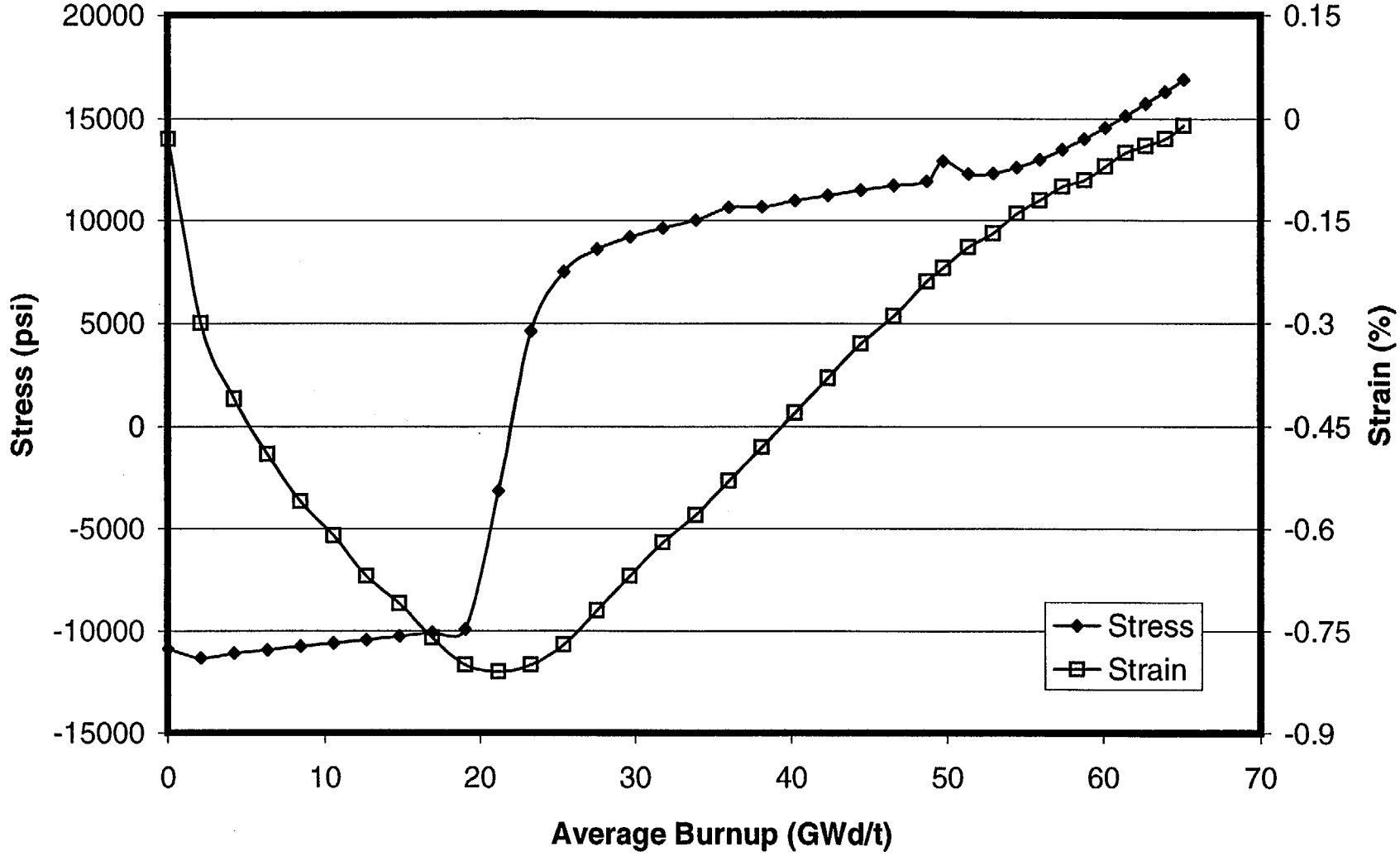

Fig. 11-6. Cladding hoop stress and hoop strain for a PWR 17x17 fuel rod with initial peak power of 7 kW/ft.

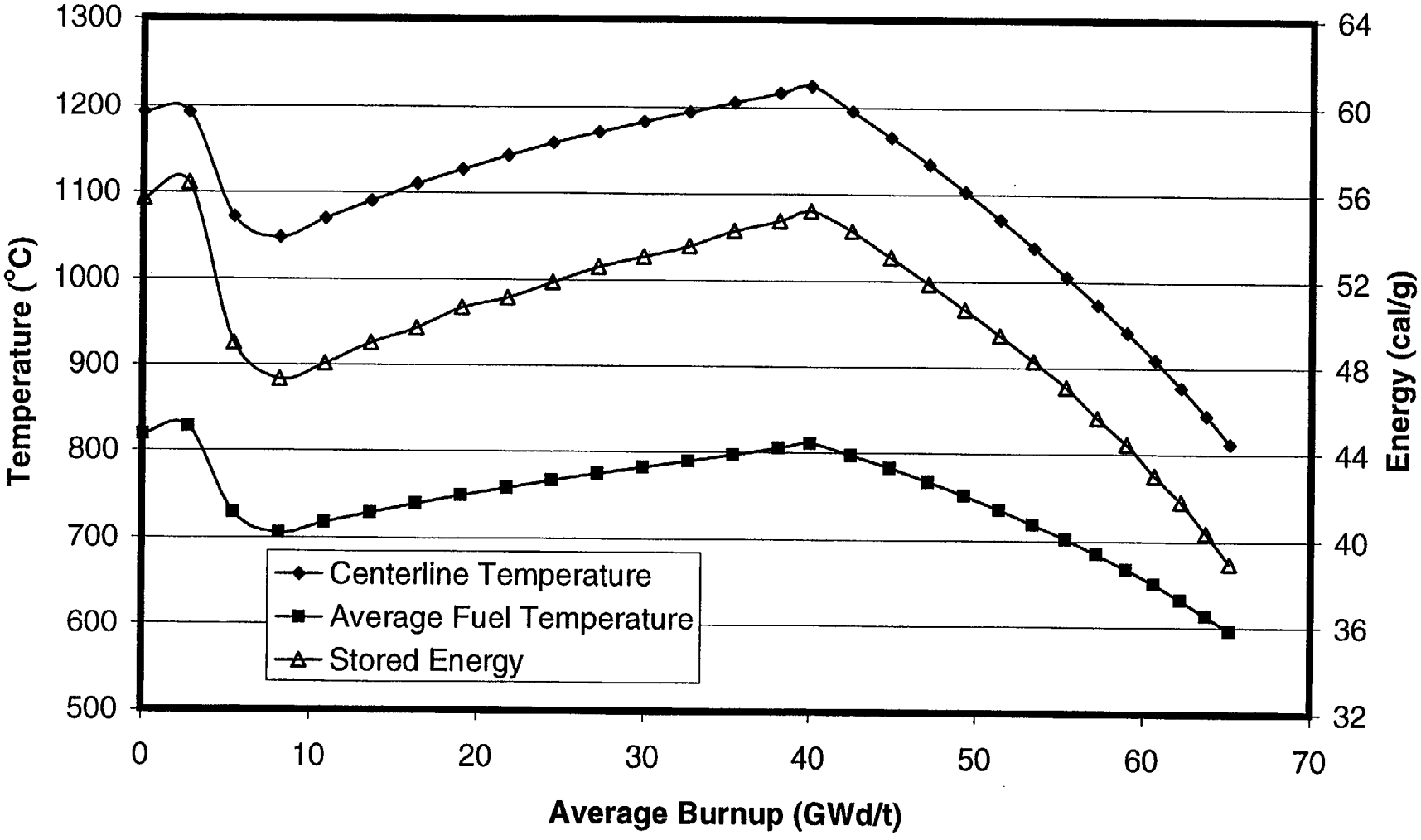

Fig. 11-7. Fuel temperatures and stored energy for a PWR 17x17 fuel rod with initial peak power of 9 kW/ft.

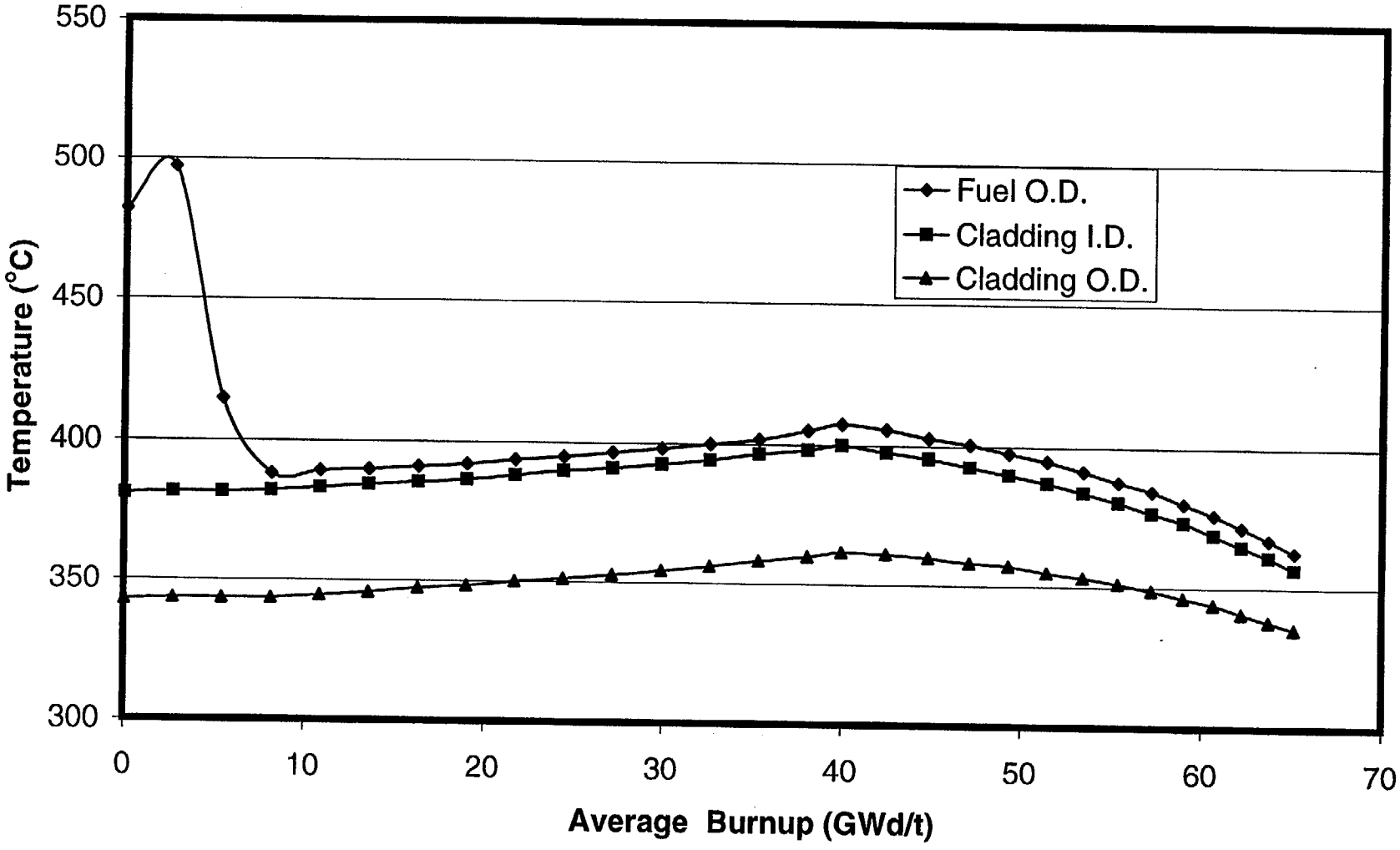

Fig. 11-8. Cladding temperatures and fuel surface temperature for a PWR 17x17 fuel rod with initial peak power of 9 kW/ft.

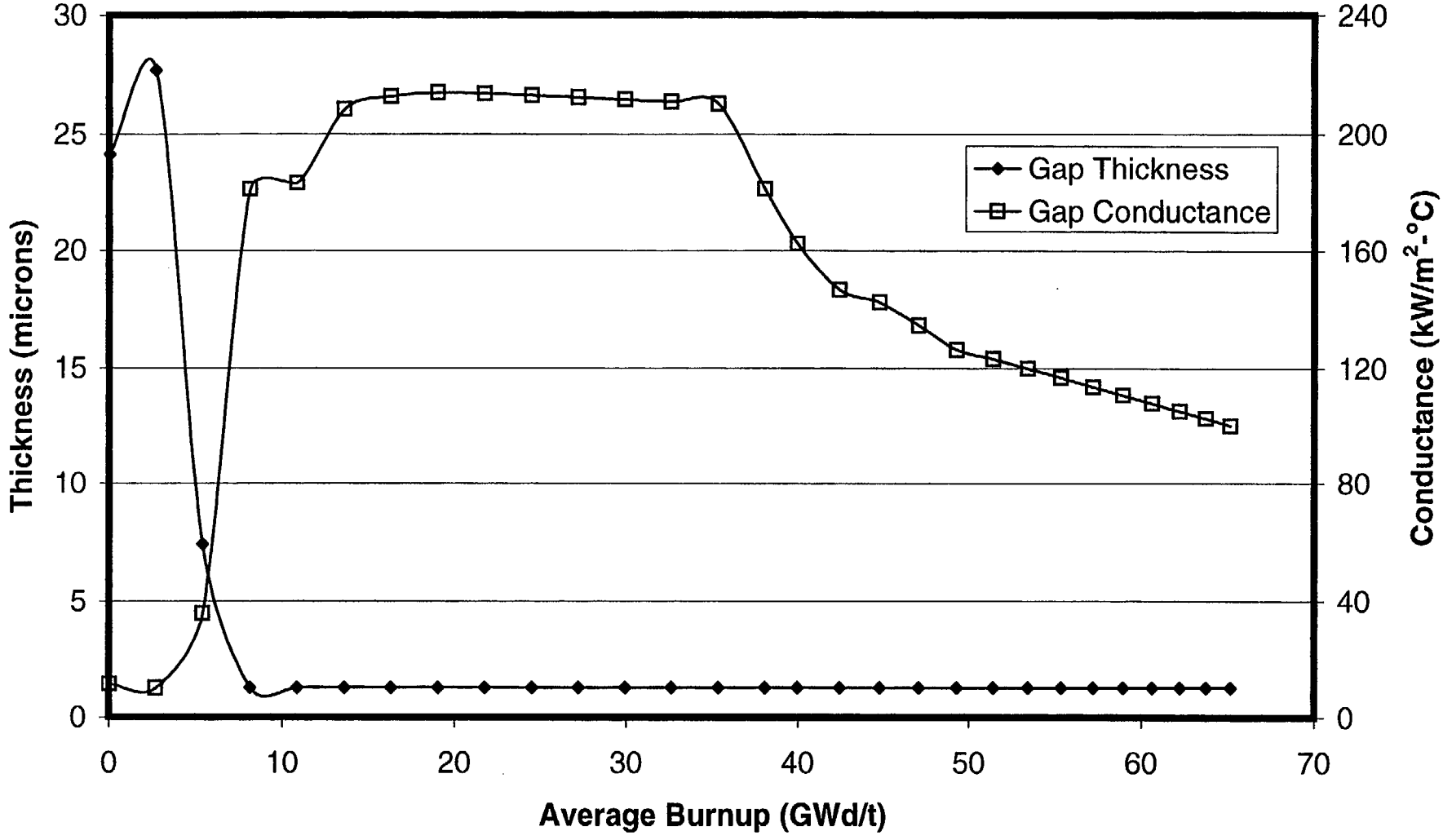

Fig. 11-9. Gap thickness and gap conductance for a PWR 17x17 fuel rod with initial peak power of 9 kW/ft.

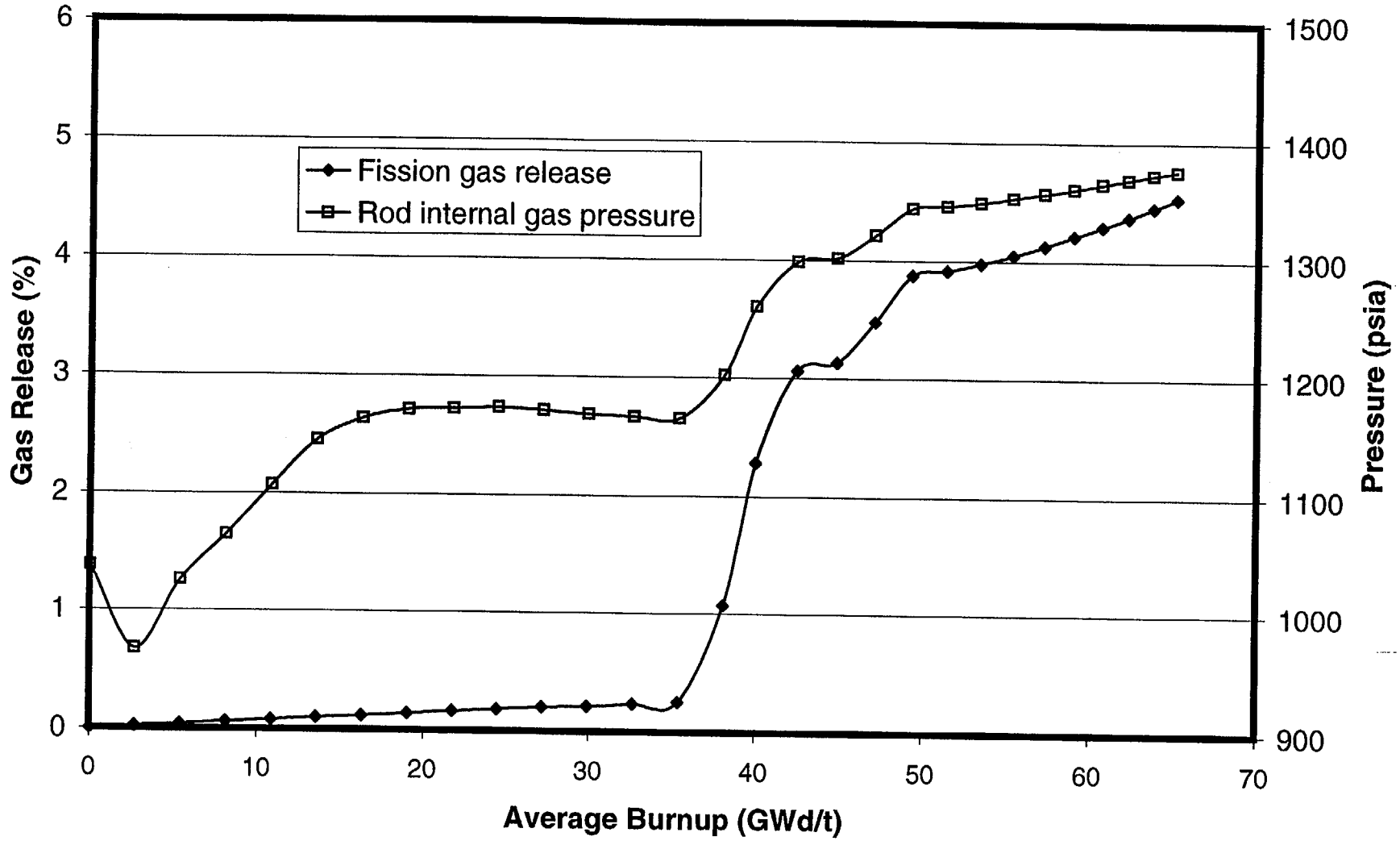

Fig. 11-10. Fission gas release and rod internal gas pressure for a PWR 17x17 fuel rod with initial peak power of 9 kW/ft.

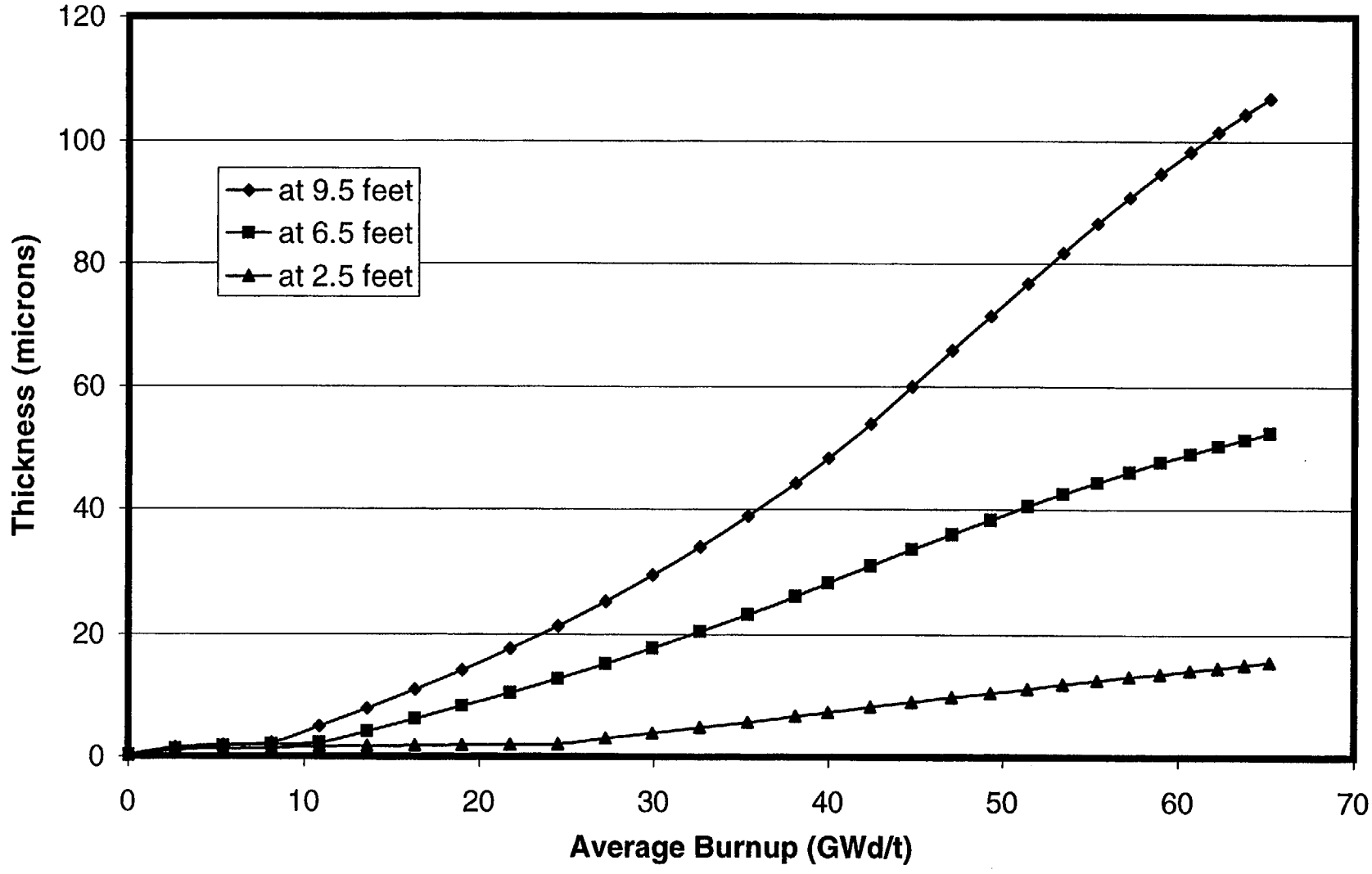

Fig. 11-11. Oxide thickness at three axial locations for a PWR 17x17 fuel rod with initial peak power of 9 kW/ft.

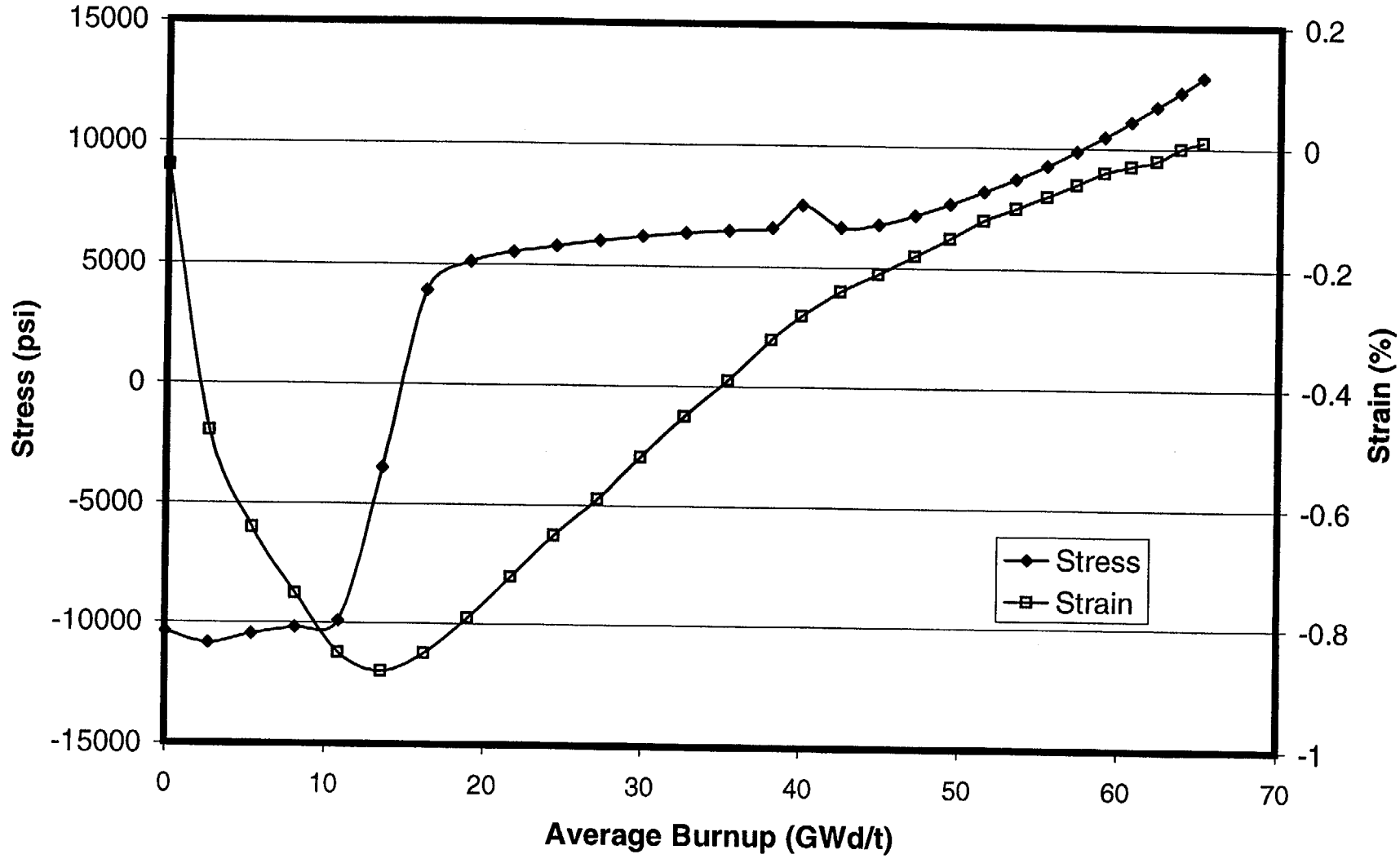

Fig. 11-12. Cladding hoop stress and hoop strain for a PWR 17x17 fuel rod with initial peak power of 9 kW/ft.

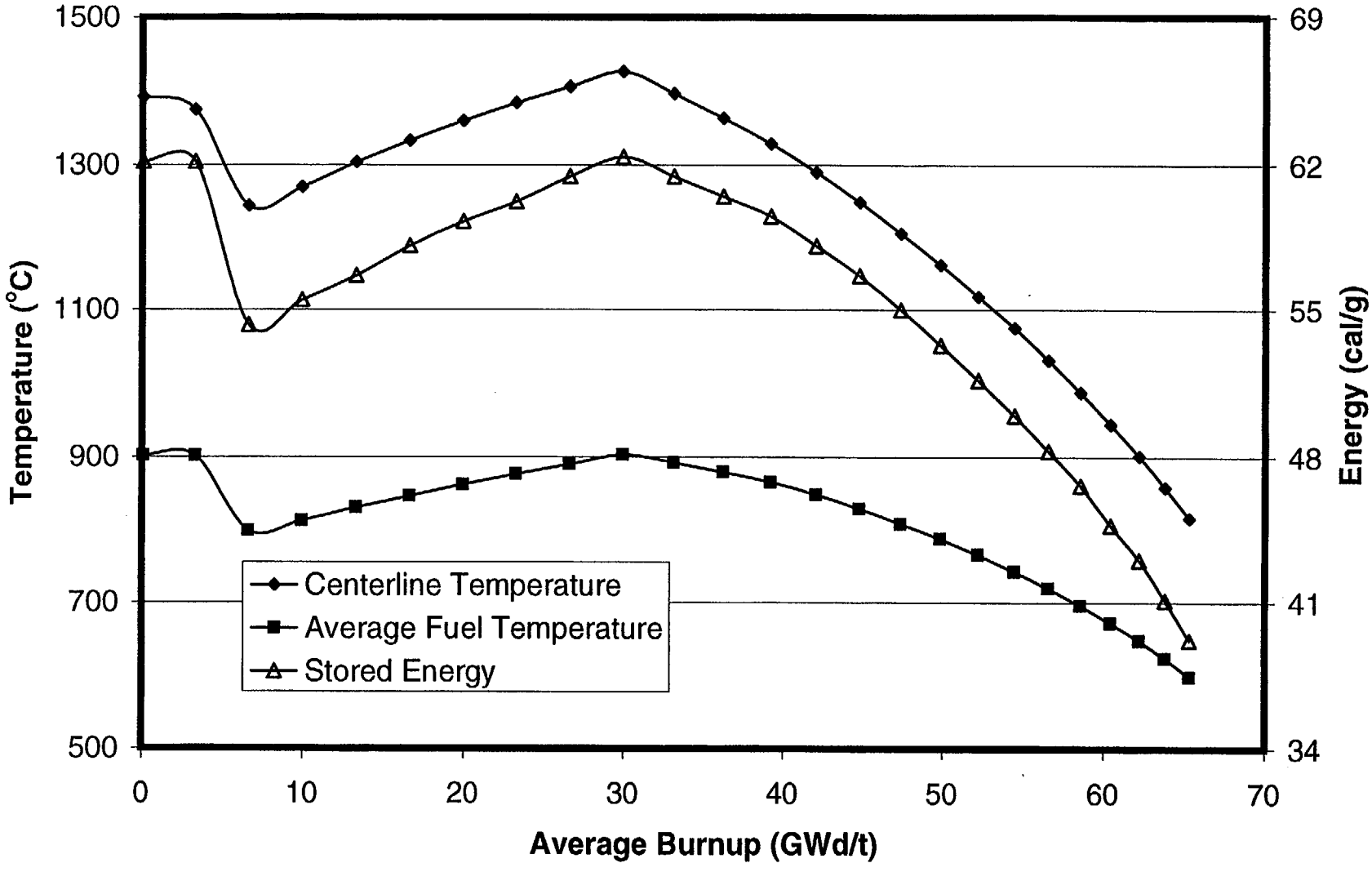

Fig. 11-13. Fuel temperatures and stored energy for a PWR 17x17 fuel rod with initial peak power of 11 kW/ft.

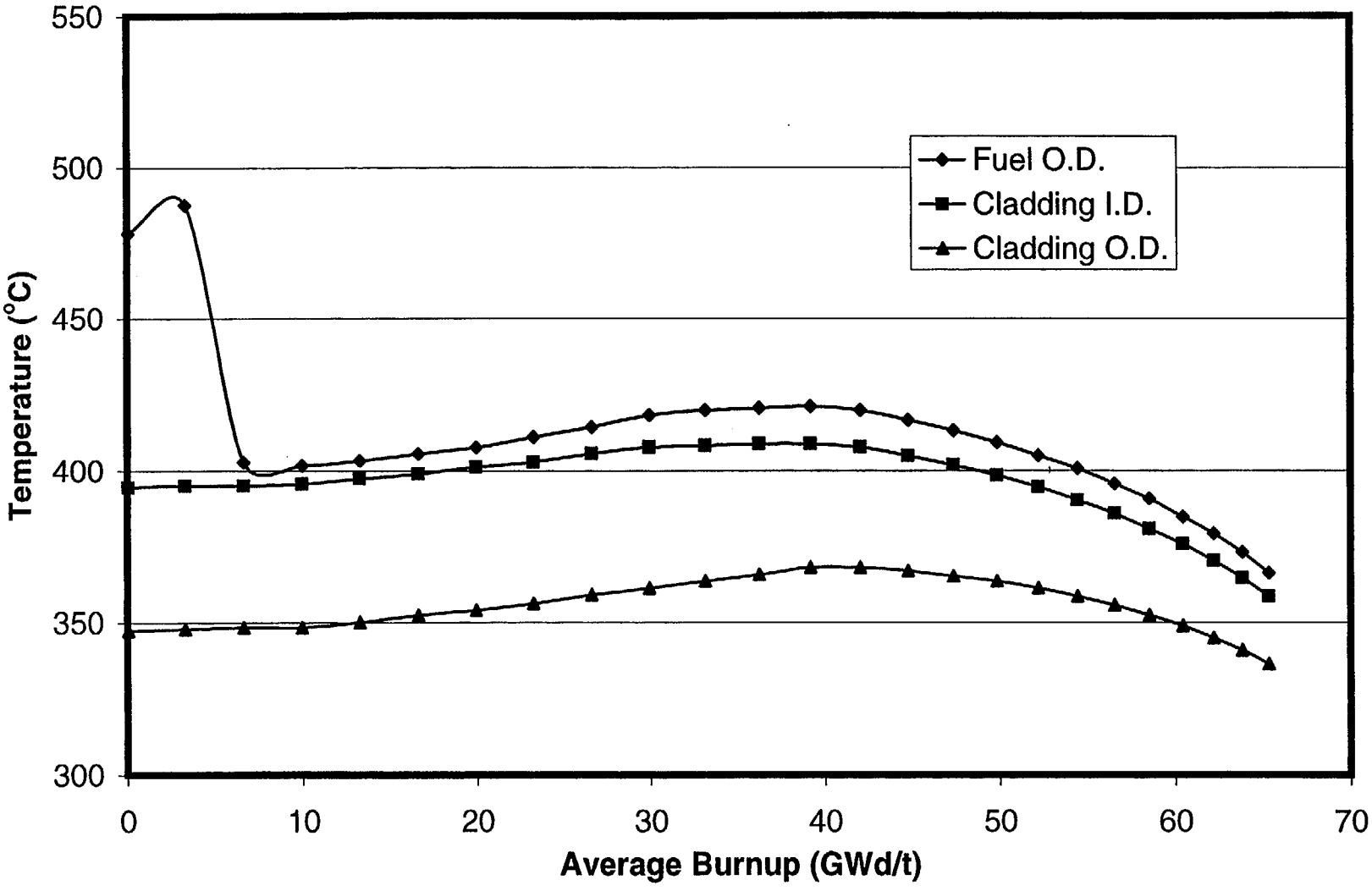

Fig. 11-14. Cladding temperatures and fuel surface temperature for a PWR 17x17 fuel rod with initial peak power of 11 kW/ft.

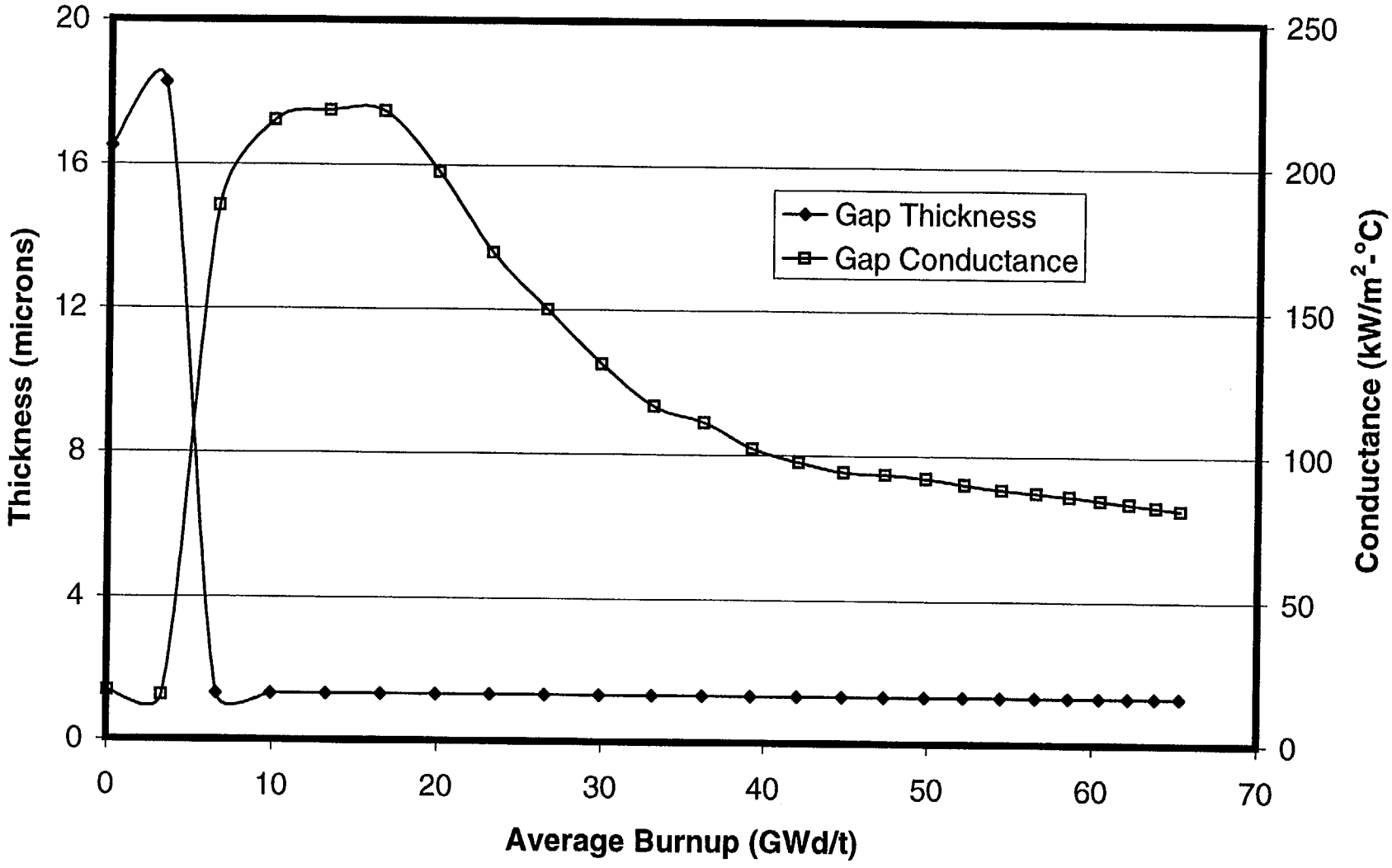

Fig. 11-15. Gap thickness and gap conductance for a PWR 17x17 fuel rod with initial peak power of 11 kW/ft.

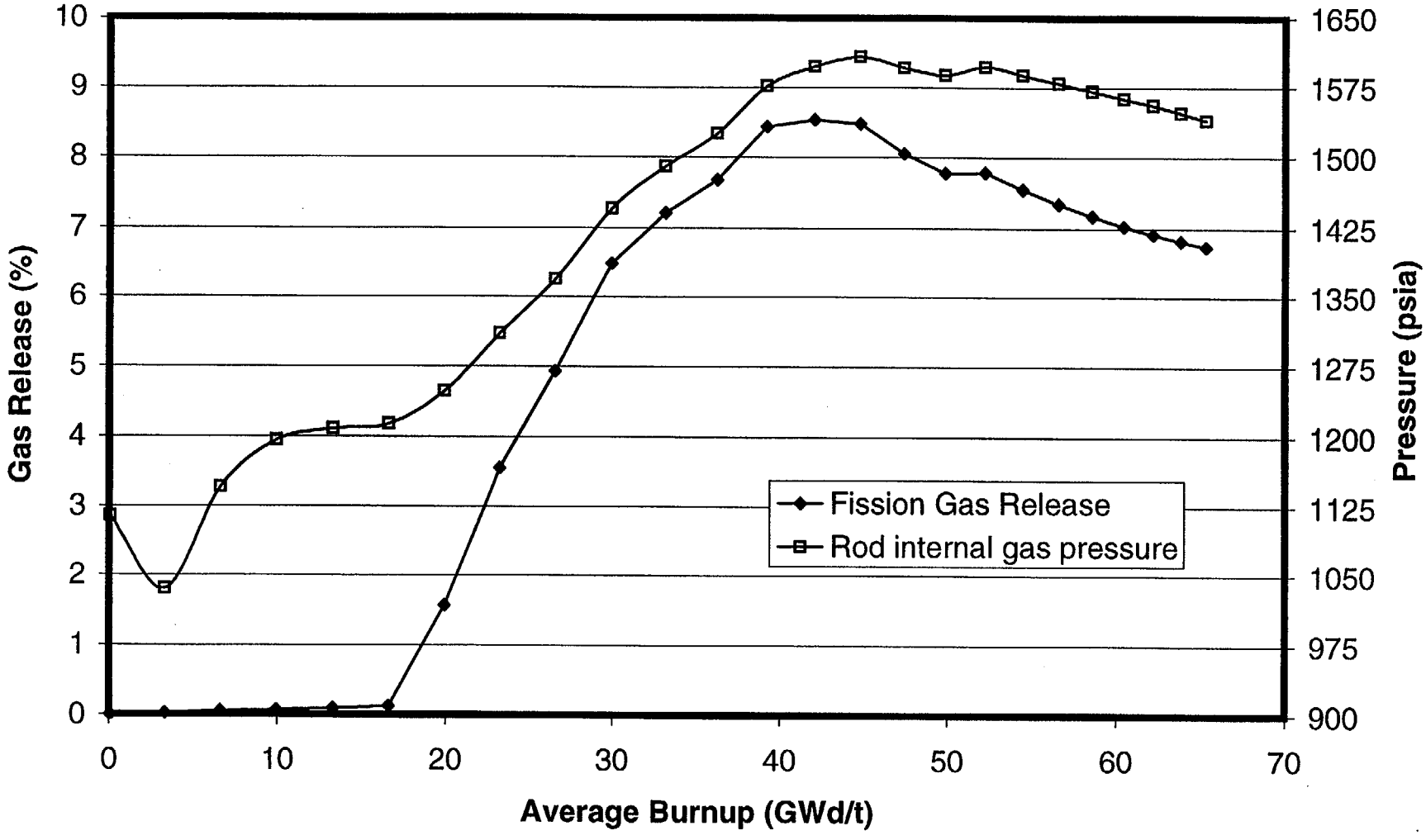

Fig. 11-16. Fission gas release and rod internal gas pressure for a PWR 17x17 fuel rod with initial peak power of 11 kW/ft.

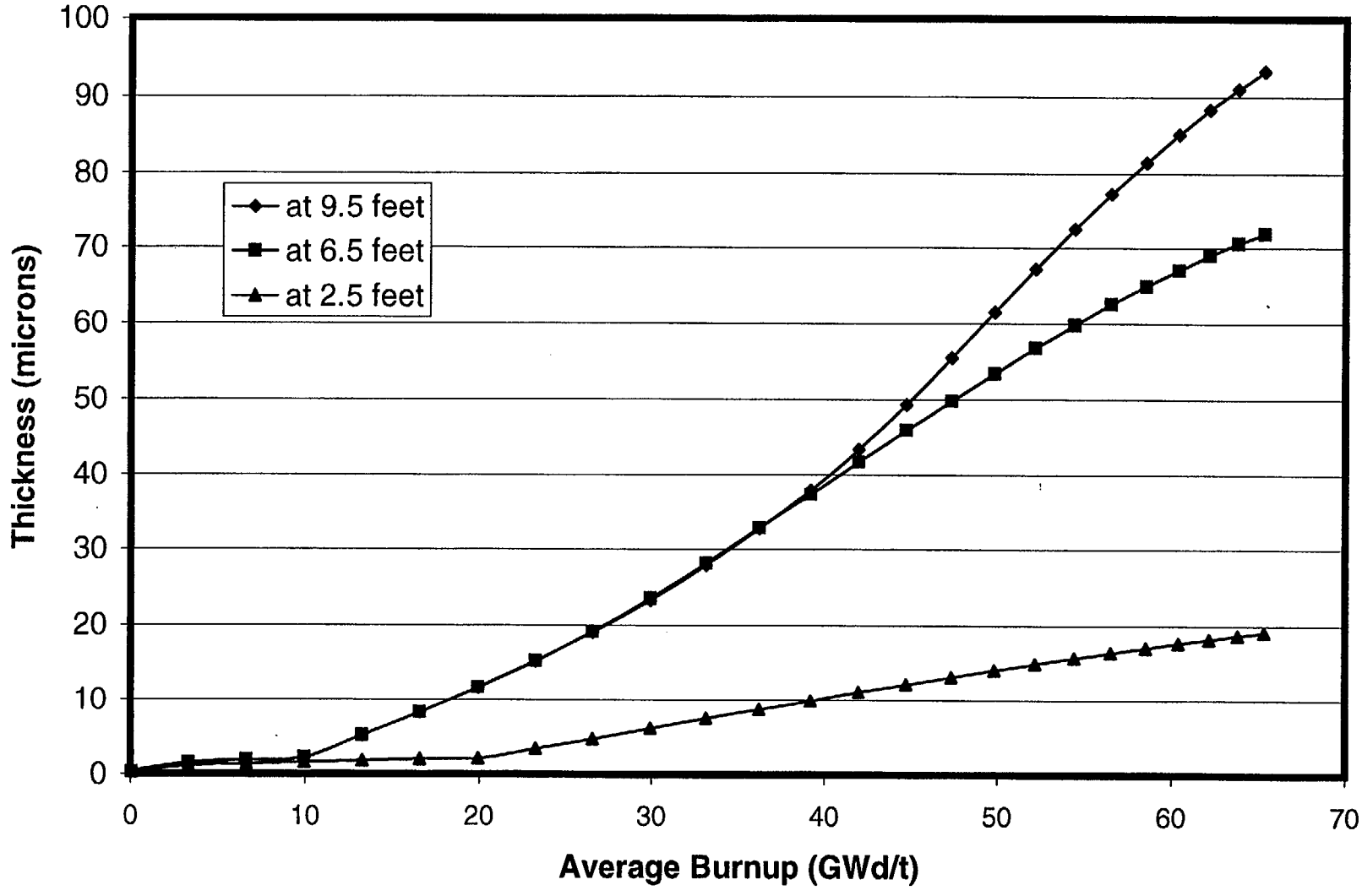

Fig. 11-17. Oxide thickness at three axial locations for a PWR 17x17 fuel rod with initial peak power of 11 kW/ft.

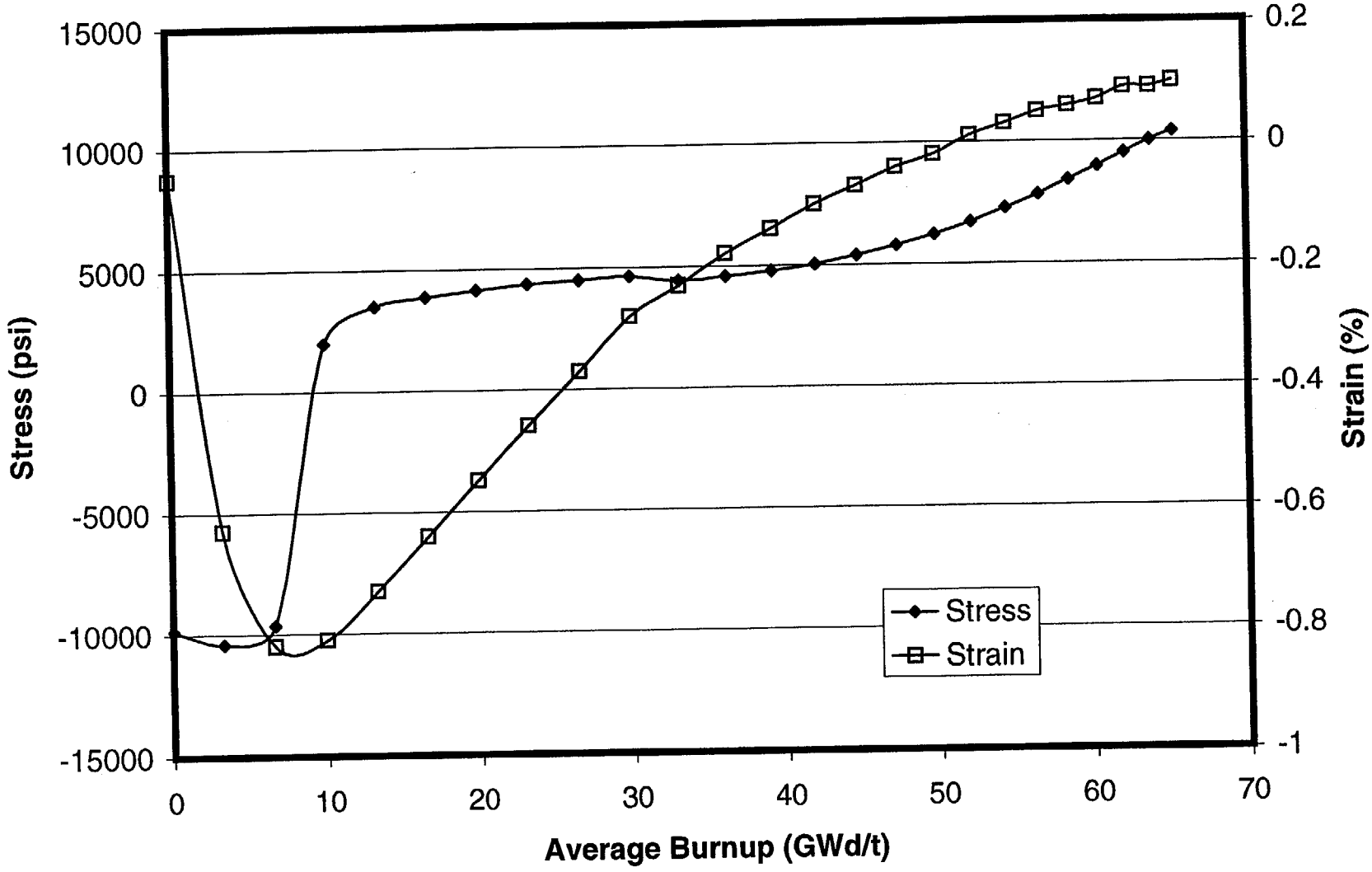

Fig. 11-18. Cladding hoop stress and hoop strain for a PWR 17x17 fuel rod with initial peak power of 11 kW/ft.

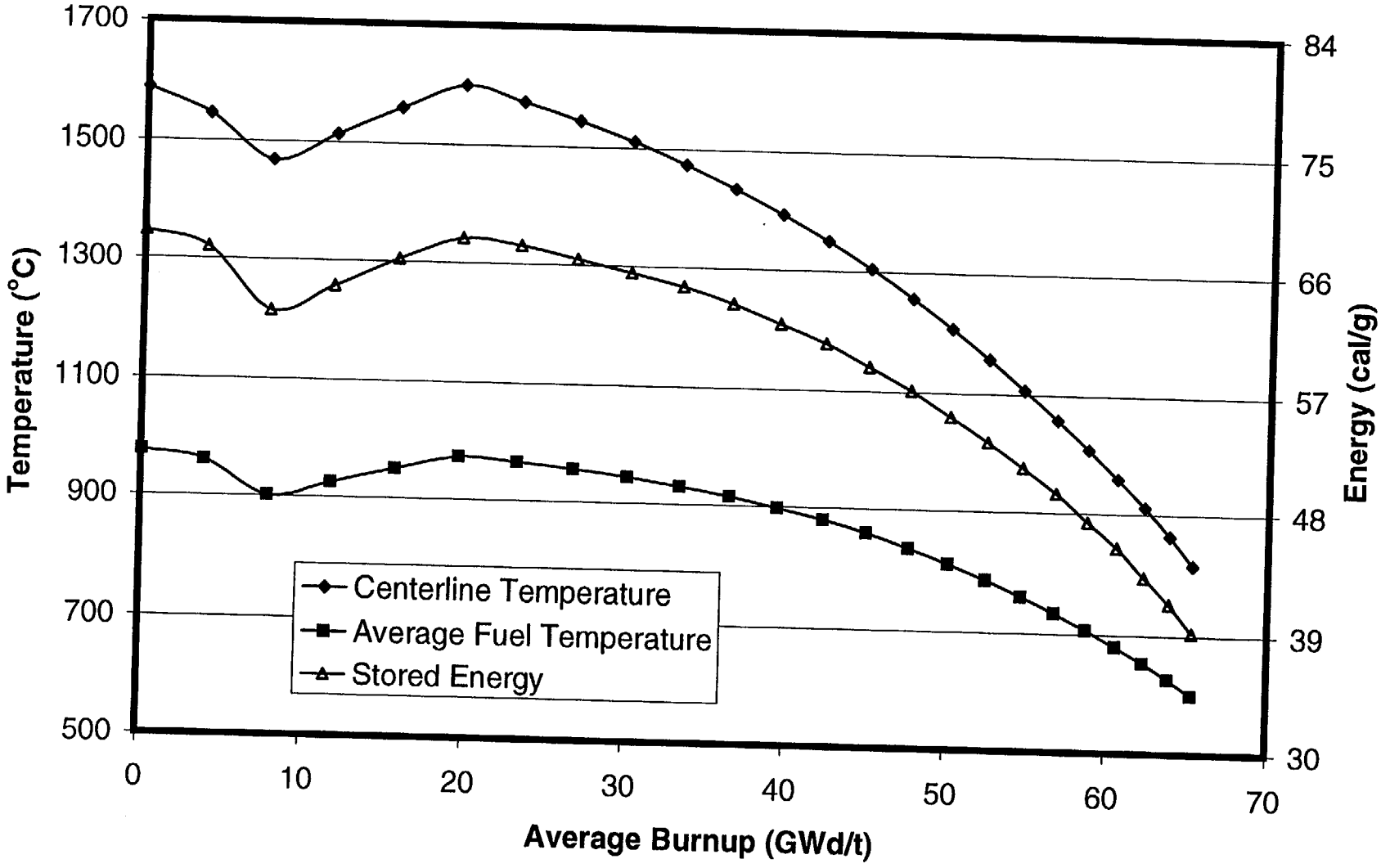

Fig. 11-19. Fuel Temperatures and stored energy for a PWR 17x17 fuel rod with initial peak power of 13 kW/ft.

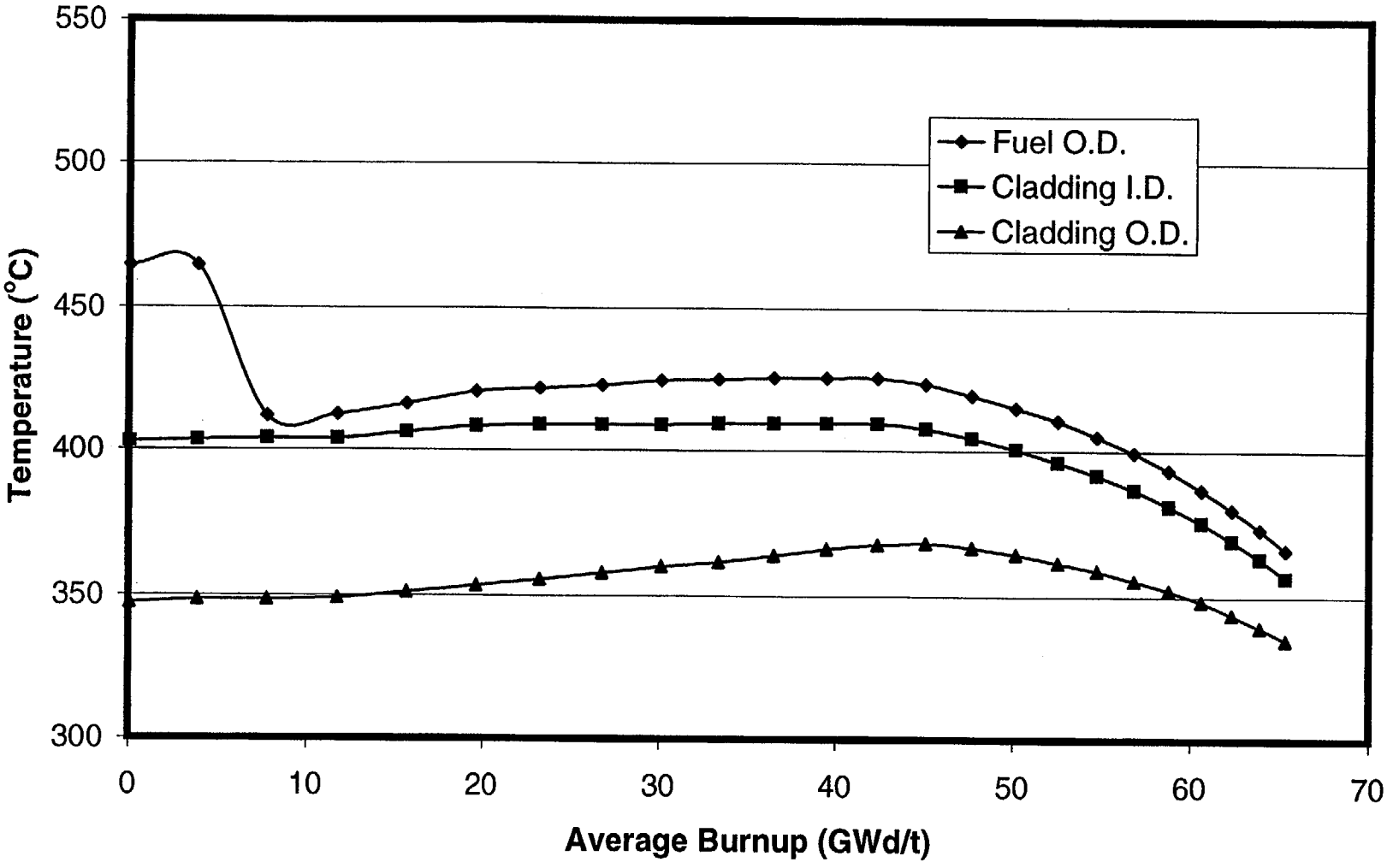

Fig. 11-20. Cladding temperatures and fuel surface temperature for a PWR 17x17 fuel rod with initial peak power of 13 kW/ft.

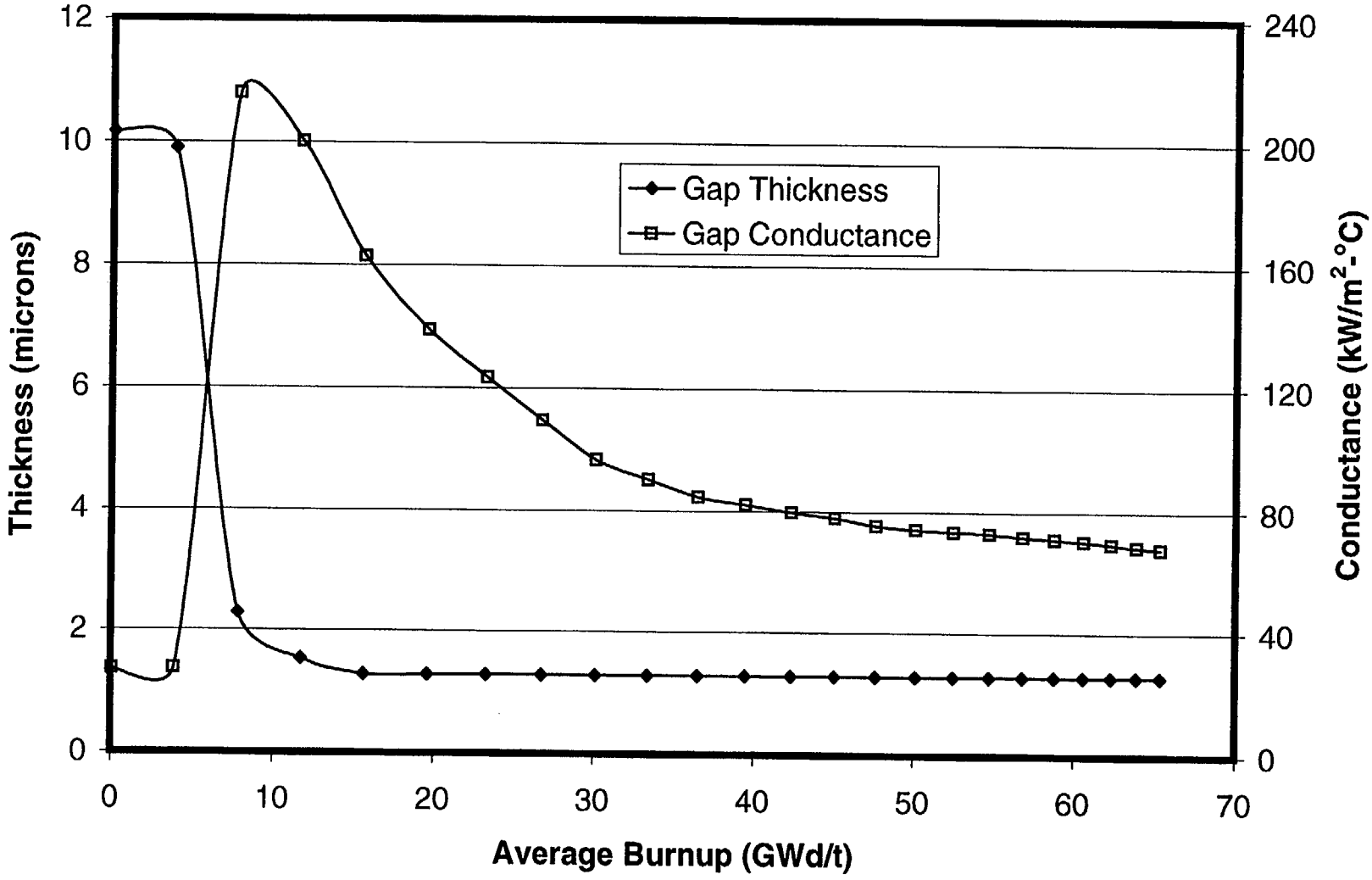

Fig. 11-21. Gap thickness and gap conductance for a PWR 17x17 fuel rod with initial peak power of 13 kW/ft.

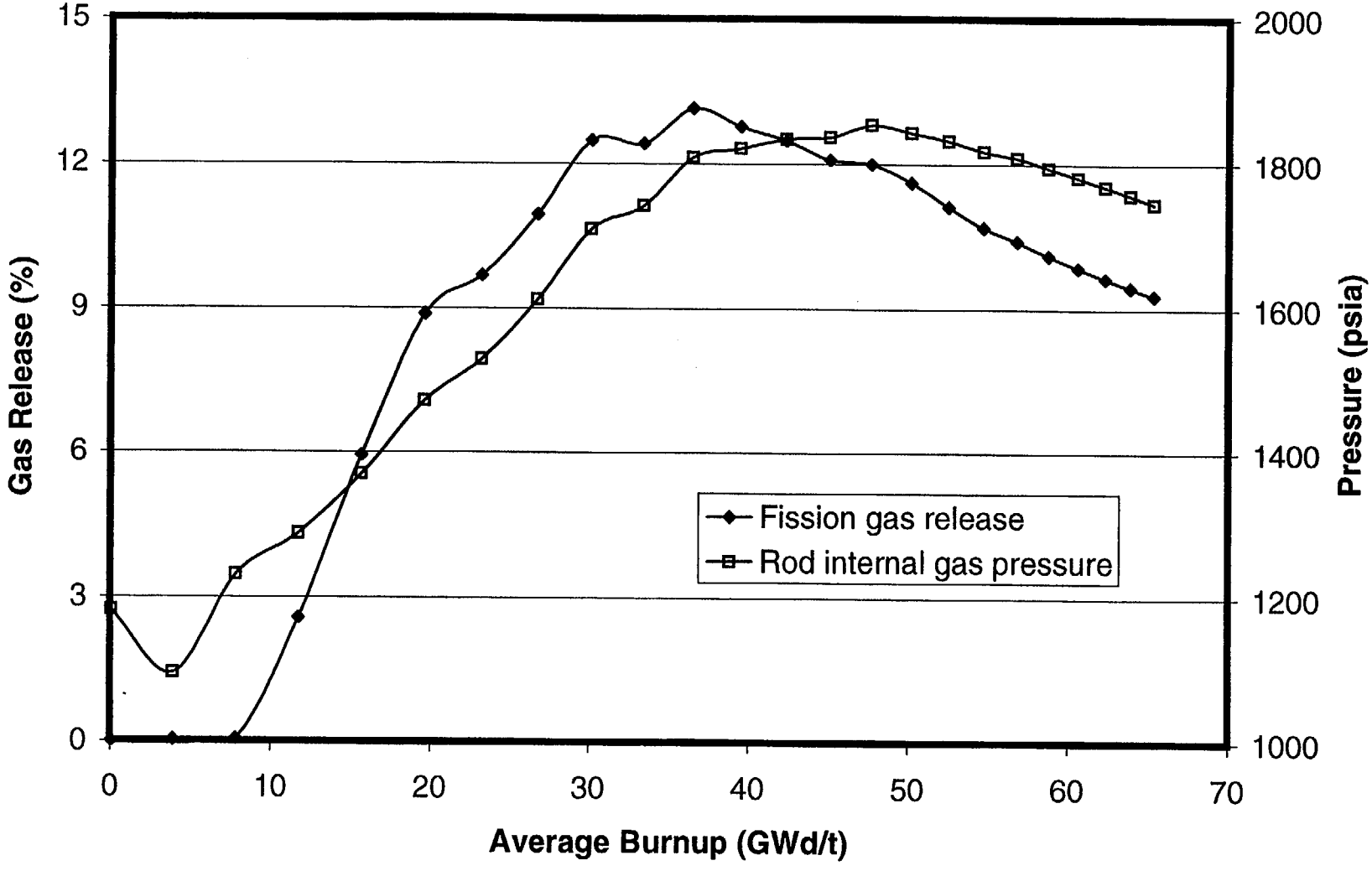

Fig. 11-22. Fission gas release and rod internal gas pressure for a PWR 17x17 fuel rod with initial peak power of 13 kW/ft.

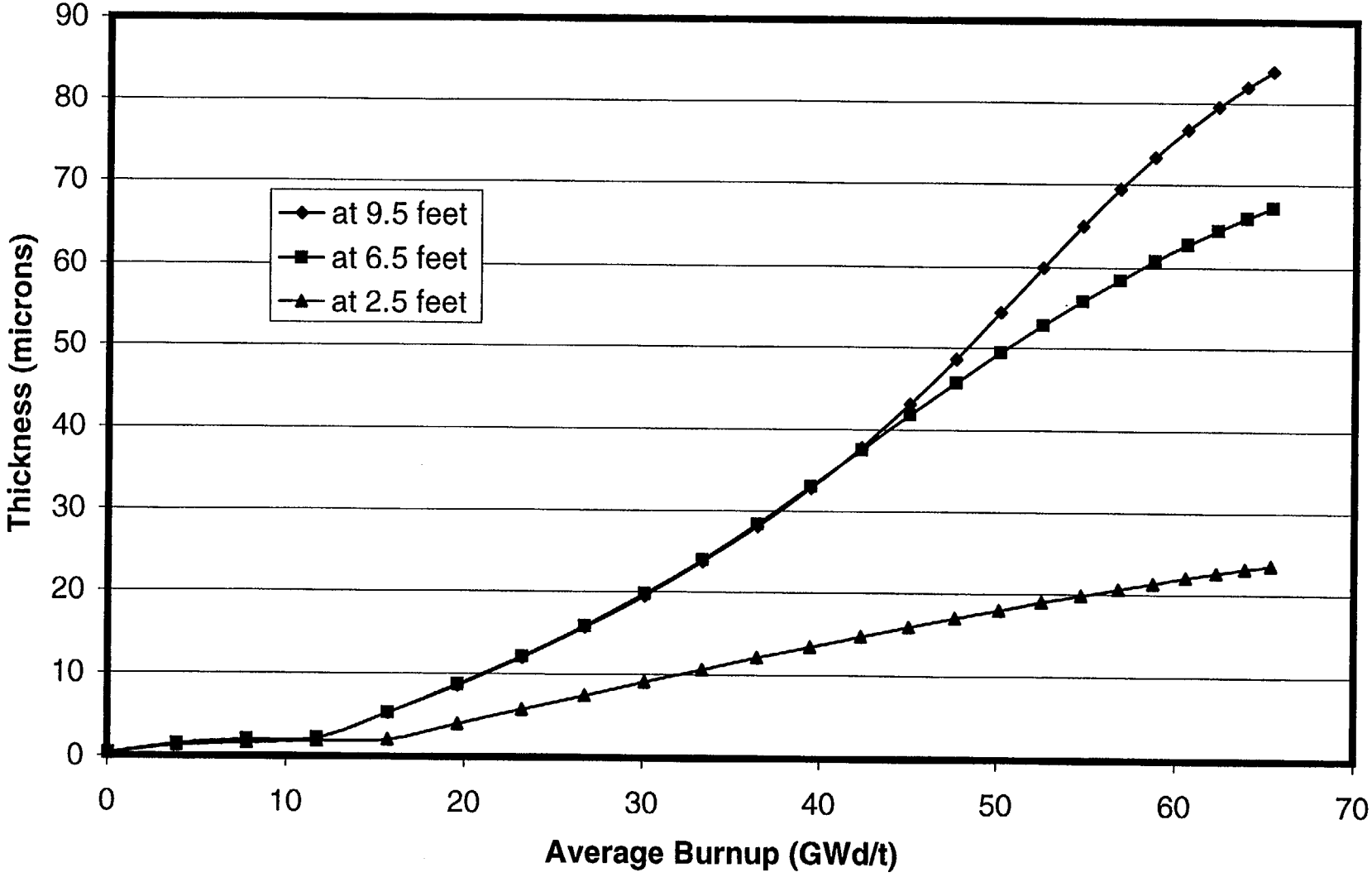

Fig. 11-23. Oxide thickness at three axial locations for a PWR 17x17 fuel rod with initial peak power of 13 kW/ft.

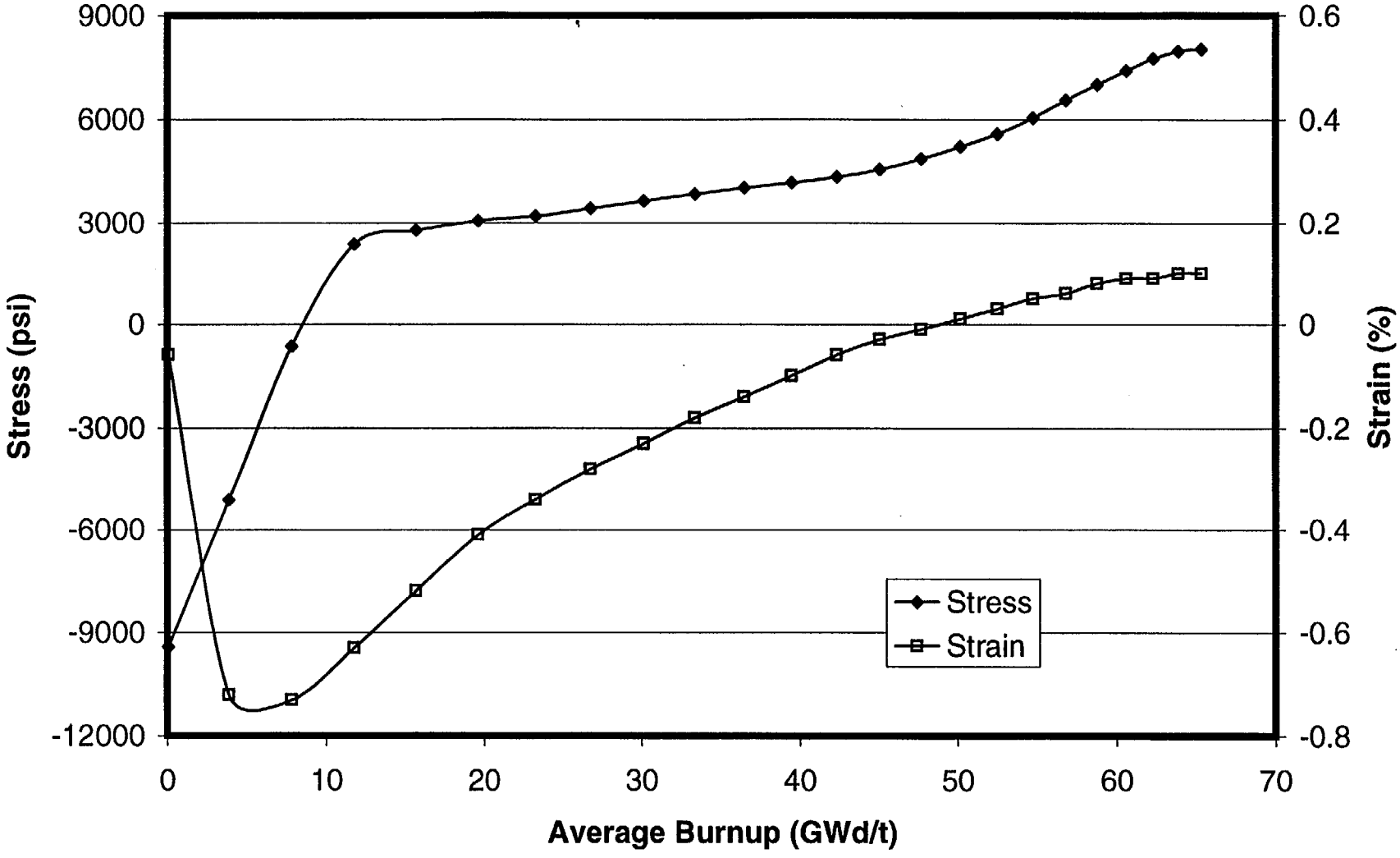

Fig. 11-24. Cladding hoop stress and hoop strain for a PWR 17x17 fuel rod with initial peak power of 13 kW/ft.

12. REFERENCES

1. D. L. Acey and J. C. Voglewede, *A Comparative Analysis of LWR Fuel Designs*, NUREG-0559, July 1980.

2. C. E. Beyer, C. R. Hann, D. D. Lanning, F. E. Panisko, L. J. Parchen, *User's Guide for GAPCON-THERMAL-2: A Computer Program for Calculating the Thermal Behavior of an Oxide Fuel Rod*, BNWL-1897, November 1975.

3. C. E. Beyer, C. R. Hann, D. D. Lanning, F. E. Panisko, L. J. Parchen, *GAPCON-THERMAL-2; A Computer Program for Calculating the Thermal Behavior of an Oxide Fuel Rod*, BNWL-1898, November 1975.

4. D. D. Lanning, C. E. Beyer, C. L. Painter, *FRAPCON-3: Modifications to Fuel Rod Material Properties and Performance Models for High-Burnup Applications,* Volume 1, NUREG/CR-6534, December 1997.

5. G. A. Berna, C. E. Beyer, K. L. Davis, D. D. Lanning, *FRAPCON-3: A Computer Code for the Calculation of Steady-State, Thermal-Mechanical Behavior of Oxide Fuel Rods for High Burnup,* Volume 2, NUREG/CR-6534, December 1997.

6. D. D. Lanning, C. E. Beyer, G. A. Berna, *FRAPCON-3: Integral Assessment,* Volume 3, NUREG/CR-6534, December 1997.

7. C. L. Painter, J. M. Alvis, C. E. Beyer, A. L. Marion, G. A. Payne, E. D. Kendrick, *Fuel Performance Annual Report for 1991,* Volume 9, NUREG/CR-3950, August 1994.

8. *General Electric Fuel Bundle Designs*, NEDE-31152P, Revision 8, Class III (only non-proprietary portions were utilized), April 2001.

9. *Characteristics of Potential Repository Wastes*, Oak Ridge National Laboratory, DOE/RW-0184-R1, Volume 1, July 1992.

Table A1. Non-proprietary BWR Fuel Design Parameters

Fuel Vendor **Array** **Version**	**GE** **8x8** **Barrier**	**GE** **8x8** **GE-4a**	**SNP** **9x9** **JP-3**	**SNP** **9x9** **JP-4,5**	**SNP** **9x9** **IX**	**SNP** **9x9** **9X**	**GE** **10x10**
Typical Number of Fuel Rods per Assembly	62	63	79	79	72	72	92
Pitch (mm, *in.*)	16.26 *0.640*	16.26 *0.640*	14.52 *0.572*	14.52 *0.572*	14.45 *0.569*	14.45 *0.569*	
Cladding OD (mm, *in.*)	12.27 *0.483*	12.52 *0.493*	10.76 *0.424*	10.76 *0.424*	10.95 *0.431*	10.95 *0.431*	
Cladding ID (mm, *in.*)	10.64 *0.419*	10.80 *0.425*	9.25 *0.364*	9.25 *0.364*	9.68 *0.381*	9.68 *0.381*	
Cladding Thickness (mm, *in.*)	0.813 *0.032*	0.863 *0.034*	0.762 *0.030*	0.762 *0.030*	0.635 *0.025*	0.635 *0.025*	
Gap Thickness (mm, *in.*)	0.115 *0.0045*	0.115 *0.0045*	0.095 *0.0037*		0.095 *0.0037*	0.105 *0.0041*	
Fuel Diameter (mm, *in.*)	10.41 *0.410*	10.57 *0.416*	9.05 *0.356*		9.50 *0.374*	9.47 *0.373*	
Fuel Pellet Length (mm, *in.*)	10.41 *0.410*	10.67 *0.420*	10.41 *0.410*				
Fuel Rod Length (m, *in.*)	4.20 *165.4*	4.09 *161.1*	4.04 *159.1*	4.16 *163.8*			
Active Fuel Length (m, *in.*)	3.68 *145*	3.71 *146*	3.68 *145*	3.81 *150*	3.81 *150*	3.81 *150*	
Plenum Length (m, *in.*)	0.241 *9.48*	0.356 *14.00*	0.243 *9.58*	0.243 *9.58*			
Average Enrichment atom%	2.06	2.64	2.92				
Fuel Density (% TD)	95.0	95.0	94.5	94.5	96.3	94.5	
System Pressure (Mpa, *psia*)	7.14 *1035*	7.14 *1035*	7.07 *1026*				
Helium fill gas pressure (kPa, *psig*)	207 *30*	0 *0*	414 *60*	414 *60*			

a. All values are from Ref. 7 except as noted

Table A2. Non-proprietary PWR Fuel Design Parameters

Fuel Vendor Array Version	ABB 14x14 CE	SNP 14x14 ABB CE	SNP 14x14 Top Rod	W 14x14 WE	B&W 15x15 Mark B	B&W 15x15 Mark BW	SNP 15x15 W	W 15x15 WE
Typical Number of Fuel Rods per Assembly	164	176	179	176	208	204	204	204
Pitch (mm, *in.*)	14.73 *0.580*	14.73 *0.580*	14.12 *0.556*	14.73 *0.580*	14.4 *0.568*	14.3 *0.563*	14.3 *0.563*	14.3 0.563
Cladding OD (mm, *in.*)	11.17 *0.440*	11.17 *0.440*	10.59 *0.417*	11.17 *0.440*	10.92 *0.430*	10.72 *0.422*	10.76 *0.424*	10.72 *0.422*
Cladding ID (mm, *in.*)	9.75 *0.384*	9.61 *0.378*	9.11 *0.359*	9.85 *0.388*	9.58 *0.377*	9.35 *0.368*	9.25 *0.364*	9.48 *0.373*
Cladding Thickness (mm, *in.*)	0.711 *0.028*	0.780 *0.031*	0.738 *0.029*	0.660 *0.026*	0.673 *0.027*	0.686 *0.027*	0.762 *0.030*	0.622 *0.024*
Gap Thickness (mm, *in.*)	0.095 *0.0038*	0.110 *0.0043*		0.085 *0.0033*	0.107 *0.0042*	0.089 *0.0035*	0.095 *0.0038*	0.095 *0.0038*
Fuel Diameter (mm, *in.*)	9.56 *0.377*	9.39 *0.370*		9.68 *0.381*	9.36 *0.369*	9.17 *0.361*	9.05 *0.356*	9.29 *0.366*
Fuel Pellet Length (mm, *in.*)	11.43 *0.450*	10.8 *0.425*		15.24 *0.600*	11.05 *0.435*	10.8 *0.425*	6.93 *0.273*	15.24 *0.600*
Fuel Rod Length (m, *in.*)	3.71 *145.9*	3.72 *146.4*	3.86 *152.0*	3.72 *146.4*	3.90 *153.7*	3.20 *125.9*	3.86 *152.0*	3.80 *149.7*
Active Fuel Length (m, *in.*)	3.48 *137*	3.40 *134*	3.66 *144*	3.48 *137*	3.60 *142*	3.66 *144 a*	3.66 *144*	3.66 *144*
Plenum Length (m, *in.*)	0.218 *8.60*		0.185 *7.28*		0.298 *11.70*	0.160 *6.30*	0.173 *6.80*	0.208 *8.20*
Average Enrichment atom%	4.1	3.5		3.13	3.46	3.58	2.65	2.92
Fuel Density (% TD) %TD	95.0	94.0	94.0	95.0	95.0	95.0	94.0	95.0
System Pressure (Mpa, *psi*)	15.5 *2250*				15.2 *2200*	13.9 *2015*	15.5 *2250*	15.5 2250
Helium fill gas pressure (MPa, *psig*)	2.07-3.10 *300-450*	2.10 *305*	2.10 *305*	1.90-2.76 *275-400*	2.86 *415*		2.00 *290*	He

a. All values are from Ref. 7 except as noted

(cont'd)

Table A2 (cont'd). Non-proprietary PWR Fuel Design Parameters

Fuel Vendor **Array** **Version**	**ABB** **16x16** **CE**	**B&W** **17x17** **Mark C**	**B&W** **17x17** **Mark BW**	**SNP** **17x17** **W**	**W** **17x17** **Vantage 5**
Typical Number of Fuel Rods per Assembly	224	264	264	264	264
Pitch (mm, *in.*)	12.9 *0.506*	12.8 *0.502*	12.6 *0.496*	12.6 *0.496*	12.6 *0.496*
Cladding OD (mm, *in.*)	9.70 *0.382*	9.63 *0.379*	9.50 *0.374*	9.14 *0.360*	9.14 *0.360*
Cladding ID (mm, *in.*)	8.43 *0.332*	8.41 *0.331*	8.28 *0.326*	7.87 *0.310*	8.00 *0.315*
Cladding Thickness (mm, *in.*)	0.635 *0.025*	0.610 *0.024*	0.610 *0.024*	0.635 *0.025*	0.572 *0.0225*
Gap Thickness (mm, *in.*)	0.089 *0.0035*	0.099 *0.0039*	0.083 *0.0033*	0.089 *0.0035*	0.065 *0.0026*
Fuel Diameter (mm, *in.*)	8.26 *0.325*	8.21 *0.323*	8.12 *0.320*	7.69 *0.303*	7.85 *0.309*
Fuel Pellet Length (mm, *in.*)	11.43 *0.450*	9.53 *0.375*	10.16 *0.400*	8.84 *0.348*	12.95 *0.510*
Fuel Rod Length (m, *in.*)	4.09 *161.0*	3.88 *152.7*	3.85 *151.5*	3.86 *152.0*	3.87 *152.3*
Active Fuel Length (m, *in.*)	3.81 *150*	3.63 *143*	3.66 *144*	3.66 *144*	3.66 *144*
Plenum Length (m, *in.*)	0.254 *10.00*	0.242 *9.50*	0.163 *6.40*	0.184 *7.26*	0.188 *7.41*
Average Enrichment atom%	2.45	3.29	3.56	3.84	3.59
Fuel Density (% TD) %TD	95.0	95.0	96.0	94.0	95.0
System Pressure (Mpa, *psi*)	15.5 *2250*	15.5 *2250*	15.5 *2250*	15.5 *2250*	
Helium fill gas pressure (MPa, *psig*)	2.07-3.10 *300-450*	3.00 *435*		2.00 *290*	He

a. All values are from Ref. 7 except as noted

NRC FORM 335 (2-89) NRCM 1102, 3201, 3202

U.S. NUCLEAR REGULATORY COMMISSION

BIBLIOGRAPHIC DATA SHEET

(See instructions on the reverse)

1. REPORT NUMBER (Assigned by NRC, Add Vol., Supp., Rev., and Addendum Numbers, if any.)

NUREG - 1754

2. TITLE AND SUBTITLE

A NEW COMPARATIVE ANALYSIS OF LWR FUEL DESIGNS

3. DATE REPORT PUBLISHED

MONTH: December YEAR: 2001

4. FIN OR GRANT NUMBER

5. AUTHOR(S)

G. M. O'Donnell, H. H. Scott, and R. O. Meyer

6. TYPE OF REPORT

7. PERIOD COVERED *(Inclusive Dates)*

8. PERFORMING ORGANIZATION - NAME AND ADDRESS *(If NRC, provide Division, Office or Region, U.S. Nuclear Regulatory Commission, and mailing address; if contractor, provide name and mailing address.)*

Division of Systems Analysis and Regulatory Effectiveness
Office of Nuclear Regulatory Research
U. S. Nuclear Regulatory Commission
Washington, DC 20555-0001

9. SPONSORING ORGANIZATION - NAME AND ADDRESS *(If NRC, type "Same as above"; if contractor, provide NRC Division, Office or Region, U.S. Nuclear Regulatory Commission, and mailing address.)*

same as above

10. SUPPLEMENTARY NOTES

11. ABSTRACT *(200 words or less)*

In 1980, NRC published a comparative analysis of LWR fuel designs, and that report served as a handy reference for typical design and operating parameters for all types of fuel then in operation in U.S. power reactors. During the past twenty years, significant changes have been made in fuel designs, burnups, and analytical computer codes. The present report is an update of the earlier report. Typical fuel design parameters are tabulated for almost all fuel types in current operation, from BWR 8x8 bundles to PWR 17x17 assemblies. Cross-section diagrams are given for BWR fuel bundles and PWR fuel assemblies. Calculated values are plotted for thirteen operating parameters including fuel centerline temperature, cladding O.D. temperature, gap conductance, rod internal gas pressure, and cladding hoop stress. The calculated values are plotted as a function of fuel burnup to 65 GWd/t for a variety of power histories, covering a range from low to high linear heat ratings, which are constant early in life but decline later in a realistic manner.

12. KEY WORDS/DESCRIPTORS *(List words or phrases that will assist researchers in locating the report.)*

Computer Code
Fuel Rod Design Data
Rod Gas Pressure
Fuel Rod Performance
Cladding Corrosion
Cladding Deformation
High Burnup
Pellet Centerline Temperature

13. AVAILABILITY STATEMENT

unlimited

14. SECURITY CLASSIFICATION

(This Page) unclassified

(This Report) unclassified

15. NUMBER OF PAGES

16. PRICE

This form was electronically produced by Elite Federal Forms, Inc.

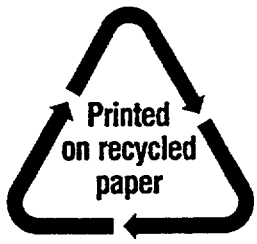

Federal Recycling Program

UNITED STATES
NUCLEAR REGULATORY COMMISSION
WASHINGTON, DC 20555-0001

OFFICIAL BUSINESS
PENALTY FOR PRIVATE USE, $300